Insertion dynamics of Kode FSL constructs with liposomes

Jolene Campbell

2023

Kode Technology Innovation
School of Engineering, Mathematical and Computer Sciences
Faculty of Design and Creative Technologies
Auckland University of Technology

A thesis submitted to Auckland University of Technology
in fulfilment of the requirements for the degree of Doctor of Philosophy

Abstract

Liposomes are used as a sophisticated delivery system for drugs and other active biomolecules. A variety of molecules can be conjugated to the liposome surface to facilitate a range of functionalities, including targeted binding of liposomes to receptor molecules on specific cells, endocytosis, intracellular delivery, triggered release of cargo, reduced opsonisation and removal by reticuloendothelial system. Currently there are 25 clinical liposome products approved by FDA and EMA, none of which are yet to have reached clinical/commercial success. Possible explanations include difficulties with scale-up and ensuring uniform production, poor correlation between animal models and humans, variation between patients and cancers, and the expense of clinical trials and regulatory requirements. In addition, limitations associated with conjugation strategies may also contribute to this lack of clinical success.

Kode technology is a rapid surface labelling technology that has been successfully used to modify and functionalise a range of biological and non-biological surfaces, including cells, viruses, and artificial membranes. Due to similarities between natural cell membranes and liposome membranes it was expected that Kode technology could be applied as a novel approach to modify liposomes without the need for complex chemical reactions.

To achieve this outcome and to understand the capabilities and limitations the aim of this research was to evaluate the modification of unwashed liposomes prepared by thin film hydration followed by extrusion and modification with Kode constructs (FSL). This included method development and characterisation (size, charge, morphology) of the resultant Kode modified liposomes. Insertion and retention dynamics of Kode modified liposomes were evaluated to determine the effects of synthesis method, concentration, temperature, time and liposome lipid composition.

Three FSL constructs, FSL-A2, FSL-biotin and FSL-FLRO4, and three methods to add them to liposomes, including lipid mix (LM), hydration (H) and post synthesis (PS) were investigated.

It was observed that all FSL constructs were very effective at labelling liposomes and did not significantly alter liposome size, morphology or stability.

Incorporation of FSL into liposomes (by H and PS methods) was temperature and time dependent, maximum insertion occurred within 2 hours 37°C and 72 hours at 4°C. The FSL spacer and head group did not appear to significantly affect this.

Transfer of FSL constructs from unwashed liposomes to other membranes (liposomes or red blood cells) was evaluated. Although no transfer to red blood cells was seen from LM liposomes transfer of FSL-A2

and FSL-biotin from liposomes prepared by H/PS methods, was in the range of 5-10%, while FSL-FLRO4 liposomes exhibited only 2% transfer. After extensive investigation it was concluded that transfer was likely due to FSL remaining in the liposome supernatant or adsorbed to the liposome surface, rather than dissociation of FSL from the liposome membrane.

The conclusions from this research are that Kode Technology can be successfully used to enable simple, rapid functionalisation of the surface of liposomes. The potential now exists to synthesise new FSL constructs with functional head groups selected to enable binding of liposomes to specific receptors on target cells/tissues.

Contents

Abstract 2
List of Figures 6
List of Tables 10
List of Abbreviations 11
Attestation of Authorship 13
Acknowledgements 14
Intellectual Property Rights 15
Chapter 1 Introduction 16
1.1 Brief History and overview 16
1.2 Liposomes 19
1.3 Micelles 20
1.4 Liposome composition 21
1.5 Lipid dynamics 23
1.5.1 Lipid polymorphism 23
1.5.2 Critical packing parameter 25
1.5.3 Lamellar bilayer phases (thermotropic phase behaviour of membranes) 28
1.5.4 Phase transition temperature 30
1.5.5 Lateral phase separation 32
1.5.6 Phospholipid movement within bilayer membranes 33
1.5.7 Phospholipid movement between membranes (between liposomes/cells) 34
1.6 Surface modification of liposomes 35
1.6.1 Conventional liposomes 35
1.6.2 Long circulating ‘stealth’ liposomes 36
1.6.3 Targeted liposomes 37
1.6.4 Stimuli sensitive liposomes 41
1.6.5 Multifunctional 42
1.6.6 Hybrid liposomes 42
1.6.7 Current methods of liposome surface modification 43
1.7 Liposome and cell interaction 46
1.7.1 Adsorption 47
1.7.2 Endocytosis 48
1.7.3 Fusion 49
1.7.4 Lipid transfer 50
1.7.5 Liposomes and RBC interaction 53
1.8 Kode technology 54
1.8.1 FSL constructs 55
1.8.2 FSL labelling of cells 59
1.8.3 FSL and liposomes 61
1.9 Liposome preparation 63

1.9.1 Thin film hydration 64
1.10 Methodology used to measure liposomes and micelles 67
1.10.1 Size and morphology 67
1.10.2 Zeta potential 71
1.10.3 Critical micelle concentration 72
1.10.4 Methods for washing liposomes 77
1.11 Research aims 79
Chapter 2 Methods and Results – FSL and Liposome Characterisation 81
2.1 FSL Characterisation 81
2.1.1 FSL constructs used in this project 81
2.1.2 Micelle size and charge 86
2.1.3 Critical micelle concentration 93
2.2 Liposome characterisation 106
2.2.1 Development of method of FSL insertion 107
2.2.2 Liposome synthesis protocol 107
2.2.3 FSL distribution in liposomes 116
2.2.4 Liposome lipid ratios 121
2.2.5 Liposome size and charge 124
2.2.6 Morphology (TEM analysis) 134
2.2.7 FSL activity (after addition to liposomes) 145
Chapter 3 Methods and Results: Dynamics of Insertion 152
3.1 FSL incorporation into liposomes 152
3.1.1 FSL-FLRO4 153
3.1.2 FSL-A2 160
3.1.3 FSL-Biotin 167
3.2 Transfer of FSL between liposomes 170
3.3 Transfer of FSL from liposome to cells 177
3.3.1 Methods 179
3.3.2 Kodecyte calibration curves 181
3.3.3 Effect of FSL concentration and method of liposome preparation 184
3.3.4 Preparation of washed liposomes 194
3.3.5 Effect of liposome age – 1 week 195
3.3.6 Effect of liposome age – 12 weeks 203
3.3.7 Effect of incubation time and temperature 208
3.3.8 Effect of liposome composition – cholesterol and charge 212
3.4 Stability of FSL modified liposomes 219
3.4.1 Size 220
3.4.2 Zeta Potential 222
Chapter 4 Discussion 226
References 244

List of Figures

Figure 1 Liposome structure..... 19
Figure 2 Classification of liposomes based on structure and size..... 20
Figure 3 Schematic diagram of a phosphatidylcholine (PC) phospholipid..... 21
Figure 4 Structure of cholesterol..... 23
Figure 5 Lipid phase structures..... 24
Figure 6 Amphiphile aggregate structures predicted by phospholipid packing parameter..... 26
Figure 7 Structure of solid ordered and liquid disordered phases..... 28
Figure 8 Lipid bilayer membrane phases..... 29
Figure 9 Possible phospholipid movement within the liposome bilayer membrane..... 33
Figure 10 Surface modified liposome..... 36
Figure 11 Passive targeting of nanoparticles by the EPR effect..... 38
Figure 12 Possible mechanisms of liposome – cell interactions..... 47
Figure 13 Endocytosis pathways..... 48
Figure 14 Transfer of lipid between membranes..... 51
Figure 15 Schematic diagram showing the structure of a Kode FSL construct..... 55
Figure 16 Chemical structures of the adipate and CMG(2) spacers used in this project..... 56
Figure 17 Schematic diagram showing different FSL spacer configurations..... 57
Figure 18 Examples of potential FSL construct conformations due to the flexibility of the CMG spacer. 57
Figure 19 Structure of 1,2-dioleoyl-sn-glycero-3-phosphoethanolamine (DOPE) phopsholipid 58
Figure 20 Different ways FSL constructs may associate with cell membranes..... 60
Figure 21 Schematic diagram of a liposome showing possible locations of FSL constructs..... 61
Figure 22 FSL mobility in phospholipid bilayer membrane..... 62
Figure 23 Liposome preparation via thin film hydration..... 66
Figure 24 Cross section view of a cryo-TEM grid and ice film..... 70
Figure 25 Schematic diagram showing particles distributed in a vitreous ice layer..... 70
Figure 26 Schematic diagram showing electric double layer of a negatively charged particle..... 71
Figure 27 Surface tension of a surfactant solution..... 74
Figure 28 Pendant drop method..... 75
Figure 29 Pyrene fluorescence emission spectrum, showing change above and below CMC..... 76
Figure 30 Example graph showing points which may be used to determine CMC..... 77
Figure 31 Chemical structure of FSL-A2, FSL-biotin and FSL-FLRO4..... 84
Figure 32 Size of FSL-A2, FSL-biotin and FSL-FLRO4 particles measured by DLS..... 87
Figure 33 Schematic diagram comparing size of FSL-A2, FSL-biotin and FSL-FLRO4..... 88
Figure 34 Size of FSL micelles..... 90

Figure 35 Size of particles present in PBS. 91
Figure 36 Zeta potential of FSL micelles. 92
Figure 37 Surface tension of FSL and SDS dispersions. 94
Figure 38 Example pendant drop images. 95
Figure 39 Emission spectra of pyrene and FSL-FLRO4+Pyrene dispersions 97
Figure 40 Fluorescence intensity ratio (I/III) vs concentration of FSL and SDS dispersions. 98
Figure 41 Graphs showing count rate data from DLS analysis of FSL and SDS dispersions. 101
Figure 42 Fluorescence of increasing concentration FSL-FLRO4 dispersions. 103
Figure 43 Avanti® Polar Lipids mini extruder 108
Figure 44 Lipid Mix (LM) method of FSL insertion into liposomes. 111
Figure 45 Hydration (H) method of FSL insertion into liposomes. 112
Figure 46 Post synthesis (PS) method of FSL insertion into liposomes. 113
Figure 47 TEM images showing liposomes prepared with or without freeze thaw step. 115
Figure 48 Possible locations of FSL within a liposome dispersion 116
Figure 49 Possible distribution of FSL constructs in liposomes prepared by the LM method. 119
Figure 50 Possible distribution of FSL constructs in (unwashed) liposomes prepared by H method. 120
Figure 51 Possible distribution of FSL constructs in liposomes prepared by PS method. 121
Figure 52 Size of FSL-A2 liposomes measured by DLS. 126
Figure 53 Size of FSL-biotin liposomes measured by DLS. 128
Figure 54 Size of FSL-FLRO4 liposomes measured by DLS. 130
Figure 55 Zeta potential of FSL labelled liposomes. 132
Figure 56 Cryo-TEM images and size distribution of 100 FSL- A2 liposomes. 135
Figure 57 Cryo-TEM images and size distribution of 100 FSL-biotin liposomes 136
Figure 58 Cryo-TEM images and size distribution of 100 FSL-FLRO4 liposomes 137
Figure 59 Size distribution of liposomes obtained from cryo-TEM. 138
Figure 60 Size comparison of liposome sizes determined by cryo-TEM and DLS. 140
Figure 61 Schematic diagram showing types of liposomes observed by cryo-TEM. 141
Figure 62 Liposome structures observed by cryo-TEM 142
Figure 63 Comparison (%) of different types of liposomes observed by cryo-TEM. 143
Figure 64 Fluorescence of FSL-FLRO4 liposomes. 146
Figure 65 Diagram showing microplate used for EIA. 148
Figure 66 EIA plates showing detection of FSL-A2 and FSL-biotin liposomes. 150
Figure 67 Schematic diagram showing possible mechanisms of FSL incorporation into liposome. 152
Figure 68 Fluorescence of liposome dispersion after the addition of 100µM FSL-FLRO4. 154
Figure 69 Fluorescence of 100 FLRO4 liposome dispersions stored at 4°C, RT, and 37°C. 157
Figure 70 Fluorescence of liposome dispersion after the addition of FSL-FLRO4 by PS method. 159

Figure 71 Fluorescence of liposome dispersion after the addition of FSL-FLRO4 by H method. 160
Figure 72 EIA technique used to detect free FSL-A2 present in liposome dispersion. 162
Figure 73 EIA detection of FSL-A2 on microwell surface after incubation with liposomes and micelles. 163
Figure 74 Detection of free FSL-A2 in 100 A2 liposome dispersions 166
Figure 75 EIA detection of FSL-biotin liposomes and micelles. 168
Figure 76 Predicted conformation of FSL-biotin constructs coating a surface. 169
Figure 77 Theoretical mechanisms of FSL transfer between liposomes. 171
Figure 78 Diagram showing EIA method used to detect transfer of FSL between liposomes. 174
Figure 79 EIA results showing transfer of FSL constructs between liposomes. 176
Figure 80 Theoretical mechansims of FSL transfer from liposomes to RBC membrane. 178
Figure 81 Agglutination reactions and scoring system in CAT. 181
Figure 82 FSL-A2 kodecyte standard curve. 182
Figure 83 FSL-FLRO4 and FSL-biotin kodecyte standard curve. 183
Figure 84 Possible mechanisms of FSL transfer from liposome to RBC. 184
Figure 85 Transfer of FSL-FLRO4 from liposomes to RBC. 186
Figure 86 Transfer of FSL-biotin from liposomes to RBC. 188
Figure 87 Agglutination reactions of A2 kodecytes 190
Figure 88 Speculated mechanism of transfer of FSL from liposomes to RBC based on results. 193
Figure 89 Proposed mechanism for transfer of FSL to RBC from a (PS) liposome dispersion 196
Figure 90 Theoretical transfer of FSL from LM liposome dispersion to RBC. 197
Figure 91 Effect of liposome age on FSL-FLRO4 transfer. 198
Figure 92 Effect of liposome age on FSL-biotin transfer. 199
Figure 93 FSL-FLRO4 overlay graphs. 200
Figure 94 FSL-A2 overlay graphs. 202
Figure 95 Transfer of FSL-biotin to RBC. 205
Figure 96 Transfer of FSL-FLRO4 to RBC. 206
Figure 97 Effect of incubation time and temperature on transfer of FSL-FLRO4 from liposome to RBC. 209
Figure 98 Effect of incubation time and temperature on transfer of FSL-biotin from liposomes to RBC. 210
Figure 99 Chemical formula of FSL-$(Me_3N^+)_2$ 213
Figure 100 Size of 100 FLRO4 liposomes with different lipid compositions. 214
Figure 101 Zeta potential of FLRO4 liposomes with different lipid compositions 215
Figure 102 Effect of cholesterol on the transfer of FSL-FLRO4 from liposome to RBC. 216
Figure 103 Effect of liposome charge on the transfer of FSL-FLRO4 from liposome to RBC. 217
Figure 104 Size of FSL-biotin liposomes over 12 weeks. 220
Figure 105 Zeta potential of FSL-FLRO4 liposomes stored for 12 weeks at 4°C. 222
Figure 106 Zeta potential of FSL-biotin liposomes stored for 12 weeks at 4°C. 223

Figure 107 Zeta Potential of FSL-A2 liposomes stored for 12 weeks at 4°C. 224
Figure 108 Schematic diagram of FSL-biotin micelles. 229

List of Tables

Table 1 Polymorphic phase preferences of common phospholipids in pure water. 27
Table 2 Phase transition temperature of commonly used phospholipids for liposome preparation..... 30
Table 3 Percentage fatty acid composition of phosphatidylcholine extracted from egg and soy..... 31
Table 4 Type of functional head group 55
Table 5 Methodology used to measure liposomes and micelles in this research 67
Table 6 CMC values calculated by Pyrene I/III spectrophotometry method 99
Table 7 Particle count rate of FSL-A2, FSL-biotin and FSL-FLRO4 dispersions (in PBS) 100
Table 8 Summary of CMC data for FSL-A2, FSL-biotin and FSL-FLRO4..... 105
Table 9 Molar ratio of liposome lipids (FSL and EPC) commonly used in this study..... 121
Table 10 Theoretical number of FSL molecules per liposome (100nm diameter) 122
Table 11 Summary of the mean size and polydispersity index of A2-liposomes. 125
Table 12 Summary of the mean size and polydispersity index of FSL-biotin liposomes..... 127
Table 13 Summary of the mean size and polydispersity index of FLRO4 liposomes 129
Table 14 Description of liposome mix samples..... 173
Table 15 Estimated percentage transfer of FSL-FLRO4 from liposomes to RBC 187
Table 16 Estimated percentage transfer of FSL-biotin from liposomes to RBC..... 189
Table 17 Agglutination scores of A2 kodecytes 189
Table 18 Estimated percentage transfer of FSL-A2 from liposomes to RBC 191
Table 19 Agglutination reactions of A2 kodecytes. 201
Table 20 FSL-A2 transfer from liposome to RBC after 12 weeks storage at 4°C. 204
Table 21 A2 kodecyte agglutination scores. 211
Table 22 Liposome lipid ratios..... 214
Table 23 PDI comparison of FLRO4 liposomes with different lipid compositions. 215
Table 24 PDI values of FSL-biotin (100µM) and blank lipoosmes stored for 12 weeks at 4°C..... 220
Table 25 Theoretical distribution of FSL constructs in liposomes prepared by LM, H and PS methods.. 233

List of Abbreviations

Ab	Antibody
BSA	Bovine serum albumin
C	Cholesterol
CMC	Critical micelle concentration
CMG	Carboxymethylglycine
CPP	Critical packing parameter
Cryo-TEM	Cryogenic transmission electron microscopy
DLS	Dynamic light scattering
DLPC	Dilauroylphosphatidycholine
DMPC	Dimyristoylphosphatidycholine
DMPE	Dimyristoylphosphatidylethanolamine
DOPC	Dioleoylphosphatidylcholine
DOPE	Dioleoylphosphatidylethanolamine
DOPG	Dioleoylphosphatidylglycerol
DPPC	Dipalmitoylphosphatidylcholine
DPPE	Dipalmitoylphosphatidylethanolamine
DSPC	Distearoylphosphatidylcholine
DSPE	Distearoylphosphatidylethanolamine
E	Egg phosphatidylcholine
EGFR	Epidermal growth factor receptor
EIA	Enzyme immunoassay
EMA	European medicines agency
EPC	Egg phosphatidylcholine
EPR	Enhanced permeability and retention
EV	Extracellular vesicle
F	FSL-FLRO4
FDA	US food and drug administration
FITC	Fluorescein isothiocyanate
FSL	Function spacer lipid (Kode technology construct)
Fuc	Fucose
Gal	Galactose
GalNAc	N-Acetylgalactosamine
GlcNAc	N-Acetylglucosamine
GRF	Growth factor receptor
H	Hydration (method of FSL addition to liposomes)
HER2	Human epidermal growth factor receptor 2
kcps	kilo count per second
L_α	Liquid disordered
L_β	Solid ordered
L_o	Liquid ordered
LM	Lipid mix (method of FSL addition to liposomes)
LUV	Large unilamellar vesicle

MLV	Multi-lamellar vesicle
mfi	Mean fluorescence intensity
mV	millivolts
MVV	Multi vesicular vesicle
NBT/BCIP	Nitro-blue tetrazolium chloride and 5-bromo-4-chloro-3'-indolyphosphate p-toluidine salt
nm	Nanometer
PBS	Phosphate buffered saline (0.9% sodium chloride, pH 7.4)
PC	Phosphatidylcholine
PDI	Polydispersity index
PE	Phosphatidylethanolamine
PEG	Polyethylene glycol
pNPP	p-nitrophenylphosphatase
PS	Post synthesis (method of FSL addition to liposomes)
RBC	Red blood cell
RES	Reticuloendothelial system
rfu	Relative fluorescence unit
SDS	Sodium dodecyl sulphate
SD	Standard deviation
SUV	Small unilamellar vesicle
T_m	Phase transition temperature
TBS	Tris buffered saline (0.9% sodium chloride, pH 9.0)
TEM	Transmission electron microscopy
v/v	Volume to volume
RT	Room temperature
(+)	FSL-(+)

Attestation of Authorship

I hereby declare that this submission is my own work and that, to the best of my knowledge and belief, it contains no material previously published or written by another person (except where explicitly defined in the acknowledgements), nor material which to a substantial extent has been submitted for the award of any other degree or diploma of a university or other institution of higher learning.

Jolene Campbell

1 June 2023

Acknowledgements

I would like to thank my supervisors Professor Steve Henry, Professor Nicolai Bovin and Dr Eleanor Williams for their generous guidance and support. I would like to especially acknowledge Dr Eleanor Williams for her invaluable suggestions and encouragement throughout my PhD journey.

I would like to thank all my colleagues at AUT Centre for Kode Technology, for their friendship, support and advice. I am grateful for the opportunity to have worked with such a fantastic group of people.

Finally, I would like to thank my family for their love, support and faith in me.

Intellectual Property Rights

Intellectual property rights comprising all aspects of the projects reported in this thesis belong to Kode Biotech Limited and shall not be passed on to a third party without explicit approval in writing from Kode Biotech Limited (www.kodebiotech.com).

Chapter 1 Introduction

Liposomes are small lipid vesicles which are frequently used in biotechnology. This chapter introduces liposomes and briefly outlines their advantages and limitations as a sophisticated drug delivery system. Liposome composition, characterisation, synthesis and existing surface modification methodologies, including limitations of current techniques, are described. As the objective of the research was to evaluate Kode technology modification of liposomes the principles of Kode technology are introduced along with a description of how this technology could be applied to the surface modification of liposomes.

1.1 Brief History and overview

Nanotechnology, the design, characterisation, production and application of nanosized materials or devices in the nanometre scale [1], is one of the most innovative technologies of the twentieth century. The use of nanotechnology and nanoparticles in medicine has revolutionised conventional therapeutic and diagnostic procedures. Since the 1990s, the use of nanoparticles as advanced delivery systems for a range of therapeutic and diagnostic applications has grown steadily. Of these nanoparticles, liposomes have been arguably the most successful [2] and account for approximately 40% of clinically approved nanoparticle therapies [3].

Liposomes were discovered by Bangham and Horne in 1964 [4] when they observed the spontaneous formation of multilamellar phospholipid vesicles in water. The term 'liposome' to describe these vesicles was first published in 1968 [5]. Initial interest in liposomes focussed primarily on their use as an artificial model membrane as they provided a unique tool which enabled the study of many fundamental membrane properties such as permeability, adhesion, fusion, and phospholipid function for the first time [6, 7].

By the 1970s it had been established that liposomes could also be used to encapsulate various compounds, such as lysozyme, chlorophyll-a, and beta-fructofuranosidase [8-10]. This led to Gregoriadis and Ryman proposing the use of liposomes as a carrier to deliver enzymes or drugs for the treatment of disease [11]. By 1973 they had demonstrated that this was possible and the potential application of liposomes as a revolutionary drug delivery system was established [12].

During the 1970s and 1980s liposomes attracted increasing interest. Improved methods of liposome synthesis and cargo encapsulation were established. Liposome properties and behaviour both *in vitro* and *in vivo* were investigated and further potential therapeutic uses were explored, such as their use as a vaccine adjuvant to increase immune response to antigen [13]. Two significant problems were quickly identified; firstly liposomes are rapidly cleared from circulation by the reticuloendothelial system [14].

Secondly, was how to engineer liposomes so that they would accumulate and then release their cargo at the desired site.

The first problem was overcome in 1990 when Klibanov et al. [15] reported that coating liposomes with the hydrophilic polymer polyethylene glycol (PEG) significantly increased circulation time, so called 'stealth' liposomes. This led on to the development of the first FDA approved liposomal drug Doxil® (PEGylated liposomes encapsulating doxorubicin) in 1995 [16].

The second challenge has yet to be resolved. Active targeted liposomes have been and continue to be extensively studied. The ability to direct liposomes to specific tissues or cells by attaching ligands such as antibodies to their surface was first proposed by Gregoriadis in 1977 [17] and methods were quickly established to couple antibody and other targeting molecules to the surface of liposomes [18-20]. However, despite 30 years of intensive research, and considerable *in vitro* success, the development of a clinical liposome product with these targeted and controlled delivery capabilities has not yet been achieved [21]. *In vivo* studies show the efficaciousness of labelled liposomes remains equivalent to unlabelled liposomes [22]. Likely explanations include difficulties with scale up, poor correlation between animal models and humans, and variation between patients and cancers [21]. In addition, limitations associated with conjugation strategies may also be contributing to this lack of clinical success.

Advantages

Liposomes can be used as a sophisticated delivery system for drugs and other active biomolecules. They are utilised across a wide range of clinical, diagnostic and analytical applications. To date 25 clinical liposomal products have been approved by the United States food and drug administration (FDA) and the European medicines agency (EMA), and many more are in development [16, 23, 24]. Liposomes are used to encapsulate a variety of bioactive molecules, including oncology drugs, antimicrobial and anti-fungal agents, anaesthetics, genetic materials e.g. DNA, RNA, siRNA etc, proteins, peptides, and molecular imaging agents [25-28]. In addition to nanotherapeutics (diagnostic, therapeutic and analytical applications) liposomes are utilised across a wide variety of additional fields including cosmetics [29], food technology [30, 31], and agriculture [32].

Liposomes offer many advantages over conventional drug formulations. Most importantly liposomes are composed of phospholipids and so are biocompatible, biodegradable and have low immunogenicity. In addition, they can improve drug pharmacokinetics by increasing accumulation at target sites while simultaneously decreasing toxicity and off-target side effects. This enables the administration of higher drug doses with reduced side effects.

Liposomes protect encapsulated molecules from degradation (redox, enzyme, pH) and removal while in the physiological environment, leading to extended circulation and increased accumulation at target sites via passive and active targeting. At the same time materials encapsulated within liposomes are not bioactive until released, this decreases toxicity and unwanted off-target effects on healthy tissues.

Liposomes are highly versatile; they can encapsulate a wide range of molecules and can be administered in many forms. Because of their bilayer structure liposomes can encapsulate both hydrophilic and hydrophobic molecules [28]. They can enable the delivery of molecules which are difficult to administer by conventional methods due to difficulties in their formulations (e.g., solubility, stability, toxicity). Liposomes can be used to deliver non-conventional biopharmaceuticals such as DNA, RNA therapeutic proteins, without the need for viral vectors [26]. They can formulated and applied in a variety of different forms [28, 33], including as a suspension [34], aerosol [35], foam [36], or semisolid such as cream [29] or gel [37]. They can be administered parentally [38-40], topically [41, 42], orally [43, 44] or via inhalation [28, 45, 46].

Liposomes can also be modified by attaching a range of molecules to their surface [47]. This can be used to engineer liposomes with a range of functionalities, including extended *in vivo* circulation (stealth liposomes) [48, 49], targeted binding of liposome to specific receptors/cells [50], promotion of cell fusion and intracellular delivery of encapsulated cargo to targeted cells (e.g. cell penetrating peptides) [51], controlled delivery (stimuli sensitive) [52], and can also help facilitate the delivery of liposomes into hard to reach environments such as crossing the blood brain barrier [53].

Limitations

Liposomes have several limitations. One of their main limitations is their short circulation time, liposomes are rapidly detected and removed from circulation by cells of the reticuloendothelial system [14]. Other limitations include poor stability *in vivo* [54] (due to both complement mediated destruction and oxidation and hydrolysis of phospholipids) [55], inconsistency of production (variation within and between batches), low targeting efficacy, drug encapsulation efficiencies can be low and leakage of encapsulated materials can occur. The controlled release of encapsulation materials at the desired site can also be problematic.

Surface modification of liposomes is a promising strategy to help overcome some of these limitations and improve their performance characteristics. The surface of liposomes can be modified with a wide range of ligands/functional molecules to engineer liposomes with multifunctional properties; for example, to facilitate targeted and specific binding to target tissues, to increase cellular uptake, to avoid uptake and removal by RES (stealth properties), to improve stability and encapsulation of cargo, and to facilitate controlled release of cargo at the desired site (stimuli sensitive).

A new approach

It was proposed that the use of Kode Technology could be a novel and simple method for the surface modification of liposomes. Kode is already established as a surface labelling method for many biological and non-biological surfaces, including cell membranes, viruses, stainless steel, nanofibers [56, 57]. This method has shown excellent performance characteristics; it is simple, stable, and reliable [56]. Since liposomes are analogous to cell membranes, it was anticipated that Kode technology can also be successfully applied to the modification and labelling of liposomes.

1.2 Liposomes

Liposomes are artificial spherical vesicles composed of one or more phospholipid bilayer membranes surrounding an internal aqueous core, Figure 1. They can range in size from several nanometres to micrometres. Liposomes are formed by the spontaneous self-assembly of amphiphilic lipid molecules, such as phospholipids, in aqueous solution. Phospholipids self-assemble with their hydrophobic lipid tails facing together within the bilayer, and their hydrophilic head groups oriented toward the aqueous phase.

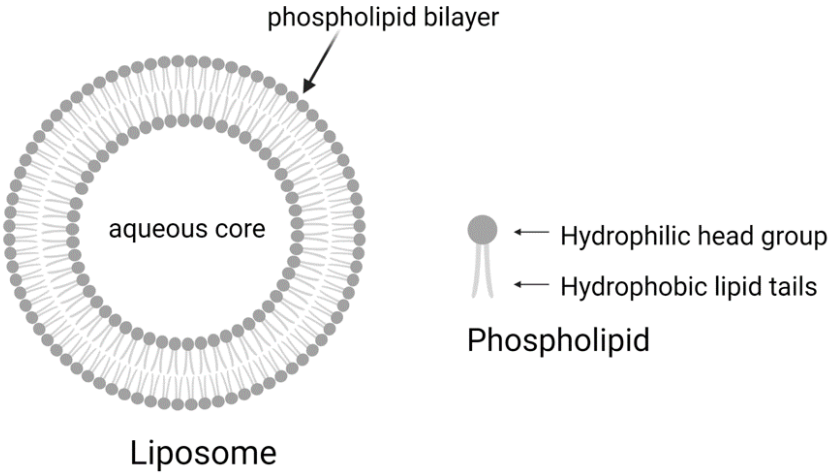

Figure 1 Liposome structure. Liposomes are composed of a spherical phospholipid bilayer membrane encapsulating an internal aqueous core.[58]

Because of their structure, liposomes have the unique ability to encapsulate molecules with different solubilities; hydrophilic molecules can be encapsulated within their aqueous core [59], hydrophobic molecules can be incorporated within the lipid bilayer or adsorbed to the liposome surface [60], and amphipathic molecules at the water lipid interface [27].

Liposomes can be classified based on their size and the organisation of their phospholipid bilayers (lamellarity). The phospholipid bilayers may be unilamellar (composed of a single lipid bilayer), multilamellar (composed of several concentric bilayers like an onion), or multivesicular in which separate smaller non-concentric bilayer vesicles are contained within a single outer bilayer, Figure 2. Unilamellar vesicles may be further divided based on their size as small unilamellar vesicles (SUV) <100nm, large unilamellar vesicles (LUV) 100-1000nm, giant unilamellar vesicles (GUV) >1000nm [61].

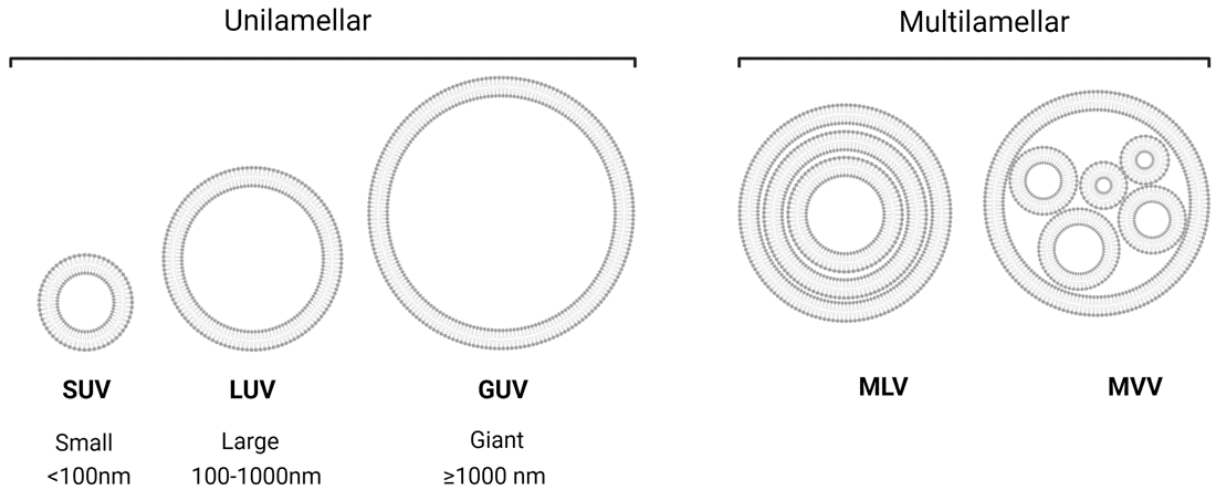

Figure 2 Classification of liposomes based on structure and size. Small unilamellar vesicles (SUV), large unilamellar vesicles (LUV), giant unilamellar vesicles (GUV), multilamellar vesicles (MLV) and multivesicular vesicles (MVV). Figure adapted from [61-63].

1.3 Micelles

In addition to forming liposomes amphipathic molecules, such as phospholipids and FSL constructs, dispersed in aqueous solution can form a range of other structures, including micelles (and a variety of other structures see 1.5.1 Lipid polymorphism). Micelles are usually composed of a single layer of molecules (not a bilayer like liposomes) and do not have an internal aqueous compartment.

Phospholipid micelles are usually very small, approximately 2-20nm in size [64]. In aqueous solution, the phospholipid molecules in a micelle arrange with their polar head groups facing outwards and their lipid tails inwards. In addition, depending on the environmental conditions reverse or inverted micelles may form, where the hydrophilic head groups are oriented toward centre and hydrophobic tails face outwards. Examples of possible micelle structures in aqueous solution are shown in Figure 5.

At low concentrations amphipathic molecules are present as monomers dispersed in an aqueous solution. Above a certain concentration, termed the critical micelle concentration (see 1.10.3 Critical micelle

concentration), the amphipathic molecules aggregate and form micelles. Kode constructs (see section 1.8 Kode technology) are amphipathic molecules and can likely form micelles. Their conformation as a monomer or micelle may influence their interaction with liposomes.

1.4 Liposome composition

Liposomes are usually composed of natural or synthetic glycerophospholipids (or sphingomyelin), and small amounts of other lipids may also be included e.g. cholesterol to improve bilayer stability and reduce permeability [27]. The lipid composition of a liposome influences its characteristics, including size, charge, bilayer structure (rigidity, fluidity, stability) permeability, encapsulation efficiency, charge, drug retention and release and circulation times *in vivo* [65]. Therefore, careful selection of phospholipids can be used to develop liposomes with optimal performance characteristics.

Glycerophospholipids

Glycerophospholipids (commonly referred to as phospholipids) are composed of a glycerol backbone linked to two hydrophobic fatty acid chains and a hydrophilic polar head group (via a phosphate group), Figure 3. Phospholipid head groups (choline, ethanolamine, serine, glycerol, and inositol) vary in size, charge, and polarity. These head groups form phospholipids called phosphatidylcholine, phosphatidylethanolamine, phosphatidylserine, phosphatidylglycerol and phosphatidylinositol respectively [65].

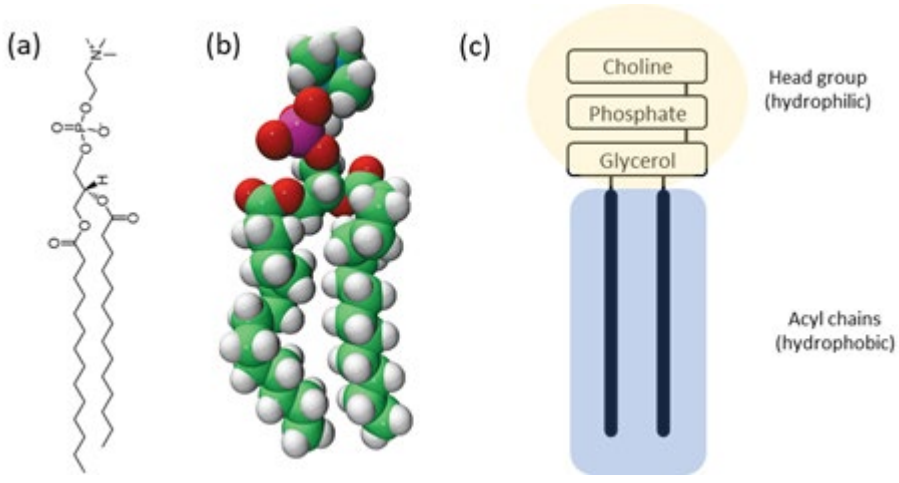

Figure 3 Schematic diagram of a phosphatidylcholine (PC) phospholipid. The (**a**) schematic chemical structure, (**b**)space filling molecular structure, and (**c**) a schematic representation of dimyristoylphosphatidylcholine (1,2-dimyristoyl-sn-glycero-3-phosphocholine) is shown. Dimyristoylphosphatidylcholine is composed of a hydrophilic choline head group attached via a phosphate residue to the glycerol backbone, which is connected to two hydrocarbon fatty acid acyl chains. Adapted from [66, 67].

Charge

Depending on the head group of the phospholipids used to prepare liposomes, they can have positive, negative and neutral charge [65]. Phosphatidylcholine (PC) and phosphatidylethanolamine (PE) are zwitterionic, and contain both positive and negatively charged regions, while phosphatidylserine, phosphatidylinositol, and phosphatidylglycerol are negatively charged [68]. There are no naturally occurring cationic phospholipids, however positively charged lipids, such as stearylamine, DOTAP (dioleoyl-3-trimethylammonium propane) and DOTMA (di-O-octadecenyl-3-trimethylammonium-propane) can be incorporated into liposomes to impart a positive charge [69, 70].

Liposome charge (via electrostatic interaction) can be used to increase encapsulation and/or interaction with molecules of the opposite charge. For example positively charged lipids can be included in liposome composition to increase interaction between the liposome and negatively charged cell membranes [70-72], positive lipids are used to increase encapsulation of negatively charged molecules such as DNA, RNA or oligonucleotides [73, 74] in the liposomes, similarly negatively charged liposomes can increase encapsulation of positively charged molecules [75].

Phospholipid acyl chains

The acyl chains of the phospholipids can also affect the liposome properties. Long saturated phospholipids pack tightly together forming liposomes which are rigid, stable and have low permeability (see section 1.5.3 Lamellar bilayer phases) [65]. In contrast, liposomes composed of shorter unsaturated phospholipids, are more permeable and less stable [70, 76, 77]. Acyl chain length can also influence encapsulation efficiencies; phospholipids with longer acyl chains enable increased encapsulation of hydrophobic drugs due to the increased lipophilic environment [78].

Phospholipid properties can also alter the liposomes stability and fusion characteristics. Phospholipids which undergo a phase transition (see 1.5.2 Critical packing parameter) in response to a change in environmental conditions (e.g. pH change) can be used to cause membrane destabilisation to facilitate cell-liposome binding and to enable triggered release of cargo at a specific. For example small amounts of PE (which undergoes phase transition at low pH) is often included in liposomes to facilitate fusion with cell membranes and intracellular drug release [51, 79].

Cholesterol

Cholesterol (up to 30mol%) is a common constituent of liposomes. Cholesterol is included to improve their membrane stability and reduce permeability [80]. Cholesterol orients itself with its hydroxyl group close to the phospholipid head groups and its carbocyclic rings aligned between the hydrophobic alkyl chains [81]. Cholesterol alters the membrane fluidity and stability, see section 1.5.3 Lamellar bilayer phases (thermotropic phase behaviour of membranes). It can also influence encapsulation efficiencies and release profiles of encapsulated molecules [78, 80, 82].

(a) (b)

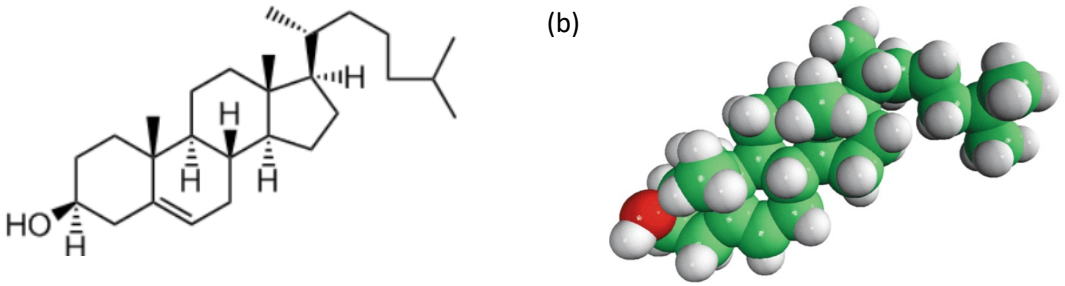

Figure 4 Structure of cholesterol. Schematic diagram showing the (a) chemical structure and (b) space filling molecular structure of cholesterol [83].

1.5 Lipid dynamics

1.5.1 Lipid polymorphism

Phospholipids are amphipathic, they contain both a hydrophilic (head group) and hydrophobic (fatty acid chains) region. When dispersed in aqueous solution they spontaneously self-assemble with their hydrophilic head groups facing toward the aqueous solution and their hydrophobic tails preferring to face toward each other away from the aqueous solution. As a result of this they can from a variety of supramolecular aggregates, with different phospholipid organisation.

The different types of aggregate structures can be classified as micelles (sphere of lipid molecules), lamellar (two dimensional bilayer formations, such as planar membrane or spherical vesicles such as liposomes), hexagonal (two dimensional tubular or cylindrical arrangements), and cubic (more complicated three dimensional structures), example structures are shown in Figure 5. The shape and morphology of the structures formed depends on both the lipid composition and environmental conditions such as pH, temperatures, presence of salts.

The self-assembled aggregates are not held together by strong ionic or covalent bonds, but instead by van der Waals forces, electrostatic interactions, hydrogen bonding and hydrophobic forces. As a result the

supramolecular structures formed are flexible or fluid like, and their association is reversible [84]. It is possible for structurally different populations (monomer, small and/or large aggregates, such as micelles and liposomes) to coexist in a thermodynamic equilibrium with each other [84, 85]. Micelles are highly dynamic, the molecules are in constant motion, the monomers exchange rapidly between micelles and the bulk solution, with a monomer existing within a micelle for between 10^{-5} and 10^{-3} seconds [84].

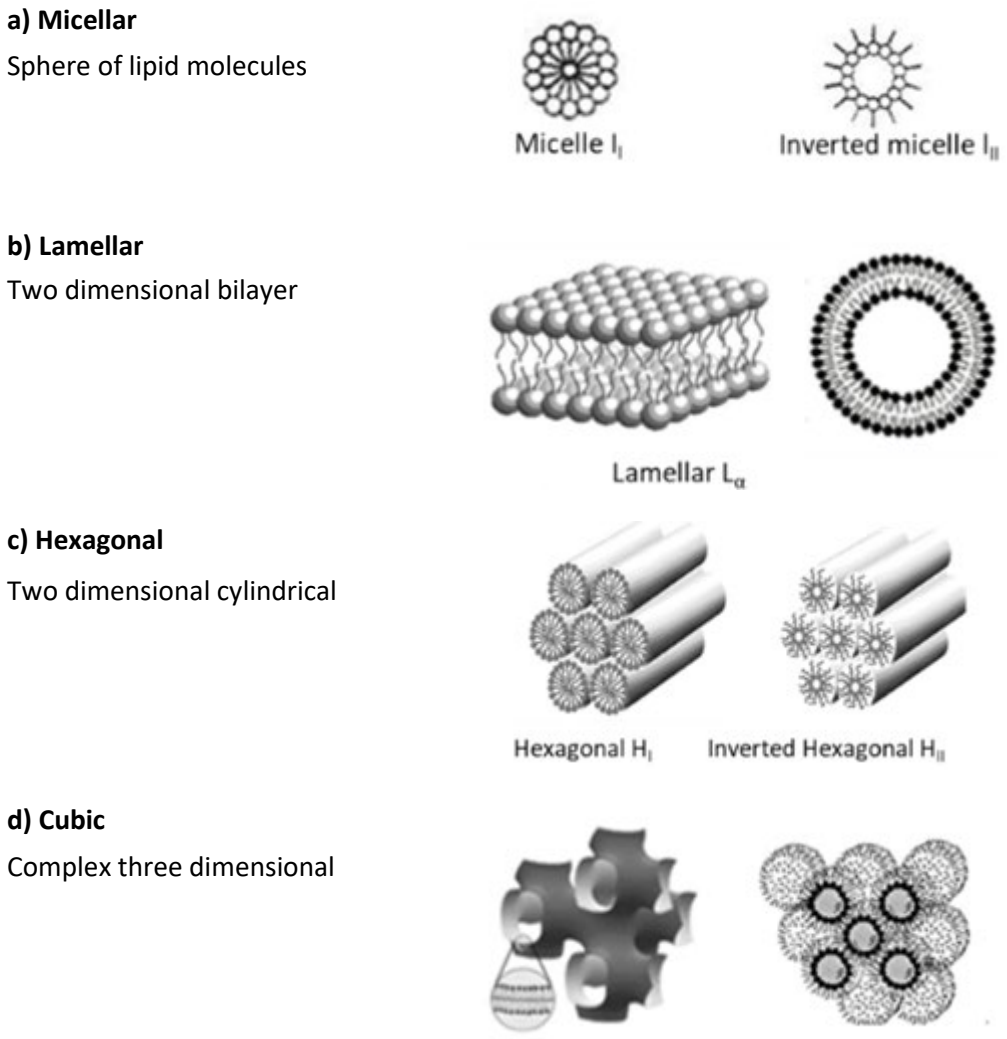

Figure 5 Lipid phase structures. Diagram showing examples of (**a)** micelle, (**b**) lamellar, (**c**) hexagonal and (**d**) cubic lipid phase structures. Figure adapted from [86].

1.5.2 Critical packing parameter

The shape and size of a phospholipid aggregate is partly dependent on the molecular geometry of its component molecules (head group, degree of unsaturation and branching of lipid acyl chains), as these influence how the molecules can best pack together. According to Israelachvili et al. [87] the structure of lipid aggregates can be predicted based on the geometry of the individual amphiphile molecules using equation 1 [88] below:

$$P = \frac{v}{a\, l_c}$$

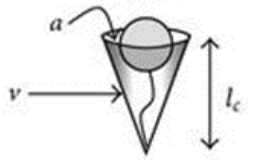

P	Critical packing parameter
v	Volume of hydrocarbon chains
a	Area of the hydrophilic head group
lc	Length of hydrophobic chains

Equation 1 Packing parameter equation

This equation calculates the 'critical packing parameter', a dimensionless parameter, which is the ratio between the volume of the hydrophobic part of the amphiphile with the optimal surface area of the hydrophilic head groups and the length of the hydrophobic chains [88]. This packing parameter can be used to predict the shape of aggregate structures likely to form in aqueous solutions, Figure 6 [85, 89].

Phospholipids which have a larger head group than their hydrocarbon area have a cone like geometry, P < 0.3, and tend to form spherical micelles. However, it should be noted that micelles only form above a defined concentration of amphiphile. This concentration is called the critical micelle concentration (CMC), see 1.10.3 Critical micelle concentration. Below the CMC amphiphiles are present as monomers (single molecules).

Phospholipids which are cylindrical in shape, with equal headgroup and hydrocarbon areas, have a packing parameter 0.5-1 and tend to form lamellar phases such bilayer membranes and vesicles, e.g. liposomes. Nearly all phosphatidylcholine and phosphatidylethanolamine phospholipids fall into this category. The primary phospholipid constituent of most liposomes is usually phosphatidylcholine for this reason.

Phospholipids with a small head group, and a packing parameter greater than one, form reverse or inverted micelles (hexagonal I and II or cubic phase). In this case the phospholipids aggregate with their hydrophilic head groups on the inside and the hydrophobic tails on the outside. Phosphatidylethanolamine with unsaturated hydrocarbon chains forms this phase.

Packing Parameter	Amphiphile Shape	Aggregate Structure	Phase
P < 0.3	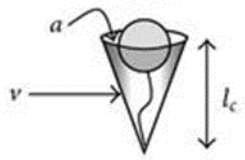	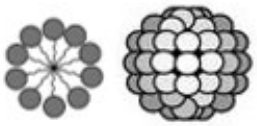 Spherical micelles	Micelle
0.3 ≤ P < 0.5		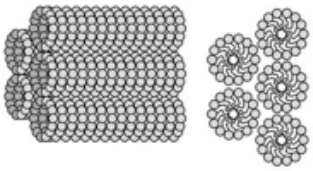 Cylindrical micelles	Hexagonal I
0.5 ≤ P < 1		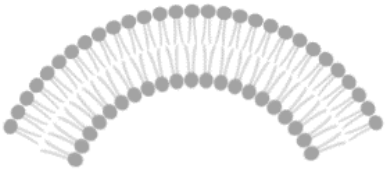 Flexible bilayers, vesicles	Lamellar (bilayer)
P = 1		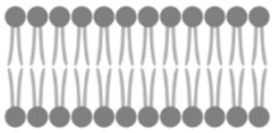 Planar bilayers	
P > 1		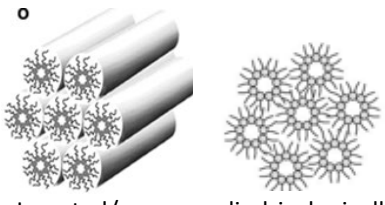 Inverted/reverse cylindrical micelles	Hexagonal II

Figure 6 Amphiphile aggregate structures predicted by phospholipid packing parameter. Adapted from [89].

Note: the above structures should not be considered mechanically, as if the molecules really are cylinders, cones etc. It must be kept in mind that in reality all lipids, even cholesterol, are highly dynamic

conformationally flexible molecules that can intertwine with each other as part of a bilayer and other supra molecular formations. For details see 1.5.6.

While the packing parameter is useful for predicting possible micelle/aggregate structures in simple model systems, caution must be used when applying to natural biological systems. In this case many other factors play a role in determining aggregate shape and structure including phospholipid concentration and interactions with other lipids and ions, thermodynamic factors such pH and temperature, and aqueous conditions. Altering these conditions can result in changes to the structure of the aggregate formed. The phase preferences of several common phospholipids in pure water are shown in Table 1 [90, 91].

Table 1 Polymorphic phase preferences of common phospholipids in pure water.

Bilayer (lamellar)	**Hexagonal II**
Phosphatidylcholine	Phosphatidylethanolamine (unsaturated)
Phosphatidylserine	Phosphatidylserine (pH <3)
Phosphatidic acid	Phosphatidic acid (pH <3)
Phosphatidylglycerol	Phosphatidic acid (pH <3) (+ Ca^{2+})
Phosphatidylinositol	Cardiolipin (+ Ca^{2+})
Phosphatidylethanolamine (saturated)	

Environmental conditions such as temperature, pH, water content influence the phase behaviour of phospholipids and can cause them to transition from one phase to another. Decreased water content, increased temperature all promote transition from lamellar to hexagonal phases. pH changes or the presence of polyvalent ions (e.g. Ca^{2+}), which neutralise head group charges, can also destabilise lamellar phases and promote the transition to hexagonal phases.

Phospholipid hydrocarbon chain unsaturation also impacts phase behaviour. For example saturated PE phospholipids form lamellar phases, whereas unsaturated PE lipids, such as DOPE, favour hexagonal structures [90].

The phase behaviour of phospholipids is an important consideration when designing liposomes. These properties can be used to trigger membrane instability, which can promote liposome fusion with cell membrane (inclusion of non-lamellar lipids can facilitate liposome-cell membrane fusion, [90, 91]) and triggered release of content (phase transition can be triggered by changing environment e.g. pH, leading to membrane destabilisation and content release) [92].

1.5.3 Lamellar bilayer phases (thermotropic phase behaviour of membranes)

Phospholipids can also adopt different states within the lamellar bilayer phase. These affect the fluidity of the bilayer membrane and are an important consideration in liposome design as they directly impact liposome stability, permeability, and cargo release characteristics.

Phospholipids within a bilayer membrane can exist in three phases; solid ordered (L_β), liquid disordered (L_α), and liquid ordered (L_o). Although there is no molecular rearrangement of the bilayer between these states, there is significant change in the properties, lateral organisation, molecular order, and the mobility of the lipid molecules within the bilayer. The transition between the solid ordered and liquid disordered states occurs at a specific temperature specific for each phospholipid, called the thermotropic phase transition temperature (T_m), see section 1.5.4 Phase transition temperature.

Solid ordered phase (L_β)

In the solid ordered phase, the phospholipid acyl chains are fully extended (*trans* conformation) and tightly packed together, Figure 7a. Intermolecular forces increase, phospholipid movement within the bilayer is reduced and the bilayer thickness increases. A phospholipid membrane in this phase is ordered, rigid, stable and relatively impermeable [93].

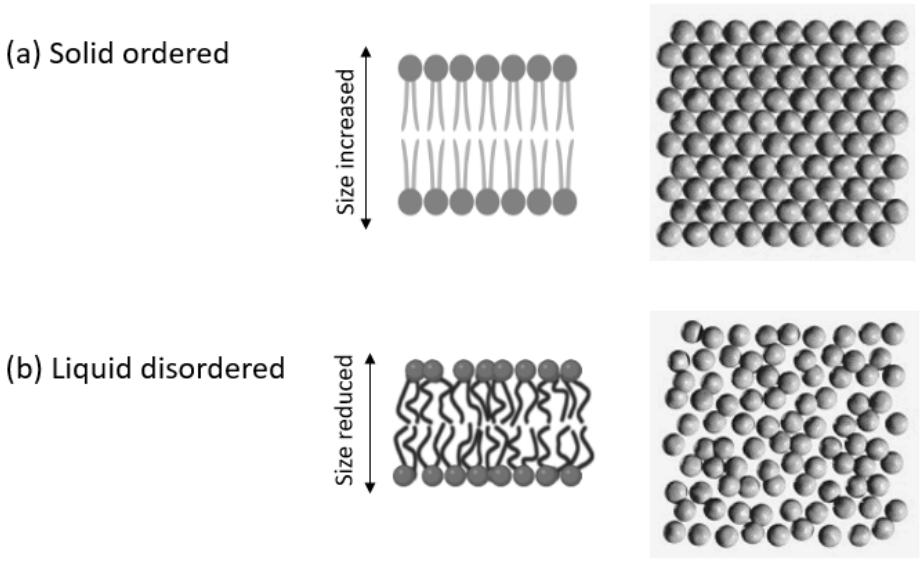

Figure 7 Structure of solid ordered and liquid disordered phases. A cross section view of bilayer is shown on the left and a top view of phospholipid head groups on the right. (**a**) Solid ordered phase shows highly ordered packing, while (**b**) liquid disordered phase shows a more irregular packing arrangement.

Liquid disordered (L_α)

In the liquid disordered phase (liquid crystalline L_α) the phospholipids are in a more fluid and randomly oriented state. The lipid acyl chains are shortened and kinked (gauche conformation). This results in each

phospholipid taking up more space and therefore the membrane becomes less densely packed, Figure 7b. Intermolecular forces and the bilayer membrane thickness are reduced. Phospholipids are not held together so tightly so the phospholipids are able to move freely within the membrane, fast bilateral and rotational phospholipid movement can occur in this phase [94]. The membrane is fluid, permeable and less stable.

Liquid ordered

The addition of cholesterol to the lamellar membrane results in the formation of an intermediate phase termed the liquid ordered phase, Figure 8. Cholesterol has the unique ability to either increase or decrease lipid order depending on the phase of the surrounding lipids. Cholesterol orients itself with its hydrophobic hydroxyl group facing the aqueous phase and its rings intercalated between the phospholipid fatty acid tails within the bilayer membrane [95]. When added to phospholipids in the solid ordered phase cholesterol disrupts the close packing and consequently reduces order. Conversely when cholesterol is added to phospholipids that are in the liquid disordered phase it increases order by straightening lipid chains and reducing their movement, leading to closer packing and an increase in the size of the bilayer. This results in the formation of an intermediate liquid disordered phase which shows rapid lipid lateral and rotation diffusion, similar to fluid disordered phase, but has packing which resembles the solid ordered phase.

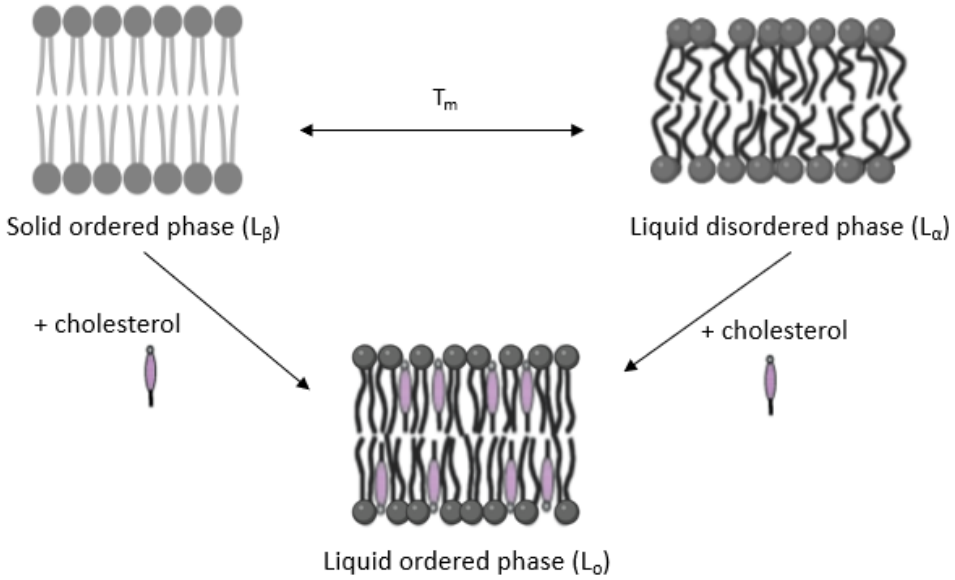

Figure 8 Lipid bilayer membrane phases. In the gel (solid ordered) phase the lipids are highly ordered and tightly packed. In the fluid (liquid disordered) phase the lipids are highly disordered, less densely packed, shortened. Membrane is thinner, more permeable and less stable in fluid phase. Addition of cholesterol increases the order of fluid phase but decreases order of gel phase, forming a liquid ordered phase. Figure adapted from [96].

The fluidity and permeability of the liposome membrane is an important consideration, particularly if a molecule/drug is to be encapsulated. If the membrane is too permeable encapsulated material will quickly leak out of the liposome. In contrast, if the liposome membrane is very rigid and impermeable (composed of phospholipids with long saturated hydrocarbon chains) release of encapsulated molecules is very slow, for example Charrois and Allen [97] showed that liposomes composed of dioleoylphosphatidylcholine (DOPC), an unsaturated phospholipid, released encapsulated drug very quickly (all released within 24 hours), while those composed of distearoylphosphatidycholine (DSPC), a saturated phospholipid, showed much slower and sustained release over seven days.

A unique feature of liposomes (and other lipid membranes) is that they have a fluid surface which allows dynamic organisation of anchored ligands, unlike other inorganic nanoparticle drug delivery systems [98]. Movement of ligands allows for optimal polyvalent binding, which can increase binding affinity [98, 99]. Membrane rigidity also effects the mechanical properties of the liposomes, rigid membrane makes the liposome less deformable, this can influence cellular uptake and penetration into the extracellular matrix [100]. Abumanhal-Masarweh et al. [101] showed that cellular uptake of liposomes was increased with increasing phospholipid acyl chain length, and the addition of cholesterol, to increase membrane rigidity, also enhanced uptake.

1.5.4 Phase transition temperature

The transition between solid ordered and liquid disordered lamellar states occurs at temperature specific to each phospholipid, called the phase transition temperature (T_m). The T_m of some commonly used phospholipids are shown in Table 2 [102, 103].

Table 2 Phase transition temperature of commonly used phospholipids for liposome preparation

Phospholipid type	**Fatty acid Length:Saturation**	**Name**	**Abbreviation**	**T_m (°C)**
Phosphatidylcholine (PC)	12:0	Dilauroyl PC	DLPC	-2
	14:0	Dimyristoyl PC	DMPC	24
	16:0	Dipalmitoyl PC	DPPC	41
	18:0	Distearoyl PC	DSPC	55
	18:1	Dioleoyl PC	DOPC	-17
	mixture	Egg PC	EPC	-15 - -5
Phosphatidylethanolamine (PE)	12:0	Dilauroyl PE	DPLE	29
	14:0	Dimyristoyl PE	DMPE	50
	16:0	Dipalmitoyl PE	DPPE	60
	18:0	Distearoyl PE	DSPE	74
	18:1	Dioleoyl PE	DOPE	-16

Above the T_m the phospholipids in are in the liquid disordered phase. Reducing the temperature below the T_m results in a transition to the solid ordered phase.

T_m is mostly affected by hydrocarbon length and saturation, but also charge and headgroup type;

- T_m increases with increasing chain length, as the hydrocarbon chain length increases van der Waals forces also increase, thus more energy is required to disrupt the ordered packing.
- Unsaturation decreases T_m, as it causes the hydrocarbon chains to kink which prevents them from packing tightly together, resulting in decreased van der Waals interaction and therefore less energy is required to disrupt the packing. Most natural phospholipids contain at least one double bond and have a low T_m as a result.
- Head group effects T_m, PC and PG with same hydrocarbon chain length have similar T_m, however PE has a higher T_m (e.g. DPPC and DPPG both have a T_m of 41°C, whereas DPPE is 63°C). This is believed to be due to stronger interactions between the PE head groups. [103].

EPC has a broad temperature transition range (T_m between minus 15°C to minus 5°C) which is well below room temperature (RT). This is because EPC is obtained from a natural source and so contains a mix of phospholipid components with a range of different fatty acid chain lengths and both saturated and unsaturated chains, Table 3. EPC has better oxidative stability than soy PC because it is composed of a greater proportion of saturated lipids [103]. Liposomes formed with EPC will be in the liquid disordered phase in the temperature ranges used in this study (4°C-37°C).

Table 3 Percentage fatty acid composition of phosphatidylcholine extracted from egg and soy

Type of Fatty Acid		Fatty Acid Composition %	
Length:saturation	Name	Egg PC	Soy PC
14:0	Myristic	0.2	
16:0	Palmitic	32.7	14.9
16:1	Palmitoleic	1.1	
18:0	Stearic	12.3	3.7
18:1	Oleic	32.0	11.4
18:2	Linolenic	17.1	63.0
18:3	γ-linolenic		5.7
20:2	Eicosadienoic	0.2	
20:3	Eicosatrienoic	0.3	
20:4	Arachidonic	2.7	
22:6	Docosahexaenoic	0.4	

1.5.5 Lateral phase separation

Different lamellar phases can co-exist together within a membrane. When more than one type of lipid is present in a bilayer membrane, the different lipids can separate into regions with distinct lipid composition, based on the physical and chemical properties of the head group and hydrocarbon tail groups [93, 104-106]. Larsen et al. [107] showed significant inhomogeneities in the composition of single liposomes from within a single population (composed of DOPC:DOPG).

The lipids may have different T_m temperatures, and therefore could be in different lamellar phases depending on temperature. Some may be solid (if temperature is below their T_m), while others may be in the liquid state (if temperature is above their T_m). Domains of tightly packed lipids (in solid phase) can form which move together laterally within a larger area of liquid disordered lipids [108-110]. The presence of cholesterol can greatly increase the formation of these domains . Examples of naturally occurring domains include lipid rafts, caveolae, coated pits, receptor and channel clusters [111]. Phase separation can affect liposome permeability due to defects in the membrane at the boundary of the two phases [112]. Liposomes therefore can show highest permeability around T_m due to the presence to two phases [98].

Lipid polymorphism can be exploited to engineer liposomes with specific behaviours. Phase changes within a liposome membrane can be used to induce liposome fusion and drug release. Liposomes can be designed to contain lipids which undergo phase transition from solid ordered to fluid disordered phases at a specific temperature, or in response to pH change. When this trigger is encountered the bilayers undergo phase transition and become more permeable leading to drug release. Imam et al. [51] showed that phase separated liposomes substantially increased liposomes to cell membrane fusion and increased intracellular delivery of lipids and model macromolecules (dextran).

Phase separation can also be used to modulate ligand density on the liposome surface, ligands can be clustered together within distinct lipid domains thereby increasing local ligand density. Increased ligand density can facilitate multivalent binding [113] and help increase binding affinity between liposomes and target cell [114]. Vu et al. showed that phase-separated liposomes with the binding ligand RGD showed 15 fold enhanced binding to Jurkat cells compared to uniform liposomes [106]. In addition, phase separation can be used to reduce steric hindrance by altering the distribution of PEG molecules (which can also be localised into distinct domains) to further enhance targeted ligand binding. Phase separation can be used to modulate the spatial presentation of both targeting and shielding molecules, and enhance the efficacy of liposome drug delivery [106].

1.5.6 Phospholipid movement within bilayer membranes

Bilayer membranes are not static, phospholipid molecules can move within and between the bilayer leaflets. This movement can be rotational, lateral, or transverse, Figure 9. If the phospholipids making up the bilayer membrane are in the solid ordered state (below their T_m) then movement of phospholipids is strongly reduced. However, if the phospholipids are in the liquid disordered state (are above their T_m) then the membrane is fluid, and the phospholipids are able to move freely.

When the membrane is in the fluid state phospholipids are to move freely in three ways;

- Rotational: phospholipids can rotate about their axis, perpendicular to the bilayer plane (this occurs very fast time scales, nanoseconds) [115].
- Lateral: phospholipids can move sideways within a bilayer leaflet, the time taken to exchange position with a neighbouring phospholipid is approximately 100 nanoseconds, (phospholipid translation diffusion coefficient is approximately 10^{-7} - 10^{-10} cm^2/s) [115] and a phospholipid molecule can travel across a typical cell in less than 30 seconds [116].
- Transverse: phospholipids can move between the inner and outer bilayer membrane (translation perpendicular to the plane of the bilayer). In a biological cell membrane transverse movement of phospholipids can occur via two mechanisms; either due to the action of lipid translocating enzymes (flippases, floppases and scramblases, in which case it happens very fast), or by spontaneous passive movement often referred to as 'flip-flop'. Passive flip-flop of phospholipid molecules between bilayers is very slow, taking place in the order of hours to days [115, 117, 118]. Flip-flop is energetically unfavourable as the polar head group of the phospholipid must pass through the hydrophobic core of the lipid bilayer.

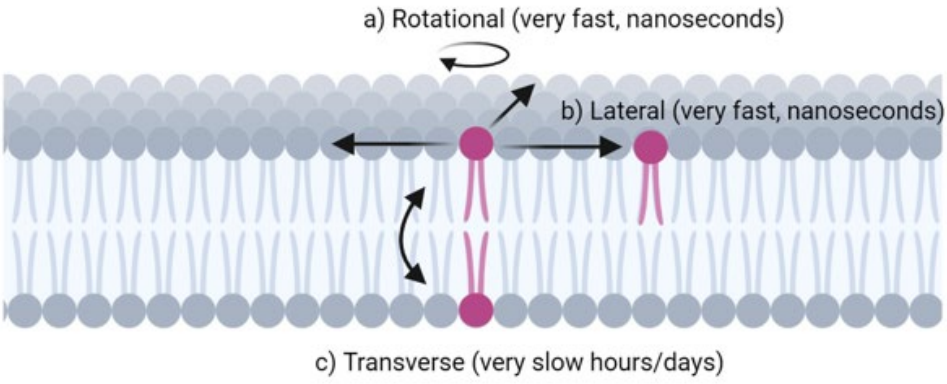

Figure 9 Possible phospholipid movement within the liposome bilayer membrane. Phospholipid movement can move be (**a**) rotational (rotate about their axis), (**b)** lateral (move sideways within the bilayer leaflet), or (**c**) transverse (move between the inner and outer bilayer leaflets) [58].

In artificial membranes, such as liposomes, which do not contain flip-flop enzymes, transverse movement between leaflets can only occur by the passive flip-flop mechanism, and therefore occurs slowly. For example in a phosphatidylcholine based liposome movement between lipid bilayers usually occurs over a timescale of days [119]. Flip-flop rate is affected by lipid chain length (longer chains impede flip-flop), membrane packing (flip-flop reduced in gel state), head group (charged non-polar head group reduce transverse movement), presence of cholesterol (decreases flip-flop above T_m by reducing membrane fluidity) and environmental factors such as temperature. Packing defects in the bilayer membrane are also known to increase flip-flop, for instance at the border of two phases liquid ordered and liquid disordered phases. Some lipids, such as cholesterol, have a high rate of spontaneous flip-flop (<1 second) [115]. Consequently, cholesterol is usually evenly distributed between the inner and outer bilayer leaflets [96].

1.5.7 Phospholipid movement between membranes (between liposomes/cells)

Phospholipids have been shown to spontaneously elute from liposome membrane and transfer to other liposomes [120-122]. The rate of transfer is dependent on temperature, fatty acid chain length and unsaturation (transfer decreases with increased chain length and increases with increased unsaturation[120]), phase of liposome membrane (transfer is greater when membrane in fluid phase [121]), size of liposomes can impact transfer (contact area shown to be decreased with increased vesicle size, transfer is greater from smaller liposomes [72]), and vesicle concentration (due to increased rate of vesicle collision[123]). Charge can be used to increase transfer. The use of charged lipids can increase electrostatic attraction between oppositely charged membranes/vesicles which can help to increase lipid transfer [71, 72]. The speed of phospholipid transfer between neutral liposomes is reported to be quite slow, taking hours to days [72, 120], while transfer between oppositely charged vesicles can be much more rapid, occurring within minutes [124]. Transfer of phospholipid has also been shown to be independent of acceptor vesicle concentration [122]. Transfer between artificial membranes (liposomes) is also reported to occur faster than transfer from cell membranes.

The rate of dissociation and transfer is also dependent on the surrounding environment. Transfer has been shown to be relatively low when the liposomes are suspended in buffer. However when suspended in plasma increased dissociation of phospholipids from the liposome can occur [121]. This may be because after dissociating the phospholipid interacts with serum lipids and plasmas and preferentially binds to these rather than transferring to a new vesicle/membrane. Münter et al. also showed that any attached group to the phospholipid (for example a fluorescent label) can alter the rate of dissociation [121].

1.6 Surface modification of liposomes

Surface modification of liposomes can be used to help improve liposome performance characteristics and to overcome some of the barriers which inhibit their effectiveness. A wide variety of molecules may be incorporated into liposomes, Figure 10, either attached to their surface or embedded within their membrane, to achieve many purposes including;

- Alter their physical characteristics i.e. charge [125], improve stability, reduce permeability, facilitate fusion with other membranes [79]
- To prevent capture by the immune system (stealth liposomes), e.g. PEGylation [49]
- Active targeting, addition of binding ligands to facilitate binding of specific cells/tissues and/or intracellular delivery. Improved binding capacity to facilitate incorporation of drugs or bio-macromolecules into target cells
- Stimuli sensitive, to enable controlled release of cargo

The following section briefly outlines the main categories of liposomes based on their surface modifications; conventional, stealth, active targeted, stimuli sensitive, multifunctional and hybrid.

1.6.1 Conventional liposomes

Conventional liposomes (i.e. with no surface modifications) are composed of natural or synthetic phospholipids often in combination with cholesterol. Depending on the phospholipid constituents used the resulting liposomes may be neutral (no charge), anionic (negatively charged) or cationic (positively charged).

Liposome charge can be used to facilitate liposome cargo incorporation, for example positively charged liposomes facilitate binding and encapsulation of negatively charged nucleic acids, such as DNA, small interfering RNA, oligonucleotides via electrostatic interactions [126]. Charged liposomes are removed from circulation faster than neutral liposomes, however negatively charged liposome enhance cellular interactions.

A significant limitation of conventional liposomes is that they are rapidly removed from circulation by macrophages of the reticuloendothelial system (RES) particularly the spleen and liver [14, 127, 128]. They are also quickly opsonised by the adsorption of plasma proteins [129]. This opsonisation leads to increased recognition and removal by RES cells and can also directly cause liposome destruction via membrane instability and complement mediated lysis [130].

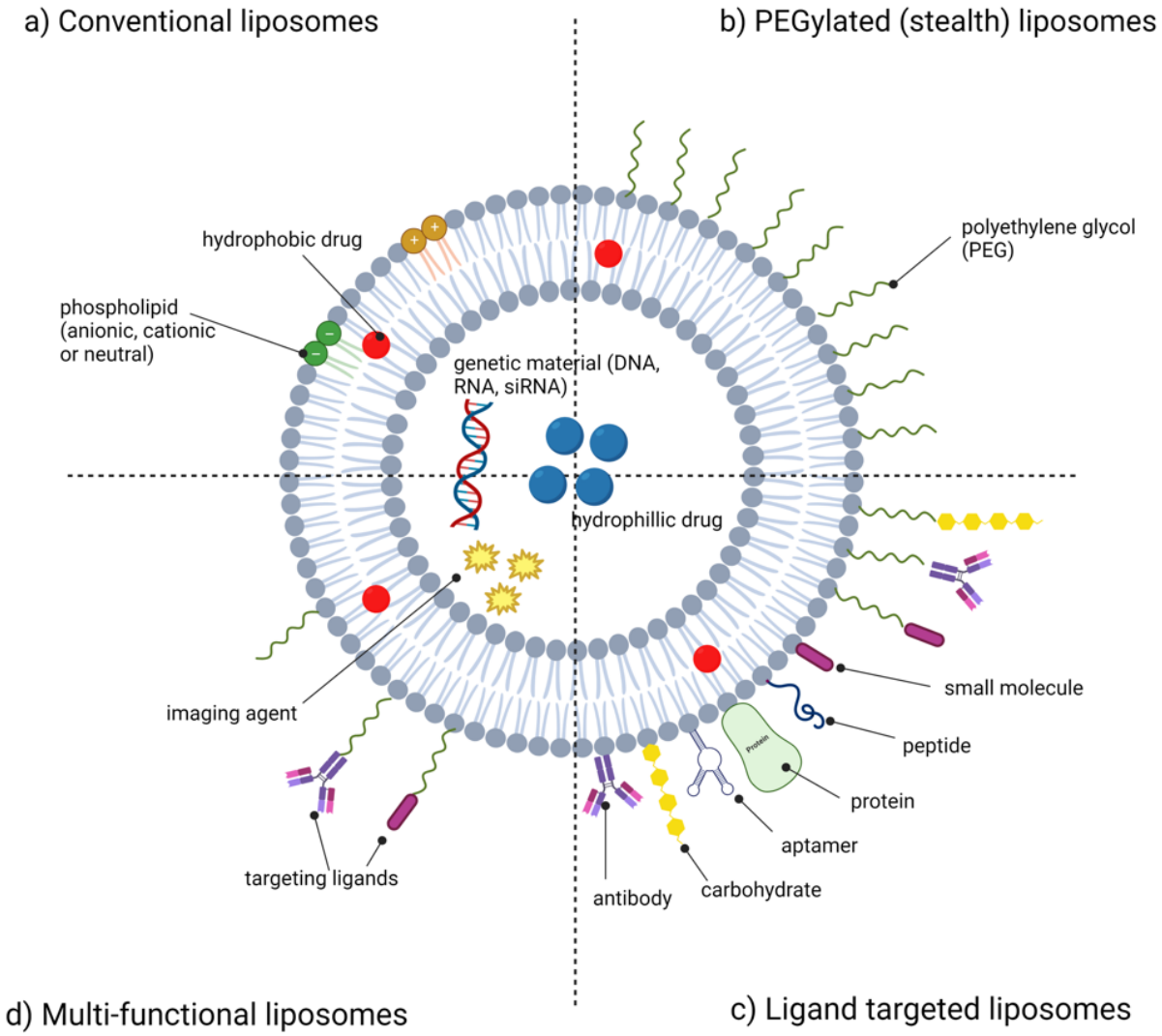

Figure 10 Surface modified liposome. Diagram showing different types of liposome surface modification; (**a**) conventional liposomes are composed of phospholipid (can be positive, negative or neutral charge) with no surface modifications, (**b**) PEGylated or stealth liposomes have PEG conjugated to their surface, (**c**) active targeted liposomes may contain a range of different ligands to promote binding and endocytosis at specific tissue, and (**d**) multifunctional liposomes which have more than one type of functionising molecule. Adapted from [58, 129, 131].

1.6.2 Long circulating 'stealth' liposomes

For liposomes to be used successfully as a drug delivery system, their rapid removal from circulation must be reduced. Currently the predominant method to achieve this is the addition of a protective coating of hydrophilic polymer chains to the surface of the liposome, the resulting long circulating liposomes are called 'stealth' liposomes. The most commonly used coating is polyethylene glycol (PEG), which has been shown to increase liposome circulation in humans from minutes to several hours [48, 127, 132].

Initial studies to create stealth liposomes via surface modification investigated the use of various types of coatings, such as monosialoganglioside, hydrated phosphatidylinositol, and other hydrophilic polymers such as PEG [49]. PEG was quickly found to be effective, economical, and relatively easy to chemically modify/conjugate, and so was quickly adopted as the primary method to allow liposomes to evade removal from circulation [48, 133]. Surface coating with PEG, termed PEGylation, decreases opsonisation of liposomes through a steric barrier hindrance mechanism, which reduces (but does not entirely prevent) liposome interaction with plasma proteins [134, 135].

PEGylation is currently the gold standard for creating long circulating 'stealth' liposomes [136]. However there are concerns regarding the toxicity and immunogenicity of PEG; PEG is non-biodegradable and long term toxicity of PEG is unknown [137]. Repeated administration can lead to accumulation of PEGylated liposomes in extremities and the development of hand-foot syndrome (palmer-plantar erythrodysesthesia) a dose limiting adverse reaction which can be mild to severe and lead to discontinuation of treatment [138]. PEG is immunogenic and can stimulate formation of anti-PEG antibodies, leading to hypersensitivity reactions and rapid clearance of liposomes on repeat administration [137]. In addition, it has been found that up to 25% of a blood donor population had anti-PEG antibodies with no known prior exposure to PEG [139-141]. Due to the drawbacks associated with the use of PEG, alternative methods to create stealth liposomes are desirable. Some proposed alternatives include use of 'self' marking peptides i.e. CD47 to prevent recognition by RES [142], or the use of other synthetic polymers such as chitosan[143, 144], pectin, polyglycerols, polyoxazolines, poly-vinylpyrrolidone, poly-acrylamide, or natural polymers such as heparin or carbohydrates [145]. To date PEG is the only stealth coating used *in vivo*.

A significant drawback/limitation of 'stealth' surface coating on liposomes is that it can reduce the effectiveness of any binding ligands attached to the surface of the liposome by preventing their interaction with target cells. PEG reduces membrane interactions by steric hinderance and can inhibit cell binding and intracellular delivery [48] One strategy to overcome this is attaching the binding ligand to the distal end of the PEG molecules [146]. However PEG polymers do not maintain a linear conformation *in vivo*, instead they fold into a globular structure and the attached ligand may be buried within the PEG structure [133]. The presence of PEG on surface of liposomes can also hinder hydrophilic drug encapsulation and impede the release of encapsulated materials [147].

1.6.3 Targeted liposomes

Following the development of stealth liposomes, which were capable of extended *in vivo* circulation, strategies to alter liposome biodistribution and facilitate their delivery to specific cells and tissues have been widely investigated. Liposome delivery to target tissue can be achieved by passive or active

targeting. Passive targeting occurs due to the enhanced permeability and retention effect (EPR), see below, which is most relevant for oncology applications [148]. Active targeting involves the addition of specific binding ligands to the surface of liposomes to facilitate binding to target cells. Although highly sought after, and despite being widely investigated and many successful preclinical trials, active targeted delivery has not yet been realised for a clinical liposomal product.

Passive targeting - EPR effect

Liposomes passively accumulate in neoplastic and inflamed tissue due to the enhanced permeability and retention (EPR) effect [149]. Tumour tissue, and inflamed tissue, develop leaky blood vessels which have enlarged inter endothelial gaps that allow particles up to 200 nm in size to pass through [133]. These leaky vessels allow nanoparticles to move through the large endothelial gaps and accumulate in the surrounding tissues. In addition, lymphatic drainage from tumour tissue is impaired. Thus, once the liposomes move into the tumour tissue via the leaky vasculature they remain there and accumulate, Figure 11.

There are some limitations to the effectiveness of EPR effect; tumour vasculature is not distributed homogenously throughout the tumour, so there can be regions within the tumour with very limited blood flow. In addition high interstitial pressure within the tumour tissue can make it difficult for liposomes to diffuse deep within tumours [150].

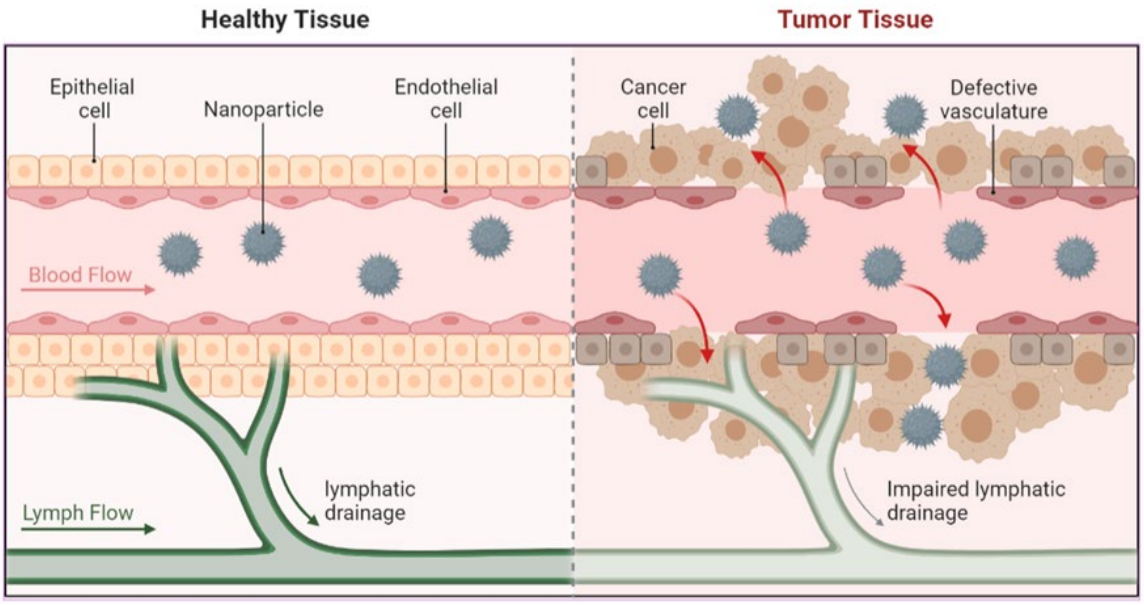

Figure 11 Passive targeting of nanoparticles by the EPR effect. Nanoparticles pass through the enlarged inter-endothelial gaps found in tumour blood vessels. Once in the tumour tissue they accumulate due to reduced removal caused by impaired lymphatic drainage. Image adapted from [151].

Active targeting - Types of ligands

Active targeting is the surface modification of liposomes with specific ligands to promote liposome binding and endocytosis at target tissues to further improve the delivery of encapsulated materials to a specific target [152]. A variety of bioactive molecules can be attached to the surface of liposomes to achieve wide range of functions, include binding to specific target cells, membrane fusion and intracellular delivery, gene therapy, enzyme activity. Example ligands include antibodies or antibody fragments [153, 154], aptamers [155], peptides and proteins [156], carbohydrates [157, 158], nucleic acids [159], and small molecules capable of being recognised by specific cell surface receptors e.g. vitamins such as folic acid [160]). The target receptor/antigen should be either selectively expressed or over expressed on the target tissues (to reduce off-target side effects). Ideally binding should also promote internalisation (receptor mediated endocytosis) The binding ligands can be directly conjugated to liposome surface or may be attached to a linker molecule such as PEG (see 1.6.7 Current methods of liposome surface modification).

- Antibodies or antibody fragments are a commonly used ligand. Antibodies enable efficient and specific binding to their target antigen. Examples include anti-Her2 to target breast cancer cells [73], anti-EGFR to target hepatocellular carcinoma cells [161]. However they are large molecules which can be immunogenic, resulting in hypersensitivity reactions and faster removal from circulation [162]. Conjugation can be problematic as antibody binding requires correct orientation/presentation to be effective. Conjugation can alter the antigen binding region resulting in reduced binding capabilities.
- Aptamers. Aptamers are single stranded short DNA and RNA oligonucleotides that selectively bind a single target [163]. Aptamer binding can trigger receptor mediated endocytosis[164]. Aptamers are small, stable, biocompatible and show low immunogenicity [163]. Their synthesis is relatively cheap and simple, and because they are chemically synthesised there is no need for the use of animals or cell culture.
- Peptide, proteins, enzymes. Peptides can all be used as binding ligand on liposome surface. Peptide targets can be divided into three categories: G-protein-coupled receptors , growth factor receptors (GFRs) and integrin receptors ($\alpha_v\beta_3$) [165]. A commonly used peptide target is the epidermal growth factor receptor (EGFR/HER) which can be overexpressed on different subclasses of cancer including breast and lung cancer, for example EGFR targeted peptide ligand D4 conjugated to PEG and added to liposomes used to target HER2 positive breast cancer [166]. Cell penetrating peptides can be used to enable which enhance internalisation without the use of receptors [167].

  Enzymes can also be incorporated into liposomes. They can be encapsulated within the internal aqueous space, incorporated within the lipid bilayers or attached to the liposome outer surface

[168]. Encapsulation of enzymes within liposomes can help to protect the enzymes from degradation and also to target their activity to desired sites [169].

- Vitamins. Many cancer cells over-express vitamin receptors, vitamins can be conjugated to liposome surface to facilitate binding to these receptors. Folate is the most used, however other vitamins such as tocopherol, pyridoxal phosphate and pyridoxine have also been investigated [47, 170, 171].
- Carbohydrates and carbohydrate-binding proteins. Various types of glycan, e.g. mannose, maltose, and lectin molecules e.g. tomato lectin, wheat germ agglutinin have also been added to surface of liposomes for a range of purposes including targeted binding to tumour cells, targeted binding to immune cells to modify immune reactions, cell membrane binding [47, 172, 173].

Challenges

Despite considerable success *in vitro* active targeting has not yet led to the successful development of a product for clinical use. Active targeted liposomes have shown only small improvement in human clinical trials. Possible reasons for this include:

- heterogeneity of target receptor expression between cancer types, between people, and expression can change as disease progresses [133].
- conjugation of the binding ligand to the liposome may impair drug release from the liposome. It may also increase opsonisation and clearance by the immune system.
- conjugation of antibody/peptides to liposome surface can alter the structure of the conjugate which impedes their binding [152].
- the presence of PEG on liposome surface (for stealth purposes) can inhibit ligand binding activity.
- methods to produce ligand targeted liposomes can be time consuming and difficult to control [73], resulting in ligand orientation which may not be optimal for binding, and heterogeneity between liposomes (both between and within batches) which reduces their reproducibility [174].
- rapid high affinity binding between liposome and target receptor can prevent diffusion of liposomes further into tumour tissues.

1.6.4 Stimuli sensitive liposomes

The addition of stealth properties and active binding ligands can help to increase liposome circulation times and their accumulation at target sites. However the liposomes' therapeutic efficacy can remain low due to slow drug release and/or poor cell penetration [175]. Ideally liposomes should retain their cargo while in circulation and release it only when they reach the target site. Strategies have been developed which utilise a physical or chemical stimulus to trigger liposome destabilisation enabling release of cargo and/or membrane fusion at the target site. Stimuli can be internal or external, internal stimuli exploit changes in the microenvironment associated with pathological conditions, such as pH changes, altered enzyme expression and oxygen concentrations [52]. External triggers use an external stimulus such as heat, light, or electromagnetic field [176];

- pH – by incorporating pH sensitive lipids and polymers into the liposome (which change formation dependent on pH leading to destabilisation of the liposome membrane and cargo release) liposomes can be designed which are stable at physiological pH (7.4) and undergo destabilisation and release of cargo at low pH. pH sensitive liposomes may be designed to release their cargo due to acidic changes associated with tumour tissue or following endocytosis to enable release from the endosome [177].
- Redox sensitive – redox gradients between intracellular and extracellular environments can be exploited to enable release of cargo intracellularly [178].
- Temperature sensitive – thermosensitive liposomes respond to heat, such as microwave, radio frequency, or infrared laser. Examples of thermosensitive molecules include gold nanorods, lysolipids, peptides [33].
- Enzyme sensitive – enzymes are often overexpressed by neoplastic and diseased cells. Engineered lipid conjugates can be included in the liposome which can be cleaved by enzyme activity. Cleavage results in either the release of an active component/drug from the lipid-conjugate or the cleavage causes destabilisation of the liposome membrane leading to cargo release from the liposome [179].
- Light responsive, photochromic moieties used to cause membrane destabilisation on exposure to light (photoisomerization, photocleavage) [180], or light activation can cause formation of reactive oxygen radicals which causes local damage e.g. Visudyne for treatment macular degeneration [181].

By using a combination of functionalising structures, liposomes may be engineered to avoid removal by the immune system (stealth liposomes), to release their cargo in sustained or triggered manner (stimuli sensitive liposomes) at the desired site (active targeting).

1.6.5 Multifunctional

By employing a combination of functional structures, liposomes properties can be carefully tuned to improve their overall efficacy. Liposomes can be engineered to avoid removal by the immune system (stealth liposomes) and to release their cargo at a specific location (active targeting) in a controlled manner (stimuli sensitive liposomes).

In addition, combinations of drugs and/or different types of therapeutic molecules can be co-delivered within a single liposome formulation. Co-delivery of multiple drugs can help decrease development of drug resistance and help improve the efficacy of the drugs. The drugs can be combined and delivered in a specific optimised molar ratio. A recent example of this is the liposome formulation Vyxeos which contains the optimal molar ratio of cytarabine:daunorubicin 5:1 for the treatment of AML [34]. It is difficult to achieve this ratio of drugs in the tissues via conventional administration methods. This formulation improves efficacy and enables administration of lower cumulative doses compared to free drug [182].

Additionally different types of functional molecules can be used in combination to improve the liposome performance. For example addition of cell penetrating peptide to liposomes surface which contains encapsulated siRNA significantly increased uptake and endosomal escape and increased efficacy of gene silencing [183]. Or the combination of an imaging agent and an oncotherapy drug within a single treatment could be useful for the ability to monitor treatment in real time [184]. Curcio et al. prepared multifunctional liposomes which had CD44 receptors for active targeting and both pH and redox stimuli responsive properties for controlled drug delivery and were loaded with doxorubicin hydrochloride for treatment of breast cancer [177].

By varying liposome phospholipid make up, surface modifications and type of encapsulated material the potential scope of liposome formulations and applications is vast.

1.6.6 Hybrid liposomes

Recently fusion of liposomes with natural cell membranes has attracted increasing interest [185]. Liposomes can be fused with membranes derived from natural cells e.g. RBC or extracellular vesicles (EV) [186]. The hybrid liposomes can combine easy surface modification, stimuli sensitive, and enhanced drug encapsulation characteristics of liposomes with immune evasion and cell targeting abilities of natural cells and exosomes [187].

Incorporating the natural membrane in the liposome helps the hybrid-liposomes to escape immune recognition and removal, natural membranes express 'self' antigens such as CD47 which prevent their phagocytosis. This enables stealth properties without the need for PEGylation. The natural membrane can also facilitate binding to target cells, EV have been shown to accumulate preferentially in their parent cells [188, 189].

1.6.7 Current methods of liposome surface modification

The surface modification of liposomes can be carried out in three ways;

- direct conjugation to a lipid component of the liposome
- conjugation via a lipid-spacer molecule
- non-covalent mechanisms.

Direct conjugation

A common method is to conjugate the functional molecule to a lipid component of the liposome, such as a phospholipid (DSPE,DOPE), cholesterol or even a single chain fatty acid such as stearate. The conjugation reaction can take place after liposomes have been formed, so the ligand is added to the surface of premade liposomes. Conjugation to premade liposomes can alter the size, shape, and charge of liposomes and impact their stability. Conjugation reactions to modify preformed liposomes include amine, carboxylic acid, thiol, maleimide, and click chemistry [190].

Alternatively, the conjugation between lipid anchor and ligand/functional molecule can be carried out before liposome synthesis. An advantage of this method is that the ligand-lipid conjugate can be fully characterised before addition to liposomes. The conjugated lipid is added with other liposome ingredients during liposome synthesis (lipid mix method), or it can be inserted into liposomes after they have been formed (post synthesis method).

A wide range of natural and synthetic phospholipids are available to prepare liposomes, however not all of them are suitable for chemical conjugation reactions. Due to its amine group phosphatidylethanolamine is widely used and can be used to conjugate to other molecules via a nucleophilic substitution and addition and/or substitution to carboxyl or carbonyl related groups. These methods have the advantage that water is used as solvent, so can be used to conjugate many biomolecules i.e., proteins.

Limitations of direct conjugation include that the conjugated molecule is located very close to the liposome surface which can impede its interaction with other cells/tissues, in addition the presence of large polymers also present on the liposome surface, such as PEG, can shield the molecule and prevent interaction with other cells/molecules. The orientation of the ligand may not be optimal and conjugation can alter the binding regions, leading to impaired binding capacity [190]. Binding reactions can be complex and require specialised equipment and expertise and it can be difficult to achieve efficient and reproducible conjugation.

Conjugation via a spacer/linker molecule

To avoid some of the limitations associated with directly conjugating the ligand to the liposome surface the ligand can be attached via a linker molecule. The ligand is conjugated to one end of a spacer/linker molecule which is attached to the lipid anchor. An advantage of using a spacer/linker molecule is that it enables an increased number of conjugation reaction types to be utilised and hence increases the number of molecules which can be conjugated [191]. The spacer/linker molecule also enables the presentation of the ligand/functional molecule away from liposome surface. This helps to prevent inhibition of reaction by any stealth coating if present and improve antigen presentation/binding with other cells/biological systems [191]. The linker can also increase the types of chemical reactions which can be utilised and increase the molecules which can be conjugated.

A commonly used linker molecule is PEG [191]. A limitation of PEG (when used for presentation of a targeted ligand) is that the PEG molecule is not rigid and can adopt folded configurations [49]. The ligand could become hidden within the folded PEG inhibiting its ability to interact with its target receptors.

Conjugation to a spacer molecule is the method used with FSL constructs, other researchers have also used similar strategy employing a range of different linker molecules [191-194].

Addition of premade conjugate to liposomes

The functional molecule (bound to a lipid anchor, with or without a linker) can be pre-formed prior to addition to liposomes. Advantages of preparing the ligand conjugate before addition to liposomes is that it allows for full characterisation of the targeted lipid prior to use. It also enables good control of the amount of targeting ligand included in liposomes. The pre-made conjugate can be added to liposomes in two ways, it can be added with other lipid ingredients during liposome synthesis, or it can be added after synthesis to pre-made liposomes.

Lipid mix method: The premade conjugate can be added during liposome synthesis by mixing with other lipid ingredients. Limitations of this method include;

- the ligand is expressed on both internal and external membranes, this can reduce density on exterior membrane which can reduce binding capacity, may also be waster of resource.
- the conjugated ligand can occupy a large volume within the liposome interior which can reduce encapsulation capability of liposomes [190] and decrease liposome stability [195], (particularly if ligand is attached to a PEG linker).
- depending on method of liposome synthesis it can expose the molecules to solvents (which may adversely affect proteins and other labile molecules).
- presence of PEG on exterior of liposome can compromise the loading capacity of hydrophilic molecules into the liposomes, therefore advantageous to add PEG-ligand conjugate after drug loading [196].

Post synthesis method: Alternatively, the ligand-lipid conjugate can be added to liposomes after they have been synthesised. The ligand-lipid molecules incorporate into the liposomes due to hydrophobic forces [197, 198]. (Many types of hydrophobic molecules, such as proteins/hydrophobic dyes can also be incorporated into liposomes via hydrophobic effect). This post insertion into pre formed liposomes is dependent on temperature, time and concentration, and membrane packing of liposome [174, 199]. Advantages of this method include its ease of use and that it avoids exposing labile molecules to solvents/harsh conditions during liposome synthesis.

Limitations include that not all the ligand-lipid conjugate may incorporate into the liposomes, and incorporation may be uneven between liposomes [174]. This can cause less consistent and replicable therapeutic effects.

A major limitation of ligand conjugated liposomes is the increased expense associated with their synthesis. In addition, it is difficult to measure and quantify ligand density on liposomes surface, it is also difficult to determine the quality of attachment (if ligand is correctly orientated, etc). This can lead to variation between liposomes and between batches, resulting in less precise and reproducible results [174].

Non-covalent binding

Bioactive molecules can also be attached to liposomes via non-covalent mechanisms. Examples include;

- electrostatic adsorption, e.g. DNA/RNA binds to positively charged liposome membrane forming a stable complex [26], positively charged chitosan binds to negatively charged liposomes [143].

- Ionic interactions by chelation, e.g. NTA-nickel-His-tag chelation can be used to bind ligand to liposomes [22].
- Biotin-streptavidin interactions can also be used, e.g. the targeted ligand is labelled with streptavidin, which then facilitates binding via a biotin-lipid anchored in the liposome membrane [22].
- Lipid anchor integration, ligands linked to a lipid anchor can be inserted into liposomes, this is a commonly used method as it easy to perform and insertion is stable [22]. The lipid anchor integrates into liposome due to hydrophobic forces.

A benefit of non-covalent binding is easier formulation, however drawbacks include potential loss of coating *in vivo*, reduced stability [200].

Biological modification

Recently fusion of liposomes with cell membranes has attracted increasing interest. Liposomes can be fused with membranes derived from natural cells or extracellular vesicles (EV) [186]. Incorporation of a natural membrane can help the liposome evade removal by the immune (the natural membrane express CD47 which protects from phagocytosis). Cancer derived EV have been shown to accumulate preferentially in their parent cancer cells, so combining them with liposome can help targeted binding of liposome-EV hybrid with tumour tissue [188].

1.7 Liposome and cell interaction

Liposomes may interact with cells via four mechanisms; adsorption, endocytosis, fusion and lipid exchange, Figure 12 [201]. Interaction between cells and liposome can be a combination of these interactions. Determining exactly which mechanisms are involved can be difficult, especially as multiple pathways of uptake may be occurring simultaneously under given circumstances. These interactions are dependent on the type of cell, the characteristics of the liposomes (including size, charge, shape, composition, and any surface modifications), and environmental factors such as the presence of serum (lipids and proteins) and temperature.

Understanding the possible interactions between liposomes and cell helps to predict the behaviour of liposomes, including cellular uptake and intracellular distribution, both *in vitro* and *in vivo*. This information is critical for the development of clinical liposome products as it can be used to help design liposomes with maximum delivery efficiency and improved biocompatibility (reduced off target effects).

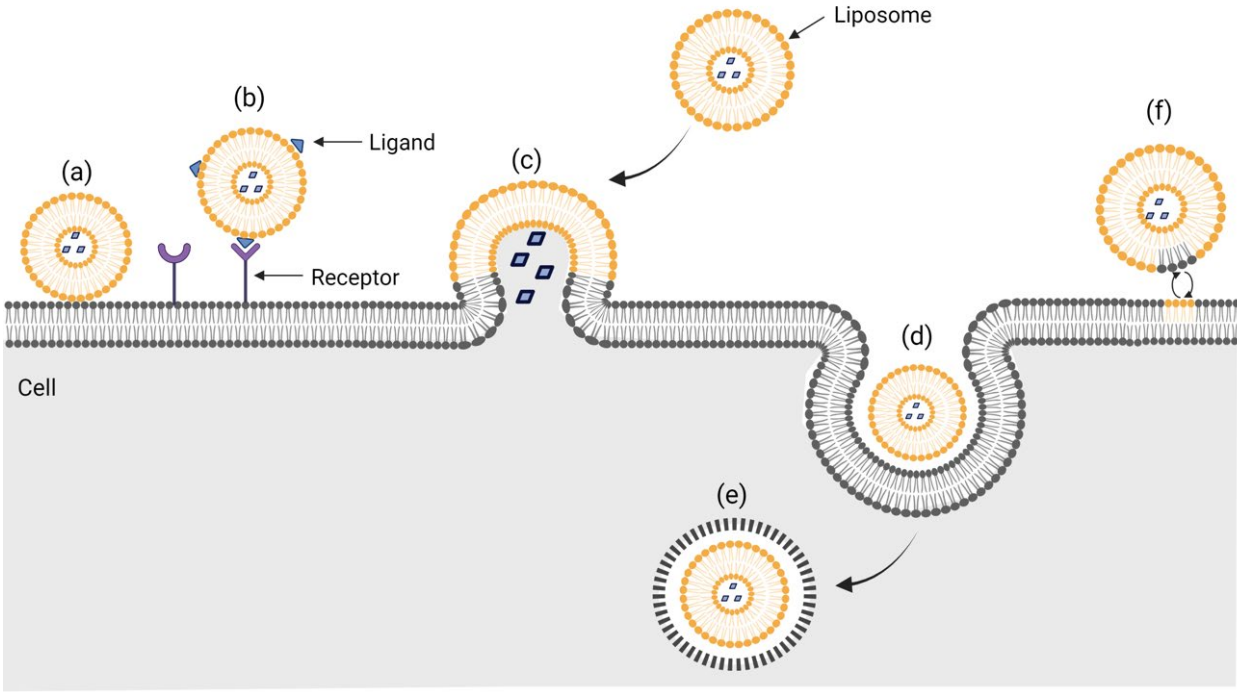

Figure 12 Possible mechanisms of liposome – cell interactions. (**a, b**) Adsoprtion; liposomes are associated with the cell membrane or glycocalyx (glycocalyx not shown, see Figure 20) but are not incorporated into the cell membrane. Adsorption can be (**a**) non-specific (due to elecrostatic, van der Waals and hydrophobic forces) or (**b**) specific (meidated via binding between a ligand and receoptor). (**c**) Fusion; liposome merges with cell plasma membrane, (**d**) endocytosis; uptake of the liposome into an endocytic vesicle (**e**), and (**f**) lipid exchange; transfer of lipids between liposome and cell plasma membrane. Created with BioRender.com.

1.7.1 Adsorption

Adsorption occurs when liposomes become stably associated with the cell surface or glycocalyx without becoming incorporated into the cell membrane or internalised within the cell [202, 203]. This type of association may be specific or non-specific. Non-specific adsorption occurs due to electrostatic, van der Waals, and hydrophobic forces. Liposomes may be loosely adsorbed to the cell membrane, in which case they can be removed by washing, or may be tightly adsorbed to the cell surface. Following adsorption lipid exchange and/or fusion may occur, but usually the liposome remains intact and there is no transfer of the aqueous content.

Specific adsorption occurs when ligands on the liposome membrane bind to specific receptors on cell surface, e.g., antibodies, transferrin etc. Liposomes adhered to cell surface may release their content, leading to high local concentrations near the cell surface, which can then be taken up by the cell either by passive diffusion or active transport.

1.7.2 Endocytosis

Liposomes can be taken up into cells by endocytosis. The intact liposome is engulfed by the cell membrane into an endocytic vesicle [202]. The liposome is then usually delivered to lysosomes for degradation, but in some cases liposome content may escape into the cytoplasm. Endocytosis can be divided into two major uptake pathways – phagocytosis (immune regulated uptake of large particles) and pinocytosis (uptake of fluid with solutes and small molecules <500nm) Figure 13.

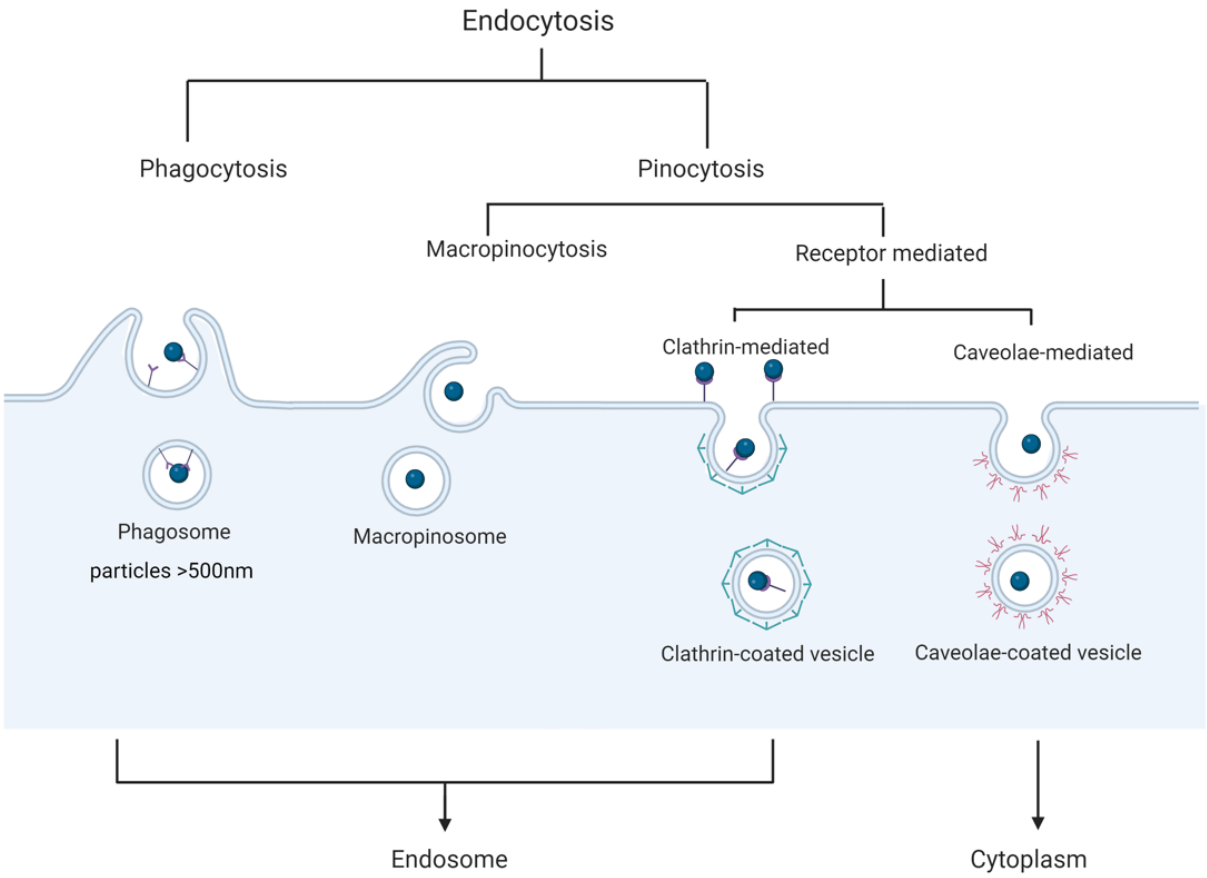

Figure 13 Endocytosis pathways. Particles can be taken up by phatocytosis and pinoctyosis mechanisms. Pinocytosis can be receptor independent (macropinoctyosis) or receptor mediated (clathrin and caveolin mediated). Adapted from [204].

Phagocytosis

Phagocytosis, Figure 13, is usually involved in the removal of large particles, in the size range 200-1500nm, such as pathogens (bacteria and yeast), or large debris/remnants of dead cells, etc. It is carried out by specialised phagocytic cells, such as macrophages, monocytes, and neutrophils, and is an important part of the immune response. This pathway is triggered by the adsorption of opsonin's such as complement or antibody onto the surface of the particle (i.e. liposome) which then bind to receptors on the phagocyte. The phagocytic cell engulfs the particle into an internal compartment (endosome), which then fuses with a lysosome, resulting in degradation of the contents. Liposomes which have not been coated with a

stealth coating such as PEG are rapidly removed from circulation via phagocytosis by macrophages of the liver and spleen [14].

Pinocytosis

The mechanism involves the uptake of small molecules and fluid from the surrounding environment, Figure 13. It occurs in most cells and is essential for nutrient uptake. It can occur by both specific (mediated by specific receptor-ligand binding process) and non-specific processes.

Receptor mediated

Receptor mediated pinocytosis, Figure 13, is a process by which cells take up specific molecules such as hormones, growth factors and other essential nutrients by specific binding to receptors on the cell surface. Receptor mediated pinocytosis can occur by clathrin or caveolin mediated pathways [205]. Receptor mediated endocytosis can be exploited to enable the internalisation of liposomes into target cells to facilitate intracellular delivery of liposomes cargo [205].

Macropinocytosis (receptor independent)

This is a non-specific uptake mechanism, Figure 13. The cell plasma membrane invaginates and engulfs extracellular fluid and any molecules within it. This pocket is internalised to form an intracellular vesicle, which then fuses with a lysosome, resulting in degradation of the contents. Very small particles <50nm can be taken up by this mechanism.

1.7.3 Fusion

Fusion occurs when the liposome phospholipid bilayer membrane merges with a cell plasma membrane, Figure 14. This does not happen spontaneously, the liposome and cell membranes need to come into close proximity followed by membrane destabilisation [206]. Liposome fusion can be induced by the inclusion of fusogenic lipids e.g. PE, and the introduction of divalent cations e.g. Ca^{2+}. The addition of binding ligands and membrane disrupting peptides can also help facilitate fusion.

During fusion liposome phospholipids integrate into cell membrane and can then rapidly diffuse within membrane [207]. Hydrophilic content from the aqueous core of liposome may be released directly into the cytoplasm of the cell or may escape into the extracellular space.

Lipids and their polymorphic behaviour are believed to play a role in membrane fusion, the formation of non-lamellar phases is closely associated with membrane fusion [90]. Factors which induce the hexagonal phase in lipid dispersions have been shown to also induce fusion of liposomes [91]. Fusion between

bilayers can be induced by the inclusion of hexagonal II forming lipids, e.g. PA, PS, unsaturated PE, plus the addition of Ca^{2+} or dehydration (to help force membranes into close proximity).

1.7.4 Lipid transfer

Lipids and/or other membrane constituents may be transferred between a cell membrane and a liposome membrane. During this process the liposomes can remain intact and content may not be released [202]. The transfer of lipids occurs only between outer membrane leaflets [208, 209]. Two mechanisms have been proposed for the spontaneous transfer of lipids between membranes: transfer of lipid during a transient membrane collision and/or lipid monomer diffusion between membranes [210-214]. Lipid exchange can also be mediated by lipid exchange proteins found in the cell membrane [210]. Transfer between liposomes has been shown to occur much faster than exchange rate with cell membranes [197].

(a) Membrane collision

In the membrane collision mechanism lipids are exchanged during a transient collision between two membranes (cell/liposome or liposome/liposome), Figure 14a. Lipids may transfer between the adjacent membranes via lipid translocation, or the collision could result in transient merging of the cell/liposome membranes, enabling the exchange or mixing of membrane lipids to occur [211, 215]. However this second mechanism is considered less likely as membrane merging/fusion is unlikely to be easily reversible [215].

(b) Monomer diffusion

In this mechanism lipid monomers dissociate from the (donor) membrane and diffuse through the aqueous phase to become incorporated into the second (acceptor) membrane, Figure 14b.

The rate of monomer transfer is affected by;

- lipid acyl chain length (shorter chains can transfer more easily, long chain phospholipids must overcome a significant energy barrier to dissociate from the bilayer into the aqueous phase) [211, 216].
- polarity of the lipid (increasing polarity enables easier transfer through the aqueous phase, hydrophobic molecules which have monomer solubility in water can freely diffuse between vesicles) [215].
- Membrane curvature can also effect transfer, high membrane curvature can increase rate of transfer [213].

(a) Collision

i. Lipid translocation

ii. Membrane merging

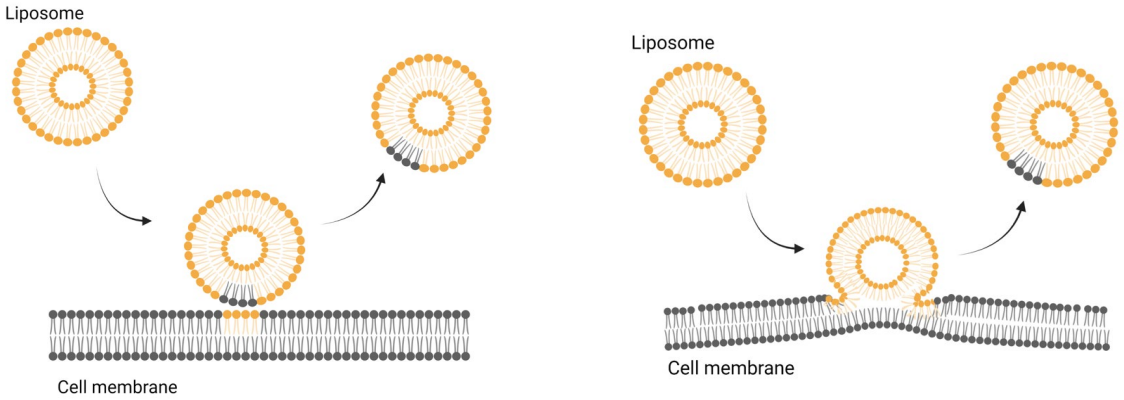

(b) Monomer diffusion

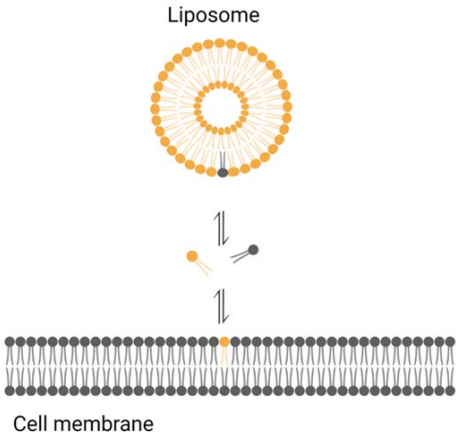

Figure 14 Transfer of lipid between membranes. following the (**a**) transient collision of two membranes, resulting in (**i)** translocation of lipid between adjacent membranes, or (**ii**) transient merging of the colliding membranes, or (**b**) transfer of lipids between membranes by monomer diffusion. Lipids may transfer between liposome and cell membranes as lipid monomers which have dissociated from the membrane and diffuse through the aqueous phase. Created with BioRender.com.

Factors which effect interaction between liposomes and cells

The interaction between cells and liposomes is dependent on the cell type, liposome morphology and composition, and environmental conditions.

- the type of cell, e.g. rapid uptake by macrophages, much slower uptake by tumour cells
- concentration
- Physical characteristics of the liposome.
    a) Size. Uptake of liposomes within the 100-1000nm range is size dependent with uptake increasing with increasing particle size [217, 218]. Very small liposomes (<10nm) are

rapidly excreted via the kidney with minimal interaction with cells. Rejman et al. [219] report that particles 50-100nm are internalised more rapidly than larger particles, and that size also plays a role in mechanism of endocytosis (particles <200nm primarily uptake via clathrin endocytosis, >200 via caveolae).

b) Charge. Charged liposomes (both positive and negative) show an increase in cell uptake, compared to neutral liposomes. Positively charged liposomes show an increased affinity for negatively charged cell membranes (via non-specific electrostatic interaction) and have the highest rate of uptake [220].

c) Liposome composition. The phospholipid composition of liposomes can influence their ability to bind and interact with cell membranes. The presence of non-bilayer forming lipids (PE and phosphatidylserine) can destabilise the liposome membrane and promote liposome-cell fusion [221, 222]. The fluidity or phase of the liposome membrane also influences uptake, uptake is significantly reduced when membrane is in the tightly packed rigid solid phase. The presence of cholesterol or saturated phospholipids increases rigidity and can decrease liposome/cell interaction [223, 224].

d) Liposome surface modification. The presence of binding ligands or stealth coatings can increase or decrease the liposome cell interactions. The addition of molecules such as antibodies or ligands (transferrin, folate) to target epitopes expressed on target cells increase uptake via specific adsorption [225, 226]. In contrast the addition of PEG or other hydrophilic polymers can be used to reduce liposome-cell interaction and consequently reduce uptake [227].

- Environmental factors

a) Temperature. The interaction between liposomes and cells is temperature and time dependent. Liposome uptake is much greater at 37°C than at 4°C [228]. In addition, temperature can affect the type of interaction that occurs, at 37°C fusion and endocytosis are more likely to occur, while at 4°C the primary processes are probably adsorption and lipid exchange [221, 228].

b) pH, presence of salts (can induce phase transition to destabilise membrane and increase uptake) [222].

c) The presence of serum lipids and proteins;

- serum lipids and proteins e.g. HDL and albumin have been shown to reduce liposome cell interaction [229].
- serum proteins can also increase cell uptake, opsonisation of liposomes with IgG and/or complement greatly increases their uptake by macrophages [221].

1.7.5 Liposomes and RBC interaction

Liposomes have been shown to interact with RBC primarily by adsorption, lipid exchange and fusion [202, 209, 216, 230]. Uptake via endocytosis is unlikely to occur as mature RBC do not carry out endocytosis [231, 232], although some studies have reported the detection of endocytosis in adult RBC [233, 234]. The interaction between liposomes and RBC is dependent on liposomes lipid composition, charge and concentration, incubation temperature and time. Increasing these parameters can increase interaction but can also increase RBC injury [224].

Cholesterol and phospholipids readily exchange between liposomes and the RBC membrane [209, 235]. RBC incubated with liposomes lose cholesterol and gain phospholipid [236]. This causes changes to RBC morphology (formation of acanthocytes, echinocytes, stomatocytes, spherocytes, size change), increases RBC osmotic fragility [237], and can eventually lead to the formation of ghost RBC (RBC which have lost their haemoglobin) and RBC haemolysis [209]. Red cell injury is dependent on liposome concentration, however at the low concentrations likely to be experienced *in vivo* the damage to RBC is minimal [224]. Inclusion of other lipids/proteins to the liposome surface can significantly increase haemolytic effect of liposome [238].

Liposomes have been shown to adsorb both loosely (removed by washing) and tightly (removed by enzyme treatment) to the RBC surface, and that liposome content was delivered to RBC cytosol indicating membrane fusion was also occurring [236]. Interaction between RBC and liposomes is enhanced by negative liposome charge, increased incubation time, higher incubation temperatures and increased liposome concentration [224]. Damage to the RBC membrane was also shown to increase with increased incubation time and temperature [236]. Holovati reported a 12% greater uptake by RBC of liposomes after 2 hours at 37°C than RT, and no uptake in same time period at 4°C [224]. Increased temperature would increase collision rate between RBC and liposomes and would also increase the fluidity of cell/liposome membranes which may create more favourable conditions for lipid transfer and/or membrane fusion to take place.

Cholesterol

Cholesterol exchanges relatively quickly between liposome and RBC membranes, reaching an equilibrium within hours [216]. Normal RBC have a cholesterol: phosphatidylcholine ratio of 0.9. When RBCs are incubated with liposomes which contain a small amount of cholesterol (ratio of cholesterol: phosphatidylcholine <0.9) cholesterol transfers from the RBC membrane to the liposome. This depletion of cholesterol from the RBC membrane increases lipid disorder and membrane fluidity, and increases the osmotic fragility of the RBC, and results in abnormal RBC morphology, usually becoming echinocytes (many small membrane projections) [235]. When liposomes contain a greater percentage of cholesterol

compared to the RBC (cholesterol: phosphatidylcholine >0.9) then cholesterol will transfer from the liposome to the RBC [202, 239]. Enrichment of cholesterol causes the RBC reduces membrane fluidity and causes changes to cell morphology [235]. However, liposomes usually contain less than 30% cholesterol (C:P ratio 0.3), so this scenario is unlikely.

Phospholipids

Phospholipids transfer between liposome and RBC [216]. This transfer occurs more slowly than cholesterol. Alterations to RBC phospholipid composition causes abnormal RBC morphology (poikilocytosis, echinocytes and acanthocytes) and eventually haemolysis. Phospholipid transfer depends on acyl chain length and saturation, phospholipids with short acyl chains and less unsaturation show much faster rates of transfer [216].

1.8 Kode technology

Kode technology is a surface engineering technology able to rapidly modify biological and non-biological surfaces using function-spacer-lipid (FSL) constructs. FSL constructs are amphiphilic molecules which are able to disperse in water and self-assemble onto biological surfaces, such as cell membranes, and non-biological surfaces such as stainless steel, nanofibers [240]. FSL constructs can be used to attach a range of bioactive functional groups onto these surfaces without the need for chemical conjugation.

Modification with these constructs is simple and is achieved by contact between an FSL dispersion and the surface/cell to be modified [56]. Modification is rapid, occurring in seconds for non-biological surfaces ([241]) or between 30-120 minutes at 37°C for biological surfaces [57, 242].

FSL have been used for a variety of applications and products, including;

- cell labelling (e.g. RBC, epithelial, endometrial, cultured cells, spermatozoa, embryos, zebra fish, viruses, bacterial viruses) [56, 243-245]
- antibody specificity mapping [246, 247]
- diagnostic assays [248, 249]
- immune system manipulation and *in vivo* neutralisation of antibodies [250]
- immunohematology quality control cells [251]
- modification of a diverse range of non-biological surfaces including stainless steel, polyester, paper [57, 240, 241].
- Inhibit toxins and cell/virus binding [252]

1.8.1 FSL constructs

FSL constructs are composed of three parts: a functional head group (F), a linker or spacer molecule (S) and a hydrophobic lipid tail (L). FSL molecules are modular, each part (lipid tail, spacer, head group) can be modified and optimised for a desired purpose.

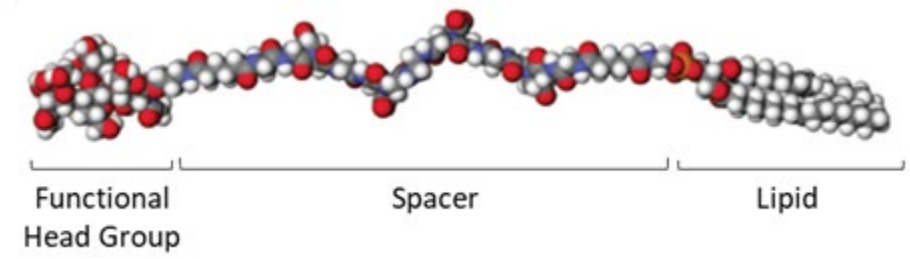

Figure 15 Schematic diagram showing the structure of a Kode FSL construct. FSL constructs consist of three parts; a functional head group, a spacer and a lipid tail [253].

Functional Head group

The functional head group is usually the bioactive component of an FSL construct. Examples include carbohydrates, peptides, proteins, antibodies, fluorophores, DNA/RNA etc. A wide range of functional head groups have already been created and characterised, Table 4.

The functional had group is used to impart a new structure and/or function to the surface being modified e.g. FSL-FLRO4 adds a fluorescent label to the modified cell/surface, FSL-biotin can be used to biotinylate a surface, FSL-A2 addition of blood group A carbohydrate.

Table 4 Type of functional head group

Functional Head Group Type	Example	Reference
Glycans	ABO, Lewis, H, P1PK, GLOV, FORS, hyaluronic acids,	[254],
Peptides	Miltenberger, Syphilis, Chagas, CMV, Sar-Cov-2	[248, 249, 255, 256]
Non glycans	Biotin, PEG_{2000}	[257]
Fluorophores	FITC, BODIPY, Atto488	[56, 244]
Radiolabels	^{125}Iodine	[245],
Antimicrobials	Selenium, Spermine	[258, 259]
Reactive groups	Maleimide, Succinimide, Click coupling	unpublished
Enzyme substrates	Sortase	unpublished
Oligonucleotides	RNA	unpublished
Antibody	Anti-IgG short chain	unpublished

Spacer

The middle section of the FSL construct is the spacer. This acts as a chemical linker between the functional head group and the lipid tail. The FSL molecules used in this project contained either an adipate or CMG(2) (carboxymethyl glycine dimers) spacer. These are the most commonly used, although other alternatives are available e.g. CMG(4), trimeric CMG (TCM) and β-DD [253].

Adipate is used as a short spacer alone and also as a conjugation linker on the ends of the CMG spacer. The adipate linker is approximately 1nm in length, while the CMG(2) spacer (composed of 2 repeating units of CMG with adipate linkers) has a length of 6.5nm in its fully extended conformation, Figure 16 [240, 253].

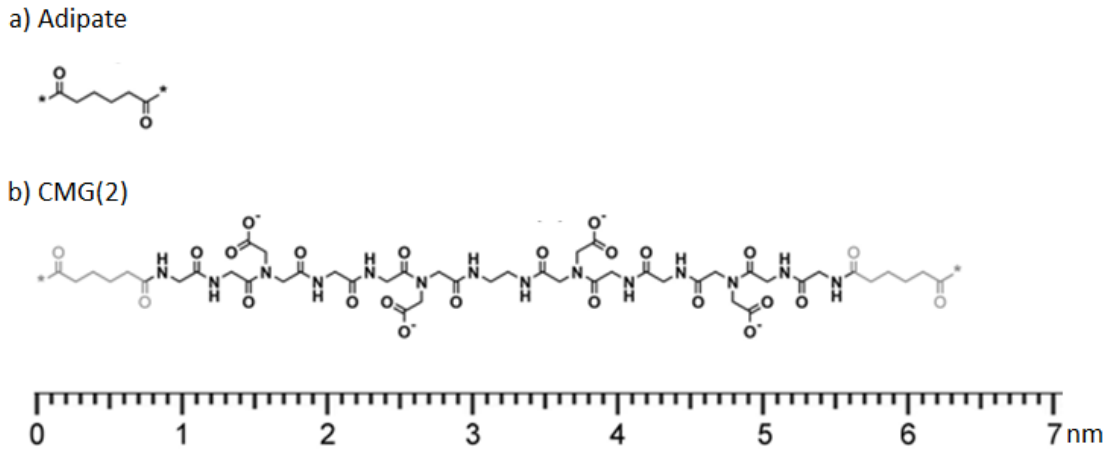

Figure 16 Chemical structures of the adipate and CMG(2) spacers used in this project [253].

The CMG spacer helps to improve the water dispersibility of the FSL constructs and improves presentation of the functional head group by spacing the functional head away from the surface. Variations in the CMG spacer structure (elongated, branched, multivalent) can be used to alter the position and orientation of the functional head group to allow optimised presentation and improve both specificity and sensitivity of reactions between head group and binding receptors [240, 253]. Figure 17 shows examples of different CMG spacer configurations.

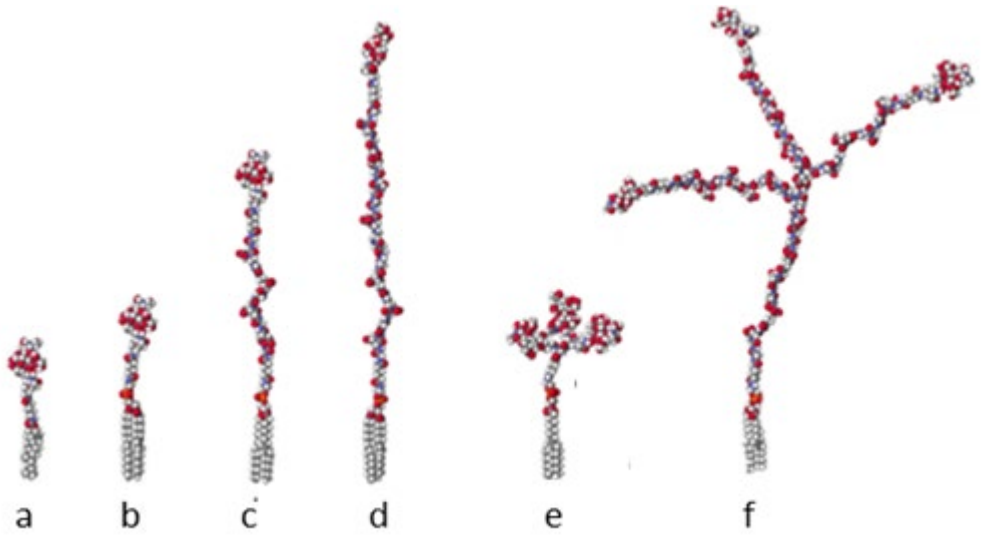

Figure 17 Schematic diagram showing different FSL spacer configurations, (a) natural glycolipid, (b) adipate spacer (c) CMG(2) spacer (d) CMG(4) (e) β-DD spacer and (f) branched TCMG spacer [253]

The spacers are designed to be biologically inert, nontoxic, and non-immunogenic, and to date no adverse reactions have been observed either *in vitro* or *in vivo* [240]. The CMG spacer has a unique 'flexible-rigid' structure, it is a relatively rigid structure however it has a high degree of flexibility about a central hinge region [253]. CMG(2) is composed of two almost identical sections which are connected by a flexible hinge region (NH-CH_2-CH_2-NH bond). The two halves are semi rigid (due to their negative charge) however the hinge region allows the two halves to rotate relatively freely. This allows the top portion (including the functional head group) to rotate and flex through a wide range of positions as shown in Figure 18. Alternative spacers, such as PEG do not offer this same flexible rigidity and can collapse to a compact conformation.

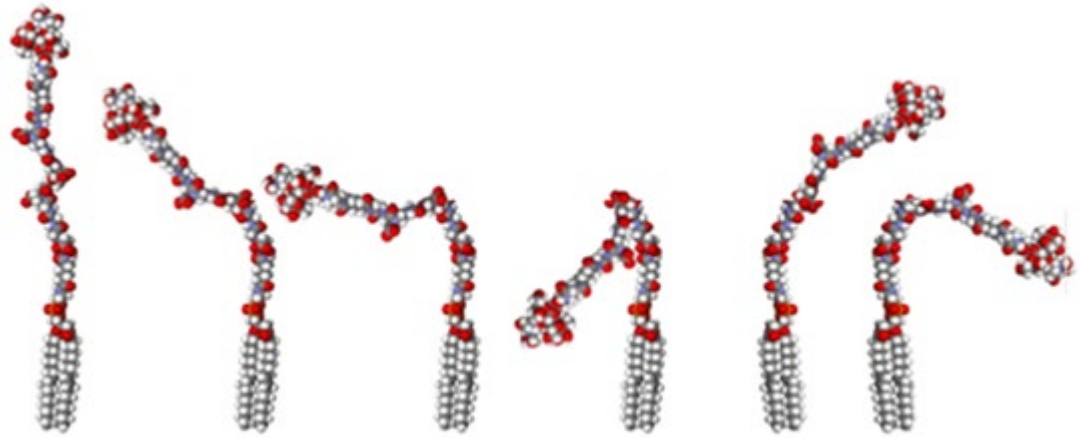

Figure 18 Examples of potential FSL construct conformations due to the flexibility of the CMG spacer. [253]

Zalygin et al. show that the majority of FSL-biotin is presented in this folded configuration and only a small number are presented in the extended upright position at any given moment [260].

Lipid Tail

The lipid tail is believed to facilitate the insertion and anchoring of the FSL constructs into biological cell membranes. A variety of lipid tails have been used, the most used being dioleoyl phosphatidylethanolamine (DOPE), cholesterol, and ceramide.

DOPE, shown in Figure 19, is the lipid tail of all three constructs used in this study. It is a phospholipid and has two unsaturated 18 carbon fatty acid chains, linked via glycerol to an ethanolamine head group. Previously it has been found that FSL constructs with ceramide and DOPE tails perform best for insertion and membrane retention of FSL constructs within biological cell membranes [240, 261].

(a)

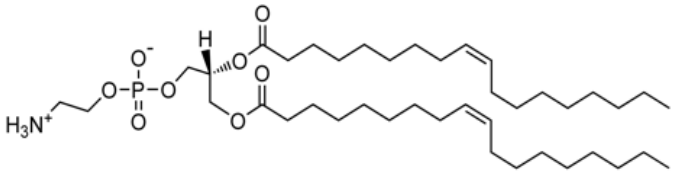

(b)

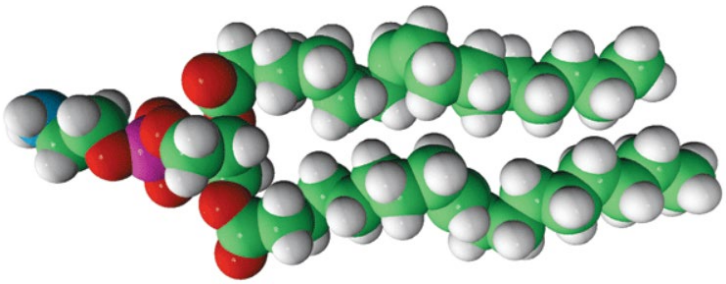

Figure 19 Structure of 1,2-dioleoyl-sn-glycero-3-phosphoethanolamine (DOPE) phopsholipid . Schematic diagram showing the (a) chemical structure and (b) space filling molecular structure of DOPE [262].

1.8.2 FSL labelling of cells

Kode technology enables rapid, simple, and non-toxic labelling of many types of surfaces, including cell membranes [56, 230]. The addition of FSL constructs to cells/viruses is non-toxic and does not appear to affect their normal function or vitality [56, 244]. The methodology to label cell membranes with FSL constructs is very simple – it is achieved by incubating together equal volumes of washed cells with the desired FSL dispersed in an appropriate buffer. It is hypothesised that the FSL constructs spontaneously insert into the cell membranes due to hydrophobic forces [56].

FSL may associate with cell membranes in several ways, Figure 20; they may insert their phospholipid tail into the cells phospholipid bilayer membrane, they may become closely associated with the membrane without integrating, i.e. via electrostatic interactions, interaction with the glycocalyx [230]. In addition, FSL constructs can label extracellular vesicles (EV) which may be present, or alternatively after binding to cell membrane cell may bud off an EV which includes the FSL construct [253].

Insertion

FSL molecules spontaneously insert non-specifically into all cell membranes [253, 261]. This spontaneous insertion is most likely driven by hydrophobic forces. Insertion is temperature dependent, occurring faster at 37°C than RT, and even slower at 4°C. The majority of insertion (around 80% of maximum) occurs within 2 hours, when incubated at 37°C [230, 242]. Insertion does not appear to be significantly affected by the size of functional head group however different FSL constructs have been shown to display slightly different insertion kinetics i.e. FSL-A2 slower insertion rate compared with FSL-FLRO4 [230]. The quantity of FSL inserted is controlled by its concentration, and more than one construct can be inserted simultaneously [254, 263].

The ability of FSL constructs to insert into cell membranes is believed to be due to their lipid tail. This spontaneous insertion is similar to the phenomenon seen with natural glycolipids, such as those of the Lewis blood group system which are known to spontaneously insert into cell membranes [264, 265]. FSL can be constructed with several types of lipid tail including cholesterol, ceramide, and phospholipid (as used in this study). The type of lipid tail can influence insertion kinetics, Slivka et al. [261] demonstrated that FSL-biotin with a cholesterol tail showed slightly improved insertion and retention characteristics compared with DOPE and ceramide tails.

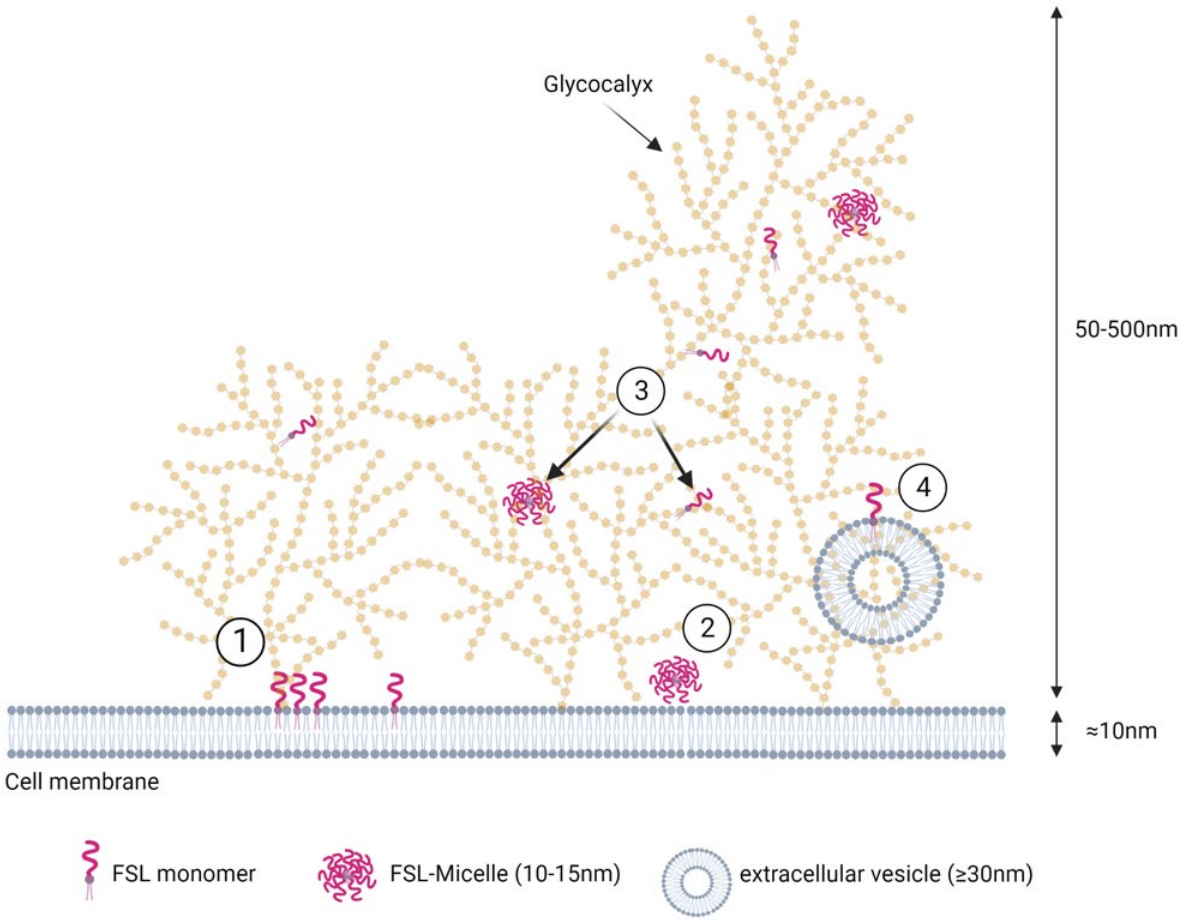

Figure 20 Different ways FSL constructs may associate with cell membranes. (**1**) They may become incorporated into the membrane by inserting their lipid tail into the membrane. (**2**) FSL micelles may adsorb or closely associate with the cell membrane but remain inatact and do not integrate into the membrane. (**3**) FSL monomers or micelles may become entrapped within the glycocalyx. (**4**) FSL constructs may label extracellular vesicles if present, or after the FSL construct has inserted into the cell membrane, the cell may bud off an EV which contains the FSL construct. It is possible that a mixture of these may occur simultaneously [58]. Not to scale. Created with BioRender.com.

Retention

Retention of FSL labelling is dependent on the type of surface/cell and the surrounding environment [230]. Viable cells show declining FSL levels within 4 hours (possible explanations for this include loss via extra-vesicle formation, membrane turnover and internalisation of the FSL constructs, loss of FSL that was entrapped within glycocalyx but not inserted into membrane back to supernatant) [230, 261]. Non-viable cells, such as RBC, or dead cells are strongly labelled and retain their labelling for much longer (days) [241]. The presence of plasma or albumin (for example in cell culture growth media) has been shown to significantly reduce labelling [57], and increase FSL loss from cell membranes [253]. *In vivo* FSL constructs are completely lost from cells within a few days, similar to that seen with natural glycolipids [266].

Location

Rapport et al. showed that the majority of FSL constructs associated with the cell membrane are integrated into the membrane with a small amount remaining entrapped within the glycocalyx [230]. FSL constructs do not appear to distribute uniformly throughout the cell membrane but instead cluster together in patches [230, 261]. FSL clusters (FSL-A2 and FSL-biotin) were observed to localise mostly outside of lipid rafts [230, 261], this may be due to the tight packing of phospholipids within the raft making it unfavourable for FSL construct to insert.

1.8.3 FSL and liposomes

Due to their structure, it was anticipated that FSL constructs will be able to integrate into the liposome phospholipid bilayer membrane, most likely via insertion of their DOPE lipid tail portion into membrane due to hydrophobic forces. Depending on the method that FSL constructs were added to liposomes, FSL constructs may be present on the internal and/or external phospholipid bilayer leaflets, and FSL monomers and/or micelles may be present in the external aqueous solution and could be encapsulated within the aqueous interior of the liposome core, Figure 21

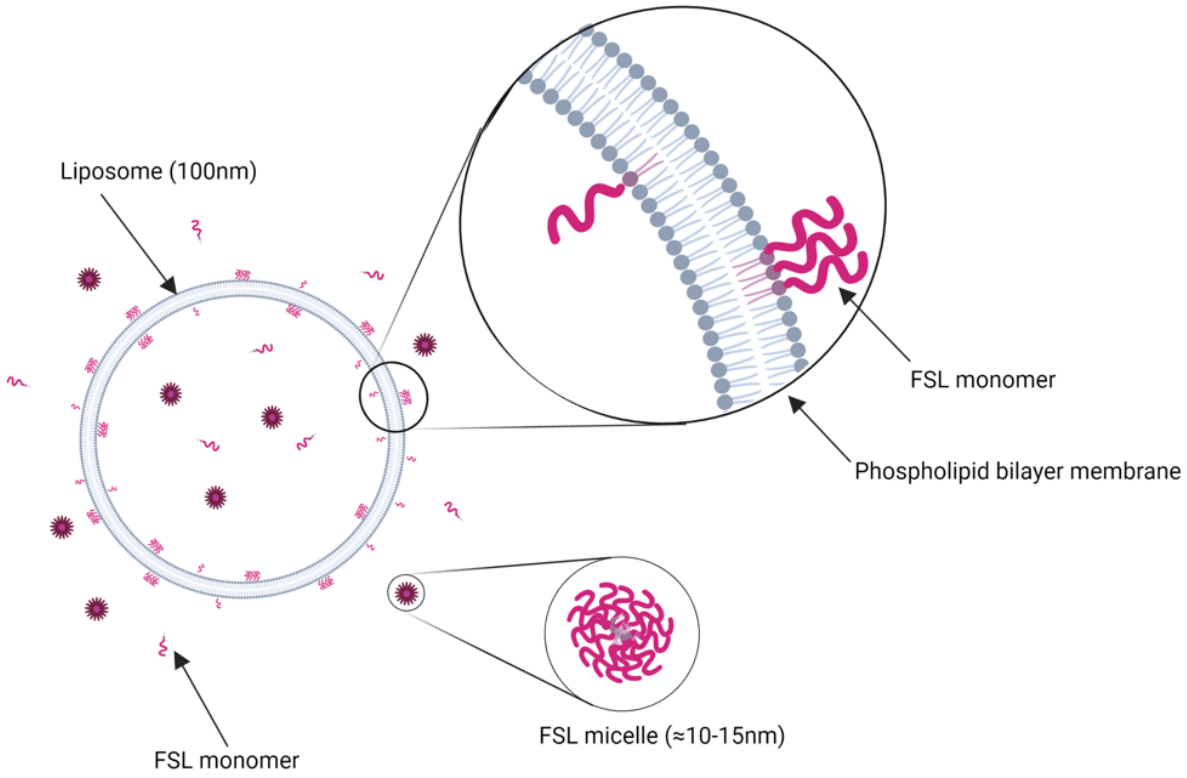

Figure 21 Schematic diagram of a liposome showing possible locations of FSL constructs. FSL constructs may potentially insert into the phospholipid membrane (internal and/or external leaflet), or they can be present as micelles encapsulated within the liposomes aqueous core or in the surrounding aqueous solution. Approximately to scale. Created with BioRender.com.

FSL construct movement within the liposome membrane

As previously discussed, section 1.5.6, phospholipids can rotate about their axis and move laterally within a phospholipid bilayer membrane (although this is dependent on temperature and phase state of membrane). Flip-flop between bilayer membranes is also possible.

The liposomes used in this study were in a fluid liquid disordered state so the FSL constructs should be capable of fast lateral and rotational movement within the liposome membrane. The ability of FSL constructs to freely move within the membrane is advantageous as it can allow the constructs to cluster together which can help to facilitate and improve multivalent binding, e.g. with IgM antibodies.

Flip-flop movement of the FSL constructs (between inner and outer bilayer membranes) is likely to be very slow if it occurs at all. FSL-A2 and FSL-biotin both have a large negatively charged hydrophilic spacer group (CMG2) attached to the phospholipid head group, which is likely to impede flip-flop.

The flexible hinge region of the CMG spacer allows movement of the functional head groups in FSL-A2 and FSL-biotin constructs from a vertical upright position through to a folded position close to the membrane surface, Figure 22 [253]. This flexibility of the FSL constructs (with CMG spacer) can allow for better presentation of the functional head group. Figure 22 shows the potential mobility of a FSL construct within liposome membrane.

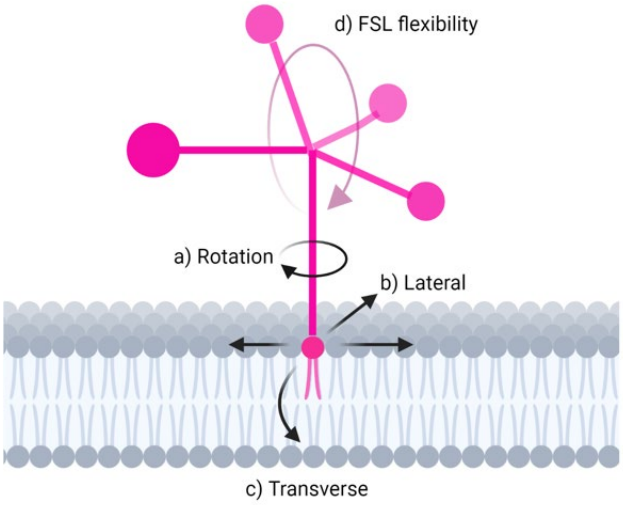

Figure 22 FSL mobility in phospholipid bilayer membrane. Schematic diagram showing the possible movement of an FSL construct with a CMG spacer within a phospholipid bilayer membrane. The FSL construct can rotate and move laterally within the membrane. The CMG spacer is semi flexible, which allows the functional head group to move from fully extended vertical down to folded at the membrane surface [253]. Not to scale. Created with BioRender.com.

1.9 Liposome preparation

Liposomes can be prepared by a wide variety of methods, from relatively simple laboratory techniques to large scale industrial manufacturing processes. Additional techniques, such as extrusion, sonication and freeze/thaw cycles, are often required after synthesis to control the size and lamellarity of the synthesised liposomes. The preparation method used to synthesise liposomes can influence the resulting liposome's characteristics such as size, charge, drug encapsulation and release kinetics, sterility, and toxicity. Control of these factors is important as liposome morphology (size and surface characteristics) directly influences the interaction between the liposomes and their environment and hence also governs their performance properties. Synthesis of monodisperse liposomes with well-defined physical characteristics is desirable to ensure predictable and repeatable behaviour of liposomes.

Preparation techniques can be divided into two broad categories, conventional and novel techniques. These are briefly discussed below followed by more detailed description of thin film hydration and extrusion, the preparation method used in this research project. For a comprehensive review of liposome preparation methods, the reader is referred to additional publications [81, 267-269].

Conventional techniques

There are four main conventional techniques used for the synthesis of liposomes; thin film hydration [4], reverse phase evaporation [270], solvent injection [271, 272], and detergent depletion [273]. In general, these methods consist of a similar process; dispersal of lipids in an organic solvent, followed by removal of the solvent and replacement with an aqueous solution. These methods require relatively simple laboratory equipment and procedures, making them well suited to laboratory scale projects. However, these methods usually result in the formation of liposomes of varying size and lamellarity, and consequently require a further processing step to control their size and lamellarity. A major drawback of conventional methods is that they expose the liposomal components (and any material to be encapsulated) to harsh conditions such as organic solvents, high temperatures and mechanical stress, which may be damaging to fragile biomolecules.

Novel techniques

Many other 'novel' methods of liposome preparation have been developed, primarily to help facilitate the scale up of liposome production for industrial scale sterile manufacture, to improve encapsulation efficiencies, and to develop methods which avoid the use of harsh solvents/temperatures associated with conventional methods [81]. Some of these result in good control of liposome size and lamellarity, while others require post formation processing the same as conventional techniques.

Many 'novel' techniques require specialised and expensive equipment and infrastructure, often making them unsuitable for laboratory scale use. Examples of novel techniques include the use of supercritical fluids methods [274], lyophilisation [275], spray drying [276], microfluidics [277], membrane contactor technology [81], and electro formation [278].

To date there is no generally accepted method which is suitable for all purposes. Each method has advantages and disadvantages related to the intended liposome composition, toxicity and sterility requirements, fragility of any encapsulated materials, intended applications and ionic strength requirements.

Post formation processing

Many liposome synthesis methods, particularly conventional, result in the formation of polydisperse liposomes with a wide range of sizes and lamellarity. A post formation processing step is then required to control the size and lamellarity of the liposomes. Post formation techniques generally use a mechanical force to disrupt the liposome membranes which then re-fuse resulting in smaller unilamellar liposomes [279]. The most commonly used methods are sonication [280], extrusion [281, 282], homogenisation (French press)[283], and freeze thaw cycles [284, 285]. These methods can expose the liposomes to high mechanical stress, which may be damaging to fragile molecules.

1.9.1 Thin film hydration

Liposomes in this study were prepared by the thin lipid film hydration method [286], followed by extrusion to form liposomes of a uniform size and lamellarity [4, 287]. Thin film hydration was selected as it is a well-established, simple and reproducible method, which is suitable for all kinds of lipid mixtures and requires relatively inexpensive and simple laboratory equipment. It is one of the most widely used methods (at laboratory scale) for liposome preparation [81, 279].

The disadvantages of this technique include the use of harsh solvents and the removal of organic solvent can be difficult and time consuming. This method is not sterile and produces liposomes with a range of sizes and lamellarity. Consequently, a second post synthesis step, extrusion, is required to control the size and lamellarity of the liposomes.

This method consists of three steps, thin lipid film formation, lipid film hydration and extrusion. These steps are discussed in more detail below, and Figure 23 shows a schematic diagram of the method.

Thin Lipid Film formation

The lipid components of the liposome, plus any other hydrophobic molecules to be incorporated, are dissolved in an organic solvent to form a homogenous dispersion. The solvent is then removed by evaporation to form a 'thin lipid film' which consists of a stack of dried lipid bilayers against the vessel wall (the so-called thin lipid film).

Hydration

The dried lipid film is then hydrated with an aqueous solution. The aqueous solution causes the lipid sheets to swell and detach from the vessel wall. The detached lipid sheets self-close, due to hydrophobic forces, to form large multilamellar liposomes of varying size. Any hydrophilic molecules present in the hydrating solution will be encapsulated within the liposome aqueous core.

Extrusion

Extrusion involves passing the multilamellar liposomes back and forth through a membrane with size defined pores. As the liposomes pass through the membrane pores they break and reform. Multiple passes through the membrane results in the formation of unilamellar liposomes with a narrow size distribution that is close to the size of the membrane pores. This method has good reproducibility and control of size.

Extrusion forms LUV with a narrow size distribution close to the size of the membrane pores. This method has high reproducibility and does not expose the liposomes to harsh conditions (unlike sonication and high pressure methods can result in degradation of lipids and encapsulated cargo). However, it is only suitable for relatively small volumes, and the technique must be carried out above the T_m of the constituent lipids.

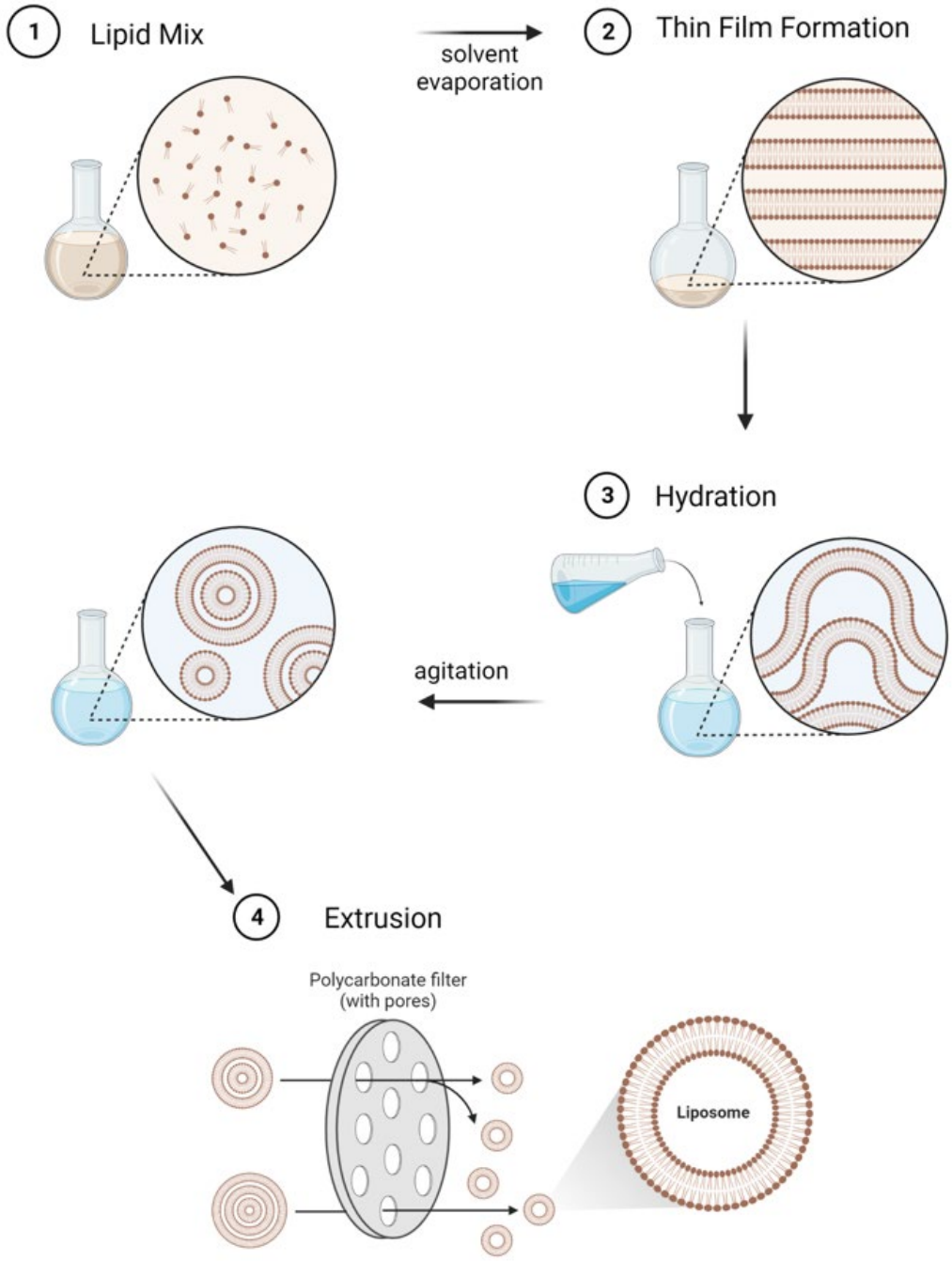

Figure 23 Liposome preparation via thin film hydration. (1) Lipids are mixed together in an organic solvent such as chloroform. (2) The solvent is removed by rotary evaporation and a dried thin lipid film is formed. (3) The thin lipid film is hydrated with an aqueous solution and large multilamellar liposomes spontaneously form. (4) The liposomes are then extruded through a polycarbonate membrane to form small unilamellar liposomes. Adapted from [288].

1.10 Methodology used to measure liposomes and micelles

The pharmacokinetics and pharmacodynamics of liposomes are dependent on their physical properties, including size, lamellar organisation, charge, composition, and surface chemistry. These factors all impact their interaction with their biological environment, including cells and the immune system The primary techniques used to measure and observe liposomes in this project are shown in Table 5 and the following sections provides a brief outline of their principles and respective advantages and limitations.

Table 5 Methodology used to measure liposomes and micelles in this research

Measurement	Technique
Size	Dynamic light scatter (DLS), Transmission electron microscopy (TEM)
Morphology	TEM
Zeta Potential	DLS
CMC	Surface tension (pendant drop method Fluorescence spectroscopy (pyrene I/III method) DLS (particle count rate)

1.10.1 Size and morphology

The size and size distribution (polydispersity index) of liposomes are important parameters, especially if liposomes are intended for therapeutic use. Liposome size determines circulation times *in vivo*; small liposomes remain in circulation longer than larger liposomes, although very small liposomes are rapidly excreted via renal filtration (<10nm). Larger liposomes are quickly removed by phagocytic cells [289].

Liposome morphology (size, shape and lamellarity) are also important factors which impact on the liposome properties. Lamellarity can influence encapsulation efficiencies and drug release kinetics, and can also effect the liposomes intracellular fate [27]. In addition, it is important to ensure liposomes are a consistent size and shape so that reproducible and predictable results can be obtained.

Methods to measure liposome size include DLS (dynamic light scatter), TEM (transmission electron microscopy), nanoparticle tracking analysis and atomic force microscopy [290]. Morphology of liposomes can be observed by electron microscopy techniques. DLS and TEM were used in this project and are discussed in more detail below

Dynamic light scattering

Dynamic light scattering (DLS), also known as photon correlation spectroscopy, uses Brownian motion to calculate the size of particles in solution. A laser light source is used to illuminate a suspension of particles and then intensity fluctuations of the scattered light are used to determine the size of the particles [290]. When light is scattered off particles in suspension, their Brownian motion (smaller particles move faster than larger particles) causes fluctuations in the intensity of the scattered light. By analysing the fluctuation of light scattered by the moving particles their diffusion coefficient (D) can be obtained. This can then be used with Stokes-Einstein equation (Equation 2) to calculate the particles diameter [291, 292].

$$d(H) = \frac{kT}{3\pi nD}$$

d(H)	Hydrodynamic diameter (m)
k	Boltzmann's constant (m^2kg/Ks^2)
T	Temperature (K)
n	Viscosity (Pa.s)
D	Translation diffusion coefficient (m^2/s) = speed of the particles

Equation 2 The Stokes-Einstein equation

The particle diameter measured by the DLS is referred to as the hydrodynamic diameter, because it is equivalent to the diameter of a sphere which would have the same translational diffusion coefficient as the measured particle. It is dependent on the actual size of the particle, the presence of surface structures which affect its diffusion speed (anything that reduces the particles speed will correspondingly change the apparent size of the particle), and also the concentration and type of ions present in the medium [293]. Ions present in the surrounding medium create an electric double layer surrounding the particle (1.10.2 Zeta potential), which can change the apparent hydrodynamic diameter. For example 60nm monodisperse latex particles will appear 15% larger in 10mM NaCl than in deionised water [293].

DLS also calculates the polydispersity index (PDI) of the particle population. This is a dimensionless value that measures the degree of particle size heterogeneity. Values less than 0.2 are considered acceptable and indicate the population is monodisperse [294].

A major advantage of DLS is that it allows the rapid measurement of a large number of liposomes in their native hydrated state [27]. However, the results obtained are a calculated average which rely on the assumption that all particles present are spherical, monodisperse (one population of particles the same size) and non-interacting. DLS is also very sensitive. Consequently, aggregated vesicles and outliers can greatly skew the calculated average result. DLS does not provide any information on the shape or concentration of the particles present.

Transmission electron microscopy (TEM)

Electron microscopy is used to characterise the size, morphology and lamellarity of liposomes. Traditional TEM techniques require the sample to be stained, usually with a heavy metal stain such as uranyl acetate, dried and then exposed to high vacuum and an intense electron beam for imaging. As a result, labile biological samples, such as liposomes, are unlikely to remain in their native hydrated spherical form. Furthermore, internal structures, such as the bilayer membrane organisation of liposomes, are unable to be seen. To avoid these problems Cryo-TEM and freeze fracture TEM are the two most commonly used techniques [295]. Cryo-TEM was used in this study and is briefly discussed below.

Cryo-TEM preparation involves applying a small aliquot of the sample onto a TEM grid, which is composed of a metal grid covered with a thin foil and perforated with circular holes. The sample is blotted with filter paper to form a thin film across the grid, and then plunge frozen in a cryogen, usually liquid ethane. This rapid freezing forms a thin layer of non-crystalline vitreous (glass like) ice. The freezing process occurs so quickly, that any particles present, such as liposomes, are immobilised in the ice before any significant alteration to their structure can occur, allowing them to be imaged in their native hydrated state. Ideally the sample remains evenly distributed throughout the ice layer and across the thin ice which spans the holes in the grid.

The advantages of this technique include that liposomes can be observed in their native hydrated state and their morphology and internal bilayer structure can be seen. The size of liposomes can be directly measured and liposome lamellarity can also be observed. Disadvantages of this technique include that only a relatively small number of liposomes can be observed, it requires specialised equipment and sample preparation techniques, and is a relatively time consuming technique.

In addition, cryo-TEM also has limitations which should be remembered when interpreting images

- Low electron dose imaging results in lower clarity and image resolution than other techniques such as traditional TEM [296].
- During sample preparation the blotting step applies shear forces to the sample during film formation, which may affect/alter sample, e.g. could flatten out liposomes making them appear larger.
- Liposomes in sections of thin ice can become flattened and appear larger [297].
- liposomes may show a preference for the grid and avoid distribution over the holes, this interaction with grid could alter observed morphology and size [298].

- Formation of non-uniform thickness ice can alter distribution of particles, this can influence the size of particles able to be imaged, larger particles may be excluded from thinner ice which usually forms towards the centre of holes, Figure 24 [299, 300].

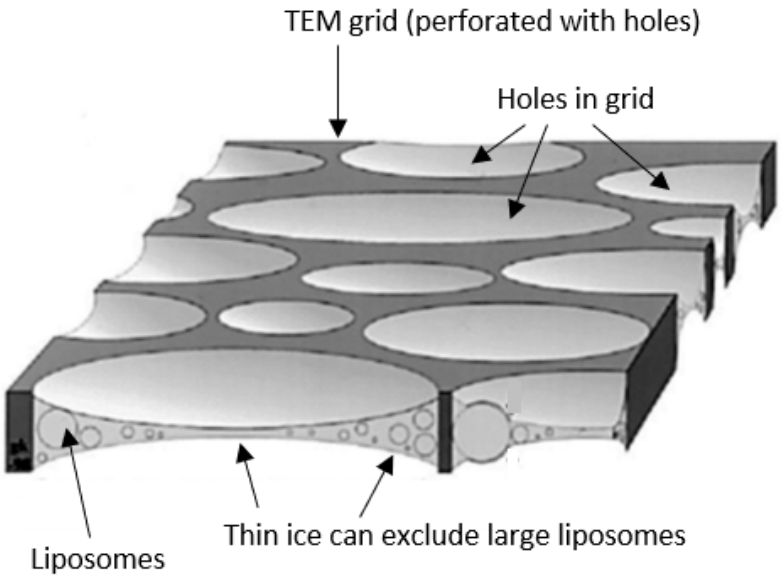

Figure 24 Cross section view of a cryo-TEM grid and ice film. Liposomes can be seen in the ice, however large liposomes may be excluded from the thin central ice. Image adapted from [301].

- Cryo-TEM results in a two dimensional image of a three dimensional object [302]. This can disguise the true shape of particles as shown in Figure 25.

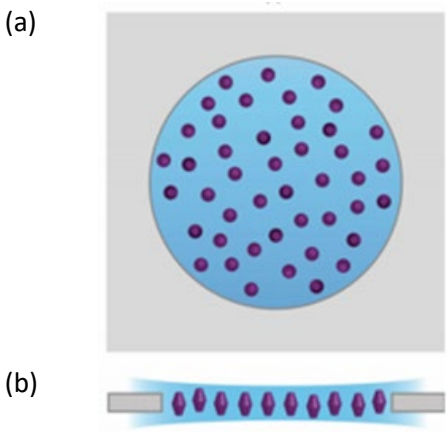

Figure 25 Schematic diagram showing particles distributed in a vitreous ice layer. (**a**) shows a view of the particles from above, as seen in cryoTEM. The particles appear to be spherical. (**b**) shows the same particles viewed from the side, where it can be seen that the particles are not spherical, illustrating how the true shape of particles may be obscured in 2D view from above. Figure adapted from [303].

1.10.2 Zeta potential

Zeta potential is the surface charge of the lipid vesicle and any surface molecules. When a charged particle is dispersed in liquid an adsorbed double layer (electric double layer) develops around the particles surface. The liquid around a particle exists in two parts, an inner region where the ions are strongly bound to the particle (called the Stern Layer), and an outer region (the slipping plane) where ions are less strongly associated. The ions within these two layers move together with the particle as a single entity. The electrokinetic potential at the slipping plane boundary is called the zeta potential, Figure 26 [290]. Beyond the slipping plane the ions no longer move with the particle.

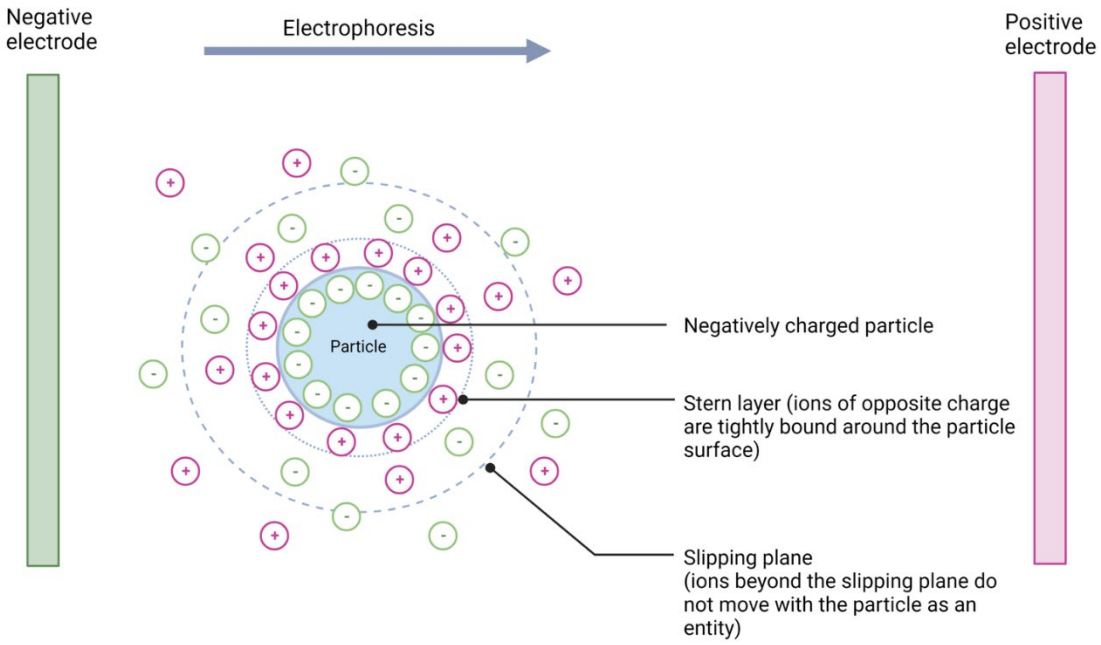

Figure 26 Schematic diagram showing electric double layer of a negatively charged particle. The surface of the particle is surrounded by a strongly adhered layer (stern layer) of oppositely charged ions. Beyond this is a diffuse layer consisting of both negative and positive charges. Ions within the slipping plane move with the particle as a single entity. During electrophoresis the particle moves toward the oppositely charged electrode (in this case the positive electrode). Image created with BioRender.com, adapted from [290].

The zeta potential is measured by electrophoretic light scatter. An electric field is applied to the dispersion, which causes the charged particles to move toward the electrode of opposite charge. As the particles move they scatter light from an incident laser. The scattered light has a different frequency to the incident light, and the frequency shift is proportional to the speed of the particles (Doppler shift) [290]. The calculated velocity of the particles is then used to calculate the zeta potential.

Factors which influence zeta potential include;

- pH, zeta potential becomes more positive and negative in magnitude with acidic and basic pH respectively [290].
- Ionic strength, zeta potential decreases with stronger ionic strength and also the presence of higher valency ions (i.e. $Ca^{2+}$and Al^{3+}), as these compress the electric double layer [290].
  Measuring zeta potential in highly conductive media (such as physiological saline) can be challenging. The high conductivity can generate heat and degrade the sample [290].
- Concentration, at higher concentrations the zeta potential decreases and the colloidal stability of the dispersion is reduced [290].

Zeta potential is often used to 'predict' the stability of a colloidal dispersion. The greater the charge on the particles the more they repeal each other, which helps to prevent aggregation (hence improving colloidal stability)[27]. It is reported in the literature that nanoparticle dispersions with zeta potentials between -10 to +10mV are unstable, ±10-30mV moderately stable and greater than ±30mV highly stable [290, 304]. However colloidal stability also depends on the attractive forces between particles such van der Waals (which are not measured by zeta potential) therefore it is possible to have stable dispersion even with a low zeta potential. Steric interactions can also contribute to colloid stability (i.e. addition of PEG to nanoparticle surface decreases zeta potential but increases colloidal stability) [290].

1.10.3 Critical micelle concentration

The critical micelle concentration (CMC) is the concentration above which micelles form in a dispersion of amphipathic molecules [305]. Below the CMC the amphipathic molecules are present as monomers within the aqueous phase, while above the CMC the monomers aggregate and form micelles. Above CMC monomers and micelles exist in a dynamic equilibrium [305].

CMC is dependent on properties of the molecule itself and also the surrounding environmental conditions. For phospholipids this includes their structure (length and saturation of hydrophobic lipid chains and size/structure of head group), charge, temperature, pH and environmental electrolytes.

CMC may be measured by a variety of methods including surface tension (Wilhelmy Plate, Du Nouy ring, Pendant drop methods)[306], electrical conductivity [307], calorimetry [308], static and dynamic light scattering [309, 310], and fluorescence (quenching) spectroscopy [62, 311].

The measured CMC result is highly dependent on the method used and interpretation of data. There is no single gold standard method to measure CMC, nor is there always a universally accepted method for how to interpret experimental data to determine the CMC point [62]. Methods are selected based on requirements and characteristics of the molecule to be measured.

In this study CMC was used to investigate the behaviour of FSL constructs in aqueous solution. The CMC of the FSL constructs was analysed using surface tension (pendant drop tensiometry) and fluorescence spectroscopy (pyrene I/III method) methods. The basic principles of these two methods are outlined below. Two additional techniques were also used to help investigate CMC; analysis of the particle count rate generated by the zetasizer and the fluorescence of FSL-FLRO4 dispersion was used to help detect formation of micelles (details of these two methods are provided in method section).

A) Surface tension

Amphipathic molecules self-assemble so that their hydrophobic portions avoid contact with water, and their hydrophilic portion remains in contact with the aqueous solution. At concentrations below CMC amphipathic molecules tend to accumulate at the aqueous phase surface edge or interface, oriented with their hydrophilic region toward the water phase and their hydrophobic portion oriented away from the water. As their concentration increases and the surface becomes saturated, the molecules will begin to suspend within the aqueous solution, first as monomers and above a certain concentration they begin to form micelles. The concentration where micelles begin to form within the aqueous solution is called the critical micelle concentration (CMC). CMC is not a distinct sharp point, but actually occurs over a narrow range of concentrations [312].

As surfactant molecules accumulate at the surface of the liquid intermolecular hydrogen bonding between water molecules is decreased, this causes a concentration dependent decrease in surface tension. At CMC the surface of the liquid becomes saturated with surfactant and all additional surfactant molecules begin to form micelles within the solution, therefore surface tension remains unchanged past that point, as shown in Figure 27.

An advantage of using surface tension to determine CMC is that no additional substances are added to the system. The addition of new molecules can potentially interact with the test molecules and alter where CMC occurs. There are several methods for measuring surface tension, Wilhelmy Plate, Du Nouy ring, and pendant drop methods)[306]. In this study the pendant drop method was used.

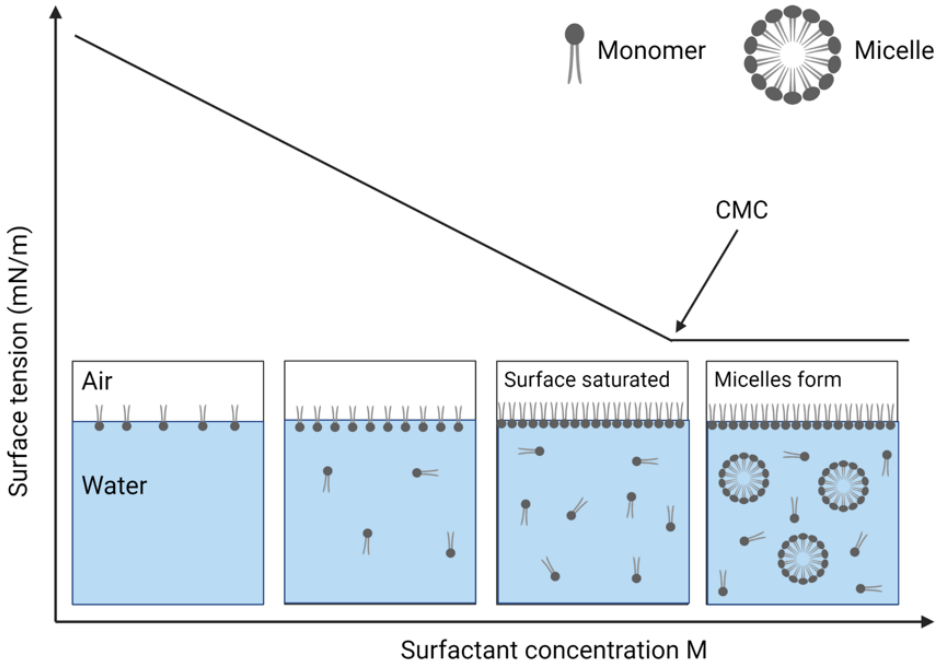

Figure 27 Surface tension of a surfactant solution. Graph shows decreasing surface tension as concentration of surfactant increases and micelles are formed.At low concentrations phospholipid molecules accumulate at water surface. As the phospholipid concentration increases the water surface becomes saturated and micelles begin to form within the water phase.[58, 313].

Pendant drop tensiometry

The pendant drop method measures the surface tension of a liquid by analysing the shape of a drop of liquid suspended from a needle [314, 315]. In the pendant drop technique, a camera is used to record the shape of a drop of liquid, as shown in Figure 28. The shape of the droplet is determined by the balance between gravity and surface forces. The software analyses the droplet's shape to determine the radius of curvature at the droplet's apex, which is then used to estimate the surface tension based on the droplet's dimensions using Equation 3 [316].

$$y = \frac{\Delta p g R_{0^2}}{\beta}$$

y	Surface tension (N/m)
$\Delta\rho$	Density difference between fluids (kg/m^3)
g	Gravitational constant (m/s^2)
R_0	Drop radius of curvature of the apex (m)
β	Bond number

Equation 3 Calculation of surface tension using droplet shape

The software allows iterative approximations to be carried out to find solutions that most closely match the obtained size profile. The advantages of this technique include that it is simple and requires only small volumes of sample, and is reported to have very high accuracy [317]. No additional molecules are added (which can themselves alter CMC values). Limitations include that reliability decreases when the shape of the drop becomes close to spherical [318].

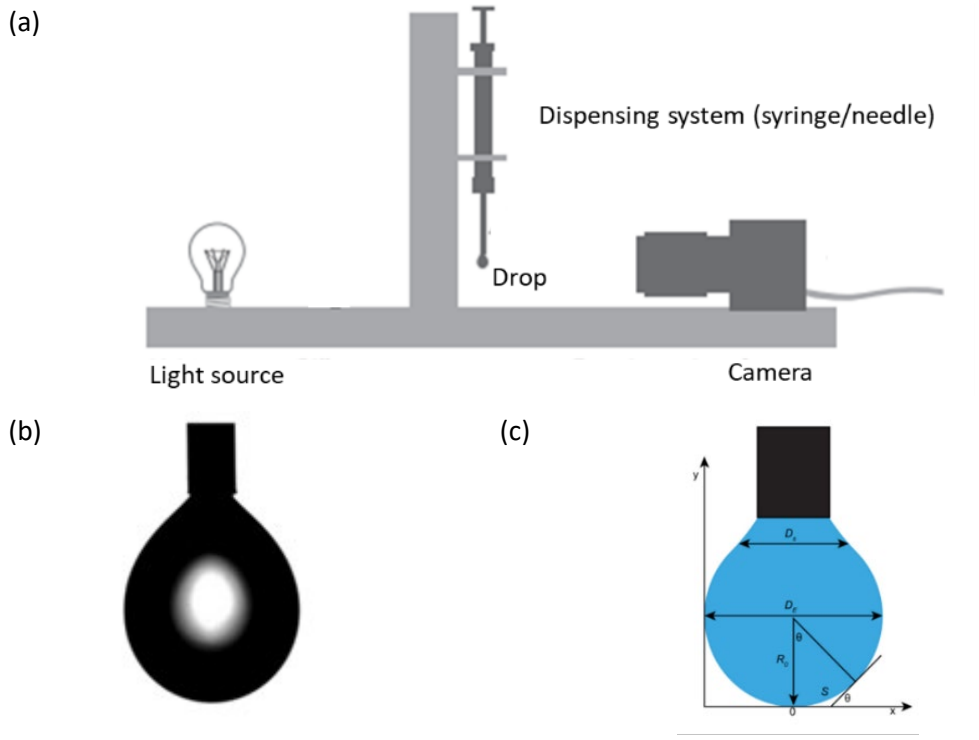

Figure 28 Pendant drop method. Schematic diagrams showing (**a**) the basic experimental set up, (**b**) a typical drop image and (**c**) drop diagram showing variables used by the software to determine surface tension. Adapted from [58, 315, 319]

B) Fluorescence spectroscopy – Pyrene 1:3 Method

Critical micelle concentration (CMC) was determined using the fluorescent dye, pyrene[62]. Pyrene emits a characteristic fluorescent spectrum in solution, with 5 vibronic bands/peaks (Figure 29). The intensity of the vibronic peaks is dependent on the solvent environment surrounding the pyrene molecule [320]. When the solution is below the surfactant CMC, the surfactant molecules are present as monomers and pyrene is exposed to the polar environment of water. In this state the ratio of the first and third vibronic peaks is high. Above the surfactant's CMC, micelles form, and the pyrene molecules preferentially bind to the hydrophobic interior of the micelles. This alters the emitted spectra of pyrene and the ratio of the two peaks decreases [305].

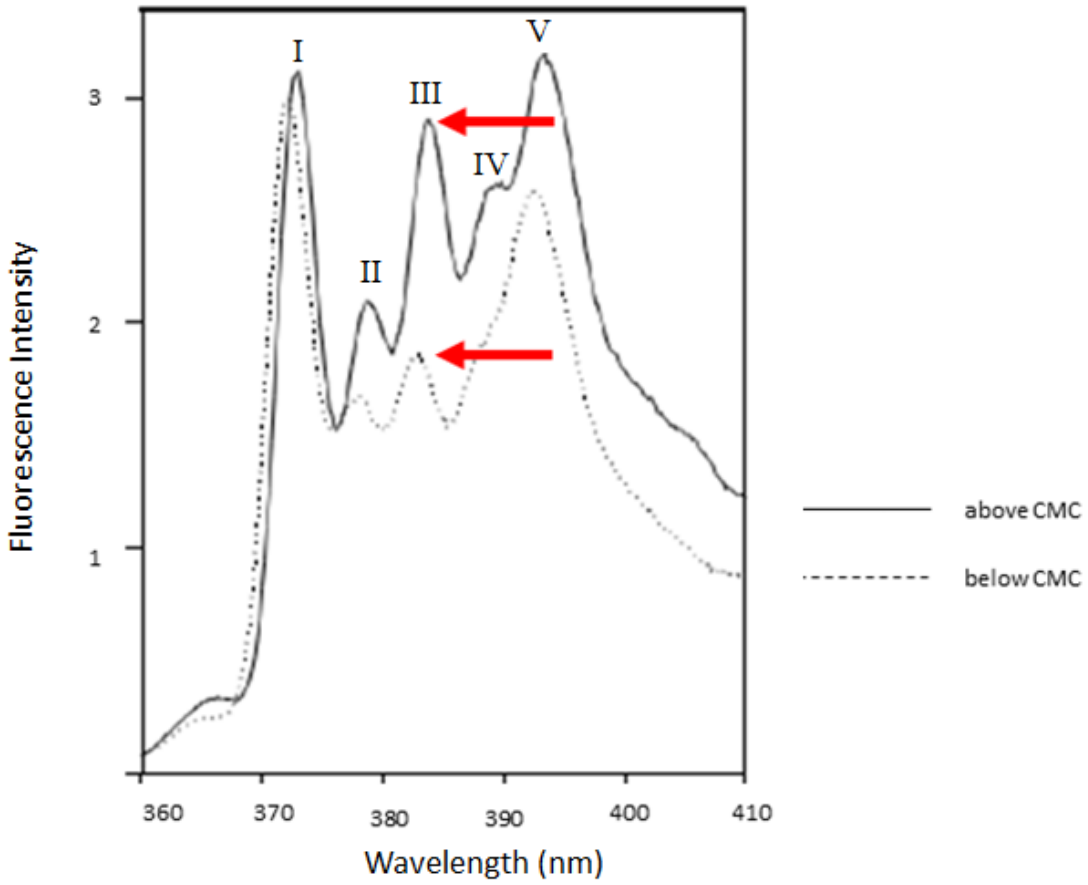

Figure 29 Pyrene fluorescence emission spectrum, showing change above and below CMC. Pyrene was mixed with two concentrations of sodium dodecyl sulphate (SDS), one above and one below CMC. Solid line shows pyrene with 0.012M SDS, which is above CMC. Broken line shows pyrene with 0.003M SDS, below CMC. A large difference can be seen between peak III of the two spectra, as indicated by red arrows. Peak I remains unchanged. Figure adapted from [305].

The ratio of the fluorescence intensities of the first and third vibronic bands of pyrene can then be graphed against surfactant concentration to give a characteristic sigmoidal curve, which is used to determine CMC [62]. However, although the pyrene 1:3 technique is a well-established method to determine CMC (in use for over 50 years), there is no defined point from the obtained graph which is universally accepted to correspond to the CMC [321]. This is because the CMC does not occur at a definite point but occurs over a range of concentrations. Most commonly in the literature the CMC point is determined as either the inflection or midpoint of the curve, point X on graph shown in Figure 32 (usually used when CMC is very low, or for non-ionic surfactants) [62, 322], or the intercept of the horizontal slope at high concentration with the rapidly varying slope of the pyrene ratio slope, point A shown in Figure 30, (better for ionic surfactants) [306, 321].

In this study two values for CMC were calculated from the acquired data; point X (the mid-point), and also point B (as shown in Figure 30). Point B is the concentration where the ratio first begins to change, and so is likely the point where micelles first begin to appear within the solution.

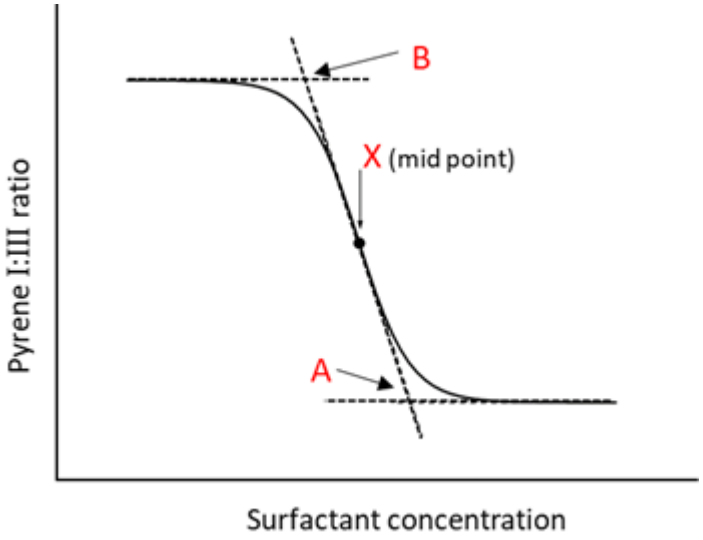

Figure 30 Example graph showing points which may be used to determine CMC. Point X is the centre of the sigmoid, and A the intersection of the straight lines extrapolated from curve (dotted) are the points most often used to calculate CMC. A third point, B, was used in this study, it represents the lowest concentration where micelles first begin to form. Figure adapted from [62].

Advantages of this method include that it directly measures micelle formation and it has good sensitivity (suitable for detecting CMC below 0.1mM [323]). Limitations include that it is very sensitive to environmental conditions and possible spectral interference if coloured or fluorescent compounds are present [323]. The addition of ethanol (necessary for pyrene solubilisation) may also affect CMC [323].

1.10.4 Methods for washing liposomes

Following the conjugation or encapsulation of bioactive molecules to liposomes it may be necessary to remove any unconjugated/non-encapsulated materials, to ensure that a homogenous liposome dispersion with reproducible characteristics is obtained. A variety of methods can be used to purify/wash liposomes to remove excess and/or unconjugated components. These include filtration, ultra-centrifugation, dialysis, ion-exchange chromatography, and size exclusion chromatography [324]. Purification/washing liposomes can be challenging. The methods are often time consuming, require optimisation for each individual liposome formulation, and they can negatively impact the characteristics of the final liposome suspension [325].

Dialysis

Dialysis involves the removal of small molecules with the use of a semi permeable membrane. The membrane has pores which allows the small molecules to diffuse out, while larger molecules are retained. It requires that the contaminating molecule is hydrophilic. The advantages of this method are that it is simple to perform and does not require expensive equipment. However, it is a time consuming technique, often requiring several lengthy incubations. The final liposome suspension can be dilute and recovery can be low [324].

Size exclusion chromatography

Gel filtration (size exclusion chromatography) is a commonly used method. Commonly used examples include Sephadex and Sepharose columns. In this method the liposomes and contaminating molecules are separated by differences in molecular weight. The larger liposomes pass through the column quickly, while the smaller particles are capable of entering the pores in the gel/beads of the column and therefore spend more time in the column and take longer to be eluted.

This method can also be time consuming, (requiring packing of the column, pre saturation of the column and multiple elutions). The column must be pre-saturated with a large excess of blank liposomes to minimise non-specific interaction between liposomes and column so it can require a large amount of product [324]. Although it can result in highly purified product, loss to column can be significant (as high as 50%) and final suspension is significantly diluted [326]. This method may not be suitable for removal of lipophilic molecules [324].

Centrifugation

Ultra-high centrifugation (100 000 – 160 000g for one hour) can be used to separate liposomes from contaminating molecules in the supernatant [324]. The liposomes form a pellet, while lower molecular weight contaminants remain suspended in the supernatant. The contaminants can then be removed with the supernatant. A drawback of this method is that the liposomes are subjected to very high g forces, and this can cause liposomes to break and leakage of any encapsulated cargo. It also requires specialised ultra-fast centrifuge.

Density gradient fractionation can also be used to separate liposomes and other molecules based on their specific gravity. In this method liposomes and contaminants are separated by centrifugation through media of different densities i.e. ficoll, dextran, sucrose. The major disadvantage of this method is that the liposome product requires additional purification steps to remove the ficoll/dextran.

Ultrafiltration is a fast and simple method. It involves passing the liposome dispersion through a semipermeable cellulose membrane, which can be selected to have a range of molecular weight cut offs. Small molecules can move through the membrane, but larger molecules can not. Advantages include that it uses low speed centrifugation (standard lab centrifuge), there is no dilution of the sample, and very small volumes can be used [324].

Ion exchange resin

An ion-exchange resin is used to bind and separate molecules using charge. For example a cation resin binds any molecules which are positively charged, while the negatively charged molecules are not attracted and can move through the resin [324].

1.11 Research aims

Currently there are 25 clinical liposome products approved by FDA and EMA [16, 23, 24]. The ability to create liposomes which can specifically accumulate at the desired site via active targeting (conjugation of specific binding ligands to their surface) is desirable. While considerable success has been achieved *in vitro* this has not, to-date, led to the same level of success in developing clinical products. There are currently no clinical liposome products with active targeting capabilities [22].

Kode technology is a rapid surface engineering technology that has been successfully used to modify and functionalise a range of biological and synthetic surfaces, including cells, stainless steel, nanofibers, plaster, nitrocellulose [253]. Due to similarities between natural cell membranes (which have been successfully modified with Kode constructs) and liposome membranes it is anticipated that FSL constructs could be used as a novel approach to label the surface of liposomes without some of the described limitations, specifically without the need for complex modification reactions. Thus, FSL constructs have the potential to be used as a targeting system for liposomes.

The aim of this research was to evaluate the modification of liposomes with FSL constructs by

1. determining if Kode constructs form micelles in aqueous solution, and if so to characterise their size, charge and CMC
2. investigating and developing methodologies to modify liposomes with Kode constructs
3. synthesising and characterising FSL modified liposomes, specifically regarding liposome size, charge, and morphology
4. measuring the dynamics of FSL liposome modification, including incorporation and retention characteristics

5. determining the stability of FSL modified liposomes.
6. establishing proof of concept that FSL constructs can be as a surface modification method to create targeted liposomes

Chapter 2 Methods and Results – FSL and Liposome Characterisation

FSL constructs are water dispersible, amphipathic molecules which have been shown to spontaneously insert into the lipid bilayer of cell membranes on contact. They have previously been used to label cell surfaces with a variety of different molecules by varying the functional head group of the FSL construct. The aim of this study was to determine if FSL constructs could also be used to provide a novel method for the surface modification of liposomes.

The first section of this chapter is focused on the characterisation of FSL behaviour in solution as understanding how FSL molecules behave in solution would help to inform how they interact with liposomes.

The second section establishes methodologies to modify/create liposomes labelled with FSL constructs. Liposomes containing FSL prepared by various methods were analysed for their properties such as size, shape, charge, to investigate the effect FSL inclusion had on the liposome's characteristics.

Chapter three investigates the dynamics of FSL insertion into liposomes, including effects of temperature, time, and method of insertion. The stability and retention of FSL labelling was investigated, including transfer of FSL between liposomes and liposome to red blood cells (RBC) as a model cell membrane.

2.1 FSL Characterisation

Amphipathic molecules are known to form a colloidal dispersion of micelles when suspended in an aqueous media (as discussed in section 1.3). Before attempting to determine how the FSL constructs would interact with liposomes it was necessary to understand how amphipathic FSL molecules behave in aqueous solutions. Therefore, initial experiments were carried out to determine if FSL constructs exist as micelles, and if so to determine the micelle size, charge, and the concentration at which they form (CMC).

2.1.1 FSL constructs used in this project

Three FSL constructs were used in this project; FSL-A2, FSL-biotin and FSL-fluorescein (FSL-FLRO4) Figure 31. These were selected to have different functional head groups; glycan (FSL-A2), vitamin (FSL-biotin), and a fluorophore (FSL-FLRO4), and two different spacer molecules, one long CMG(2) (FSL-A2 and FSL-biotin), and one short adipate (FSL-FLRO4). By using different functional head groups and spacer moieties it was hoped that any difference in interaction with liposomes caused by variation of these structures could be detected. These three constructs have been well studied previously and can be

detected and measured using a variety of relatively simple laboratory techniques: flow cytometry, fluorescent microscopy, immunoassay, and haemagglutination [230, 240, 246, 253].

FSL-A2

The FSL-A2 construct has a carbohydrate head group, consisting of four monosaccharides, it is the blood group A type 2 antigen, (GalNAcα1-3(Fucα1-2)Galβ1-4GlcNAcβ). The carbohydrate head group is attached to a CMG(2) spacer and a DOPE tail, as shown in Figure 31a. The A type 2 carbohydrate antigen is naturally expressed on RBC, and when present defines the phenotype of blood group A. Fully extended FSL-A2 construct measure approximately 9nm [260].

FSL-A2 can be detected via its reaction with anti-A reagents by techniques such as haemagglutination and enzyme immunoassay techniques. FSL-A2 has been shown to label RBC [254], and a variety of cell lines (Jurkat, Raji, JCT116p53+), murine embryos [56, 230], and also a wide range of non-biological surfaces including metals (aluminium, gold, copper, stainless steel, titanium), plastics and polymers (i.e. cellulose acetate, natural rubber, nylon, polyvinyl chloride, polystyrene), glass, and paper [57].

FSL-biotin

The FSL-biotin construct has a monomer of biotin (vitamin B7) as its functional head group. This is attached via a CMG(2) spacer to a DOPE tail, as shown in Figure 31b.

FSL-biotin can be detected via its reaction with avidin (streptavidin/neutravidin). A secondary indicator label attached to the avidin/streptavidin, for example a fluorescent/enzyme label, or surfaces such as beads, is necessary to enable visualisation of the reaction. FSL-biotin has been shown to successfully biotinylate many different types of surfaces including RBC, cell lines, viruses, stainless steel, plastic, paper, spermatozoa, embryos [244].

FSL-fluorescein (FSL-FLRO4)

The functional head group of this construct is the fluorophore fluorescein. It is composed of an adipate spacer with a DOPE lipid tail, as shown in Figure 31c. Due to its fluorescent head group this construct can be directly detected by fluorescent microscopy and flow cytometry.

FSL-FLRO4 has previously been used to label a wide range of cells and surfaces including RBC [56], embryos [56], zebrafish [56, 243], viruses [56, 244, 245], cell lines [230], bacteria [258], and *in vivo* imaging [243].

All FSL constructs (GlycoNZ, NZ) were obtained in powdered form [240]. FSL constructs were reconstituted to prepare 2mg/mL stock dispersions and stored at -80°C in 50µL aliquots. Immediately before use stock FSL dispersions were allowed to come to RT and the required volume removed and used to prepare liposome dispersions or diluted with PBS to prepare FSL micelle dispersions. Any remaining stock FSL dispersion was returned to -80°C storage, up to a maximum of three freeze cycles.

During liposome preparation FSL constructs can be added at 3 different stages of the liposome synthesis, depending on the stage of addition FSL constructs are required to be diluted in either an aqueous diluent or in a solvent diluent. Therefore, two types of FSL stock solution were prepared for each construct;

1. Stock solution dispersed in an aqueous diluent. PBS was used for all three constructs; it was selected as it is the diluent used for liposome synthesis. Additionally, it is compatible for applications involving cells and with most biological assays.
2. Stock solution dispersed in a solvent. FSL-A2 and FSL-biotin were prepared with chloroform:methanol 97:3, while FSL-FLRO4, which is not soluble in chloroform, was prepared with methanol.

All solutions containing FSL-FLRO4, including liposomes and cells, were stored protected from light.

(a) FSL-A2 (blood group A type 2 (GalNAcα1-3(Fucα1-2)Galβ1-4GlcNAcβ))

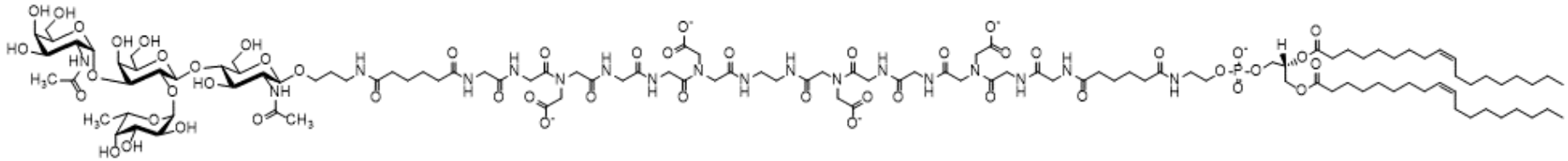

(b) FSL-biotin

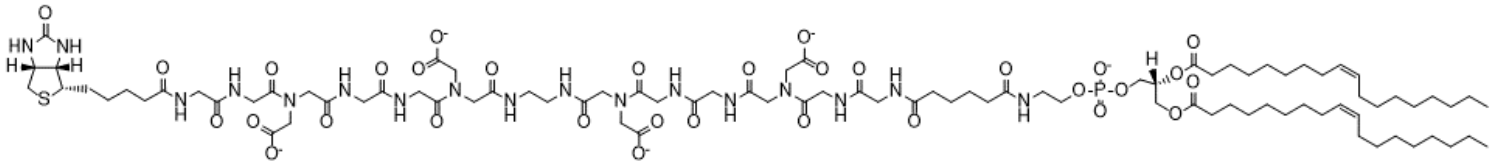

(c) FSL-FLRO4 (fluorescein)

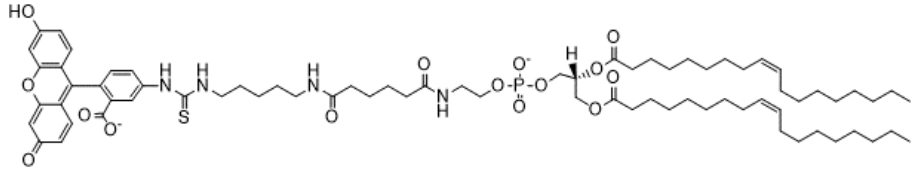

Figure 31 Chemical structure of FSL-A2, FSL-biotin and FSL-FLRO4. (**a**) FSL-A2 is composed of carbohydrate head group (blood group A type 2 antigen) joined via a CMG(2) spacer to a DOPE phospholipid tail. (**b**) FSL-biotin is composed of a biotin head group attached via a CMG(2) spacer to a DOPE phospholipid tail (**c**) FSL-FLRO4 is composed of fluorescein head group attached via an adipate spacer to a DOPE phospholipid tail. See Figure 33 for space filling versions of these constructs.

Kode terminology

The majority of the terminology used in this research to describe processes utilising FSL constructs has been published previously [241] and is outlined below;

- Modification of surfaces or cells with FSL constructs is termed koding.
- A cell, which has been modified with an FSL construct, is termed a kodecyte.
- Cells koded with a given concentration of an FSL construct are named as follows: "µM concentration-FSL name-kodecytes". For examples RBCs labelled with 100µM FSL-biotin are termed 100 biotin kodecytes.

For this research project additional terminology was required to describe and distinguish processes involving unlabelled liposomes and liposomes labelled with FSL constructs, and RBC koded with FSL constructs via interaction with koded liposomes as follows:

- The concentration of FSL used to prepare the liposome is noted in the same way as for kodecytes, for example, a liposome dispersion 'labelled' with 100µM FSL-biotin is termed 100 biotin liposomes.
- The protocol by which liposomes were prepared and FSL was incorporated is noted by the addition of initials H (hydration), LM (lipid mix) or PS (post synthesis) to the liposome description. For example, liposomes prepared with 100µM FSL-biotin which was added to liposomes by the lipid mix protocol are termed 100 biotin liposomes-LM.
- For brevity and clarity in some graphs, tables and figures liposomes are described by their method of preparation alone i.e. lipid mix (LM), hydration (H), or post synthesis (PS). In this case the concentration of FSL added to liposome would be the same for all types of liposomes and noted in the accompanying legend.

2.1.2 Micelle size and charge

Dispersions of FSL were analysed by dynamic light scattering (DLS) technique to determine if micelles were present, and if so to measure the size and charge of the particles.

Method

Dispersions containing varying concentrations of FSL constructs were prepared by diluting an appropriate aliquot of (aqueous) FSL stock solution in 1mL of PBS. The FSL dispersions were allowed to stand for 30 minutes at RT before analysis by DLS.

DLS analysis was conducted using a Malvern Zetasizer Nano SP. The Nano SP contains a 4mW He-Ne laser, operating at wavelength of 633nm, and an avalanche photodiode detector (APD). The analyser uses non-invasive back scatter technology which detects scattered light at an angle of 173°. This maximises light detection while maintaining signal quality, to enable very sensitive detection and measurement of nanoparticles at low concentrations. The analyser was set to automatically determine the optimum measurement position and correct attenuation. Size measurements were carried out in polystyrene cuvettes (Mediray, Cat# GR614101) at RT. Three size measurements of at least 10 seconds duration each were carried out and the mean result reported. Detectable size range of Malvern Zetasizer is reported to be 0.3nm -15µm [293]. Zeta potential measurement were performed in folded capillary cell (ATA Scientific, Cat# DTS1070). Three measurements were carried out and the mean result reported.

Results

Size and Critical Micelle Concentration

DLS analysis detected the presence of nanoparticles in dispersions of all three FSL constructs. The mean particle size (three experiments repeated independently) is shown in Figure 32.

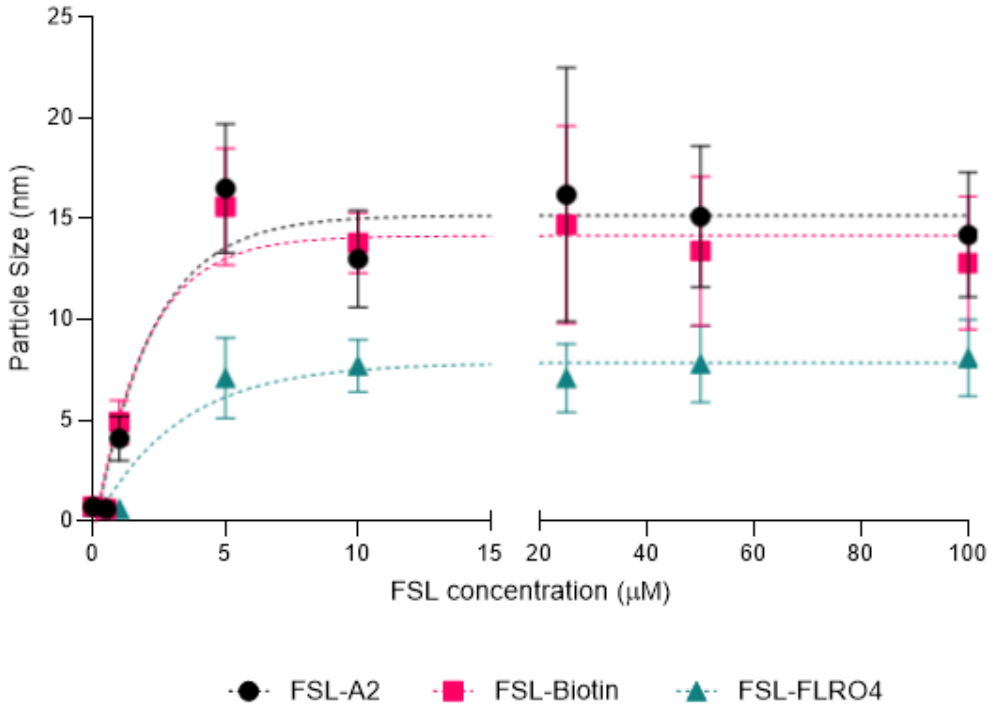

Figure 32 Size of FSL-A2, FSL-biotin and FSL-FLRO4 particles measured by DLS. FSL's were suspended in PBS, pH 7.4. Note a change in scale at the break in the x axis. Mean ± SD, n=3

The size (diameter) of the detected nanoparticles increased in size below 5µM, before reaching a plateau around 5-10µM. Above this point the size of the detected micelles remained unchanged despite increasing FSL concentration, in the range tested (≤100µM). The addition of more FSL constructs results in formation of a greater number of micelles, not a continuing increase to the size of the micelles present. These results indicate micelles are beginning to form at approximately 5µM concentration, therefore the CMC of all three constructs when dispersed in PBS pH 7.4, is approximately 5µM (when measured by DLS).

FSL-A2 micelles showed a mean particle size (diameter) of 15nm, FSL-biotin micelles were slightly smaller with a mean size of 14nm, both constructs have CMG(2) spacers. FSL-FLRO4 (which has a smaller adipate spacer) micelles were significantly smaller, with a mean size of only 8nm.

A probable explanation for difference in micelle size is that FSL-FLRO4 is a smaller molecule than FSL-A2 and FSL-biotin shown in Figure 33. FSL-FLRO4 has an adipate spacer, which is ≈1.0nm long. In contrast FSL-A2 and FSL-biotin have a CMG(2) spacer which is much longer at ≈6.5nm.

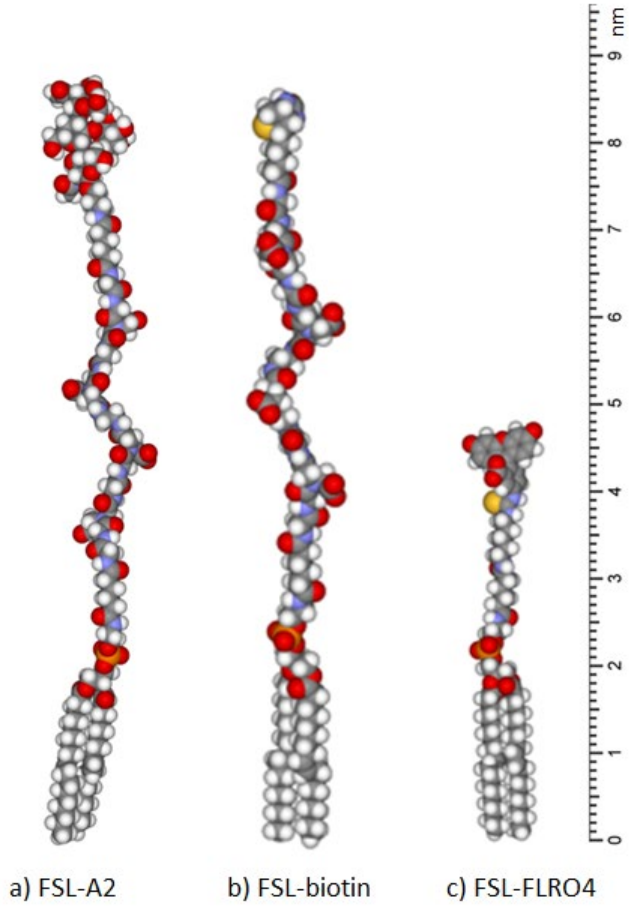

Figure 33 Schematic diagram comparing size of FSL-A2, FSL-biotin and FSL-FLRO4. Diagram comparing the sizes of (**a**) FSL-A2, (**b**) FSL-biotin and (**c**) FSL-FLRO4 constructs (in fully extended conformation). Fully extended FSL-A2 and FSL-biotin constructs measure approximately 9nm. Fully extended FSL-FLRO4 measures 5nm [253, 260].

DLS size data analysis

The default measurement generated by Malvern Zetasizer software is size as a function of scattered light intensity. However, this measurement (intensity) does not give any information regarding the number of particles present in the detected populations. Care must be taken when interpreting this data, particularly when dual populations are present. Large particles scatter exponentially more light than small particles, therefore a very small number of large particles, such as dust/bubble contamination, can give the false appearance of a significant population of large particles. The zetasizer software can convert the obtained intensity data to number of particles. This allows the relative number of particles in each population to be compared [292].

The graphs in Figure 34 show the DLS data obtained for 100µM FSL dispersions of (a) FSL-A2, (b) FSL-biotin, and (c) FSL-FLRO4 in PBS pH 7.4. Both types of graph (of the same data) for each FSL are shown. Graphs labelled (i) show size as a function of scattered light intensity, while the graphs labelled (ii) show size as a

function of the number of particles. Figure 35 shows DLS graphs of the diluent, PBS, used to prepare the micelle solutions.

In Figure 34 the graphs displaying (i) size by intensity show two populations for all three FSLs: a population of small particles approximately 10nm in size and a population of larger particles greater than 100nm in size. This larger sized population is not seen in the graphs (ii) which show size by number of particles. This indicates that the larger size particles account for only a very small number of the total particles (<1%). This larger population is also seen in the PBS solution (Figure 35), therefore is most likely due to artefacts such as dust contamination.

Because these larger particles only account for a very small percentage of particles present (and are likely dust contamination) and the vast majority of particles present were in the 10nm population, only the size of the smaller particles has been reported in Figure 32. Only the graphs from 100µM dispersions are shown, however the same pattern of results was observed for all concentrations tested.

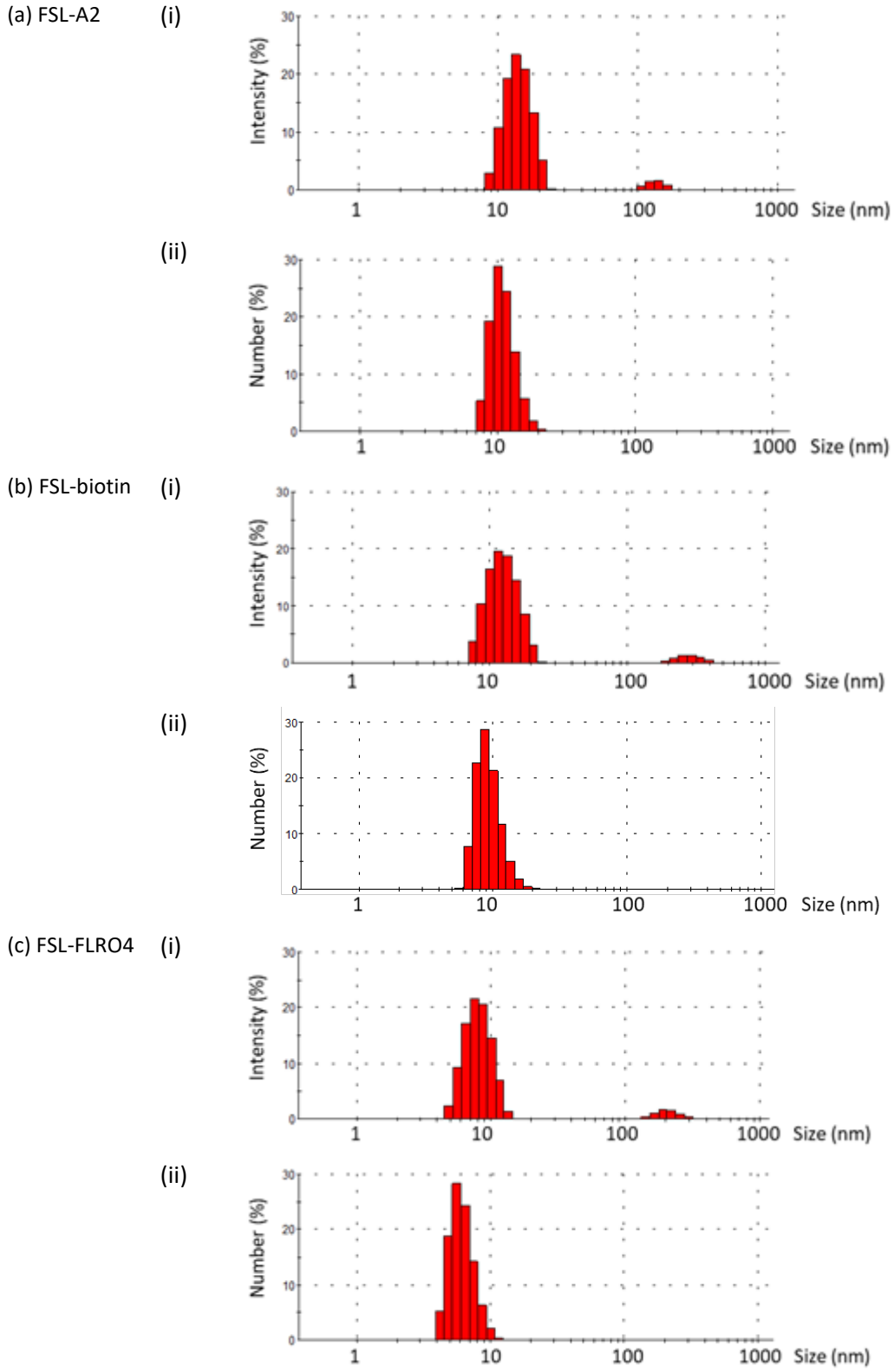

Figure 34 Size of FSL micelles. DLS graphs showing size (diameter) of particles present in (**a**) 100µM FSL-A2, (**b**) FSL-biotin, and (**c**) FSL-FLRO4 dispersions. FSL constructs were dispersed in PBS pH 7.4. Size is shown as (**i**) a function of light intensity and by (**ii**) number. Two populations are seen in the (**i**) size by intensity graphs, however the larger population is not seen in (**ii**) size by number graphs, indicating larger population accounts for ≤1% of total number of particles. This larger population was also seen in PBS diluent and is likely dust contamination.

Figure 35 shows the size of the particles present in the PBS solution used to prepare the FSL micelle solutions. Like the FSL micelle solutions two populations are present when shown by particle intensity (i), but only one when size is shown by number of particles (ii). When size is shown by number of particles a population of particles less than 1nm in size is seen.

The number of particles present in the PBS was very low, much less than in the FSL micelle solutions (see Table 7 for count rate data). Particles are measured by count rate of the particles per second (kilo count per second, kcps). Count rate of particles in PBS ≈20-30 kcps, while in 100µM FSL solutions >150 kcps.

(a) PBS (i)

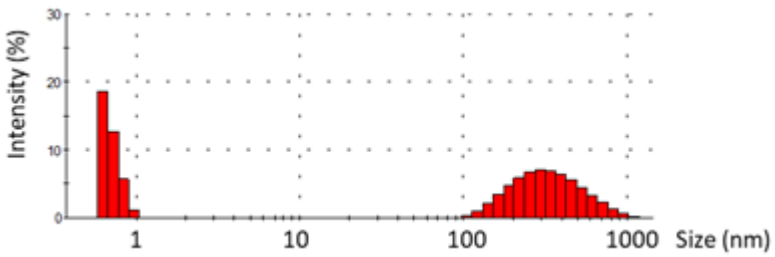

(ii)

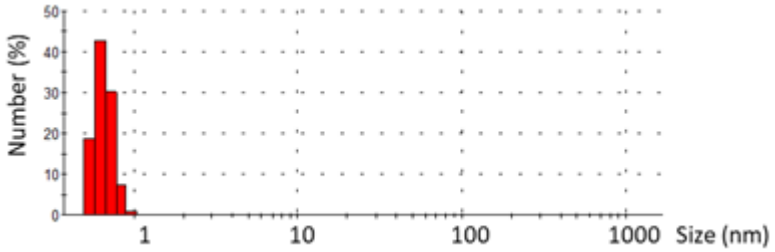

Figure 35 Size of particles present in PBS. DLS graphs showing size (diameter) of particles present in PBS (pH 7.4) diluent used to prepare FSL micelle dispersions. Size is shown as (**i**) a function of light intensity and (**ii**) by number. Two populations are seen in the (i) size by intensity graphs, however the larger population is not seen in (**ii**) size by number graphs, indicating larger population accounts for ≤1% of total number of particles.

Zeta Potential

The zeta potential (net electrical charge) of the micelle particles present in the FSL dispersions were measured by DLS. Figure 36 summarises the zeta potential (charge) data. FSL constructs were dispersed in PBS, pH 7.4.

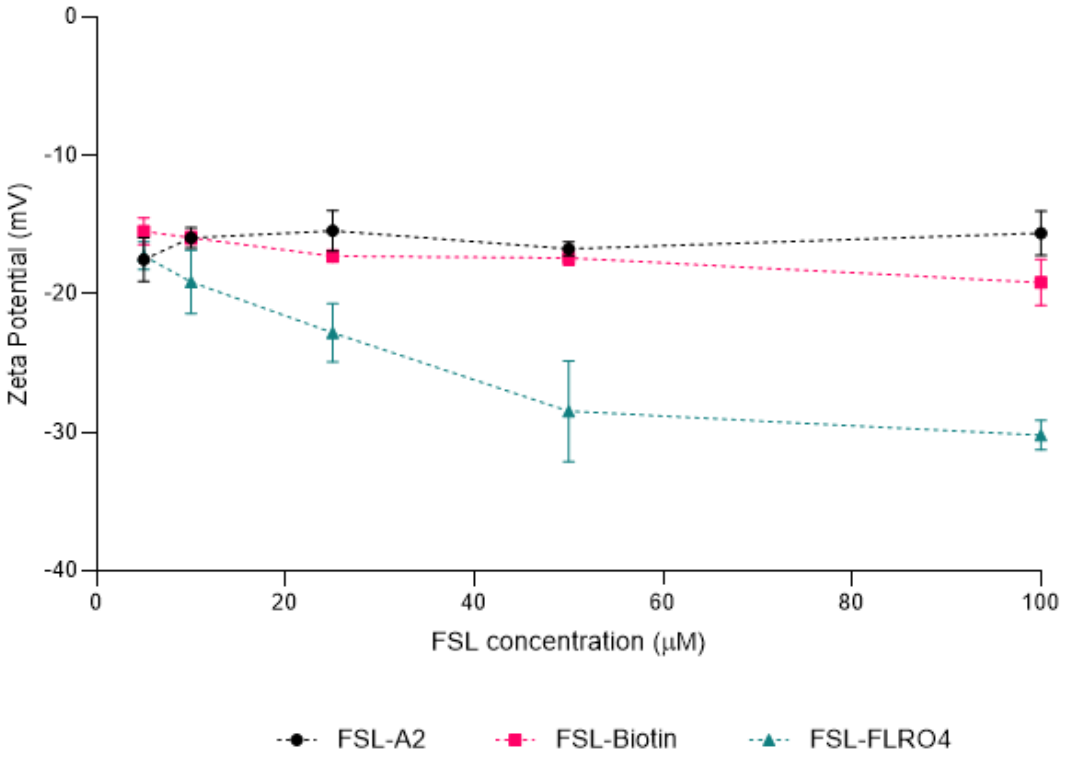

Figure 36 Zeta potential of FSL micelles. DLS was used to measure the zeta potential of micelles present in increasing concentration FSL dispersions (5, 10, 25, 50, and 100µM) suspended in PBS. The micelles of all three constructs, FSL-A2, FSL-biotin and FSL-FLRO4, were negatively charged. Results show mean ± SD, n=3.

The zeta potential (charge) of the FSL-A2 and FSL-biotin particles did not significantly change with increasing concentration, remaining between approximately negative 15 and negative 19mV. In contrast, the FSL-FLRO4 dispersions showed a significant concentration dependent increase in negative charge between 0-50µM, increasing from negative 17 (5µM) to negative 29mV (50µM). From 50-100µM charge plateaued remaining at approximately negative 30mV.

Summary

Micelles (or micelle like nanoparticles) were detected in dispersions of all three FSL constructs (in PBS), from 5µM concentration. When measured by DLS and dispersed in PBS, the CMC for all three constructs was approximately 5µM. FSL-A2 and FSL-biotin micelles had a diameter of approximately 15nm, and FSL-FLRO4 micelles were 7nm. The micelles of all three constructs had a negative zeta potential.

2.1.3 Critical micelle concentration

Once it was established that micelles were likely to be present in the FSL dispersions within our experimental range, further experiments were carried out in an attempt to determine the concentration at which micelles begin to form, the so-called CMC. Due to known methodological variability three techniques were used;

a) Surface tension (pendant drop tensiometry)
b) Fluorescence spectroscopy (pyrene 3:1)
c) DLS analysis (count rate and correlation data)

A) Surface tension – Pendant drop tensiometry

Surface tension was measured by the optical pendant drop method [315] using an Ossila contact angle goniometer (Ossila Ltd, Cat# L2004A1) and software.

Method

1. A series of dilutions of each FSL were prepared in PBS and allowed to stand for 30 minutes at RT.
2. Sodium dodecyl sulphate (SDS) (BDH, cat# 30175) was also analysed (as a known control) and was diluted in superconductivity grade water (so that results could be compared to literature).
3. A drop of each FSL dispersion was suspended from a blunt needle, the drop is pushed out until close to falling. An image of the drop was acquired using the digital camera immediately before the drop falls. Acquiring the droplet image just before detachment provides the most accurate and precise measurement [315].
4. The software analyses the shape of the drop to calculate its surface tension.
5. The needle and syringe were cleaned by rinsing six times with ethanol then six times with PBS/water between samples.
6. Measurements were carried out in triplicate and the mean result reported.

The mean surface tension was graphed against logarithm of the concentration, Figure 37. Below the CMC it was expected that surface tension would be linearly dependent on surfactant concentration. Above CMC surface tension is independent and no longer changes. The CMC point can be calculated from the intersection of the linearly decreasing region and a horizontal line passing through the plateau region at high concentrations (as shown in Figure 37(d)) [327].

Results

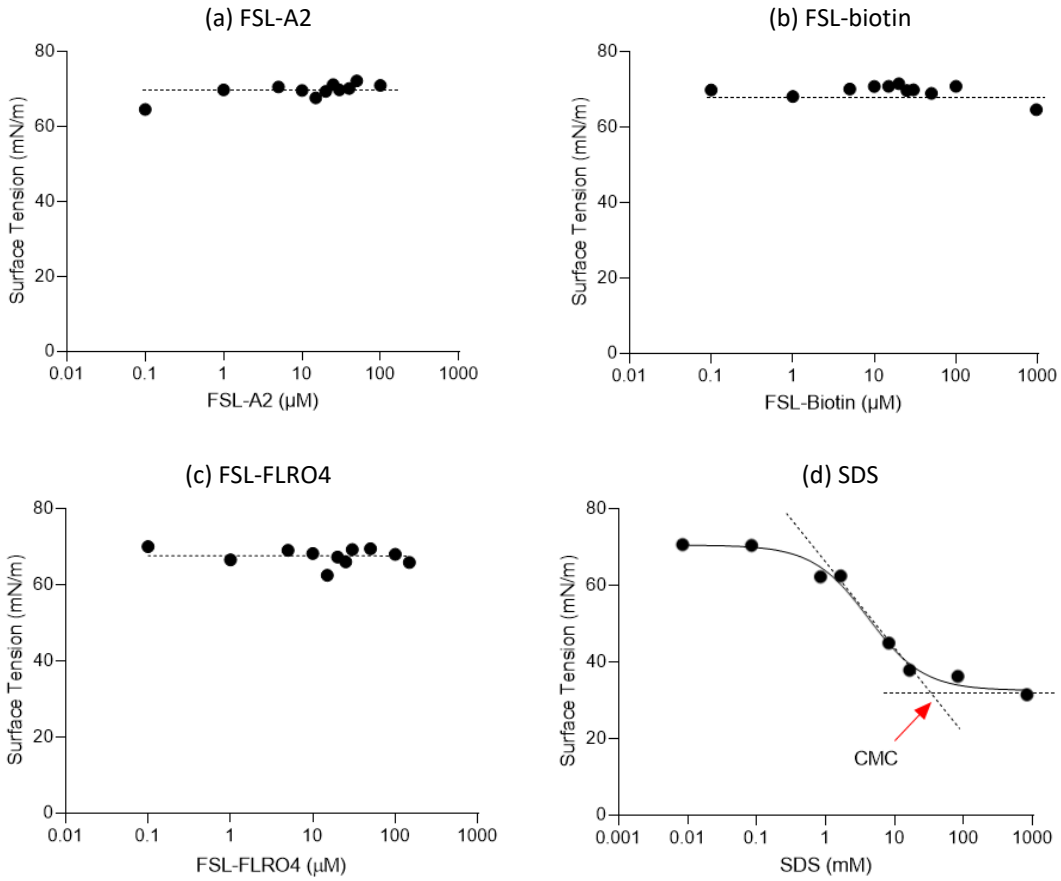

Figure 37 Surface tension of FSL and SDS dispersions. Graphs showing the surface tension of increasing concentration (**a**) FSL-A2, (**b**) FSL-biotin, (c) FSL-FLRO4, and (**d**) SDS dispersions The FSL dispersions showed no change in surface tension, thus no observed CMC value. The surface tension of SDS showed expected concentration dependent decrease. The CMC of SDS was calculated to be 14mM (dispersed in water). FSL's were dispersed in PBS, SDS in water. Note the different x axis scale for SDS.

SDS showed the expected concentration dependent decrease in surface tension. The CMC was calculated to be 14mM (intersection of two lines as indicted on graph), which is slightly higher than reported in literature. SDS was used as a known sample to validate the experiment protocol was working, and this was successfully achieved.

Dispersions of all three FSL constructs showed no change in surface tension, remaining at approximately 70mN/m (slight variation seen between 69-72mN/M), even when very high concentration stock solutions were tested. The surface tension of pure water is 72mN/m.

Because the surface tension of FSL dispersions did not change this technique was unable to determine the CMC of the FSL constructs.

During this experiment it was observed that the FSL dispersions showed a tendency for the suspended droplets to 'climb' the outer surface of the needle, rather than forming a droplet suspended evenly from

the needle base, example image shown below in Figure 38. Despite thoroughly cleaning the needle with water and ethanol between samples this problem continued to occur.

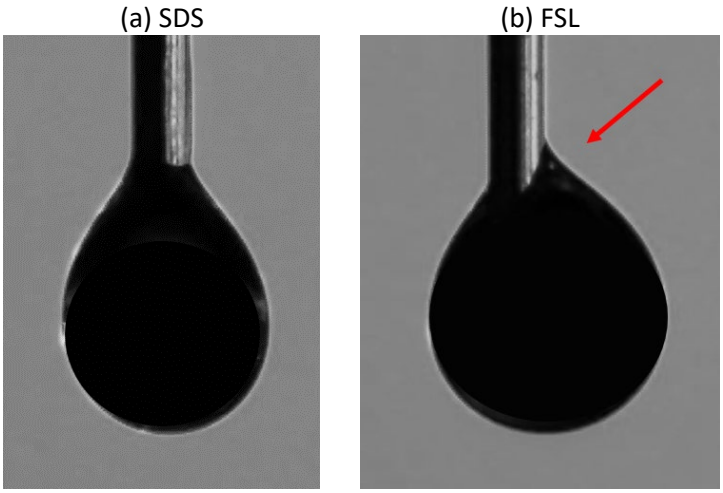

Figure 38 Example pendant drop images. Example images of SDS and FSL pendant drops showing FSL droplet climbing up the side of the needle, indicted by red arrow. This created an **(b)** asymmetrical drop, compared to **(a)** a symmetric droplet of SDS. Image altered to remove reflection from droplet.

This technique does not directly measure the formation of micelles, it actually measures changes to surface tension caused by the amphipathic molecules before CMC is reached. These results show that the FSL constructs do not alter the surface tension of the solution. Possible explanations for this include;

- The climbing of the droplet is most likely due to FSL constructs forming a monolayer on the surface of the needle, making the surface hydrophilic. The needle is then wetted, allowing the droplet to 'climb' the surface of the needle. This does not occur with SDS because it has a single lipid tail, unlike the FSL constructs used in this study which have a double lipid tail (i.e. DOPE). This ability of FSL constructs to wet the surface of the needle makes this method unsuitable.
- It may be energetically unfavourable for the constructs to assemble at the surface/air interface. FSL constructs may prefer to dimerize (dynamically) by their lipid residues rather than to adsorb at the surface of the water and contact with the air. The hydrophobicity of air is significantly lower than the hydrophobicity of the DOPE tail, therefore the FSL constructs may prefer to remain in solution and do not align at the water/air phase. A similar phenomenon is known to happen for some long chain surfactants, polymers and proteins, e.g. BSA, these molecules adopt an orientation/conformation that requires rearranging to allow adsorption at the liquid/air interface and as a result they prefer to diffuse back into the bulk rather than adsorb at the interface [328, 329].

Summary

The pendant drop method was unable to determine the CMC of the FSL constructs due to no detectable change in surface tension. However, it showed that FSL's are good 'wetting' agents.

B) Fluorescence spectroscopy – Pyrene 1:3 method

A fluorescence spectroscopy technique was then used to measure CMC. This technique directly measures the formation of micelles [311], unlike the previous method (tensiometry) which measured the concentration of monomers at the liquid-air interface.

Method

1. A stock solution of 0.1mM pyrene (Sigma Cat#82648-1G) in methanol was prepared.
2. Dilutions of FSL were prepared in PBS and then a 50µL aliquot of the pyrene solution was added, to give a final pyrene concentration of 1 $x10^{-6}$ M in each tube.
3. The volume of each tube was made up to 3 mL with PBS (pH 7.4).
4. The samples were then incubated for 30 minutes at RT protected from light.
5. The fluorescence emission spectra of each sample were measured using an Agilent Cary Eclipse Fluorescence Spectrophotometer. Excitation wavelength was set at 334nm, and emission spectra measured between 360-410nm. Emission slits were set to 2.5nm. Measurements were carried out at 22˚C.
6. The ratio of intensities at 373nm and 384nm, corresponding to pyrene's first and third vibrational bands, were graphed as a function of FSL concentration.
7. SDS diluted in superconductivity grade water were also analysed as a known control.
8. This experiment was repeated twice

Preliminary investigation to determine suitability for use with FSL-FLRO4

Since the pyrene method is based on detection of fluorescence, it is not ideally suited to measuring a molecule which is also fluorescent, such as FSL-FLRO4. It was unknown if the fluorescence of FSL-FLRO4 would interfere with the pyrene fluorescence emissions. The excitation wavelength used for Pyrene was 334nm, and emission was measured at 373 and 383nm. The excitation wavelength of FITC is 492nm and emission is 519nm [330]. Because the excitation and emission wavelengths of FITC and pyrene did not overlap, it was expected that there would be no issues. A preliminary test of 100µM FSL-FLRO4 dispersion with 0.1M pyrene was run to determine if the expected spectra of pyrene could be seen in presence of FSL-FLRO4. The results are shown in Figure 39.

The pyrene emission spectra, as expected, was not altered by the presence of FSL-FLRO4. The vibrionic peaks were clearly visible and there was no significant distortion caused in the pyrene/FSL-FLRO4 emission spectra, Figure 39. Therefore, it was decided to analyse FSL-FLRO4 by this method

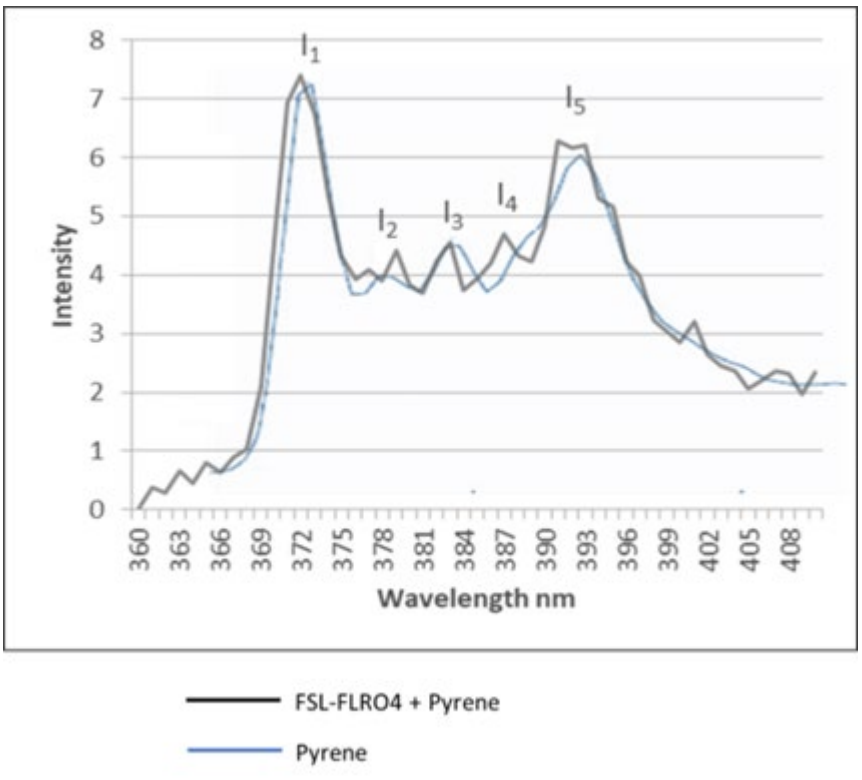

Figure 39 Emission spectra of pyrene and FSL-FLRO4+Pyrene dispersions The standard emission spectra of a pyrene (2 x10^{-6} M) (blue line) is overlaid with the emission spectra obtained from FSL-FLRO4+pyrene dispersion (black line). The vibronic features of the pyrene emission spectrum are present with no obvious distortion caused by addition of FSL-FLRO4.

Results

The expected sigmoid shaped graphs were obtained for FSL-A2, FSL-biotin and SDS samples, as shown in Figure 40. FSL-FLRO4 however did not show a typical sigmoid shape, the second plateau was not reached in the concentration range tested.

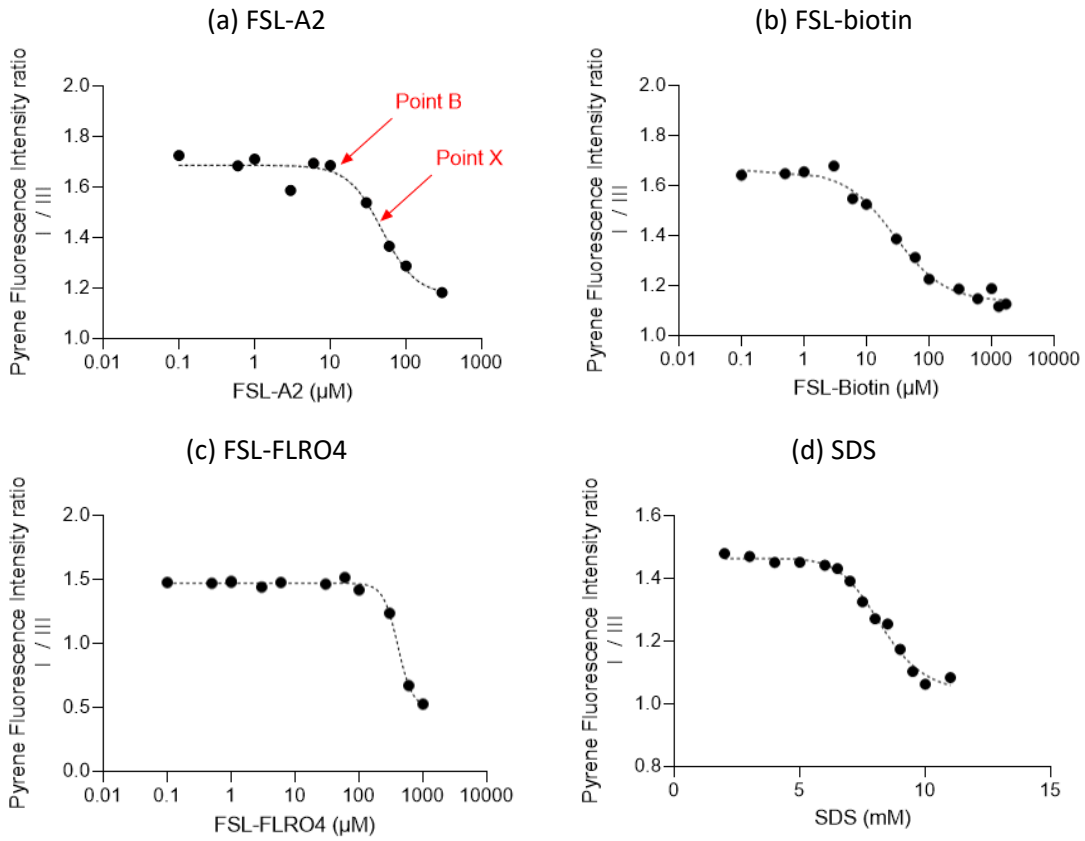

Figure 40 Fluorescence intensity ratio (I/III) vs concentration of FSL and SDS dispersions. CMC values were calculated from point B and point X as indicated by red arrows on graph a. FSL constructs were dispersed in PBS pH 7.4. SDS was dispersed in water. Note different x axis scale for SDS and FSL-FLRO4.

The CMC of SDS (dispersed in water) was calculated to be 8.5mM by mid-point (point X), which is in good agreement with the literature, (8.2mM [62]). SDS was included as a known sample to validate the experiment protocol was working.

The CMC of FSL-A2 and FSL-biotin (dispersed in PBS) was calculated using the midpoint inflection value (point X) to be 48μM and 28μM respectively. The FSL-biotin results were similar to that obtained by Zalygin et al. [260] who reported a CMC of 13μM for FSL-biotin using same technique.

A classic sigmoid curve was not obtained for FSL-FLRO4. The second plateau was not reached. Due to availability limitations of the construct additional higher concentration points could not be tested to determine if a plateau could be reached. Therefore, the mid-point could not be calculated for FSL-FLRO4. Point B was calculated for all three constructs, this showed micelles are beginning to appear at 10µM for FSL-A2, 3µM for FSL-biotin and 136µM for FSL-FLRO4. The FSL-FLRO4 result is significantly higher than the other two FSL constructs. The CMC values calculated from these results are summarised in Table 6.

Table 6 CMC values calculated by Pyrene I/III spectrophotometry method

Sample	Calculated CMC		Literature
	Inflection (Point A) µM	Intersection (Point B) µM	
FSL-A2	48	10	
FS-Biotin	28	3	13µM[260]
FSL-FLRO4	nd*	136	
SDS	8.5mM	6.5mM	8.2mM[62]

nd* could not be determined

FSL constructs dispersed in PBS, SDS dispersed in water

Summary

When measured by the Pyrene 1:3 method using the traditional midpoint of the sigmoid graph as the CMC point, the CMC (in PBS) of FSL-A2 was 48µM, FSL-biotin was 28µM and FSL-FLRO4 could not be determined. When the alternative point B was used, the CMC for FSL-A2 was 10µM, FSL-biotin 3µM and FSL-FLRO4 136µM.

C) DLS count rate

When the zetasizer measures particle size, it also measures the count rate of the particles per second (kcps). This information can be used to help establish when micelles are beginning to form in the solution. Below the CMC the number of particles detected (count rate) is expected to be low and similar to that of the diluent/background noise. Once the CMC is reached and micelles begin to form, the number of particles within the dispersion increases. Therefore the concentration where the count rate begins to increase will correspond to the CMC [310].

Method

Experiments were conducted using a Malvern Zetasizer Nano SP analysing different concentration dispersions of FSL-A2, FSL-biotin, FSL-FLRO4 in PBS. Each solution was measured by the zetasizer as detailed previously (section 2.1.2). The generated count rate data is shown in Table 7. SDS dispersed in water was evaluated in parallel as a control with known CMC parameters.

Results

Table 7 Particle count rate of FSL-A2, FSL-biotin and FSL-FLRO4 dispersions (in PBS)

FSL Concentration µM	Particle Count Rate (kcps)		
	FSL-A2	FSL-biotin	FSL-FLRO4
100.0	240	170	154
50.0	136	106	88
25.0	78	81	55
10.0	70	45	41
5.0	40	38	33
1.0	26	27	32
0.1	30	34	26
(PBS) 0	22	32	32

When the count rate is graphed against concentration, the CMC can be calculated from the intersection of the line extrapolated from the flat plateau section and the rapidly increasing slope (example shown by red lines in Figure 41a) [331]. It was calculated that micelles began to appear in FSL-A2 dispersions at 19µM, FSL-biotin at 14µM and FSL-FLRO4 at 22µM concentration. Graphs used to obtain these values are shown in Figure 41.

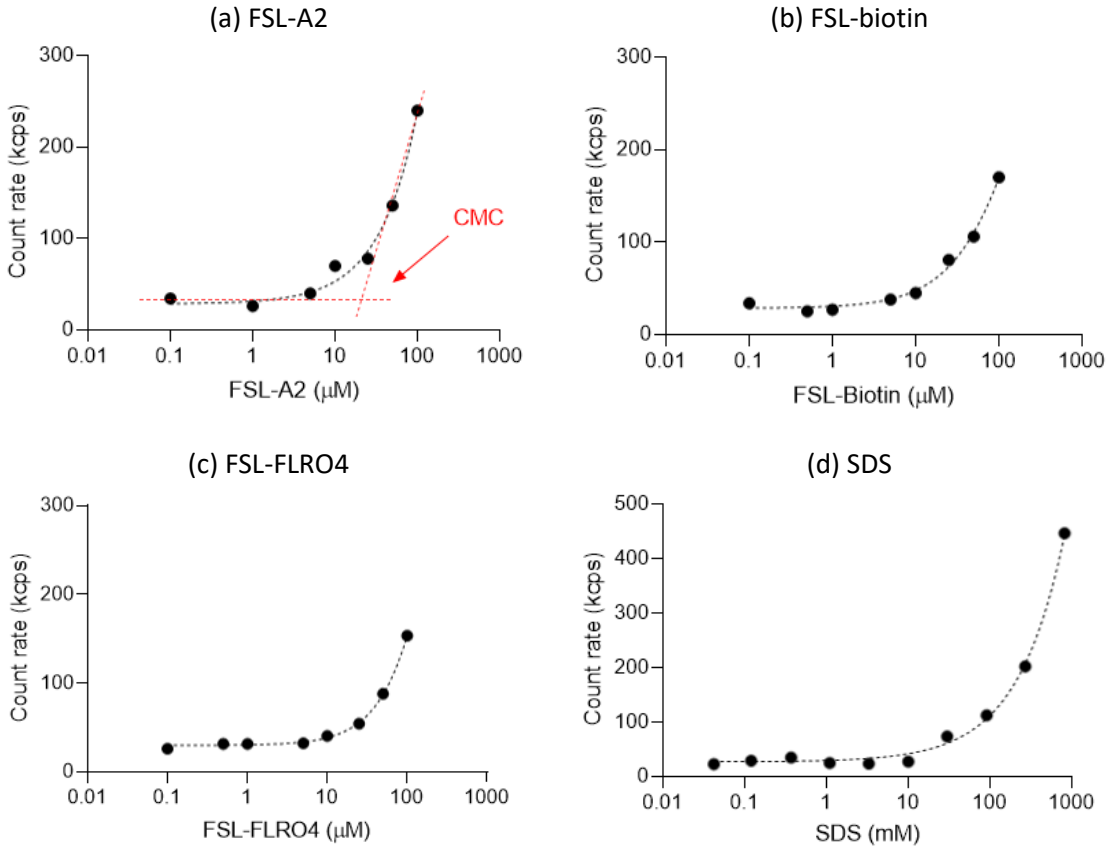

Figure 41 Graphs showing count rate data from DLS analysis of FSL and SDS dispersions. CMC values were calculated from intersection of two extrapolated lines as indicated in red on graph (a). CMC was calculated to be 19μM for FSL-A2, 14μM for FSL-biotin and 22μM for FSL-FLRO4 (dispersed in PBS). CMC of SDS was calculated to be 30mM (dispersed in water). Note different axis scale for SDS.

Summary

Using the DLS count rate data all three constructs showed similar CMC results, the CMC (in PBS) was calculated to be 19μM for FSL-A2, 14μM for FSL-biotin and 22μM for FSL-FLRO4.

D) FSL-FLRO4 - spectrophotometry

An additional technique, fluorescence emission, was used to evaluate the CMC of FSL-FLRO4. While this is not a traditionally used method for CMC determination, it is well known that fluorophores can self-quench when in close proximity with each other, such as when in micelle formation [332]. Therefore, it was hypothesised that by measuring the fluorescence of increasing concentration FSL-FLRO4 dispersions the CMC point might be identified. It was expected that above the CMC the fluorescence of the dispersion would not increase further with increasing FSL concentration. This is because after the CMC all additional FSL will from micelles and consequently be quenched.

Method

1. Dilutions of FSL-FLRO4 (between 0.005 - 400µM) were prepared in PBS and allowed to stand for one hour at RT.
2. A 100µL aliquot was then removed from each dilution and the fluorescence was measured by spectrophotometry using a Tecan Spark® 10M (Tecan.com) (excitation 495nm, emission 520nm)
3. This experiment was repeated on three separate occasions.

Results

The fluorescence of the FSL-FLRO4 dispersions initially increased with increasing FSL concentration, reaching a maximum of 50,000 relative fluorescent units (rfu) at approximately 100µM. Above this concentration fluorescence of the dispersions remained unchanged, even at very high concentrations (up to 400µM), as shown in Figure 42.

The plateau in fluorescence from 100µM indicates that addition of all further FSL above this concentration were most likely forming micelles, which are quenched and therefore contribute no fluorescence. These results indicate that the CMC for FSL-FLRO4 is ≈100µM. These results are not too dissimilar to the result obtained by pyrene method (2.1.3B) in which FSL-FLRO4 CMC was 136µM.

While the increase in fluorescence between 0-90µm was mostly linear, the region between approximately 30 and 50µM was not, shown in red circle (Figure 42). This region showed an uneven increase in fluorescence, there appeared to be two small plateau regions (indicated by red arrows) separated by a sharp increase in fluorescence (Figure 42). These results indicate that the CMC for FSL-FLRO4 is ≈100µM (when measured by spectrophotometry and dispersed in PBS, pH 7.4).

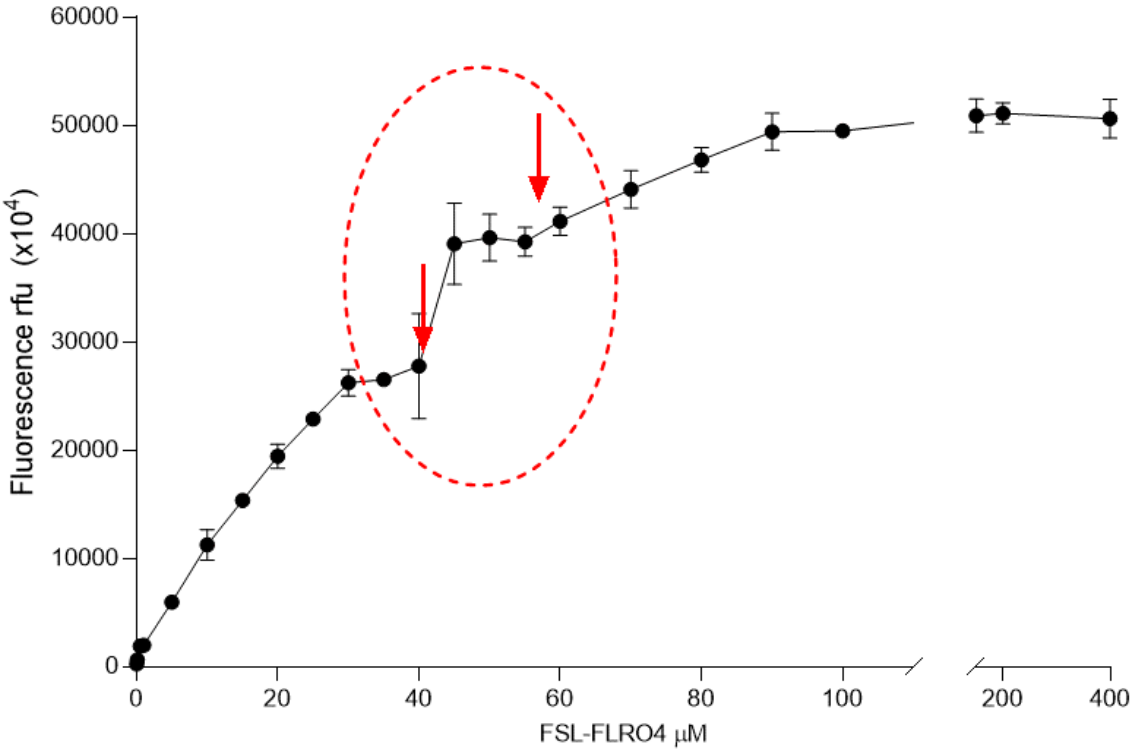

Figure 42 Fluorescence of increasing concentration FSL-FLRO4 dispersions. Fluorescence of the FSL-FLRO4 dispersions increased with increasing FSL-FLRO4 concentration, to reach a maximum of ≈50,000 rfu at approximately 90μM. Above this concentration fluorescence no longer increased and remained at ≈50,000 rfu, as shown in inset graph (concentrations 0-400μM). The increase in fluorescence between 0-90μM was mostly linear, except for the region between 30-60μM, shown in red circle. In this region increase in fluorescence was not linear, and two plateau regions can be seen, as indicated by red arrows, separated by a sharp increase in fluorescence. Note change in scale after break in x axis. Results shown are mean ± SD, n=3.

Summary

These results show that above 100μM all additional FSL-FLRO4 constructs form micelles, therefore by this technique the CMC of FSL-FLRO4 (dispersed in PBS, pH 7.4) is 100μM.

CMC summary

Table 8 summarises the CMC results obtained from the four methods used. Variation was seen between constructs and between results obtained by the different methods. Note that in all cases the FSL constructs were dispersed in PBS (pH 7.4) and SDS in water. In summary these results showed that the CMC of the FSL constructs, when dispersed in PBS were:

- The CMC for FSL-A2 lies within the range 10-50μM, and is likely around 20μM
- The CMC of FSL-biotin is within the range 5-30μM, likely around 14μM.
- The CMC of FSL-FLRO4 was more difficult to determine. The DLS results showed that micelles are forming from concentrations as low as 5μM, and DLS count rate data results gave a CMC of 22μM. In contrast the two fluorescent based methods (pyrene and spectrophotometer) gave much higher CMC values of 100-130μM.

These results and the micelle size results (section 2.1.2 Micelle size and charge) show that micelles were detectable in FSL dispersions from concentrations as low as 5μM for all three constructs. The FSL concentrations used in this study were usually between 10-100μM, therefore these results show that although the CMC may not have been reached, micelles are present in FSL dispersions from 5μM for all three constructs.

According to literature it is likely that even above CMC some monomers will remain in the dispersion alongside the micelles [333, 334]. Therefore, FSL dispersions (greater than 5μM) will contain both micelles and monomer, although the exact ratio is unknown, and so will be referred to as FSL micelle/monomer dispersions.

Table 8 Summary of CMC data for FSL-A2, FSL-biotin and FSL-FLRO4

Sample	**Calculated CMC (μM)**						
	Method of Analysis						
	Pendant drop		**Pyrene I/III**			**DLS**	**Fluorescence**
	Measured	*Literature*	Measured		*Literature*	Measured	Measured
			Point B	Point X			
FSL-A2	nd*		10	48		19	na*
FSL-biotin	nd*		3	28	*13*[260]	14	na*
FSL-FLRO4	nd*		136	nd*		22	100
SDS	14mM	*8.0mM*[335]	6.5mM	8.5mM	*8.2mM*[62]	30mM	na*

nd* could not be determined

na* not applicable

FSL constructs dispersed in PBS, SDS dispersed in water

2.2 Liposome characterisation

Although previous studies have shown that FSL constructs insert rapidly into cell membranes, it was not known if FSL constructs could be successfully incorporated into liposomes, and if so, what effects this would have on the modified liposomes.

A standard protocol for liposome synthesis with three methods for addition of FSL were established. Due to the synthesis technique used FSL constructs could be added to liposomes at three separate stages of their synthesis. It was considered possible that the addition of FSL at different stages could result in variation of FSL distribution within the liposome bilayer membranes. All three methods were employed and compared throughout this project.

After establishment of a standard protocol, initial experiments were carried out to determine what effect the addition of FSL has on liposomes. Liposomes were prepared with varying concentrations of FSL and their physical properties, such as size, shape, bilayer organisation, and charge, were characterised and compared with liposomes containing no FSL.

Basic liposome characteristics were then measured by several methods;

- dynamic light scatter technique (DLS) was used to measure liposome size and charge,
- transmission electron microscopy (TEM) was used to observe liposome morphology and membrane organisation and to confirm DLS size measurement,
- spectrophotometry and enzyme immunoassay were used to detect and confirm presence of FSL.

The primary aims of these experiments were:

- to determine if FSL constructs can incorporate into liposomes, and if so the efficiency of this incorporation.
- to determine what effect (if any) FSL incorporation has on the following liposome characteristics; size, charge, morphology (shape and bilayer organisation), and stability.
- to determine if the method of FSL insertion causes any detectable difference to liposome properties.

2.2.1 Development of method of FSL insertion

Liposomes in this study were prepared by the thin lipid film hydration method. Followed by extrusion using a mini extruder to form liposomes of a uniform size and lamellarity [4, 287]. This method was selected as it is a well-established, simple, and reproducible method which requires relatively inexpensive and simple laboratory equipment. It is one of the most widely used methods (at laboratory scale) for liposome preparation [81, 279]. It consists of three steps, thin lipid film formation, lipid film hydration and extrusion, as discussed previously in section 1.9 Liposome Preparation and shown in Figure 23.

The FSL molecules used in this study are soluble in both aqueous and solvent solutions. Because of this property three different methods for FSL modification of liposomes were investigated in this study;

a) Lipid mix (LM): FSL molecules suspended in solvent (FSL-A2 and FSL-biotin in chloroform:methanol 97:3, and FSL-FLRO4 in methanol) were added with the other lipid ingredients at the lipid mix stage. A diagram of this method is shown in Figure 44.
b) Hydration (H): FSL molecules (dispersed in PBS) were added to the aqueous solution (PBS) used to hydrate the thin lipid film. Shown in Figure 45.
c) Post synthesis (PS): FSL molecules dispersed in aqueous solution (PBS) were added to the liposome dispersion after synthesis was completed (i.e. after extrusion to fully formed liposomes). Shown in Figure 46.

2.2.2 Liposome synthesis protocol

Materials and Reagents

Phosphatidylcholine (L-α-phosphatidylcholine)

Egg phosphatidylcholine (EPC) was obtained as a powder from Sigma USA (1,2-Diacyl-sn-glycero-3-phosphocholine (Sigma, Cat#P3556)) and used without further purification. It was suspended in chloroform:methanol 97:3 to prepare a 500mg/mL stock solution which was stored in a glass vial at -80°C for up to 6 months.

FSL constructs

FSL constructs were reconstituted to prepare 2mg/mL stock solutions which were stored at -80°C. FSL stock solutions were prepared in both aqueous (PBS) and solvent diluents. FSL-A2 and FSL-biotin solvent stock solutions were prepared with chloroform:methanol 97:3. FSL-FLRO4 is not soluble in chloroform so solvent stock solutions of this FSL were prepared in methanol. All solutions, including liposomes,

containing FSL-FLRO4 were stored protected from light. Stock FSL solutions were diluted to prepare working concentration immediately prior to use.

PBS

All PBS used during liposomes synthesis, including for preparation of stock FSL dispersions, was autoclaved and filtered through a 0.22µm filter (Merck, Cat# SLGV033RS) prior to use to remove contaminating particles.

Avanti® Polar Lipids Mini-Extruder

In this study the liposomes were extruded using an Avanti® mini-extruder (Merck, Cat# 610020). This device consists of two gas tight syringes which are connected by a filter holder. This allows for the back and forth passage of the sample through an Avanti® polycarbonate membrane filter 0.1µm (Merck, Cat#610005-1). The extruder was assembled with two filter support membranes (Sigma, Cat# 610014) placed on either side of polycarbonate membrane filter, as shown in Figure 43.

As large multilamellar liposomes pass through the filter pores they break and reform into smaller unilamellar liposomes. The size of the resulting liposomes is approximately dictated by the size of the pores in the membrane filter. A minimum of 11 passes through the membrane is recommended to form uniformly sized unilamellar liposomes [336, 337].

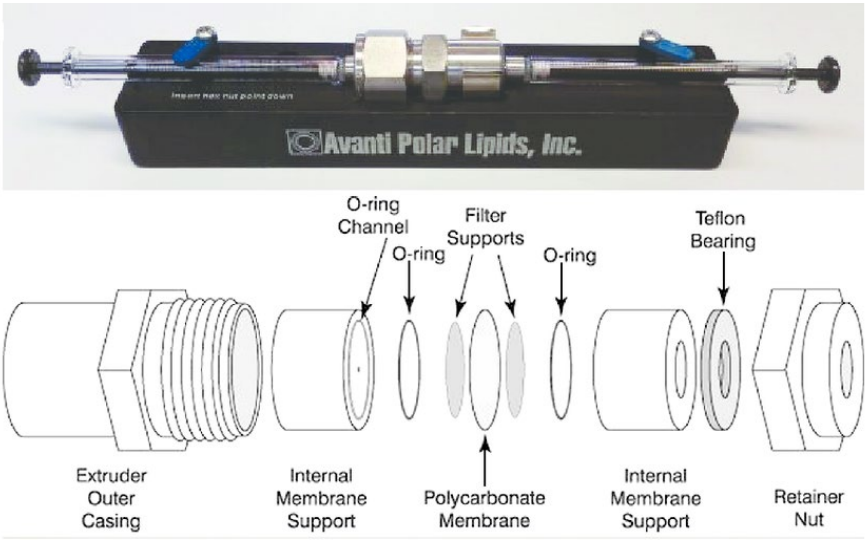

Figure 43 Avanti® Polar Lipids mini extruder. Image adapted from [336].

Basic Liposome Preparation Method

The following method is for the preparation of a 1mL liposome dispersion at 10mg/mL lipid concentration with an approximate size (diameter) of 100nm. All synthesis procedures were carried out at RT (18-22°C) unless otherwise noted.

1. Thin film preparation

1.1. A 10mg/mL solution of egg phosphatidylcholine (EPC) was prepared by diluting appropriate volume of EPC stock solution with chloroform:methanol 2:1.

1.2. A 1mL aliquot of 10mg/mL EPC solution was placed into an evaporating flask and the solvent removed by evaporation using a rotary evaporator at 40°C (Büchi, Switzerland). This formed a thin lipid film on interior surface of flask.

1.3. If the next step (hydration) was not carried out immediately the thin films could be stored in a vacuum desiccator overnight at 4°C.

2. Hydration

2.1. The dried thin film was hydrated with 1mL of PBS to form a 10mg/mL lipid solution. The choice of hydrating solution is dependent on the intended application of the liposome dispersion. In this project phosphate buffered saline pH 7.4 was used, unless otherwise noted, as this is suitable for use in most biological assays.

2.2. The flask was agitated for 10-15 minutes to help re-suspend the dried lipid film and then allowed to stand for a minimum of two hours at RT, or overnight at 4°C.

3. Extrusion

3.1. The liposome solution was extruded by passing the solution back and forth 19 times through a 0.1µm polycarbonate filter, using an Avanti® mini-extruder. The mini extruder was assembled and used according to manufacturer's instructions [336].

3.2. Liposome dispersions were stored at 4°C and used within 7 days of synthesis, unless otherwise noted.

Note: Extrusion must be carried out above the T_m of all the lipid components (to ensure liposome membrane in liquid disordered state). T_m of EPC is <0°C (see Table 2), therefore there was no requirement to heat the liposome dispersion during extrusion as the liposome membrane is in liquid disordered state at RT.

4. Addition of FSL

FSL constructs were added to liposomes at three different stages of the liposome synthesis: lipid mix, hydration and post synthesis. The basic liposome synthesis method was followed as detailed above, with variation to the following steps as described below. After addition of FSL liposomes were stored at least 24 hours at 4°C before use, unless otherwise noted.

Lipid Mix (LM) addition of FSL

1.1 An appropriate aliquot of FSL stock solution (suspended in solvent) was added to the EPC solution before drying down to form the thin lipid film, see Figure 44.

Hydration (H) addition of FSL

2.1 An appropriate aliquot of FSL stock solution (in PBS) was added to 1mL of PBS, which was then used to hydrate the thin lipid film, see Figure 45.

Post Synthesis (PS) addition of FSL

3.2 After extrusion an appropriate aliquot, depending on concentration required, of FSL stock solution (suspended in PBS) added to the fully formed liposome solution, see Figure 46.

Liposome washing

The FSL modified liposome prepared in this research were used without an additional wash/purification step after the addition of FSL constructs. A primary objective of this research was to design a simple method for modification of liposomes using Kode constructs. It was anticipated that FSL constructs could be applied as an 'add on' addition to fully formed liposomes without the need for additional purification (washing steps). Purification (washing) can be time consuming and can negatively impact the quality of final produce (dilution, loss of product, leakage of encapsulated materials).

Therefore, unwashed liposomes were used so that the mechanisms of FSL construct interaction with liposomes could be determined. It was hoped this would enable the identification of potential limitations and advantages, in order to determine how FSL can be best used for labelling liposomes.

a) Lipid mix (LM) method of FSL insertion

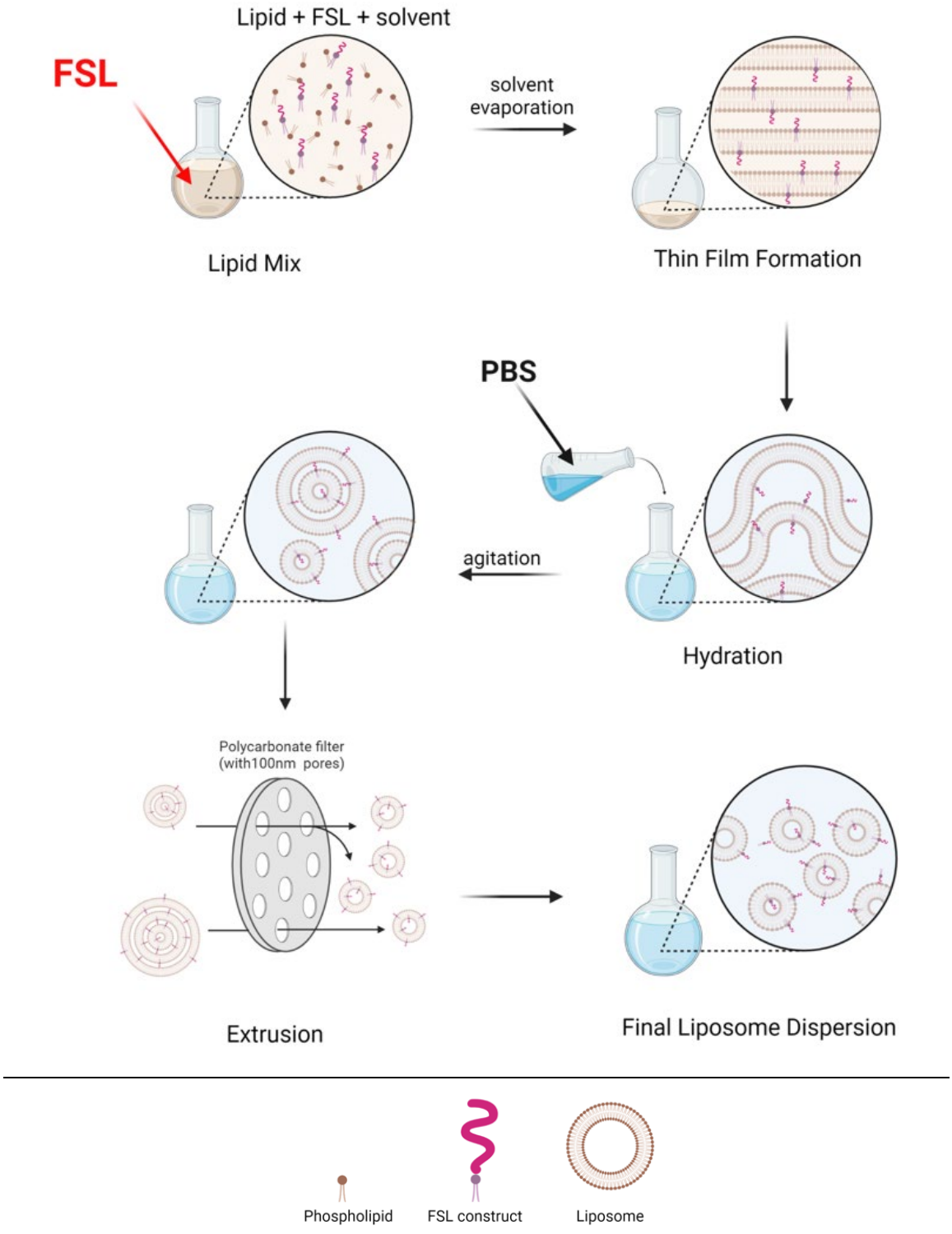

Figure 44 Lipid Mix (LM) method of FSL insertion into liposomes. FSL constructs are added with the lipid ingredients before formation of the thin lipid film. Image not to scale. Adapted from [288]

b) Hydration (H) method of FSL insertion

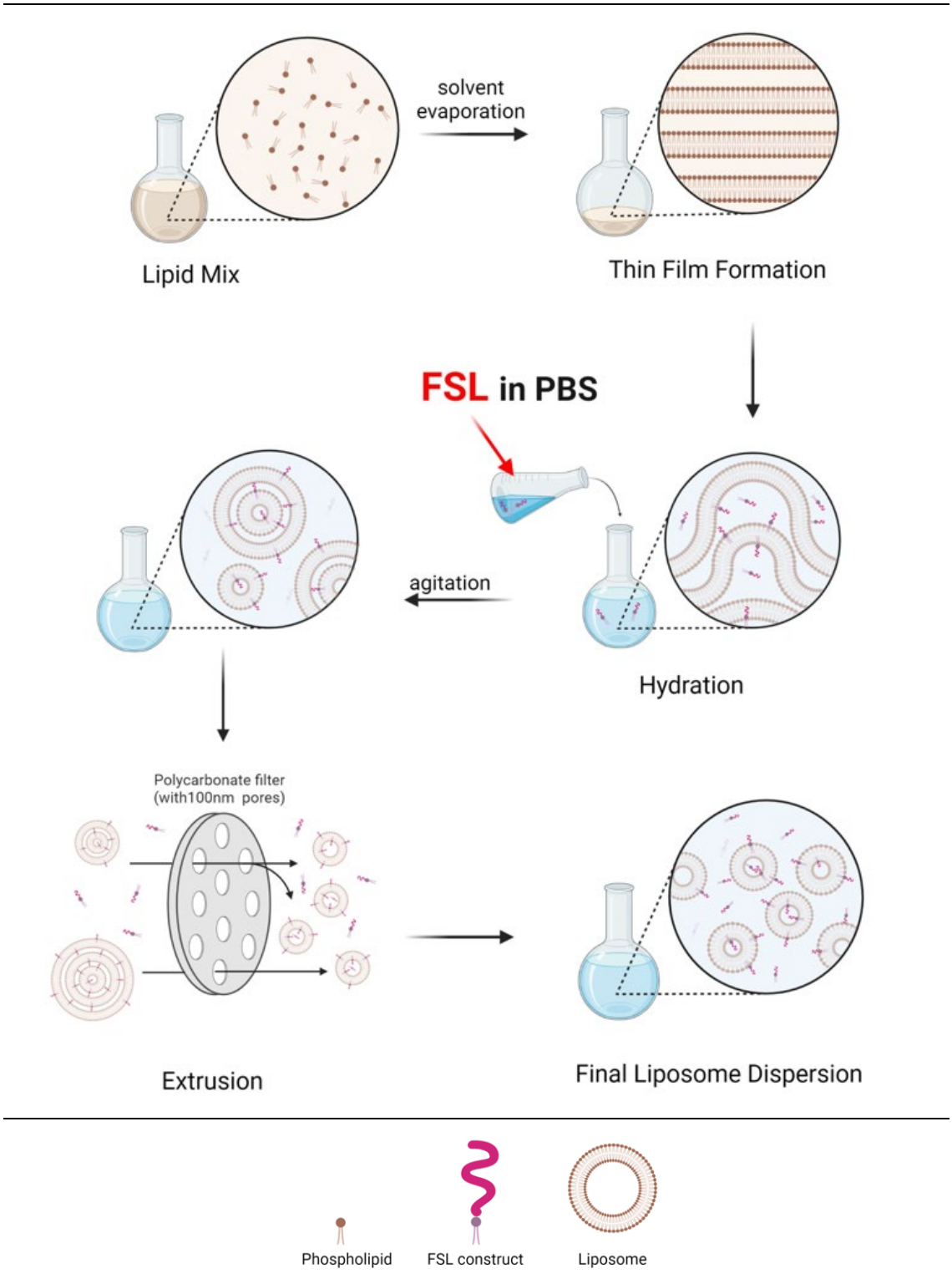

Figure 45 Hydration (H) method of FSL insertion into liposomes. FSL constructs are added with the aqueous hydrating solution. Image not to scale. Adapted from [288]

c) Post synthesis (PS) method of FSL insertion

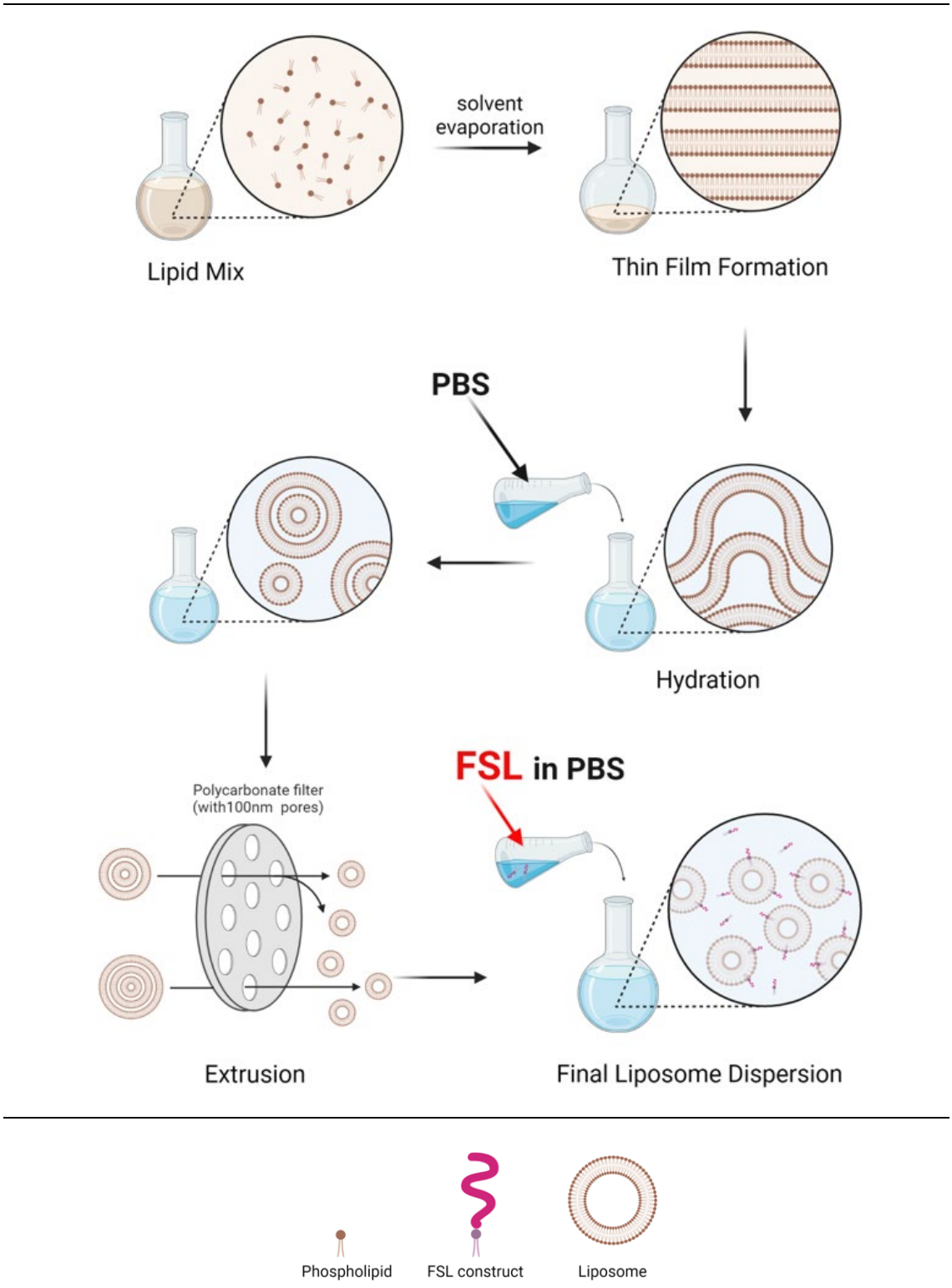

Figure 46 Post synthesis (PS) method of FSL insertion into liposomes. FSL constructs are added to fully formed liposomes. Image not to scale. Adapted from [288]

Freeze thaw step

A freeze thaw step (comprised of multiple freeze/thaw cycles by submerging in liquid nitrogen and thawing at 37°C) is often employed in liposome preparation. The purpose of this step is to help reduce lamellarity [284] and to increase encapsulation of water soluble molecules and equilibrate solute concentration between liposome interior and exterior environment [338]. Multiple freeze thaw cycles disrupt the liposome membrane which helps to increase encapsulation by allowing drug molecules to diffuse into the liposome, in addition cryo-concentration (where water freezes and excludes molecules into a concentrated area, this can help to increase diffusion of drugs into the liposome which the dispersion is in a semi frozen state [339].

Initial experiments were conducted both with and without the freeze/thaw step included in the method. The freeze thaw step was carried out after the two hour hydration step and before extrusion; the liposome dispersion was submerged in liquid nitrogen for approximately one minute until completely frozen, and then immediately thawed by placing in 37°C water bath, this was repeated five times.

TEM analysis showed that no morphological differences between liposomes prepared with freeze/thaw step and those without. However, it is possible that the freeze/thaw process could alter FSL distribution within the liposomes prepared by H and LM methods. The freeze/thaw step would not affect the distribution of FSL in PS liposomes, as in these liposomes the FSL is added after the freeze/thaw has been performed.

During the period these experiments were conducted access to liquid nitrogen was limited. In addition, the ability to prepare liposome samples with excellent reproducibility to allow comparison of results between different liposome batches and between experiments was of fundamental importance to this study. Therefore, as no morphological differences were observed when the freeze/thaw step was included, (and as encapsulation studies were not performed in this project – freeze/thaw step known to improve encapsulation) this step was omitted. By refining the synthesis protocol and removing unnecessary steps, it was hoped that reproducibility between batches would be improved.

Example images of liposomes prepared with and without the freeze/thaw step are shown in Figure 47. No morphological differences were observed.

a) Liposomes prepared with freeze/thaw step

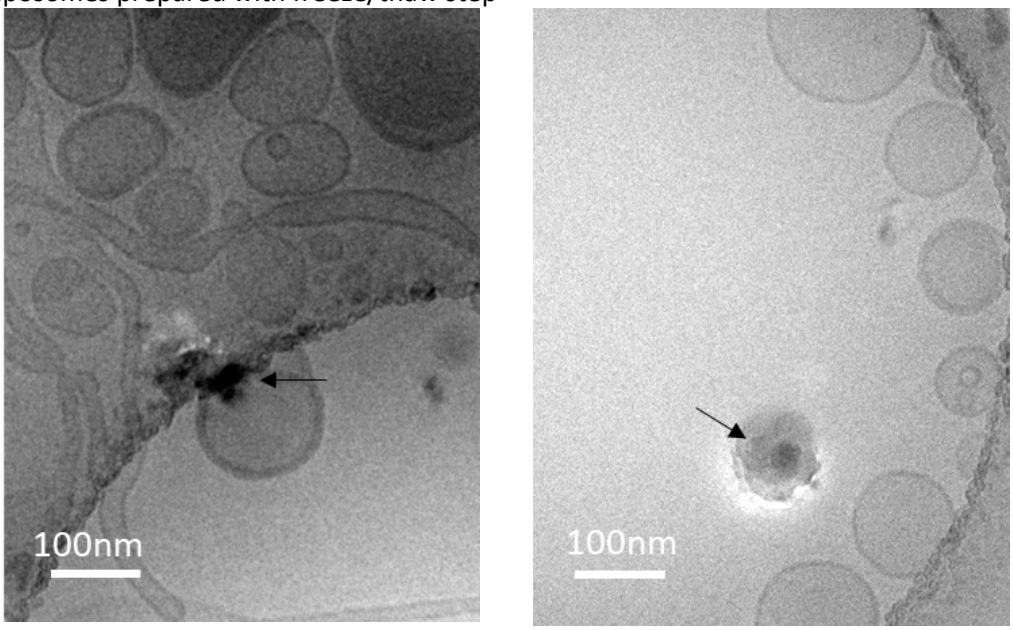

b) Liposomes prepared without freeze/thaw step

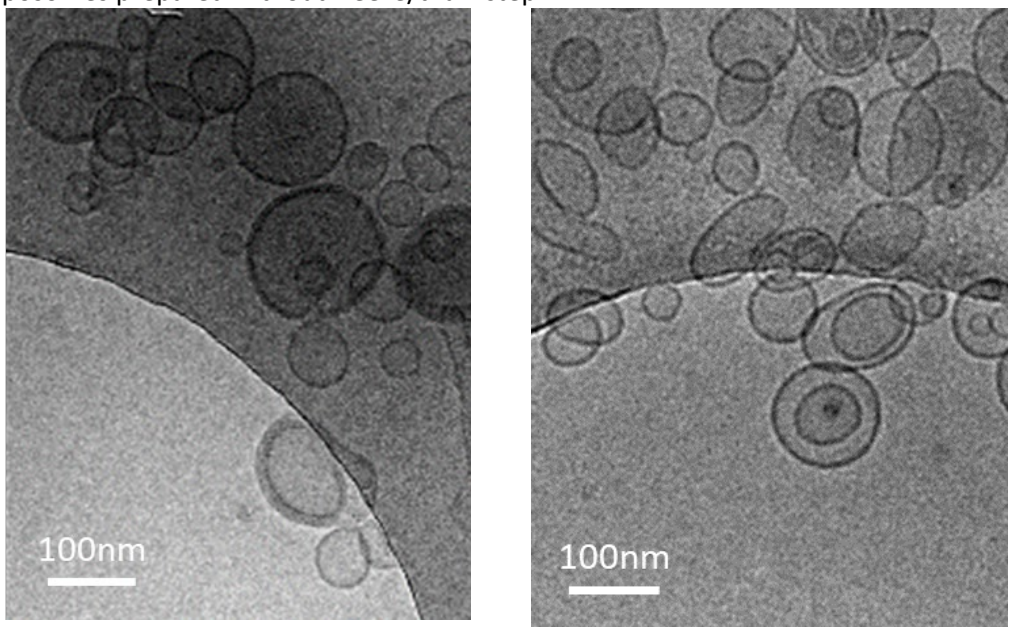

Figure 47 TEM images showing liposomes prepared with or without freeze thaw step. (**a**) Images in top row show liposomes prepared with five times freeze/thaw step and extruded through 100nm membrane. Black arrows show ice artefact. (**b**) Images in bottom row show liposomes prepared without the freeze thaw step, extruded through 100nm membrane. No significant morphological differences were observed.

2.2.3 FSL distribution in liposomes

The effect on the final liposome product of adding FSL constructs, at these three different points of synthesis was not known. However, several theoretical possibilities of FSL distribution which could result from these three different methods are discussed below.

It was anticipated that FSL constructs could easily and rapidly integrate into the liposome phospholipid bilayer membrane (internal and/or external leaflets). In addition, because liposomes were not washed after addition of FSL, depending on method of preparation unincorporated FSL (monomers and/or micelles) could also remain in the liposome dispersion; either in the external supernatant and/or encapsulated within the aqueous interior of the liposome core, as shown in Figure 48. It should also be noted that the initial FSL distribution formed during synthesis may change over time.

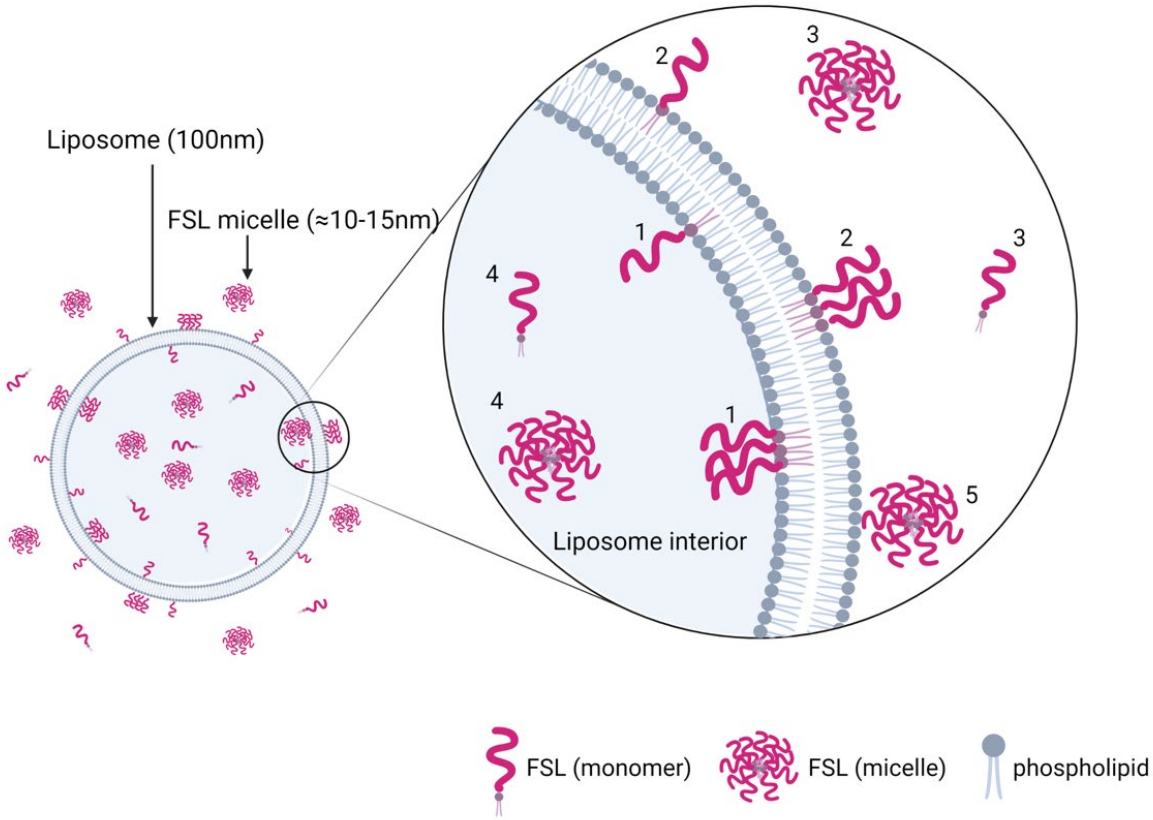

Figure 48 Possible locations of FSL within a liposome dispersion FSL may integrate into the liposomes (**1**) inner bilayer leaflet and (**2**) outer bilayer leaflet. FSL (monomer/micelle) may be present in the (**3**) supernatant surrounding the liposome and it can be (**4**) encapsulated within the internal aqueous compartment, and (**5**) FSL micelles may associate with bilayer membrane without becoming incorporated into it (diagram approximately to scale). Created with BioRender.com.

Liposomes in this study were composed of egg phosphatidylcholine (EPC). EPC was chosen as the primary liposome constituent for several reasons; phosphatidylcholine phospholipids have a critical packing parameter of ≈0.6 and consequently form stable bilayer membranes/vesicles (see section 1.5.2)[340]. In addition, EPC has a T_m of minus 15°C to minus 5°C. Throughout this study the liposomes were always above the T_m of EPC and therefore the liposome membranes were always in a liquid disordered phase (see section 1.5). This was advantageous as it made it easier to work with the liposomes as all synthesis procedures could be carried out at RT (extrusion must be carried out above T_m, other phosphatidylcholines have much higher T_m, see Table 2, and require heating). In addition, because the liposome membrane was in the liquid disordered phase this meant that FSL constructs would be able to freely move laterally within the membrane and rotate about their axis.

It is known that some lipids show a tendency to cluster together and form domains [105, 109]. It was not known how FSL constructs would behave, they may distribute evenly throughout the membrane after synthesis, or may show a preference to cluster together. It should be noted that the detection system, especially if a multivalent system was used such as streptavidin (which can bind up to four biotin molecules) and IgM (which has 10 antigen binding sites), could cause clustering as a consequence of labelling. In addition, the presence of >30% cholesterol associated with domain formation [341].

Movement of FSL between bilayer leaflets (flip-flop) is possible, however this is likely to be very slow if it occurs at all (due to large hydrophilic head group/spacer of FSL constructs which would impede their ability to move through the hydrophobic inner membrane space) [115, 117, 118]. Therefore, if asymmetry exists between inner and outer membranes it is unknown exactly how long this would persist but is likely to be days at least.

While it is known that FSL can move from monomers/micelles present in the dispersion to being associated/incorporated in the liposome membranes, it was not known whether all FSL would incorporate into the liposomes leaving no monomer/micelles remaining in the supernatant or if a portion of FSL would remain unbound in the supernatant as monomer/micelles. Furthermore, it was not known if after binding/associating with the liposome if FSL could leave the liposome membrane and move back into the supernatant.

FSL inserted by Lipid Mix (LM) protocol

In this method the FSL is incorporated into liposomes during the first step of synthesis, Figure 44. The FSL constructs are suspended in solvent together with all of the other lipid ingredients e.g. EPC. The solvent is removed by evaporation to form thin lipid films. Because the FSL constructs have been suspended together with the other lipids the FSL is expected to distribute throughout the lipid films (which go on to form the liposome membrane). Therefore, the final liposomes can have FSL located on their inner and/or outer leaflets of the bilayer membrane.

An important consequence of this method is that no FSL monomers or micelles are present in the final liposome dispersion, all of the FSL constructs are incorporated into the lipid film during the first stage of liposome synthesis, and therefore all FSL is incorporated into the liposome membrane.

The FSL constructs may or may not be evenly distributed throughout the liposome membranes. If the FSL constructs are evenly distributed throughout the dried lipid films, this would lead to an even distribution of FSL between internal and exterior bilayer leaflets of the synthesised liposomes. However, an uneven distribution could also occur. The drying down process (to from thin lipid film) can lead to 'de-mixing' of different phospholipid moieties [342]. As solvent is removed the concentration of lipid in the remaining dispersion increases. The lipid moiety with the lowest solubility will precipitate first, forming thin lipid layers before the more soluble lipid begins to form lipid layers. If this de-mixing occurs lipid layers will form which have very different compositions, resulting in formation of liposomes with uneven distributions of the lipid components. Furthermore, at higher concentrations FSL constructs may show a preference to cluster together rather than distribute homogenously (even if de-mixing does not occur).

Therefore, as a result the final liposome dispersion may consist of a mix of liposomes with very different FSL distributions; FSL could be found on interior membrane leaflet only, exterior leaflet only, both leaflets, clustered, not clustered, or in any combination of these, see Figure 49.

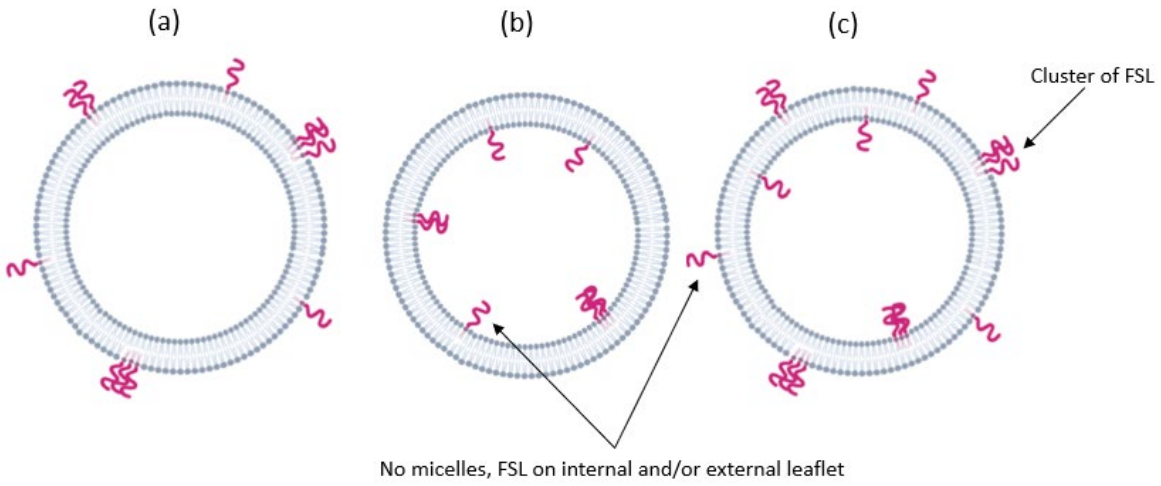

Figure 49 Possible distribution of FSL constructs in liposomes prepared by the LM method. No free FSL (monomer or micelle) is present. FSL may be present on (**a**) external surface of liposomes only, (**b**) on internal surface of liposome, or (**c**) on both the external and/or internal surface of the liposomes. FSL may be evenly distributed or could be clustered together. A mixture of liposomes with different expressions of FSL could also be present. Diagram approximately to scale. (Note: liposome shown are ≈60nm diameter, not 100nm as synthesised in this study). Created with BioRender.com.

After liposome formation FSL molecules are likely to rapidly diffuse laterally within a membrane, so distribution may become more evenly dispersed within each leaflet with time (hours). Alternatively, if FSL constructs prefer to cluster together they may become more clustered with time.

Although it is possible for phospholipids to translocate between membranes (flip-flop) as discussed above and in section 1.5.6 this movement, if it occurs, is expected to be very slow, especially in the case of FSL-A2. Therefore, if uneven distribution exists between inner and outer membrane leaflets at synthesis it is likely to persist for some time (>days) [115, 117, 118] .

FSL inserted by Hydration (H) protocol

In this method the FSL constructs are suspended in the aqueous solution used to hydrate the thin lipid films, as shown in Figure 45.

Because the FSL constructs (monomer/micelle) are added during hydration while thin lipid films are detaching and closing to form vesicles, FSL monomer/micelles will be encapsulated within the liposome internal aqueous cavity, as well as being present in the external supernatant. Therefore, FSL can label both the interior and exterior leaflets of the liposome membrane. In addition, because liposomes were used unwashed, FSL monomer and/or micelles will be present both within the internal aqueous core of the liposome and in the external supernatant.

As with lipid mix liposomes FSL can move freely laterally within membranes, so they could distribute evenly throughout leaflet, or could cluster together. Figure 50 shows the possible locations of FSL in liposome dispersion after addition by hydration method.

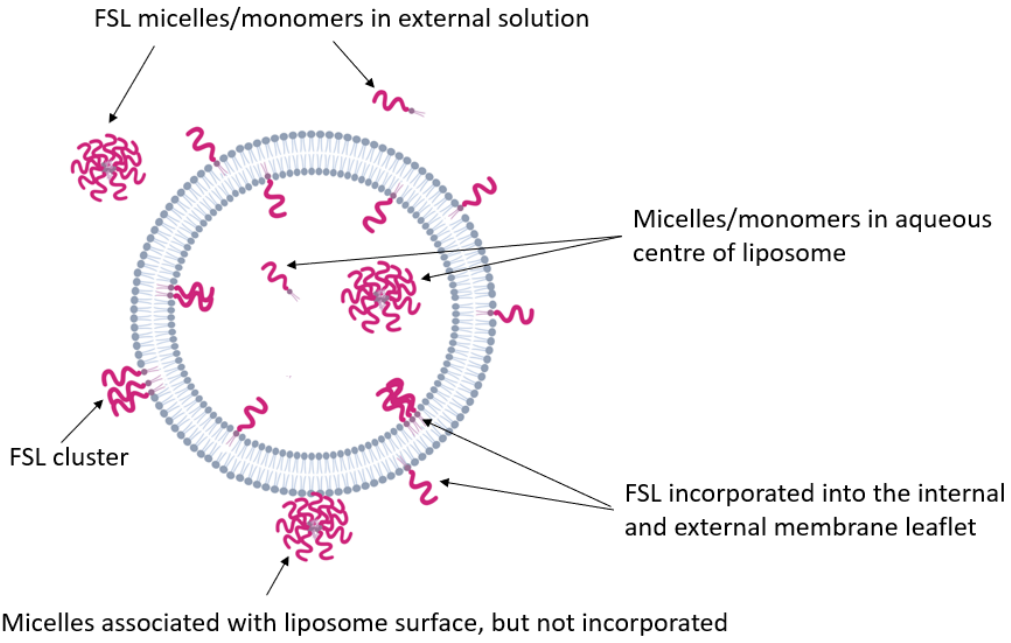

Figure 50 Possible distribution of FSL constructs in (unwashed) liposomes prepared by H method. FSL is present on external and internal liposome membrane. FSL may be evenly distributed or could be clustered together. Free FSL (monomer or micelle) is present within the liposome aqueous centre and in the supernatant surrounding the liposome. FSL micelles may bind/associate with liposome membrane without FSL constructs becoming incorporated. Diagram approximately to scale. (Note: liposome shown are ≈60nm diameter, not 100nm as synthesised in this study). Created with BioRender.com.

FSL inserted by Post Synthesis (PS) protocol

In the PS method FSL is added after the liposome synthesis is complete, as shown in Figure 46. Because the liposomes are fully formed before the FSL is added there is no opportunity for FSL to enter the liposome interior and label the internal leaflet. FSL can insert into the exterior bilayer leaflet, and because the liposomes were used unwashed FSL monomers/micelles will be present in the supernatant.

FSL can move freely within the external leaflet so distribution could be even or clustered, as discussed previously flip-flop is unlikely to occur. Free FSL (monomer/micelle) will be present in the external supernatant only, and not within the liposome's aqueous interior, as shown in Figure 51.

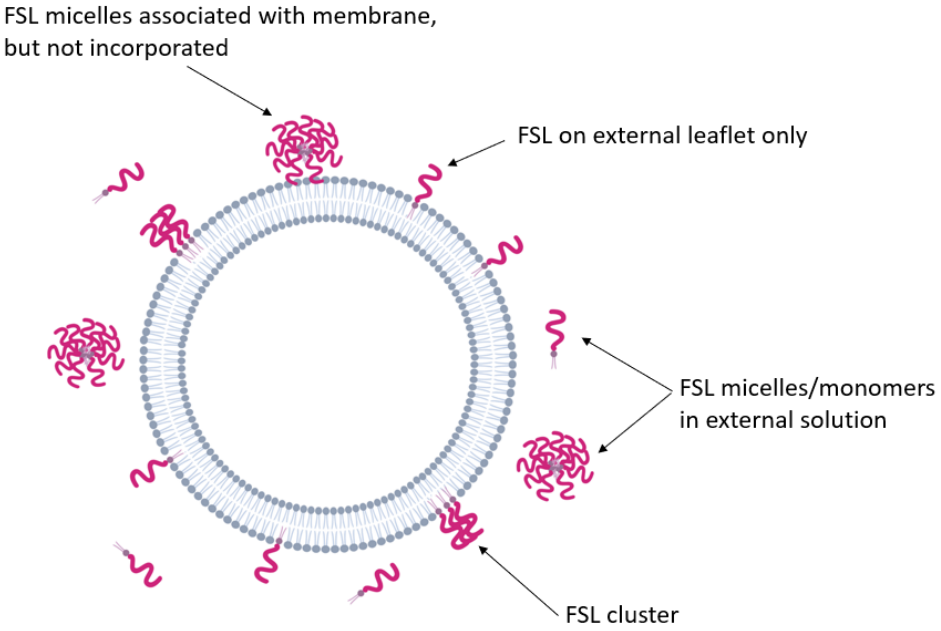

Figure 51 Possible distribution of FSL constructs in liposomes prepared by PS method. FSL constructs are only present on exterior of membranes. Free FSL is present in the supernatant. FSL incorporatd into the membrane may be evenly distributed or could be clustered. FSL micelles may bind/associate with membrane without becoming incorporated. . Diagram approximately to scale. (Note: liposome shown are ≈60nm diameter, not 100nm as synthesised in this study). Created with BioRender.com.

2.2.4 Liposome lipid ratios

Liposomes in this study were prepared using EPC at a concentration of 10mg/mL, which equates to 12.3 $\times 10^{-3}$ M. Table 9 shows the liposomal molar ratio of EPC and FSL, for the range of FSL concentrations commonly used in this study. FSL mol% is the percentage of FSL constructs in the liposome (by molecule).

Table 9 Molar ratio of liposome lipids (FSL and EPC) commonly used in this study

FSL µM	EPC µM	FSL mol%	Lipid Ratio FSL:EPC
250	12,300	2.00	2.5:123
100	12,300	0.80	1:123
50	12,300	0.40	0.5:123
10	12,300	0.08	0.1:123

Theoretical calculation of number of FSL constructs per liposome

The approximate number of FSL molecules per liposome can be calculated. The following mathematical equation can be used to determine the number of lipid molecules in a liposome [343]. This information can then be used to calculate the number of FSL molecules per liposomes as shown in Equation 4.

$$N_{tot} = \frac{\left[4\pi\left(\frac{d}{2}\right)^2 + 4\pi\left[\frac{d}{2} - h\right]^2\right]}{a}$$

N_{tot}	Total number of lipid molecules in liposome
d	Diameter of liposome
h	Thickness of the bilayer (5nm)
a	Lipid head group area (for PC 0.71nm^2)

Equation 4 Total number of lipids in a unilamellar liposome

In this equation the surface area of each of the two monolayers is calculated and added together. The total surface area is then divided by the surface area of one lipid molecule (a) to find the approximate number of lipid molecules in a liposome with a particular diameter. The head group area of EPC is 0.71nm^2, therefore the above equation can be simplified as shown in Equation 5.

$$N_{tot} = 17.69 \times \left[\left(\frac{d}{2}\right)^2 + \left(\frac{d}{2} - 5\right)^2\right]$$

Equation 5 Number of lipid molecules in a 100nm unilamellar phosphatidylcholine liposome

Using Equation 5 the number of lipid molecules in a 100nm diameter EPC liposome will be approximately 80,000. From this we can calculate that when 100µM FSL is added to liposomes; the molar ratio is 1:123 FSL:EPC, or 0.8 mol%, therefore there will be approximately 640 FSL molecules per liposome (80,000 × 0.8% = 640). Table 10 lists the number of FSL molecules per 100 nm liposome for several FSL concentrations commonly used in this project.

Table 10 Theoretical number of FSL molecules per liposome (100nm diameter)

FSL µM	FSL mol%	Approximate number of FSL molecules per liposome
250	2.00	2000
100	0.80	640
50	0.40	320
20	0.20	160
10	0.08	64

These calculations rely on several assumptions;

- that all the liposomes are unilamellar and 100nm in size,
- that FSL distributes uniformly across all available liposomes,
- that all FSL is incorporated into the liposomes. In lipid mix this is likely but will not be the case for the other two methods of FSL insertion; FSL is known to readily coat surfaces so at least some FSL will be lost to the vessel surfaces and laboratory apparatus (e.g. extrusion filter membrane). It is also possible that some FSL could remain in solution phase and never insert.

Due to method of FSL addition, liposomes prepared by lipid mix (LM) and hydration (H) method can have FSL on both the internal and external liposome bilayer membranes (see section). While liposomes prepared by post synthesis (PS) method labelling should only occur on the external surface of the liposome. Therefore, (assuming all FSL inserts, and LM liposomes have a relatively homogenous distribution) PS liposomes should have a much higher density of FSL molecules on their surface than LM and H liposomes.

For example, a 100nm liposome labelled with 100μM of FSL, then the PS liposomes will have a maximum of 640 FSL constructs on their external surface, while LM and H will have only a maximum of 350, assuming all FSL becomes homogenously inserted. (The external leaflet contains 55% of lipid molecules, and internal membrane contains 45%).

These calculations are approximate only, however they are useful to provide a rough guide to relative ratios of EPC and FSL and possible theoretical maximum insertion numbers as a consequence of the three different methods of FSL addition.

2.2.5 Liposome size and charge

Experiments were conducted using a Malvern Zetasizer Nano SP. Automatic attenuation setting and non-invasive back scatter optics at 173° angle were used. The correlation curves and the intensity weighted distributions were obtained using the built in analysis software.

Method

1. Liposomes were prepared containing varying concentrations of FSL according to protocol 2.2.2.
2. Control liposomes containing no FSL (blank liposomes) were prepared and tested in parallel.
3. Each liposome sample was thoroughly mixed and diluted 1:100 in PBS for analysis (dilutions were allowed to stand at RT for at least 30 minutes before analysis).
4. Size measurements were carried out in 4mL polystyrene cuvettes (Mediray, Cat# GR614101), and zeta potential measurements using a folded capillary cell (ATA Scientific, Cat# DTS1070)
5. All measurements were performed at 22°C and repeated in triplicate and the mean result reported. For each size measurement at least 12 acquisitions of 10 seconds each were performed.

Statistical analysis of size was carried out using PRISM GraphPad. To determine if size of liposomes was significantly altered by addition of FSL, mean size measurements were compared to a control liposome sample containing no FSL. Non parametric Kruskal-Wallis test and post hoc Dunn's test were used. The polydispersity index (PDI) is a measure of sample homogeneity, values <0.2 are considered acceptable and indicate a homogenous liposome dispersion. Each measurement was repeated three times and the mean and standard deviation reported below.

This experiment was repeated on at least two separate occasions, with similar pattern of results seen each time, one representative experiment is shown below.

Results - Size

FSL-A2

The DLS graphs (Figure 52) show that all samples contained a monodisperse population of particles of similar size. No major differences between samples were detected. Table 11 summarises the size and PDI results.

Table 11 Summary of the mean size and polydispersity index of A2-liposomes.Liposomes were prepared containing increasing concentrations of FSL-A2, by LM, H and PS protocols.

Preparation Method	FSL-A2 µM	Size nm			PDI	
Blank (control)	0	141	± 0.4		0.07	± 0.01
Lipid Mix (LM)	10	140	± 0.9		0.08	± 0.01
	25	154	± 0.5		0.15	± 0.00
	100	133	± 0.7		0.09	± 0.01
	250	140	± 0.2		0.07	± 0.07
Hydration (H)	10	145	± 1.3		0.06	± 0.01
	25	147	± 0.8		0.06	± 0.00
	100	140	± 0.5		0.07	± 0.02
	250	148	± 1.2	*	0.12	± 0.00
Post Synthesis (PS)	10	143	± 1.1		0.21	± 0.01
	25	143	± 1.2		0.08	± 0.02
	100	144	± 0.5		0.06	± 0.00
	250	147	± 1.9	**	0.07	± 0.01

Mean ± standard deviation, n=3 *P<0.05 **P<0.01

Liposomes ranged in size from 133 to 148nm. No significant difference in size was detected between control liposomes (containing no FSL) and liposomes containing ≤100µm FSL, for all three methods of insertion.

A statistically significant increase in liposome size was detected after addition of 250µM FSL-A2 by both hydration (P= 0.0325) and post synthesis (P=0.004) methods. Size increased from 141nm (blank) to 148 (H) and 147nm (PS). While this was a statistically significant result, the actual change was small, less than 10nm (≈5% increase in size) in both cases.

The PDI values obtained for all samples were <0.2, except for the 250µM Hydration sample which was 0.22, indicating liposomes were monodisperse. Addition of FSL did not cause the PDI to increase.

a) Lipid Mix (LM)

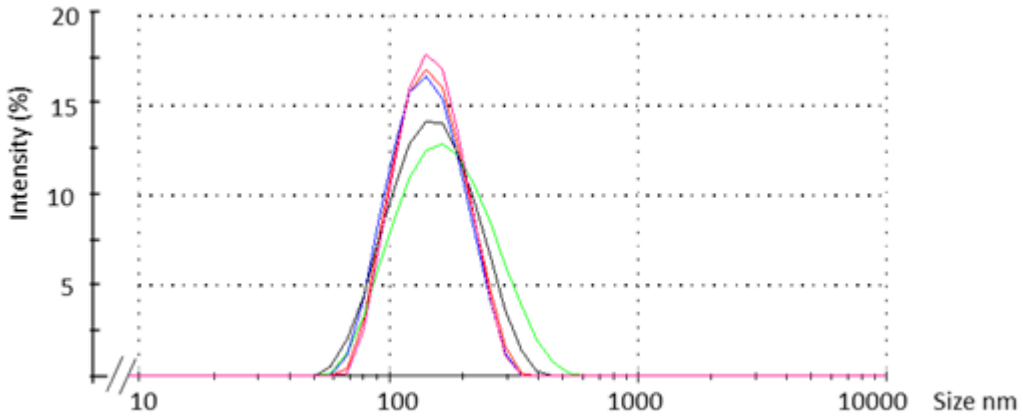

b) Hydration (H)

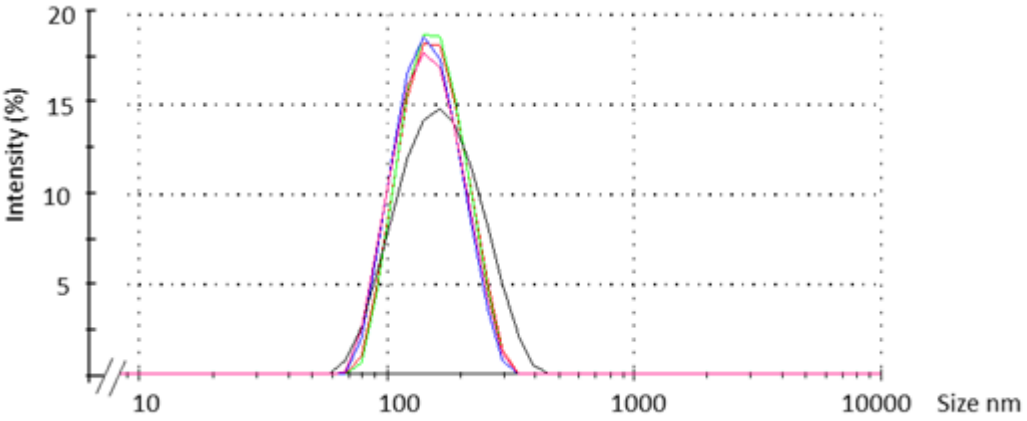

c) Post Synthesis (PS)

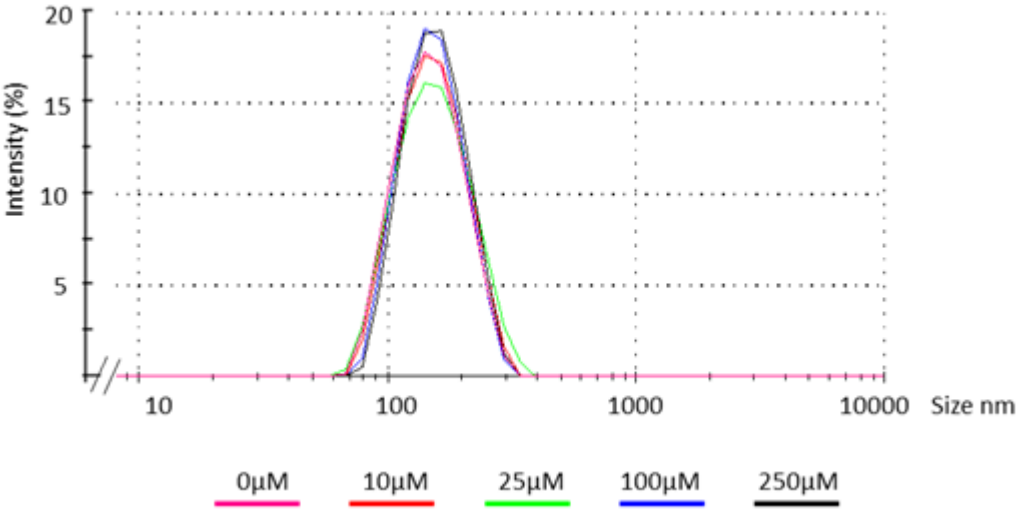

Figure 52 Size of FSL-A2 liposomes measured by DLS. Liposomes were prepared containing varying concentrations of FSL-A2 (0, 10, 25, 100, and 250µM) incorporated by (**a**) lipid mix, (**b**) hydration, and (**c**) post synthesis protocols. Because no particles were detected in the regions of 0-10nm the x axis scale is started at 10nm. Liposome populations were monodisperse and no difference was seen between methods of FSL insertion.

FSL-biotin

The DLS graphs, Figure 53, show that all samples contained a monodisperse population of particles of similar size. No major differences between samples were detected. Table 12 summarises the size and PDI results.

Table 12 Summary of the mean size and polydispersity index of FSL-biotin liposomes. Liposomes were prepared containing increasing concentrations of FSL-biotin by LM, H and PS protocols.

Preparation Method	FSL-biotin µM	Size nm			PDI	
Blank (control)	0	163	± 2.4		0.22	± 0.02
Lipid Mix (LM)	10	154	± 3.1		0.13	± 0.01
	25	151	± 4.5		0.11	± 0.01
	100	134	± 2.8	*	0.08	± 0.01
	250	133	± 3.1	*	0.09	± 0.00
Hydration (H)	10	155	± 1.6		0.09	± 0.02
	25	146	± 2.6		0.09	± 0.01
	100	145	± 4.3	*	0.06	± 0.02
	250	145	± 1.7	*	0.11	± 0.01
Post Synthesis (PS)	10	154	± 2.1		0.10	± 0.02
	25	152	± 3.1		0.12	± 0.03
	100	151	± 3.1		0.08	± 0.01
	250	144	± 1.9	**	0.12	± 0.04

Mean ± standard deviation, n=3 *P<0.05 **P<0.01

Liposomes ranged in size from 144 to 163nm.

A statistically significant decrease in liposome size was detected after addition of 250µM FSL-biotin (compared to liposomes containing no FSL) by all three methods of insertion, lipid mix (P=0.041), hydration (P=0.0325) and post synthesis (P=0.010). Mean size decreased from 163nm (blank liposomes) to 133, 145, and 144nm (lipid mix, hydration, post synthesis) respectively.

In addition, lipid mix (P=0.024) and hydration (P=0.033) liposomes containing 100uM FSL-biotin also showed a statistically significant decrease in size, from 163nm down to 134 and 144nm (lipid mix, hydration) respectively.

The PDI values obtained for all liposomes sample containing FSL-biotin were <0.2 indicating liposomes were monodisperse. Addition of FSL did not cause PDI to increase.

a) Lipid Mix (LM)

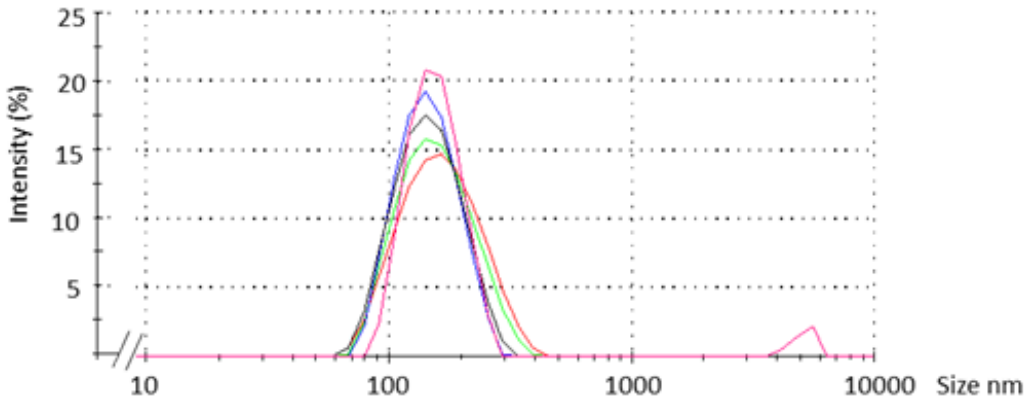

a) Hydration (H)

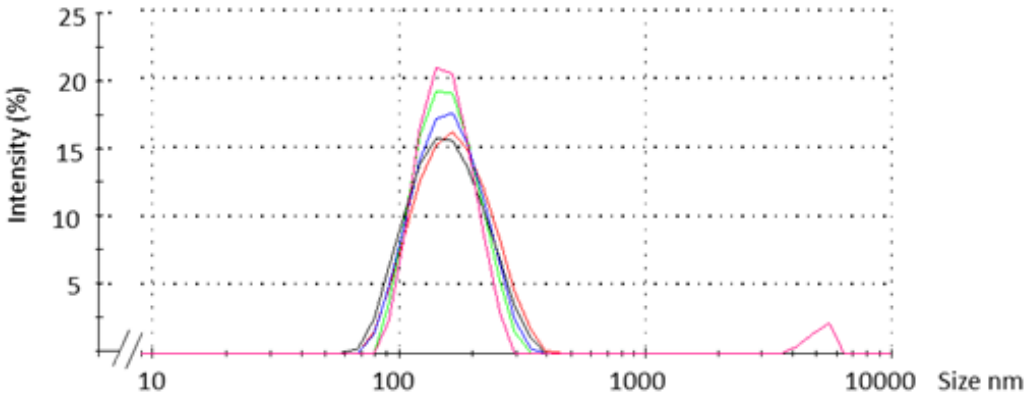

b) Post Synthesis (PS)

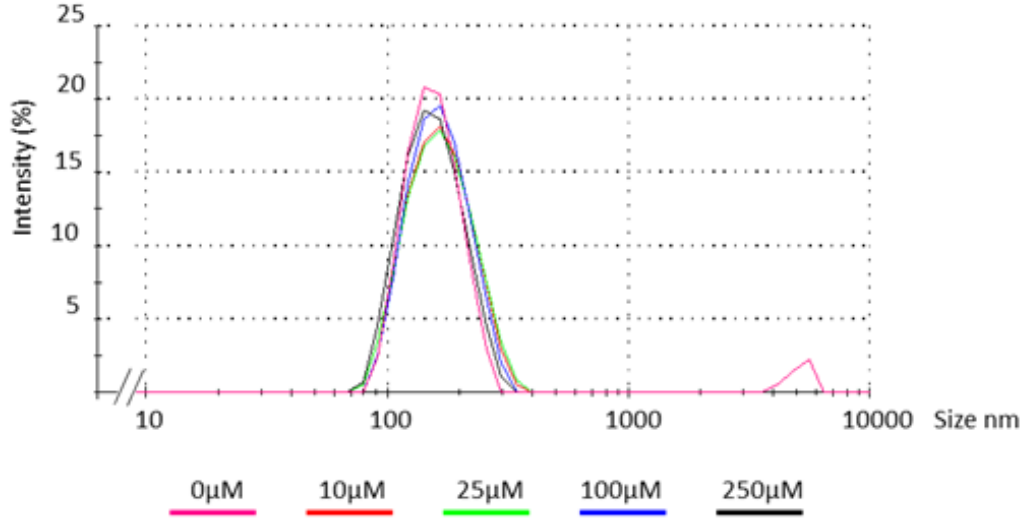

Figure 53 Size of FSL-biotin liposomes measured by DLS. Liposomes were prepared containing varying concentrations of FSL-biotin (0, 10, 25, 100, and 250µM) incorporated by (**a**) lipid mix, (**b**) hydration, and (**c**) post synthesis protocols. Because no particles were detected in the regions of 0-10nm the x axis scale is started at 10nm. Liposome populations were monodisperse and no difference was seen between methods of FSL insertion. A population of large particles was seen in PBS sample (0µM sample), most likely due to dust contamination.

DLS measures the Brownian motion of a particle (by analysing light scatter) and uses this to determine the size of the particle - larger particles move more slowly and scatter more light. Because the diameter calculated by DLS is actually related to how a particle diffuses through a liquid, it is termed the hydrodynamic diameter. Anything which effects the particles diffusion speed will also alter the apparent size of the particle. Any change to the particles surface can affect diffusion speed, by altering the fluid layer associated with particles [344].

FSL-FLRO4

The DLS graphs, Figure 54, show that all samples contained a monodisperse population of particles of similar size. No major differences between samples detected. Table 13 summarises the size and PDI results.

Table 13 Summary of the mean size and polydispersity index of FLRO4 liposomes Liposomes were prepared containing increasing concentrations of FSL-FLRO4, prepared by LM, H and PS protocols.

Preparation Method	FSL-FLRO4 µM	Size nm		PDI	
Blank (control)	0	147	± 4.7	0.07	± 0.00
Lipid Mix	10	153	± 2.8	0.12	± 0.01
	25	148	± 2.5	0.09	± 0.01
	100	143	± 1.2	0.07	± 0.00
	250	132	± 1.3	0.08	± 0.00
Hydration	10	152	± 2.2	0.11	± 0.01
	25	143	± 2.0	0.06	± 0.01
	100	158	± 2.7	0.11	± 0.01
	250	147	± 1.4	0.09	± 0.02
Post Synthesis	10	144	± 0.6	0.07	± 0.01
	25	143	± 0.9	0.06	± 0.01
	100	142	± 0.5	0.08	± 0.02
	250	143	± 1.3	0.06	± 0.01

Mean ± standard deviation, n=3

Liposome sizes ranged in size from 132 to 158nm.

No significant difference in size was detected between control liposomes (containing 0µM FSL) and liposomes containing FSL-FLRO4 for all concentrations and by all three methods of insertion.

Polydispersity index (PDI) values were ≤ 0.2, indicating liposomes were monodisperse. Addition of FSL did not cause PDI to increase.

a) Lipid Mix (LM)

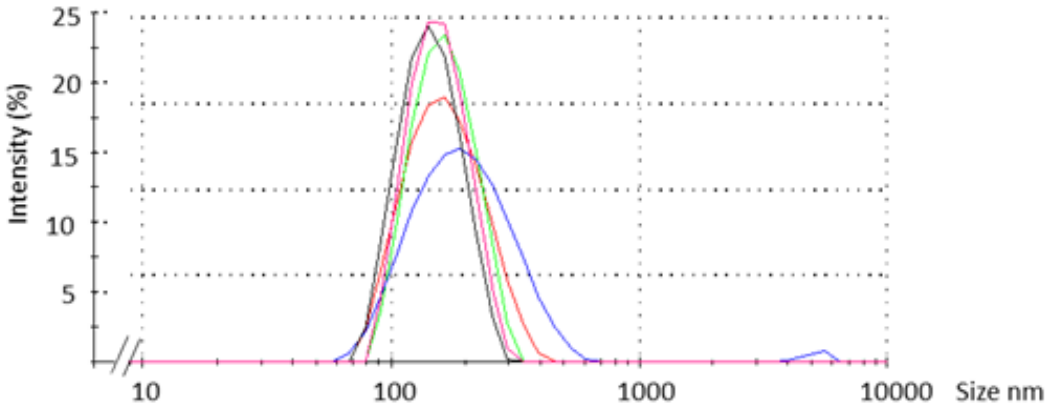

b) Hydration (H)

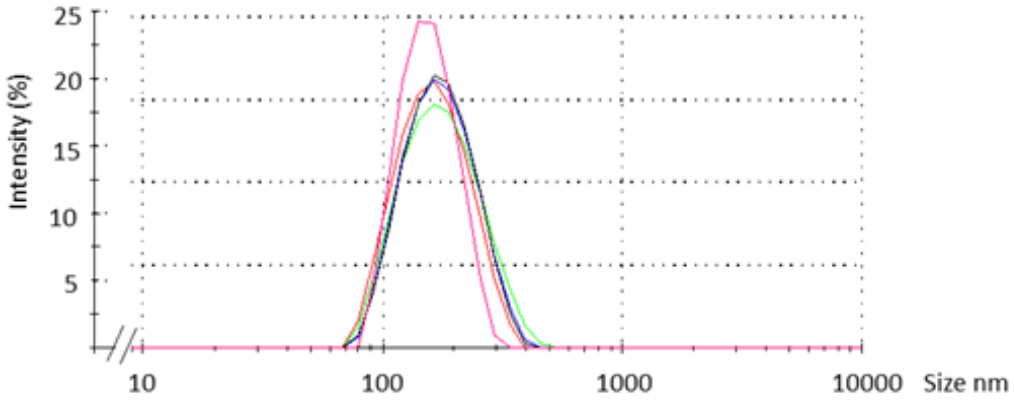

c) Post Synthesis (PS)

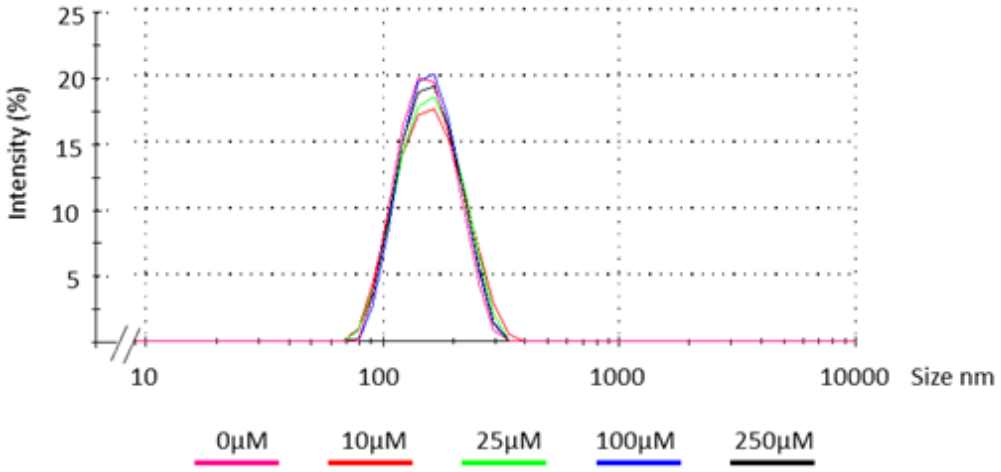

Figure 54 Size of FSL-FLRO4 liposomes measured by DLS. Liposomes were prepared containing varying concentrations of FSL-FLRO4 (0, 10, 25, 100, and 250µM) incorporated by (**a**) lipid mix, (**b**) hydration, and (**c**) post synthesis protocols. Because no particles were detected in the regions of 0-10nm the x axis scale is started at 10nm. Liposome populations were monodisperse and no difference was seen between methods of FSL insertion.

Summary

The addition of FSL constructs at concentrations less than 100µM cased no change to liposome size.

FSL-FLRO4 did not alter liposome size at all concentrations tested.

Addition of larger concentrations (100-250µM) of FSL-A2 and FSL-biotin did cause some small changes to liposome size. The addition of 250µM FSL-A2 caused slight increase in liposome size, while 100 and 250µM FSL-biotin caused slight decrease in liposome size.

The variation in liposome size appeared to be more pronounced when FSL was added by PS method, which was not unexpected as in these liposome FSL was added after extrusion (step in method which sizes liposomes).

Results -Zeta Potential

Addition of FSL-A2 and FSL-FLRO4 constructs caused small increase in negative charge. FSL-biotin caused a significant concentration dependent increase in negative charge as shown in Figure 55.

a) FSL-A2 liposomes

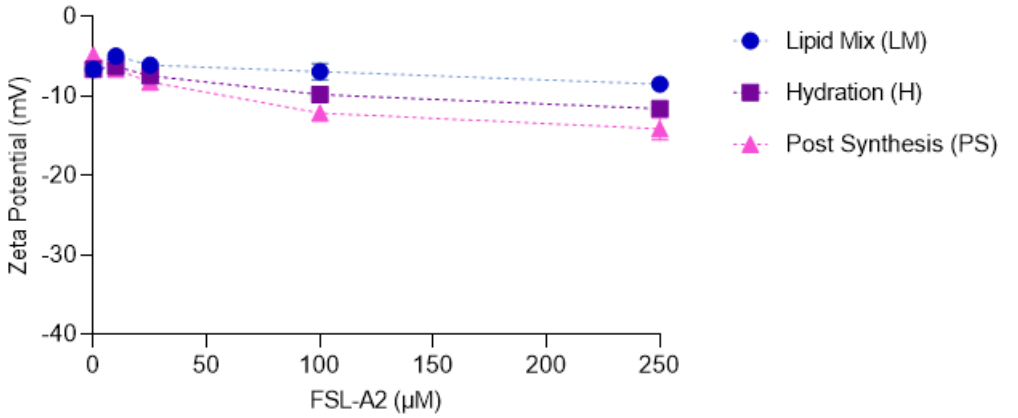

b) FSL-biotin liposomes

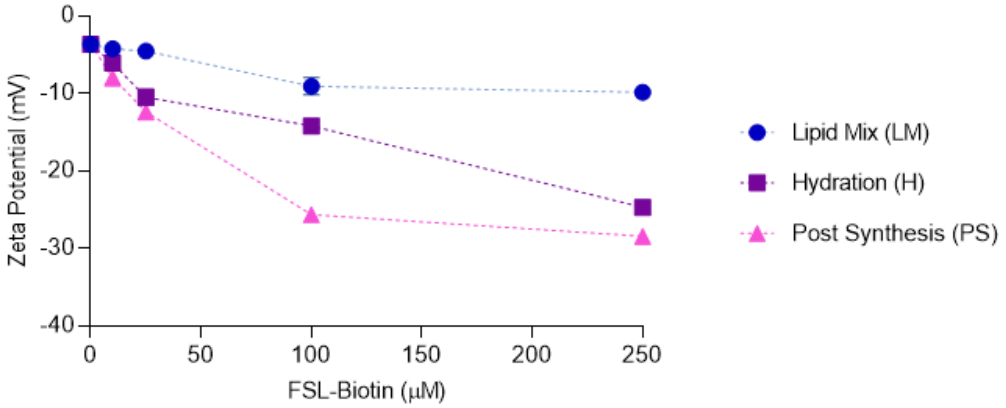

c) FSL-FLRO4 liposomes

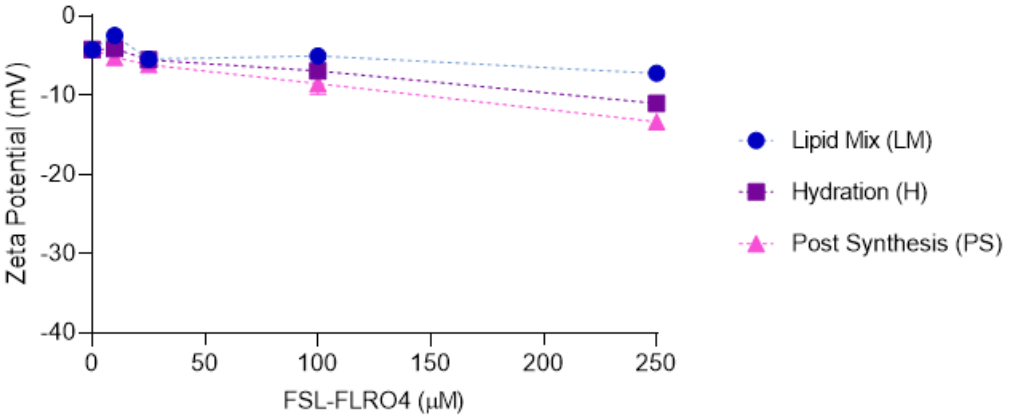

Figure 55 Zeta potential of FSL labelled liposomes. Graphs show the zeta potential of liposome prepared with varying concentrations of (**a**) FSL-A2, (**b**) FSL-biotin, and (**c**) FSL-FLRO4 added by lipid mix, hydration and post synthesis methods. Post synthesis liposomes showed greatest increase in charge, lipid mix the least change. FSL-biotin liposomes showed the greatest increase in negative charge.

All three FSL constructs are negatively charged (see micelle characterisation section 2.1.2) so it was expected that their incorporation into liposomes would increase the liposomes negative charge. Interestingly, addition of FSL-biotin caused the greatest increase in (liposome) charge even though the FSL-FLRO4 micelles were more negatively charged than FSL-biotin micelles.

For all three constructs addition of FSL by the post synthesis protocol showed the greatest increase in charge, while lipid mix method showed the least change. Addition of 250μM FSL-biotin caused a significant increase in liposome charge; from -3.7mV (blank) to -9.9mV, -24.7mV, and -28.4mV after FSL was added by LM, H, and PS methods respectively.

Addition of FSL-A2 and FSL-FLRO4 resulted in only a slight increase in liposome negative charge, for FSL-A2 zeta potential increased from -6.6mV (blank) to -8.5mV (LM), -11.6mV (H), and -14.1mV (PS). Addition of FSL-FLRO4 resulted in an increase from -4.2mV (blank) to -7.2mV (LM), -11.0mV (H), and -13.3mV (PS).

Zeta potential values above +30mV and less than -30mV are considered strongly cationic or anionic [304]. Only the liposomes containing FSL-biotin (H and PS) became strongly anionic.

Summary

The addition of FSL-A2, FSL-biotin and FSL-FLRO4 increased the zeta potential of liposomes in a concentration dependent manner. However, the addition of FSL-A2 and FSL-FLRO4 resulted in only a very small increase in zeta potential, while addition of FSL-biotin by H and PS methods caused a significant increase in negative charge.

Addition of FSL via the post synthesis method resulted in the greatest increase in zeta potential for all three constructs. A possible explanation for this is that when FSL is added to liposome by PS method it is only able to insert into the external surface of the liposome phospholipid bilayer (see section 2.2.2). In contrast, for both lipid mix and hydration methods FSL can become incorporated on the interior surface of liposome bilayer membrane and free FSL (monomers/micelles) can be sequestered within the liposomes internal aqueous core (H method liposomes). Consequently, liposomes prepared by PS method may express a higher surface density of FSL on their exterior compared with liposomes prepared by other two methods, and hence have a greater negative surface charge.

2.2.6 Morphology (TEM analysis)

Cryogenic transmission electron microscopy (cryo-TEM) was carried out to determine if the addition of FSL causes any alteration to liposome morphology (size, shape, and/or membrane organisation). Cryo-TEM enables the visualisation of liposomes including their membrane organisation. It also provides opportunity to measure the size of liposomes by a second method to confirm size data obtained from DLS. As DLS size measurement is derived via mathematical calculation from light scatter it is advisable to confirm this data with TEM (an empirical measurement).

Cryo-TEM preparation involves applying a small aliquot of the sample onto a TEM grid. TEM grids are composed of a metal grid covered with a thin foil, which is perforated with a regular repeating array of circular holes. The sample is blotted with filter paper to form a thin film across the grid, and then plunge frozen in cryogen, usually liquid ethane.

Method

1. Liposome samples were prepared containing 100µM of each FSL, inserted by all three insertion protocols (protocol 2.2.2). Liposomes containing no FSL were prepared and analysed in parallel as a 'blank' control.
2. Liposome samples were diluted 1:3 in PBS.
3. A 1.5µL aliquot of each liposome sample was plunge frozen in ethane onto plasma treated quantifoil grids (1.2/1.3 300 mesh on 300 copper) using a Vitrobot Mark IV (Thermo Fisher Scientific). Blot time of 6 seconds and drain time of 1 second was used.
4. The prepared grids were imaged under low dose conditions on a Tecnai 12 TEM (Thermo Fisher Scientific) running at 120kV. Defocus was typically set at -3µm.
5. The diameter of liposomes was calculated from images using Fiji Image J software. A minimum of 200 liposomes were counted for each sample. Liposomes which were tubular in shape (see Figure 61) were excluded from size analysis (as diameter cannot be accurately determined). All liposomes in an image were counted.

Results -Size

The TEM size results and representative images of all three FSL constructs and three methods of insertion are shown in Figures 56-58. Control liposomes containing no FSL and prepared in parallel with the test liposomes are also shown. All liposome samples were extruded through 100nm membrane. Preliminary analysis of varying concentrations was carried out, results not shown. The results for 100µM only are shown, no difference was observed with other (10 and 50µM) concentrations.

100µM A2 liposomes

(a) Lipid Mix

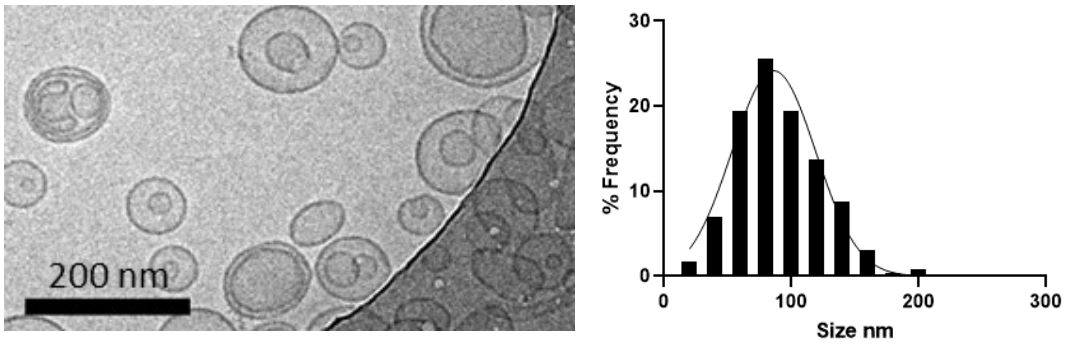

(b) Hydration

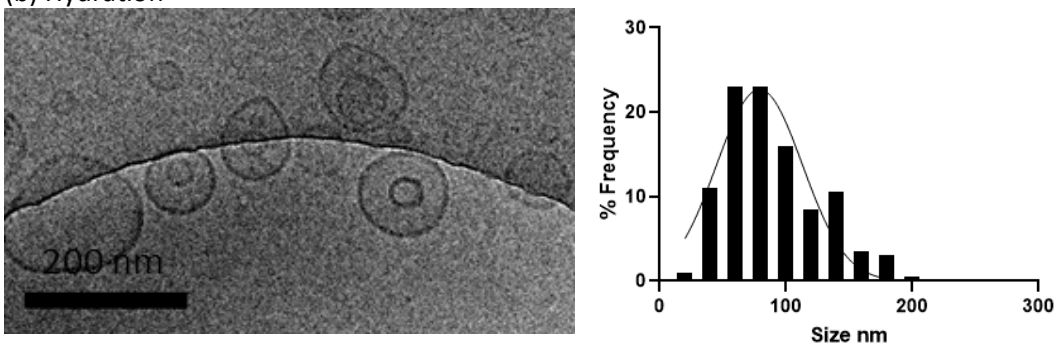

(c) Post Synthesis

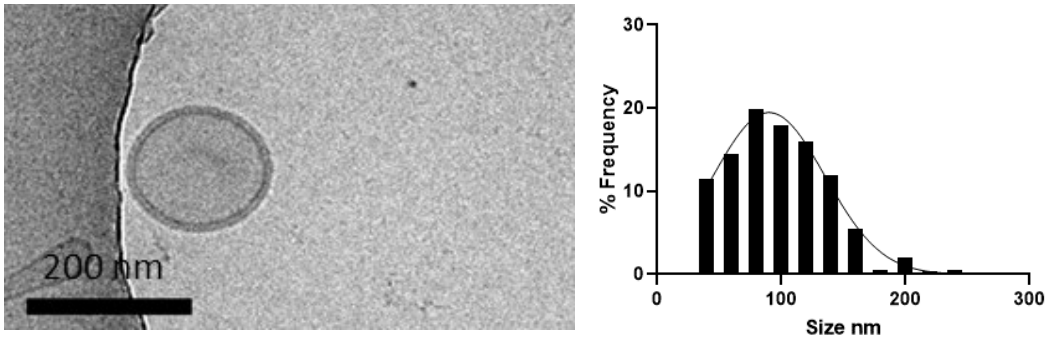

(d) Control liposomes (0µM FSL)

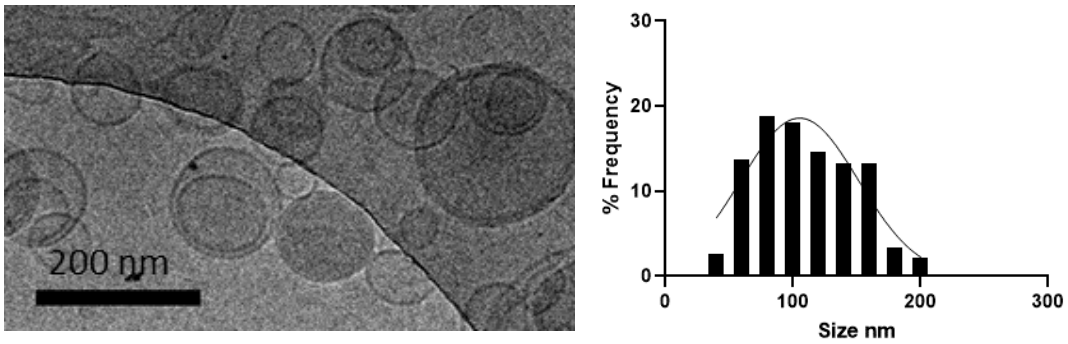

Figure 56 Cryo-TEM images and size distribution of 100 FSL- A2 liposomes. Liposomes were prepared with 100µM FSL-A2 added by (**a**) lipid mix, (**b**) hydration, and (**c**) post synthesis protocols. (**d**) Control liposomes containing no FSL were also analysed. Note: the circle seen is the images is the edge of one of the holes which perforate the grid, the lighter grey area is the space within the hole, while the darker area is the grid.

100µM Biotin liposomes

(a) Lipid Mix

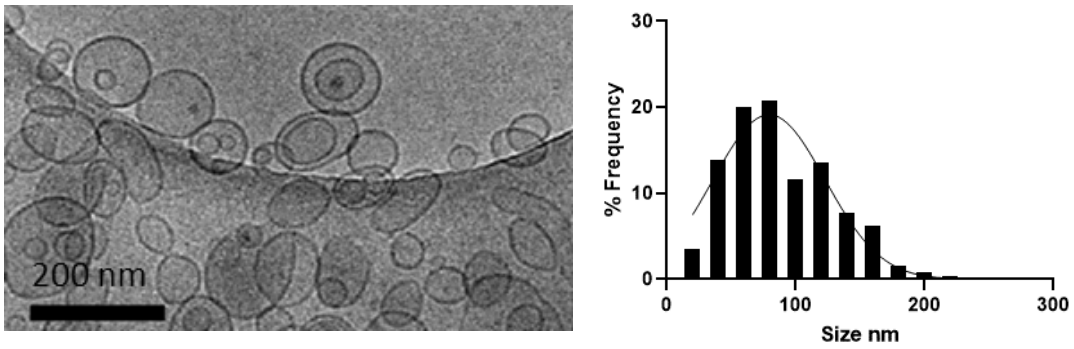

(b) Hydration

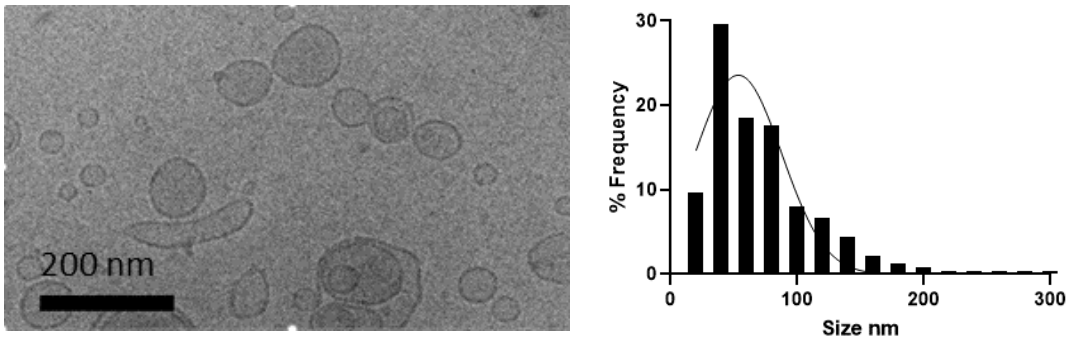

(c) Post Synthesis

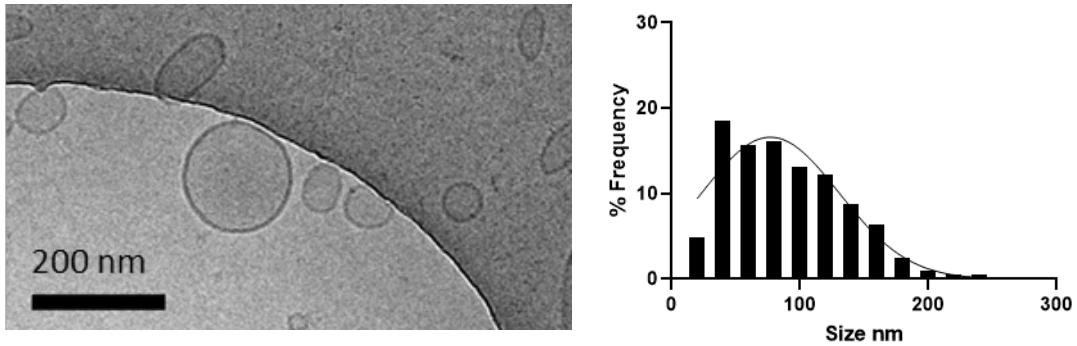

(d) Control liposomes (0µM FSL)

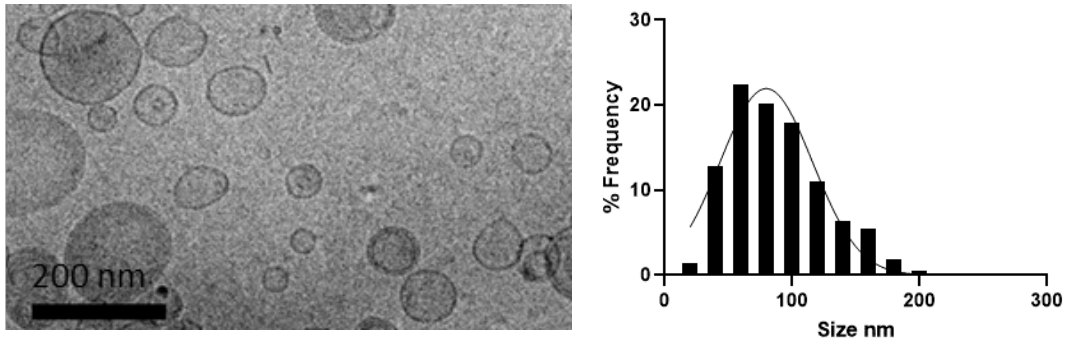

Figure 57 Cryo-TEM images and size distribution of 100 FSL-biotin liposomes Liposomes were prepared with 100µM FSL-biotin added by (**a**) lipid mix, (**b**) hydration, and (**c**) post synthesis protocols. (**d**) Control liposomes containing no FSL were also analysed.

100µM FLRO4 liposomes

(a) Lipid Mix

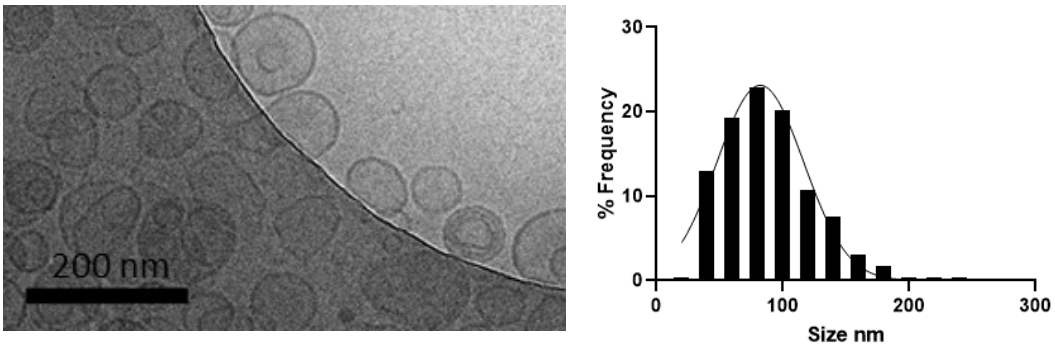

(b) Hydration

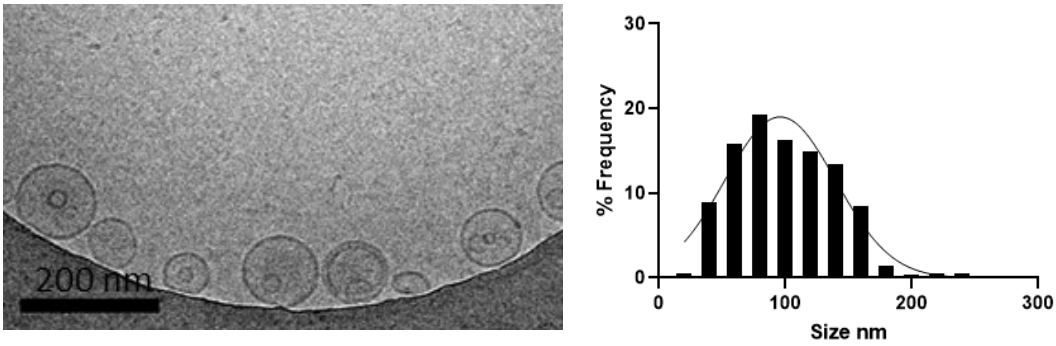

(c) Post synthesis

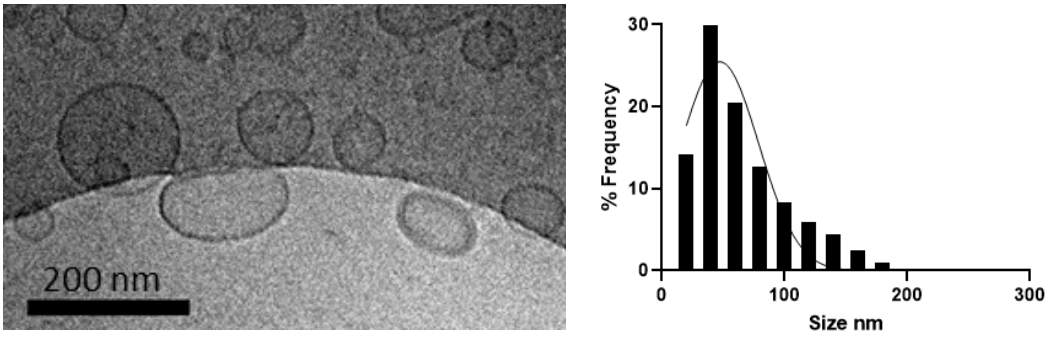

(d) Control liposomes (0µM FSL)

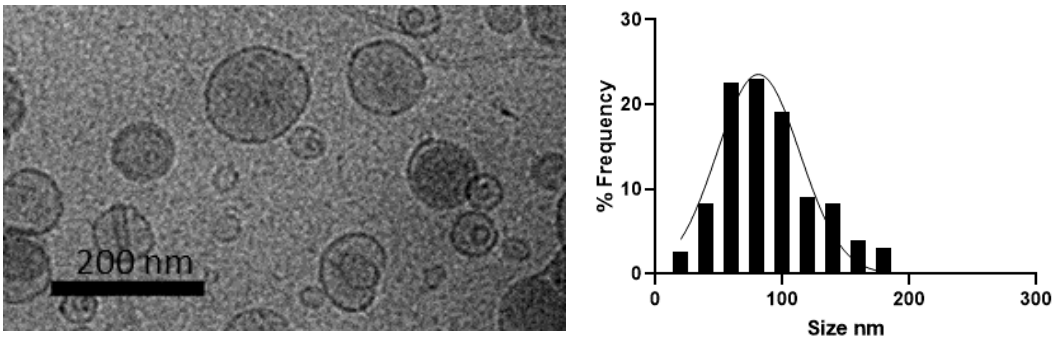

Figure 58 Cryo-TEM images and size distribution of 100 FSL-FLRO4 liposomes Liposomes were prepared with 100µM FSL-FLRO4 added by (**a**) lipid mix, (**b**) hydration, and (**c**) post synthesis protocols. (**d**) Control liposomes containing no FSL were also analysed.

The control liposomes (containing no FSL) and liposomes containing FSL all showed a range in size, from 20nm up to approximately 250nm, except biotin liposomes (prepared by hydration method) which showed the greatest variation in size, ranging from 12nm up to a maximum of 320nm. Despite this variation, the box and whisker graph, Figure 59, shows that middle 50% of populations were similar in size range, and similar mean size.

Most of the liposome samples had a mean size (diameter) of approximately 90nm, except for Biotin liposomes-hydration and FLRO4 liposomes-Post synthesis samples, which had smaller mean diameters of 72 and 65nm respectively. No effect on size related to type of FSL construct included or preparation method was observed by TEM.

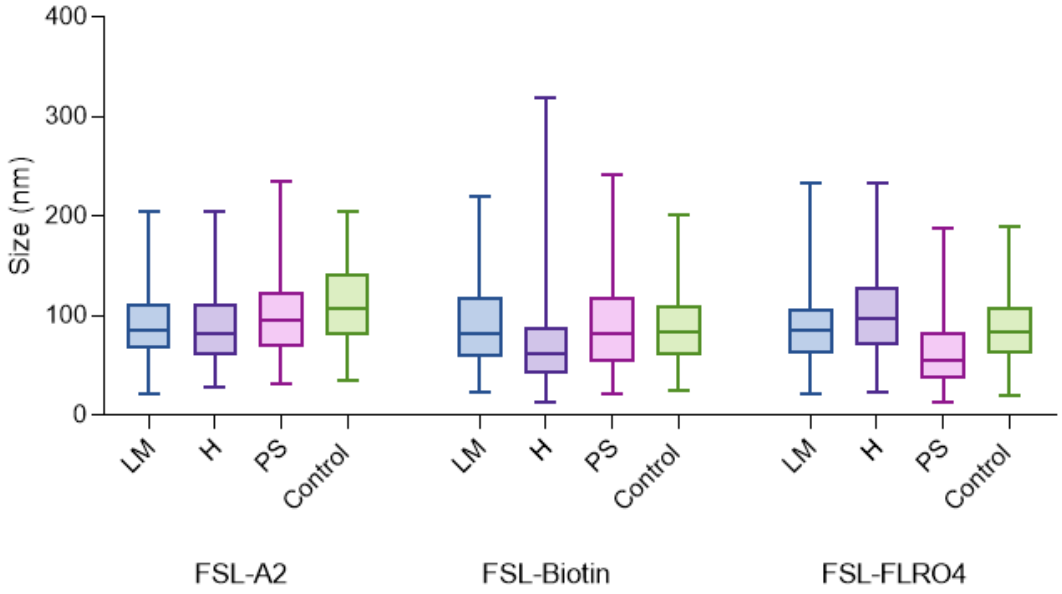

Figure 59 Size distribution of liposomes obtained from cryo-TEM. Liposomes were prepared containing 100µM FSL-A2, FSL-biotin or FSL-FLRO4 by Lipid Mix (LM), Hydration (H) and Post Synthesis (PS) protocols. Control liposomes containing no FSL were also analysed. No effect on size related to type of FSL construct included or preparation method was observed. A wide range (10-320nm) in size was seen, mean liposome size was approximately 100nm for all samples.

Size comparison – TEM vs DLS

The size data obtained by TEM analysis was compared with size data obtained by DLS analysis (of the same samples). The results are shown in Figure 60.

The mean size of liposomes measured by cryo-TEM was smaller than that measured by DLS for all samples. In addition, the TEM size measurements showed a much greater variation in size than DLS. Several factors contribute to observed discrepancies between the two methods;

- DLS measures the hydrodynamic diameter of particles in solution, whereas TEM measures the diameter of the liposomes from their membrane surface.
- DLS has a much higher sample size than TEM, millions of particles are counted by DLS compared to only hundreds (200) by TEM analysis [290].
- TEM preparation may alter the size of liposomes, during the blotting step liposomes are exposed to high shear forces, which may could alter their size.
- DLS derives particle size via a mathematical calculation, an assumption of this is that the particles present are spherical and monodisperse.

While liposomes appear to slightly more diverse than expected from DLS results, overall the results support each other, and confirm that liposomes are present, majority of which are unilamellar and within expected size range (approximately 100nm).

(a) 100µM A2 liposomes

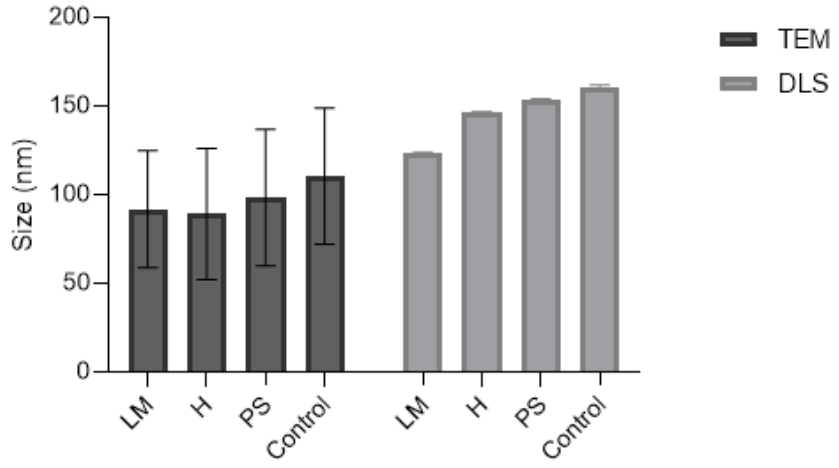

(b) 100µM biotin liposomes

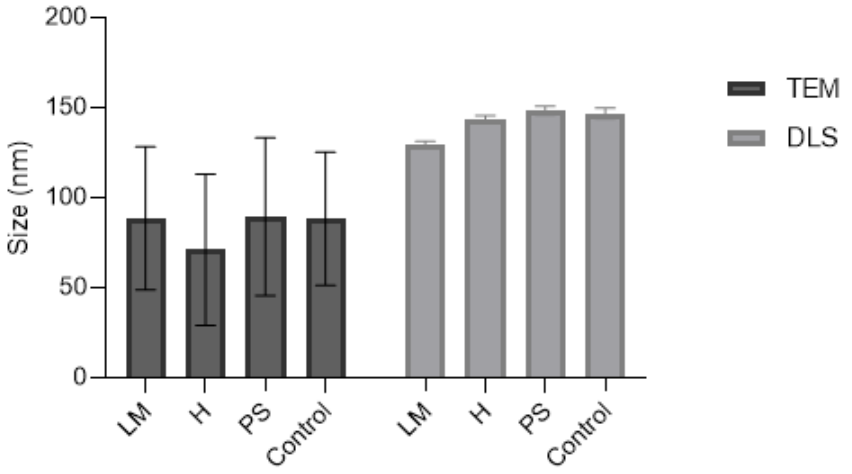

(c) 100µM FLRO4 liposomes

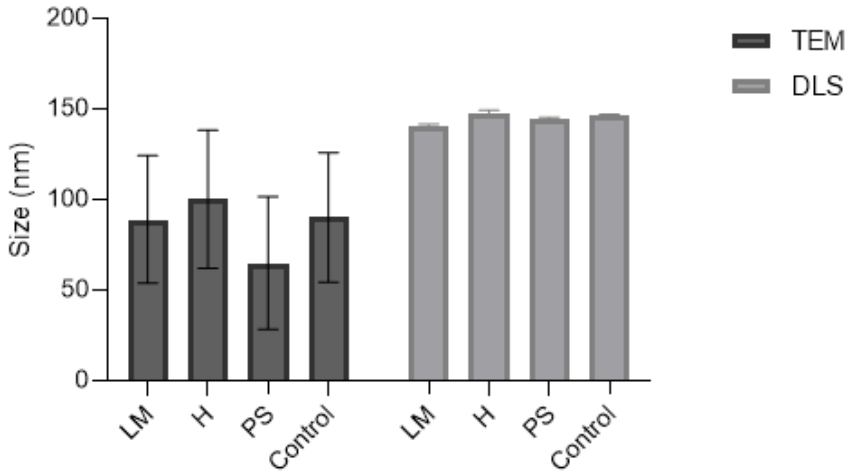

Figure 60 Size comparison of liposome sizes determined by cryo-TEM and DLS. The mean size of liposomes measured by cryo-TEM was smaller than that measured by DLS for all samples. The TEM size measurements showed a much greater variation in size than DLS

Results - Morphology

The following liposome morphologies/structures, Figure 61, were observed in all samples including the control liposomes which contained no FSL;

- unilamellar vesicles, both small <100nm and large >100nm, (SUV/LUV)
- multi-vesicular vesicles (MVV)
- multi-lamellar vesicles (MLV)
- long narrow tube-shaped vesicles, sometimes also containing spherical or pear shaped areas

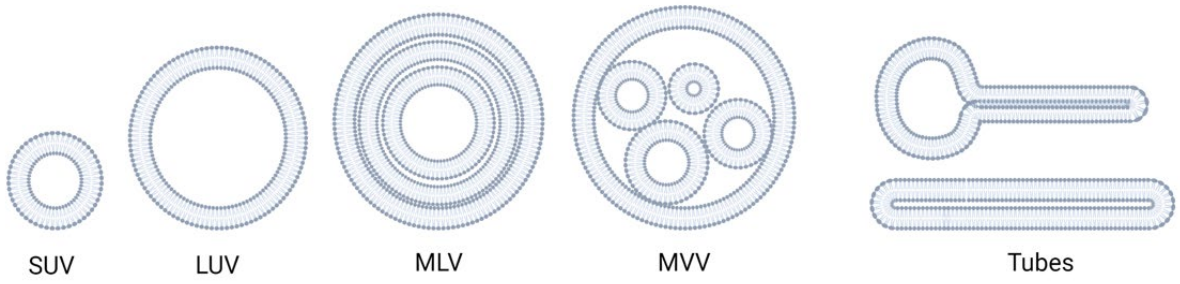

Figure 61 Schematic diagram showing types of liposomes observed by cryo-TEM. Small unilamellar (SUV), large unilamellar (LUV), multilamellar vesicles (MLV) and multi-vesicular vesicles (MVV) and vesicles with long narrow tube like projections were seen. Created with BioRender.com.

Figure 62 shows representative TEM images of each type of observed liposome/vesicle morphology. The majority of liposomes observed were unilamellar liposomes (>70% in all samples). Both small (<100nm) and large (>100nm) unilamellar liposomes were seen. Multi-lamellar and multi-vesicular liposomes were also observed, accounting for up to 20% of observed vesicles.

Liposomes which had a thin elongated tubular/cylindrical structures were also observed, shown in Figure 62 (b and d). These vesicles sometimes also contained a sphere- or pear-shaped portion attached to tubular section within one vesicle. These tubular vesicles accounted for up to 10% of observed vesicles. From the TEM images it is impossible to know if these elongated tubular structures were cylindrical, similar to a sausage, or if they were actually a flat discoid shape that is oriented perpendicular to the plane of view. While their presence was an interesting observation, as they were also present in control samples (containing no FSL) they were not investigated further in this project. Similar vesicles have been reported in the literature and a proposed explanation for their formation is the lateral phase separation of different amphiphiles within the liposomes [345-347].

It was observed that the liposomes showed a clear preference for the grid, often resulting in poor distribution of liposomes over the grid holes. This is a common difficulty experienced with cryo-TEM [298]. It is possible to experiment with different grid materials to prevent this, unfortunately this was beyond the scope of this study. The grid is perforated with multiple round holes. Ideally the liposomes

should be suspended within the ice that spans the holes of the grid. This is desirable as it removes any interaction between liposome and grid surface, which can influence the observed size and shape of liposome. In the following images (b, c, and d) the edge of the circular holes in the grid can be seen (lighter grey area), and the grid itself is the darker grey region. Figure 63, shows the percentage frequency of the different vesicle morphologies observed.

a) Large unilamellar vesicles (LUV)

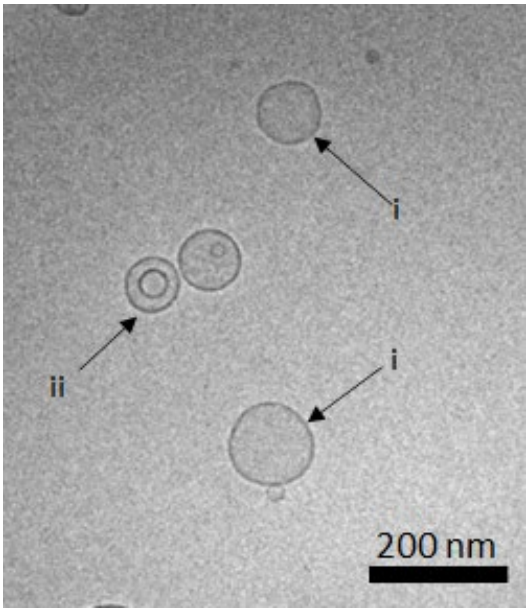

b) Multi-lamellar vesicles (MLV)

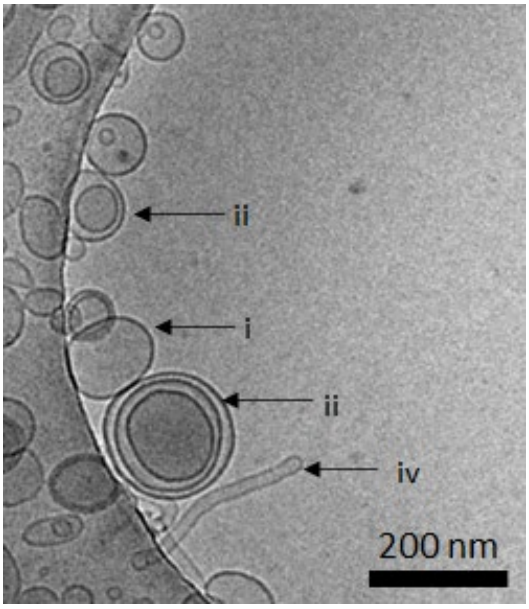

c) Multi-vesicular vesicles (MVV)

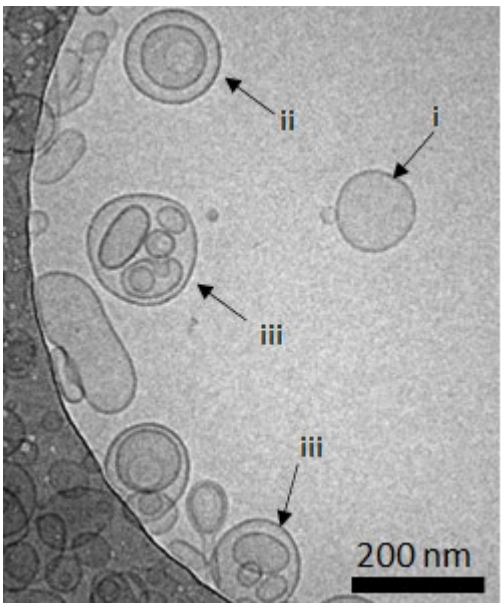

d) Elongated tubular vesicles

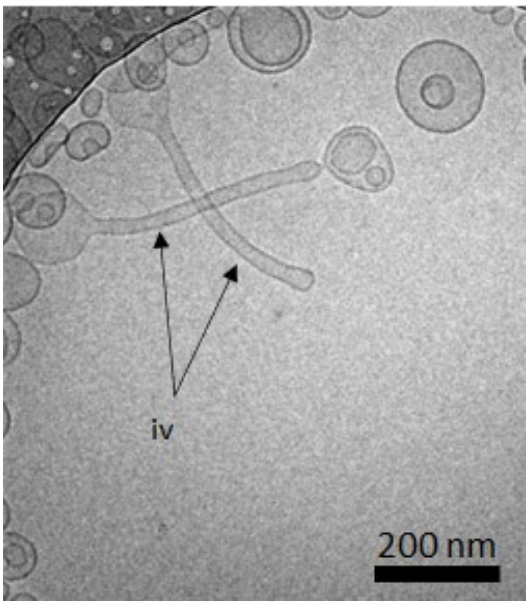

Figure 62 Liposome structures observed by cryo-TEM; Example TEM images showing examples of (**i**) unilamellar liposomes (LUV) shown in images (a, b, c), (**ii**) multilamellar liposomes (MLV) shown in images (b, c), **(iii**) multi-vesicular liposomes (MVV) shown in image (c), and (**iv**) elongated tubular structures shown in image (d), as indicated by black arrows.

(a) FSL-A2

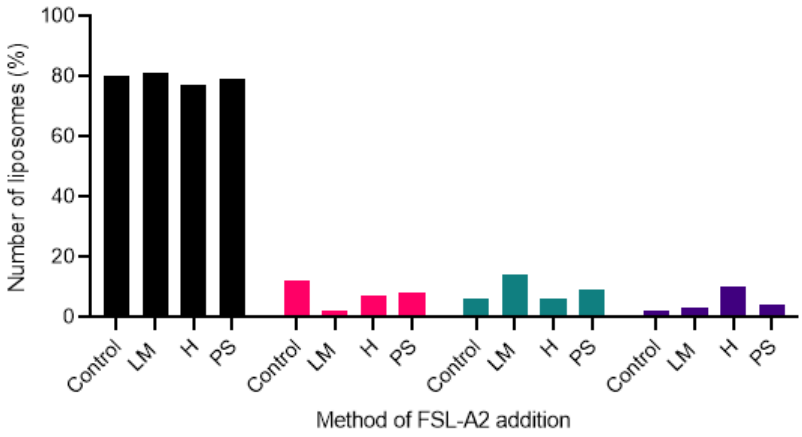

(b) FSL-biotin

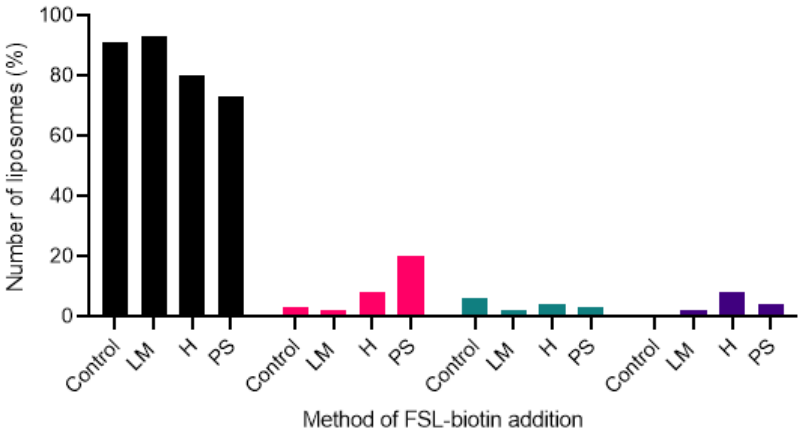

(c) FSL-FLRO4

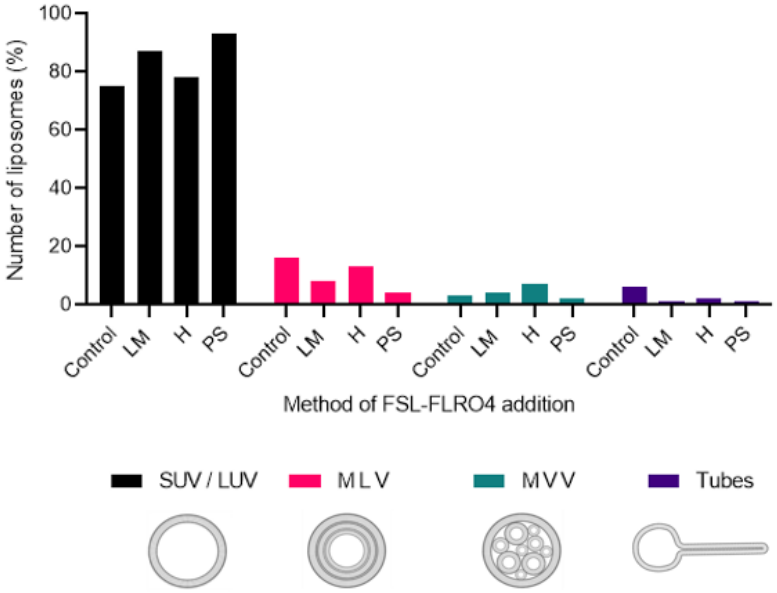

Figure 63 Comparison (%) of different types of liposomes observed by cryo-TEM. Liposome dispersions containing 100µM (**a**) FSL-A2, (**b**) FSL-biotin and (**c**) FSL-FLRO4 were prepared by LM, H and PS methods. Control liposomes, containing no FSL, prepared in parallel were also analysed. Four types of structure were observed (see Figure 62); small/large unilamellar vesicles (SUV/LUV), multilamellar vesicles (MLV), multivesicular vesicles (MLV), and long 'tube' like vesicles. All dispersions were composed of primarily unilamellar vesicles with a small percentage (<20%) of MLV, MVV and tubes. All structures were present in the control liposome dispersions (containing no FSL). No significant variation in the number of different structures was seen between FSL constructs or method of FSL addition, n≥200.

A slight increase in the number of tubular vesicles, compared to control liposomes (containing no FSL) was seen in FSL-A2 and FSL-biotin hydration liposomes. The frequency of tubular vesicles increased from 2% to 10% (FSL-A2) and from 3% to 8% (FSL-biotin). FSL-biotin PS liposomes also showed a slightly increased percentage of MLV vesicles. However due to the relatively small sample size (≈200 liposomes counted for each sample only) it is possible that these increases are due to experimental variation. Further work to repeat these experiments, with additional batches, and increased sample size number is required before determining if this is a true increase in number of tubular vesicles.

With the exception of FSL-A2 and FSL-biotin liposome dispersions (which both have a CMG spacer) and appeared to show a slight increase in number of tubular vesicles, there was no other observable difference in the type or frequency of the different morphologies seen between control liposomes containing no FSL and test liposomes containing FSL.

Summary

TEM analysis showed that samples contained a majority of unilamellar liposomes, with mean size slightly less than 100nm.

The addition of FSL, regardless of FSL type or method of insertion, did not appear to cause any significant change to liposome size, morphology or membrane organisation.

2.2.7 FSL activity (after addition to liposomes)

The aim of the following experiments was to determine if FSL molecules remain chemically intact and that the head part of the FSL molecule (F) retains its original properties – to fluoresce in the case of FSL-FLRO4 and to be recognisable by reactive proteins in the case of FSL-A2 and FSL-biotin. After FSL incorporation into liposomes the following experiments were carried out to confirm if the FSL head group remained active. The fluorescence of FSL-FLRO4 was directly measured by spectrophotometry, while FSL-A2 and FSL-biotin were detected using an enzyme immunoassay (EIA) technique.

FSL-FLRO4

Method

1. Liposome dispersions were prepared containing varying concentrations of FSL-FLRO4 inserted by lipid mix, hydration and post synthesis methods (protocol 2.2.2),
2. The fluorescence intensity of 100µL aliquots of each liposome dispersion was measured using Tecan Spark® 10M (Tecan.com) in duplicate. Excitation was at 495nm, and fluorescence emission measured at 520nm.
3. Equivalent concentration solutions of FSL constructs alone diluted in PBS were also measured. These were referred to as FSL-micelle dispersions (although they may contain FSL monomers and/or FSL micelles).

Results

The liposome dispersions were fluorescent. Fluorescence increased with increasing FSL-FLRO4 concentration, as shown in Figure 64. At lower concentrations (<50µM) this increase appeared to be linear, but at higher concentrations (>100µM FSL-FLRO4) fluorescence appears to plateau. LM dispersions continue to increase in fluorescence as the FSL is integrated into the liposome membrane and is not free in dispersion.

A difference in level of fluorescence was observed depending on method of FSL insertion into liposomes. Liposomes with FSL added via the lipid mix protocol showed the highest levels of fluorescence, measuring more than 50,000 rfu after addition of 250µM FSL-FLRO4. Liposomes prepared by hydration and post synthesis methods showed similar and much lower levels of fluorescence, reaching 27,000 and 18,000 rfu respectively after addition of 250µM FSL-FLRO4.

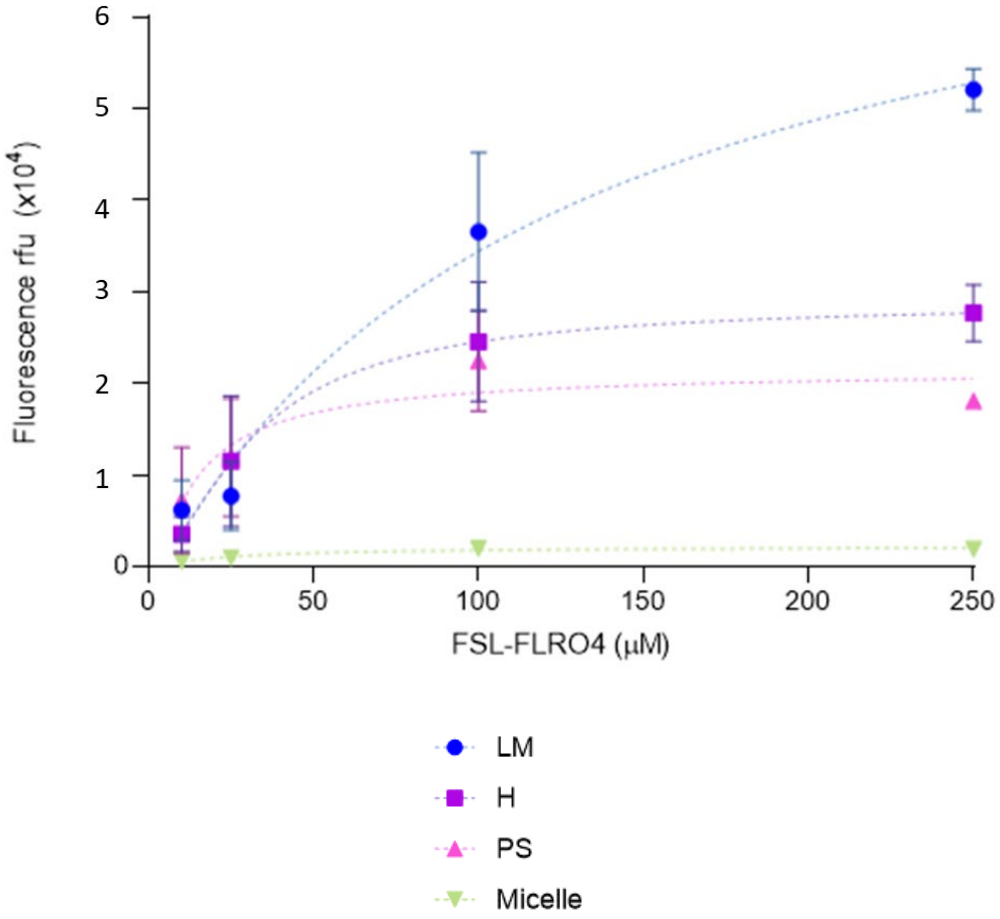

Figure 64 Fluorescence of FSL-FLRO4 liposomes. Liposomes were prepared containing varying concentrations of FSL-FLRO4 by LM, H and PS protocols. Dispersions of FSL FLRO4 micelles (no liposomes) were also measured for comparison. A difference in level of fluorescence was observed depending on method of FSL insertion into liposomes. Lipid mix liposomes showed highest levels of fluorescence and post synthesis the least. FSL-micelles showed very low levels of fluorescence compared to liposomes.

In contrast, the FSL micelle dispersion, containing FSL molecules alone (no liposomes), showed comparatively low levels of fluorescence, reaching just 1,900 rfu at 250µM FSL-FLRO4. This is also likely due to self-quenching of the fluorophore while in micelle formation.

A possible explanation for this plateau is that as the concentration of FSL-FLRO4 within the liposome membrane increases self-quenching may occur (FSL constructs may cluster together within the membrane further contributing to this effect). It is well known that emissions from a fluorophore are often 'self-quenched' when the fluorophore is present at a high concentration or in an aggregate state (i.e. micelle) [332, 348].

Alternatively, 100µM was calculated to be the CMC point of FSL-FLRO4 by fluorescence method and 130µM by pyrene method (see 2.1.3). Therefore, above 100µM all additional FSL molecules form micelles

(Figure 42). This may result in reduced incorporation of FSL into liposome membrane at concentrations greater than 100µM, micelle FSL may not transfer to liposome as readily as monomer FSL. Once CMC is reached all additional FSL forms micelles (which are quenched), rather than transferring to the liposome (and unquenching). Consequently, the fluorescence intensity of the dispersion does not change. Transfer of amphipathic molecules to liposomes above CMC is reported to be reduced compared to transfer from monomers [195].

This experiment does not provide information regarding the location of FSL constructs within the liposome. However, a clear difference in fluorescence between the micelle and liposome dispersions was seen. This change in fluorescence indicates that the FSL constructs are not remaining as FSL monomers/micelles when added to liposomes, and therefore provides indirect evidence that FSL constructs are incorporating into the liposome. However, how much of the FSL incorporates is also unknown.

FSL-A2 and FSL-biotin

To detect FSL-A2 and FSL-biotin an enzyme immunoassay technique was used. This technique was used because it had previously been well established for the detection of FSL constructs [246] and all necessary equipment and reagents were readily available. Detection of FSL on liposomes by flow cytometry would have been an ideal technique for this experiment, however access to a suitable flow cytometer, configured to detect nano-sized particles was not available.

The EIA technique enables the colorimetric detection of FSL-A2 or FSL-biotin molecules immobilised onto nitrocellulose paper. A microplate was constructed as described by Barr et al. [246], Figure 65. FSL-A2 was detected using a murine monoclonal antibody directed against the A antigen functional head group, followed by a secondary alkaline phosphatase conjugated anti-mouse antibody. FSL-biotin was detected using streptavidin conjugated alkaline phosphatase. The enzyme substrate NBT/BCIP was then used to detect the presence of the alkaline phosphatase by forming a coloured precipitate.

The assay protocols are described below and are based on the method of Svensson et al. [349] and Barr et al. [246]. All immunostaining was carried out at RT.

Immunostaining for the detection of FSL-A2

1. A microplate was constructed as described Barr et al. [246], media gloss paper (Spicers, New Zealand) was laminated with 80µm document laminating film (which had been prepared with reaction well shapes cut from one side). A 2mm acrylic template covered with double sided adhesive tape was laser cut to shape and adhered to the laminated paper sheet to form 96 reaction wells with a 10mm diameter, as shown in Figure 65.

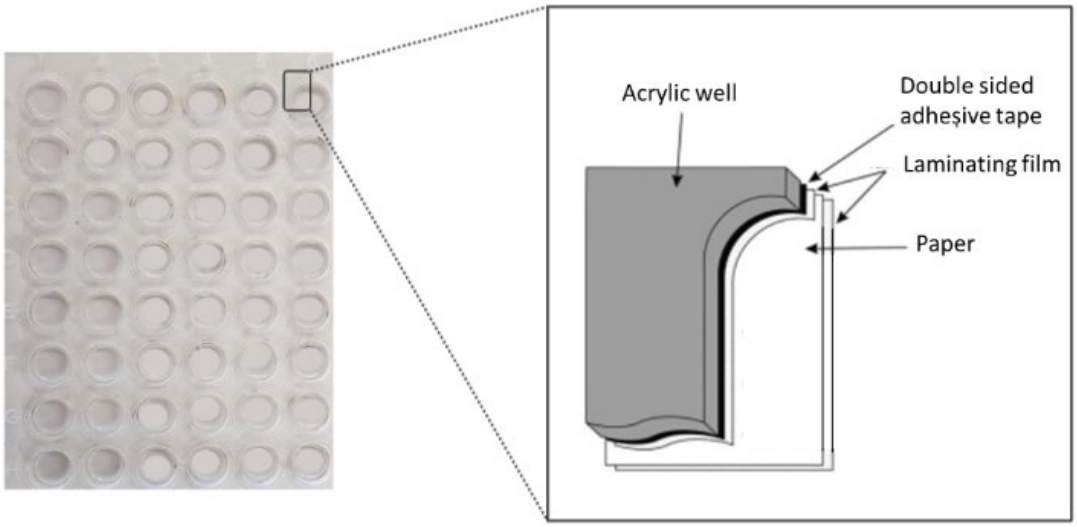

Figure 65 Diagram showing microplate used for EIA. Enlarged section shows schematic diagram of the microplate reaction well and the five layers of components used in assembly. Adapted from [246].

2. A 1µL aliquot of each liposome dispersion was dropped onto paper surface (in duplicate) within reaction well and allowed to dry. The liposomes are passively immobilised onto the microplate surface.
3. Blocking step: 2% Bovine Serum Albumin (BSA) (Gibco, Cat# 30063-572, NZ) in phosphate buffered saline (PBS) was flooded onto the surface of wells for 30 minutes, then removed by decanting.
4. Monoclonal anti-A reagent (Immucor, Cat# 0006400), diluted 1:4 in 2% BSA PBS. 100µL was added to all wells and incubated for one hour.
5. The EIA plate was washed three times with PBS, pH 7.4, and once with tris buffered saline (TBS) (50mM Tris, 150mM NaCl, 1mM $MgCl_2$ pH=9.0) by filling each well with 100µL for each wash and decanting.
6. The secondary antibody anti-mouse IgM/G/A conjugated to alkaline phosphatase (Chemicon Cat# AQ502A) was diluted 1:1000 in 2% BSA TBS and 100µL was added to each well and incubated for 30 minutes.
7. The wells were washed three times with PBS and once with substrate buffer (100mM Tris, 100mM NaCl, 50mM $MgCl_2$, pH=9.5).

8. The substrate NBT/BCIP (nitro-blue tetrazolium chloride and 5-bromo-4-chloro-3'-indolyphosphate p-toluidine salt, ThermoFisher Cat# 34042) was diluted 1:4 in substrate buffer and 100µL aliquots were added to each well for colour development of the assay.
9. The assay was stopped by washing with water after 15 minutes at RT.
10. The surface was dried and stored unprotected at RT.

Streptavidin conjugated assay for the detection of FSL-biotin

1. A 1µL aliquot of each liposome dispersion was dropped onto the surface of a microwell (in duplicate) and allowed to dry. Equivalent strength FSL micelle dispersions (i.e., FSL diluted in PBS alone) were also tested in parallel.
2. Blocking step: 2% BSA PBS was flooded onto the surface of microwells for 30 minutes, then removed by decanting.
3. 100µL of Streptavidin conjugated with alkaline phosphatase (Sigma, Cat#S2890-1MG) diluted to 1µg/mL in 2% BSA TBS was added to each well and incubated for 30 mins.
4. The wells were washed three times with TBS and once with substrate buffer.
5. The substrate NBT/BCIP was diluted 1:4 in substrate buffer and 100µL aliquots were added to each well for colour development of the assay.
6. The assay was stopped by washing with water after 15 minutes at RT, and the plate was allowed to air dry at RT.

Note: these methods can probably only detect FSL located on exterior surface of liposomes, as it would be expected that FSL located within liposome interior is unavailable to interact with antibody while the liposome remained intact.

Results

The results show successful detection of the FSL-A2 and FSL-biotin in all samples. A purple coloured precipitate developed with all FSL labelled liposome samples, and the FSL micelle dispersions, Figure 66. Blank liposomes (containing no FSL) and wells containing no liposomes were included as negative controls and as expected showed no colour development.

Results

a) FSL-A2

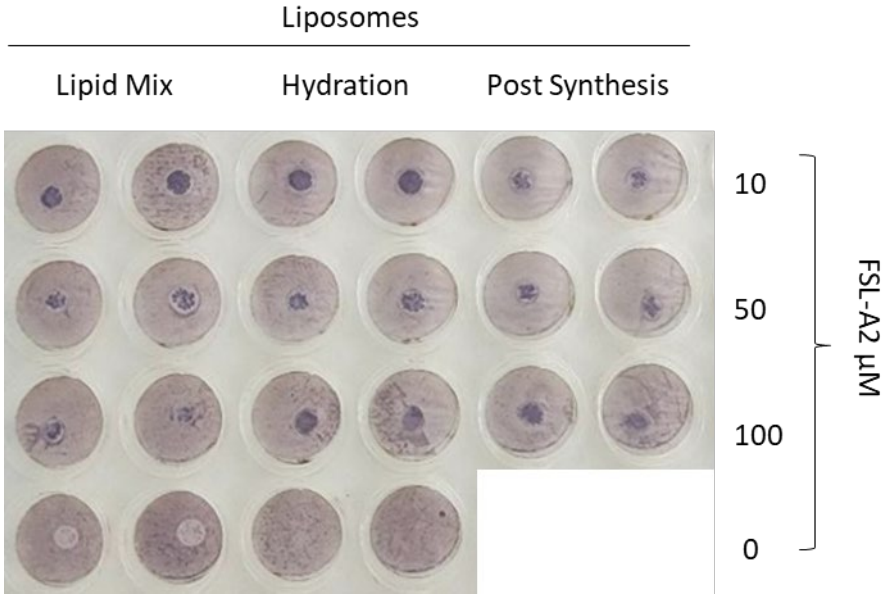

b) FSL-biotin

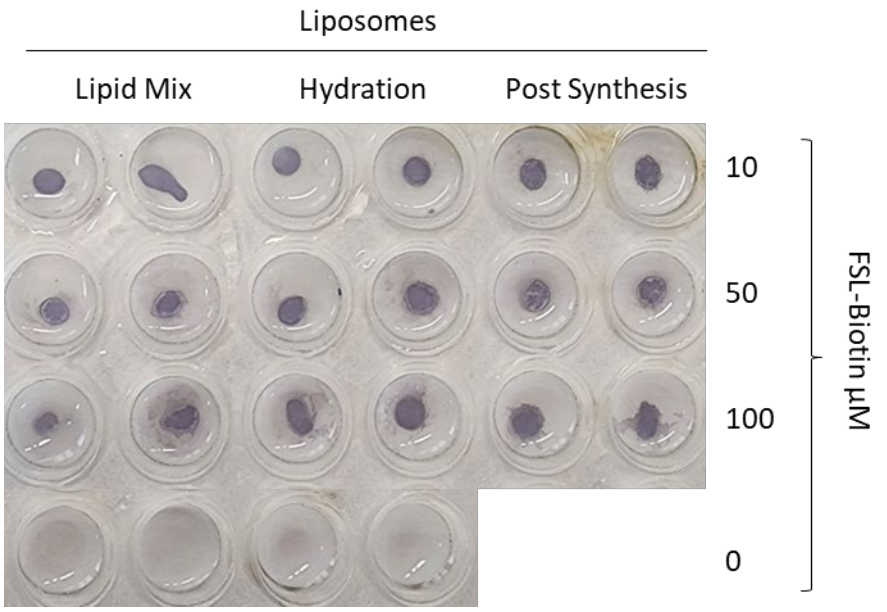

Figure 66 EIA plates showing detection of FSL-A2 and FSL-biotin liposomes. Liposome dispersions were detected by immunoassay on nitrocellulose microwell plates. The liposomes are passively immobilised onto the microplate surface and then detected by EIA. **(a)** The presence of A2 functional head group was detected by addition of murine monoclonal anti-A antibody, followed by a secondary antibody (an anti-mouse immunoglobulin) labelled with alkaline phosphatase. **(b)** The presence of biotin functional head group was detected by addition of streptavidin labelled with alkaline phosphatase. After addition of NBT/BCIP substrate the alkaline phosphatase precipitated the NBT/BCIP to form a purple colour. Colour development occurred with all FSL concentrations and all three methods of insertion.

These results confirm that the functional head group of FSL-A2 and FSL-biotin remained biologically active (detected by antibody/streptavidin). However, the location of the FSL construct within the liposome dispersion is unknown;

- any free micelle/monomer FSL remaining in the dispersion will be detected by this EIA technique and give a positive result.
- during this EIA technique the spherical structure of liposomes is unlikely to have been maintained after drying onto the paper surface. Potentially, FSL molecules that may have been sequestered within the liposome interior (either labelling the interior of bilayer membrane or present as monomer/micelle within liposomes aqueous core) may have become exposed and available for interaction as the liposomes deformed and dried onto paper. Whereas in their intact native form these would not be available to react with external reagents such as antibody/streptavidin.

Summary

The bioactivity of the functional head group of the FSL constructs did not appear to be affected by the addition to liposomes. FSL-A2 and FSL-biotin were successfully detected by EIA, and the FSL-FLRO4 liposome dispersions were fluorescent.

However, a difference in level of fluorescence was observed depending on method of FSL-FLRO4 insertion into liposomes. LM liposomes were brightest, and post synthesis the least bright. Addition of FSL by PS and H methods resulted in liposomes with similar levels of fluorescence.

The most interesting observation was that FSL-FLRO4 micelles showed much lower (96%) levels of fluorescence compared to FSL-FLRO4 liposomes, this is most likely because the FSL-FLRO4 is quenched when in micelle form (close proximity of fluorescent molecules can lead to self-quenching [332, 348]).

Chapter 3 Methods and Results: Dynamics of Insertion

This chapter of results focusses on the insertion and retention dynamics of FSL constructs within liposome membranes. The efficiency of FSL insertion into liposomes and the effects of temperature, time, FSL concentration, charge and lipid composition were investigated. The stability and retention of FSL within the liposome membrane was also studied. This investigation included the transfer of FSL between membranes (liposome to liposome and liposome to cell).

3.1 FSL incorporation into liposomes

The following experiment investigated the kinetics of FSL insertion into the liposome membrane. The effects of temperature, time, and method of FSL addition (LM, H or PS) were investigated. Figure 67 shows possible mechanisms of FSL incorporation into to liposomes.

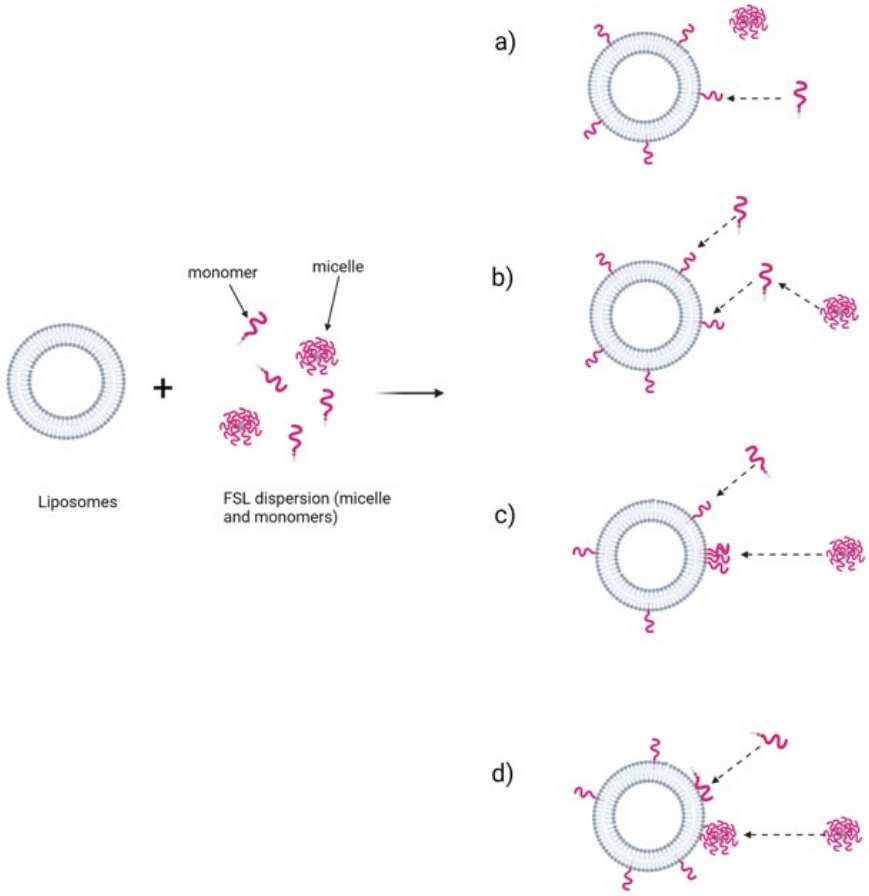

Figure 67 Schematic diagram showing possible mechanisms of FSL incorporation into liposome.(**a**) FSL monomers incorporate into liposome, no transfer of FSL from micelle. (**b**) FSL monomers may dissociate from micelle and can then incorporate into the liposome. (**c**) FSL micelle may adsorb to surface of liposme and then incorporate into the liposome membrane. (**d**) FSL micelles/monomers may adsorb to surface of liposome but do not incorporate into the liposome membrane. (Diagram approximately to scale, except liposomes ≈60nm diameter, not 100nm as synthesised in this study). Created with BioRender.com.

3.1.1 FSL-FLRO4

Spectrophotometry was used to measure changes in fluorescence of a liposome dispersion after the addition of FSL-FLRO4. In section 2.2.7 it was observed that FSL-FLRO4 micelle dispersions produce very little fluorescence in comparison to FSL-FLRO4 liposome dispersions (Figure 64). This is most likely because FSL-FLRO4 in micelle form self-quenches due to the fluorescein molecules being in close proximity to each other. When the FSL-FLRO4 incorporates into the liposome membrane the FSL molecules can move further apart and become unquenched. Consequently, fluorescence emission increases. It was hypothesised that this phenomenon could be used to measure the incorporation of FSL into liposomes by observing change in fluorescence of the liposome dispersion after the addition of FSL-FLRO4.

Initial experiment - 24 hours

An initial experiment was performed to establish the suitability of this technique. It was anticipated that after the addition of FSL-FLRO4 to a liposome dispersion that the fluorescence of the overall dispersion (which consists of a mixture of liposomes plus FSL micelles and/or monomers) would increase as more FSL incorporated into the liposome membranes.

Liposomes were prepared containing FSL-FLRO4 added by PS protocol. Immediately following the addition of FSL the liposome sample was divided into three aliquots which were stored at 4°C, RT and 37°C. At various time points an aliquot was removed from each and the fluorescence of the liposome dispersions measured.

Method

1. Blank liposomes (composed of EPC only) were prepared and divided into three 1mL samples.
2. An aliquot of FSL-FLRO4 stock solution was added to each of the 1mL of blank liposome samples, so that each contained 100µM FSL-FLRO4.
   Note: the liposome dispersions are subsequently referred to as 'FLRO4 liposomes', although they most likely consist of a mixture of liposomes plus FSL monomers and/or FSL micelles.
3. One sample was then stored at 4°C, one at RT, and one at 37°C for up to 24 hours.
4. An aliquot of 100µL was removed from each of the three FLRO4 liposome samples at various time points (5 mins, 15 mins, 30 mins, 1 hr, 4 hr, and 24 hr) during the 24 hour incubation and the fluorescence of the aliquots were measured by spectrophotometer. (Excitation 495nm, emission 520nm).

Results

Figure 68 shows the fluorescence of the FLR04 liposome dispersions stored at 4°C, RT and 37°C for 24 hours after the addition of 100µM FSL-FLRO4. (Note: after the addition of FSL-FLRO4 the liposome dispersions contain a mixture of liposomes and FSL-FLRO4 micelles and monomers but are simply referred to as FLRO4 liposomes).

The fluorescence of the FLRO4 liposome dispersions stored at all three temperatures increased with time. The increase was temperature dependent, where fluorescence increased more quickly at 37°C than RT, and was much slower at 4°C.

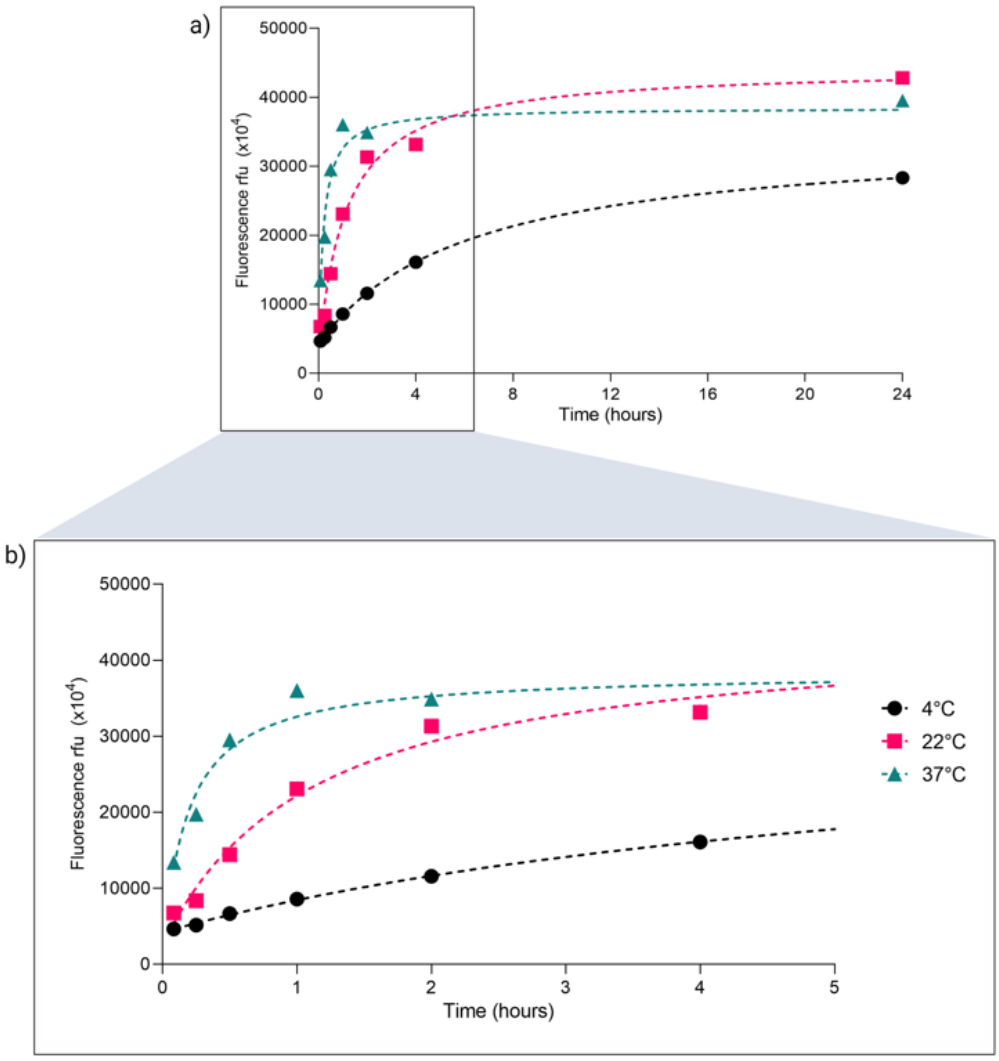

Figure 68 Fluorescence of liposome dispersion after the addition of 100µM FSL-FLRO4. The liposome dispersions were stored at 4°C, 22°C and 37°C for 24 hours immediately following the addition of FSL-FLRO4. Graph (**a**) shows fluorescence over 24 hours and graph (**b**) shows fluorescence during first 5 hours. The fluorescence of the liposome dispersion increased after the addition of FSL-FLRO4, fluoresence increased more quickly at 37°C than RT, and most slowly at 4°C. Liposomes stored at 37°C and RT reached a maximum fluorescence after approximately 1-4 hours incubation.

The maximum rfu obtained was 42,000 (24 hrs at RT). The FLRO4 liposomes incubated at 37°C showed a rapid increase in fluorescence before reaching a plateau of 39,000 rfu after approximately 1 hour incubation. FLRO4 liposomes stored at RT showed a slightly slower rate of increase, reaching a similar plateau (42,000 rfu) after approximately 4 hours incubation.

The fluorescence of the FLRO4 liposomes stored at 4°C showed a much slower rate of increase and were continuing to increase and had not reached the maximum rfu by 24 hours. The level at 24 hours was similar to that obtained at 30 mins at 37°C and 1.5 hours at RT.

The change in fluorescence is believed to correspond with movement of FSL from micelle (where it is quenched) into the liposome membrane (where it can fluoresce). Therefore, these results show that FSL insertion into liposomes is temperature dependent, occurring more quickly at 37°C and RT, and much slower at 4°C. FSL-FLRO4 incorporation has reached maximum insertion after ≈1 hours at 37°C and after 4 hours at RT.

Extended experiment – 1 week

The previous experiment was repeated for an extended time frame of one week, to determine if liposomes stored at 4°C would reach a similar plateau. In addition, liposomes prepared by all three methods of FSL addition (lipid mix, hydration, and post synthesis) were tested in parallel.

Liposomes were prepared by lipid mix, hydration and post synthesis methods and then immediately stored at three different temperatures, 4°C, RT and 37°C. The fluorescence of the liposome dispersions was then measured at various time points. The liposomes stored at 4°C and RT were monitored daily for seven days. The liposome dispersions stored at 37°C were monitored for 24 hours only. As shown in the previous experiment liposomes stored at 37°C have probably reached a maximum level of insertion within 2 hours incubation. Unfortunately, storing liposomes at 37°C for one week was not practical because liposomes in this study are prepared in PBS with no antibacterial preservative added and incubation at 37°C for an extended period could result in bacterial contamination and sample degradation. Experiments were repeated three times (results shown are mean ± standard deviation).

Method

1) Liposome dispersions containing 100µM FSL-FLRO4 were prepared by LM, H and PS methods of preparation (protocol 2.2.2).
2) Immediately following synthesis, the dispersions were divided into three 1mL samples which were stored at 4°C, RT and 37°C.
3) A 100µL aliquot was removed from each dispersion and the fluorescence emission measured by spectrophotometer (excitation 495nm, emission 520nm) at time 0, 2 hours and 24 hours. Following this the dispersions stored at 37°C were discarded, and the remaining dispersions (stored at 4°C and RT) were tested daily for a total of seven days.

Results

Figure 69 shows the change in fluorescence of FLRO4 liposome dispersions, after the addition of 100µM FSL-FLRO4, stored at 4°C, RT and 37°C.

The results show that the movement of FSL into liposomes is both temperature and time dependent for the first 24 hours or less. Differences were also observed between liposomes prepared by different methods. Liposomes prepared by LM method showed no change in fluorescence, at all storage temperatures and incubation times. These liposomes also showed the highest levels of fluorescence (max rfu 52,000).

The liposomes prepared by PS and H methods showed an initial increase in fluorescence before reaching a plateau (approximately 30,000 rfu). The liposomes stored at 4°C showed a much slower rate of increase and reached maximum fluorescence after approximately 24-48 hours incubation. The fluorescence of liposomes stored at RT and 37°C increased more quickly and reached the plateau within 4 hours (as seen in previous experiment).

a) Lipid Mix (LM) liposomes

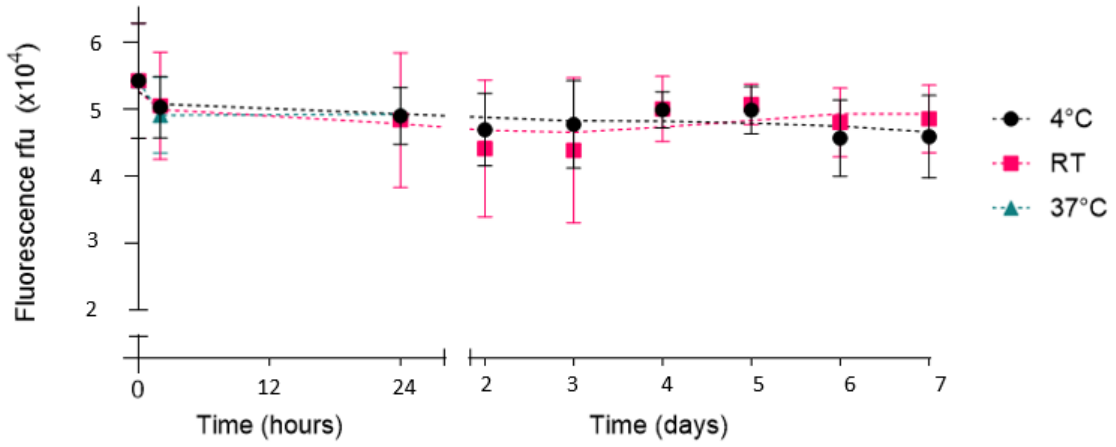

b) Hydration (H) liposomes

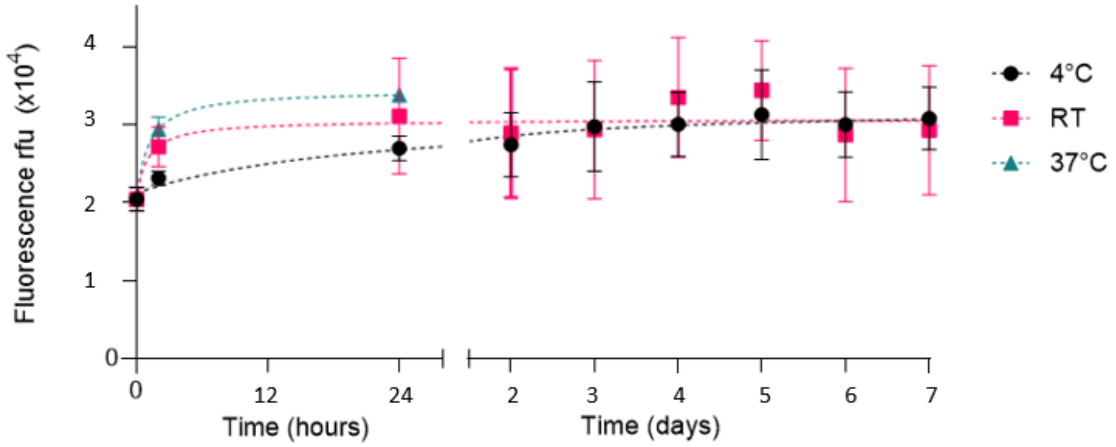

c) Post synthesis (PS) liposomes

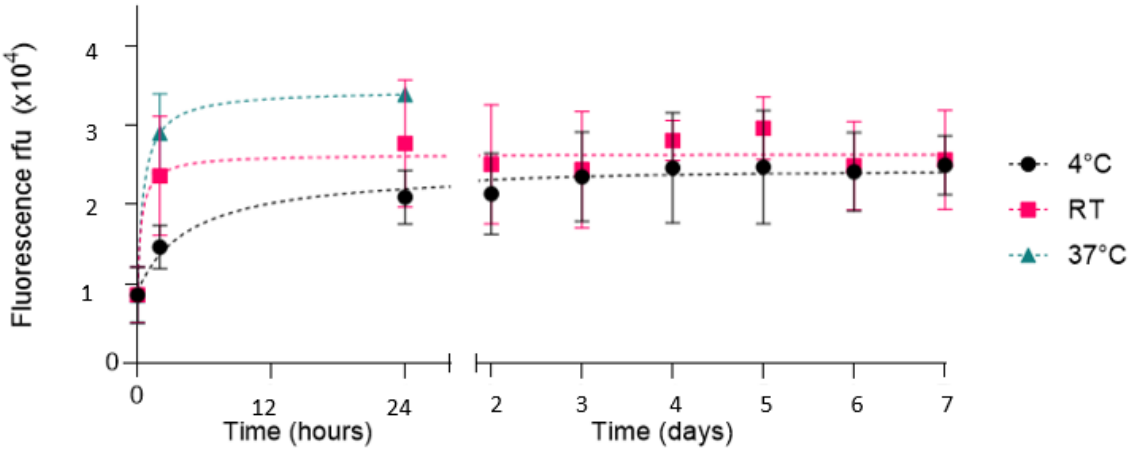

Figure 69 Fluorescence of 100 FLRO4 liposome dispersions stored at 4°C, RT, and 37°C. Liposome dispersions containing 100µM FSL-FLRO4 were prepared by **(a)** LM, **(b)** H, and **(c)** PS methods. H and PS liposomes showed an initial increase in fluorescence before reaching a plateau after 2 days at 4°C, and within 2-4 hours at RT and 37°C. LM liposomes showed no change in fluorescence at all storage temperatures. The liposome dispersions stored at 4°C and RT were tested for one week, while the liposomes stored at 37°C were only tested for 24 hours. Results shown are mean ± SD, n=3.

Comment

The liposomes prepared by lipid mix method showed no change in fluorescence over time regardless of temperature of storage. This is most likely because when the liposomes prepared by this method (LM) all of the FSL-FLRO4 constructs are integrated into the liposome membrane during the first step of liposome synthesis (see section 2.2.2). Because the FSL constructs are fully incorporated into the liposome membrane there are no micelle/monomer FSL is present and consequently there is no movement of FSL from quenched micelle form into the liposome membrane (where it becomes unquenched) and therefore no change in fluorescence is observed.

In the PS and H methods of preparation the FSL-FLRO4 is added to liposomes either after liposomes are completely formed (PS) or part way through their synthesis (H). In both methods FSL constructs are added to the liposome dispersion in micelle/monomer form (quenched). Earlier evidence suggests that micelles are forming at concentrations as low as ≈5µM (see 2.1.2 and 2.1.3), therefore the FSL dispersions used in this study would likely consist of a mixture of monomers and micelles (relative ratios unknown). The fluorescence of the PS and H liposome dispersions increase with time most likely as FSL moves from the quenched micelle form and integrates into the liposome membrane (becoming unquenched), as shown in Figure 70 and Figure 71.

PS and H liposomes dispersions reach a maximum fluorescence (≈3-3.5 $x10^4$ rfu) which is less than the level shown by LM liposomes (5 $x10^4$ rfu). Possible explanations include

- Because the liposome dispersions are unwashed, it is possible that some 'free' FSL micelles/monomers remain in the supernatant of the H and PS liposome dispersions. Since micelles are quenched, if they are present in HS and PS dispersions, they could account for the lower fluorescence observed in these dispersions compared with LM liposomes, which contain no micelles.
- In PS/H liposomes FSL micelles could adsorb to the liposome surface without becoming integrated into the membrane, this could result in them remaining in close contact (without integrating into the membrane they would be unable to diffuse through the membrane and spread out) and hence remaining quenched.
- quenching of FSL in liposome membrane may begin to occur as concentration in external membrane increases. The FSL constructs may cluster together which could lead to quenching.

It is possible that a combination of these is occurring.

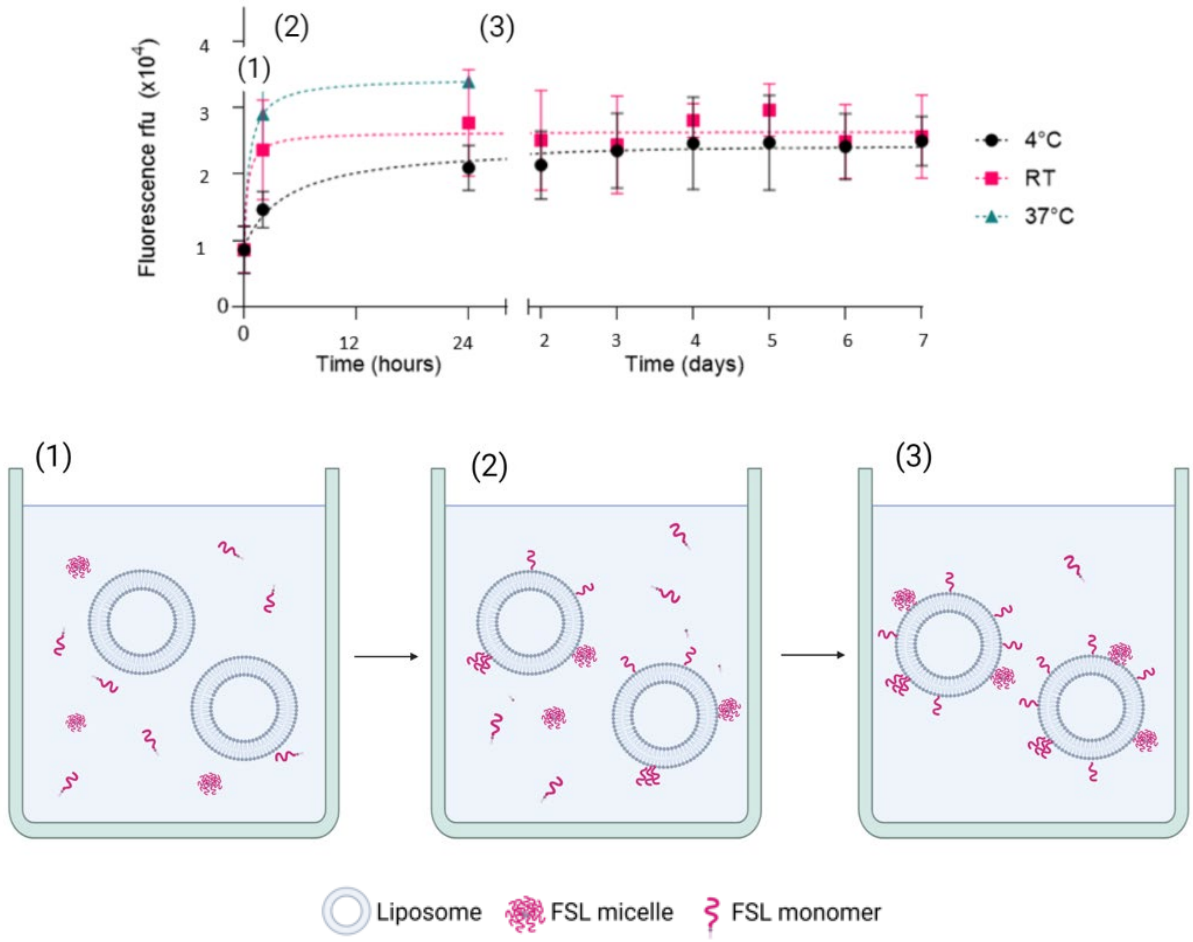

Figure 70 Fluorescence of liposome dispersion after the addition of FSL-FLRO4 by PS method. Speculated schematic of dynamic situation shown at various time points (**1**-**3**). (**1**) Initially the liposome dispersion contains unlabelled liposomes and a high concentration of FSL micelles/monomers. FSL is present in liposome supernatant only. (**2**) As the FSL constructs incorporate into the liposome the concentration of the monomer/micelle FSL in the dispersion decreases. The fluorescence of the dispersion increases as the FSL moves from quenched micelle form to unquenched in liposome membrane. (**3**) Fluorescence of dispersion reaches a maximum and then remains constant. Diagram approximately to scale. (Note: liposome shown are ≈50nm diameter, not 100nm as synthesised in this study). Created with BioRender.com.

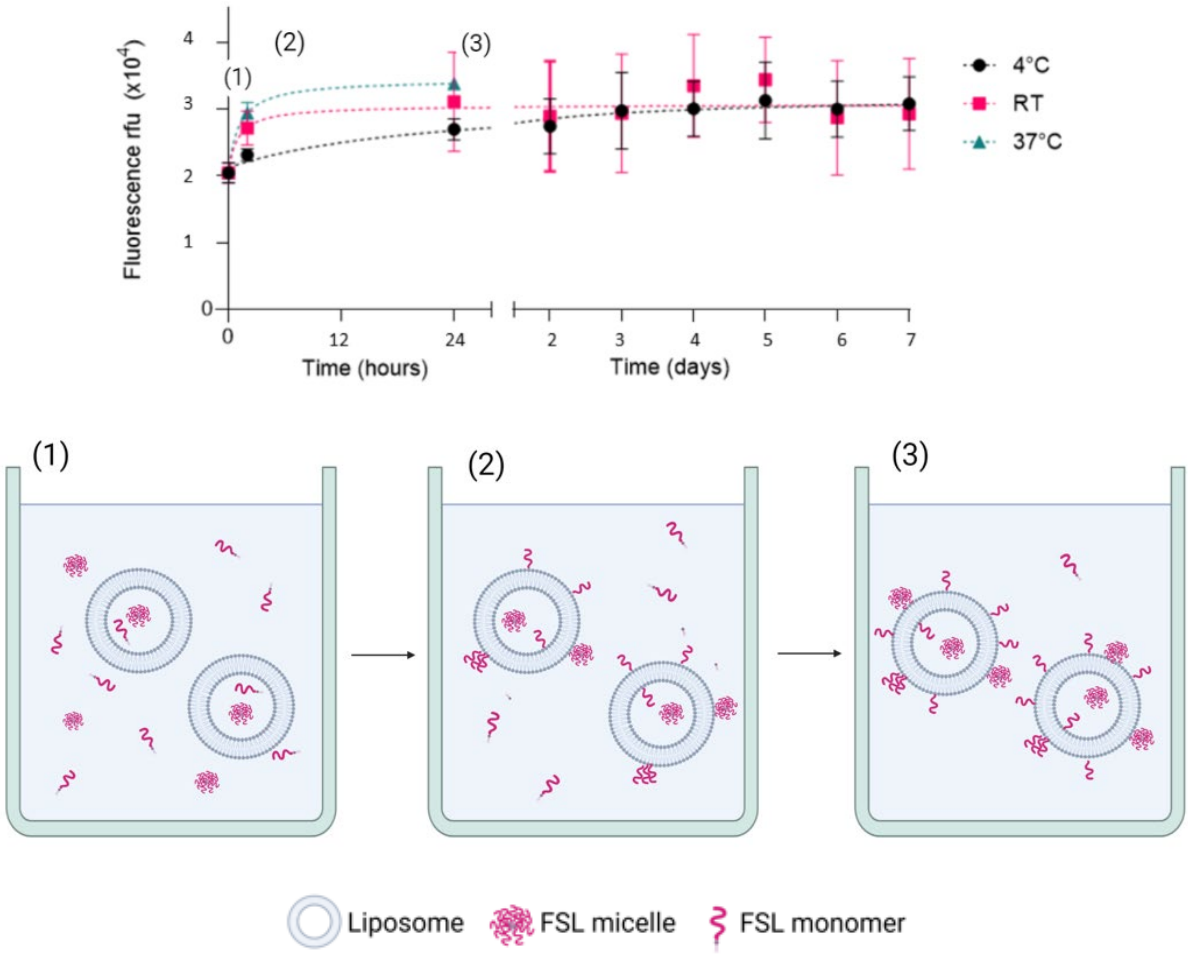

Figure 71 Fluorescence of liposome dispersion after the addition of FSL-FLRO4 by H method. Speculated schematic of dynamic situation shown at various time points (**1-3**). (**1**) initially the liposome dispersion contains unlabelled liposomes and a high concentration of FSL micelles/monomers. FSL is present both within liposome interior and in the external supernatant. (**2**) As the FSL constructs incorporate into the liposome the concentration of the monomer/micelle FSL in the dispersion decreases. The fluorescence of the dispersion increases as the FSL moves from quenched micelle form to unquenched in liposome membrane. (**3**) Fluorescence of dispersion reaches a maximum and then remains constant. Diagram approximately to scale. (Note: liposome shown are ≈50nm diameter, not 100nm as synthesised in this study). Created with BioRender.com.

3.1.2 FSL-A2

To investigate if insertion of FSL into liposomes is affected by differences in head group/spacer the insertion kinetics of FSL-A2 were also investigated. Previous work has established that micelle FSL-A2 present in a solution will readily coat surfaces on contact, such as microwell plates, and that EIA can then be used to detect this immobilised FSL-A2 [246]. It was found during this study that A2 liposomes did not bind to EIA wells. Therefore, EIA was used to measure the amount of micelle/monomer FSL present in a liposome dispersion. The unincorporated micelle/monomer FSL-A2 coats the surface of the wells and could then be detected by EIA. By measuring the change in free FSL-A2 within the liposome dispersion over time, the movement of FSL from micelle into liposomes could be indirectly observed.

Method overview

The presence of FSL-A2 bound to the microplate surface was detected using anti-A followed by a secondary anti-antibody enzyme conjugate. The presence of FSL-A2 was detected by a colour change when the enzyme substrate was added. If no free FSL-A2 was present, the primary and secondary antibodies are unable to bind and were washed away. In this case there was no colour change when the substrate was added.

If FSL-A2 is present as micelle/monomers within the liposome dispersion, it binds to the microplate surface, resulting in a positive reaction (colour change) by EIA. If no micelle/monomer FSL-A2 is present in the liposome dispersion, then a negative reaction (no colour change) is obtained.

Therefore, as FSL moves from micelle/monomer form (present in the liposome dispersion supernatant) and associates/integrates into the liposome membrane, the EIA results will change from positive (colour change) to negative (no colour change). Figure 72 shows a schematic diagram of this EIA technique.

EIA method

1. Wells (96 well culture plate, Greiner Bio-one, Cat# 650180, Mediray) were blocked with 2% BSA PBS for 1 hour at RT.
2. The liposome samples were diluted 1:3 in PBS and 50µL aliquots were added to the plate in duplicate and incubated for 30 minutes at RT.
3. The plate was washed four times with PBS.
4. Murine monoclonal IgM anti-A (Anti-A Series 1, Immucor Cat# 0006400) reagent was diluted 1:4 in 2% BSA PBS. Aliquots of 50µL were added to all wells and incubated for 30 minutes at RT.
5. The plate was washed three times with PBS and then once with TBS.
6. The secondary antibody, anti-mouse IgG/A/M alkaline phosphatase conjugated antibody (Chemicon Cat# AQ502A, USA), was diluted 1:1000 in 2% BSA TBS and 50µL aliquots were incubated in wells for 30 minutes at RT.
7. The plate was washed three times with TBS and then once with substrate buffer (100mM Tris, 100mM NaCl, 50mM $MgCl_2$, pH=9.5).
8. The substrate p-nitrophenylphosphatase (pNPP) (Sigma Aldrich Cat# P7998-100ml) was added to plate and the absorbance was read at 405nm after 30 minutes incubation at RT.

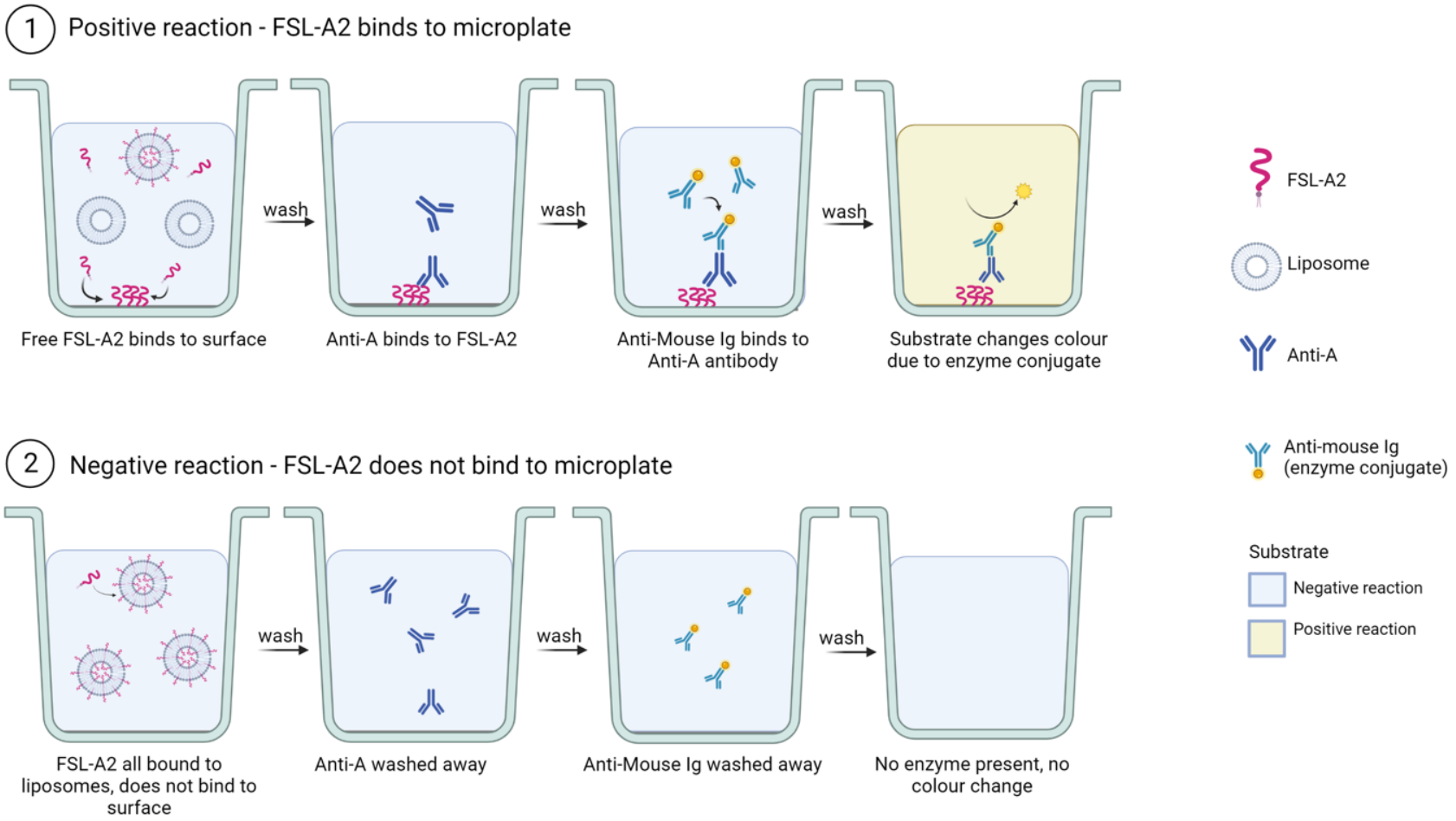

Figure 72 EIA technique used to detect free FSL-A2 present in liposome dispersion. (**1**) Free FSL-A2 is present in supernatant alongside liposomes and binds to the microwell surface. The surface bound FSL-A2 was then detected using anti-A and a secondary anti-antibody with an alkaline phosphatase conjugate . When substrate is added the presence of alkaline phosphatase causes the solution to turn yellow. (**2**) When there is no free FSL in liposome dispersion (it has all incorporated into liposomes) the anti-A and secondary anti-antibody are unable to bind to the plate and are washed away, consequently there is no colour change when the substrate is added. Note: anti-A is actually an IgM reagent, but for simplicity is represented with an IgG in this diagram. Created with BioRender.com.

Initial experiment to determine if FSL-A2 liposomes bind to microplate surface

An initial experiment was conducted to determine if FSL-A2 liposomes were able to bind to the microplate surface and cause a positive reaction by EIA.

1. Liposomes containing 50µM FSL-A2 were prepared by LM, H and PS methods of preparation (method 2.2.2).
2. The liposomes were stored at 4°C for 5 days (to ensure maximum FSL insertion into liposome had occurred).
3. An aliquot was removed from each liposome sample and analysed by EIA (method below).
4. Liposomes containing no FSL were tested in parallel as a negative control (labelled blank).
5. Dispersions of FSL-A2 in PBS (1, 10 and 50µM) were prepared also tested in parallel. Note that although these are labelled as micelle dispersions in Figure 73, they may also contain FSL monomers.

Results

Figure 73 shows the EIA reactions of 50 A2 liposomes prepared by LM, H and PS protocols, and FSL-A2 micelle/monomer dispersions.

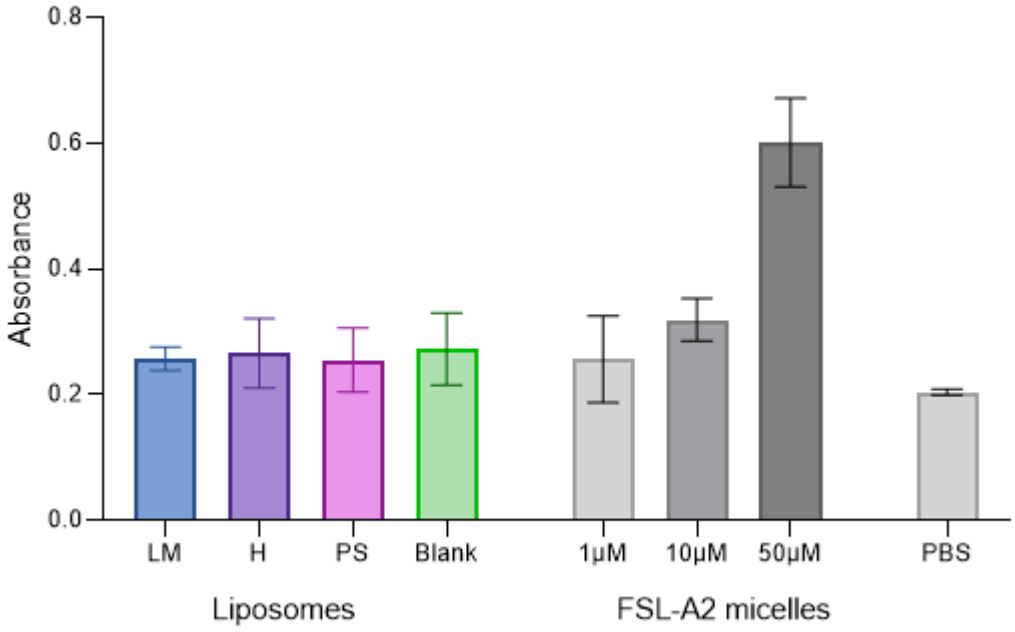

Figure 73 EIA detection of FSL-A2 on microwell surface after incubation with liposomes and micelles. FSL-A2 was not detected by EIA on microwell surface after incubation with all three 50µM A2 liposome suspensions (LM, H PS), same reactivity observed as negative controls (blank liposomes containing no FSL and PBS). FSL-A2 was detected on microwell surface after incubation with 10µM and 50µM FSL-A2 micelle dispersions (note FSL dispersion labelled micelles but may also contain monomers). Mean ±SD, n=2.

All the A2 liposomes, regardless of method of FSL insertion, showed negative reactions, they had the same absorbance (0.25) as the blank liposomes (0.27) and PBS (0.20). The 1µm FSL-A2 dispersion also showed a negative reaction (0.25).

The 10µM and 50µM FSL-A2 micelle/monomer dispersions showed positive reactivity (0.32 and 0.60 respectively).

The results show that the A2 liposomes had no reactivity by this EIA technique, the A2 liposomes did not bind to the plate. In contrast the FSL-A2 micelles/monomers (≥10µM concentration) resulted in a positive reaction. Therefore, this technique appears to be suitable to detect 'free' monomer/micelle FSL present within a liposome dispersion. Only micelle/monomer FSL results in positive reaction, once the FSL has incorporated into liposome it is not detected, therefore allowing indirect measurement of FSL insertion/association into the liposomes.

Detection of movement of FSL-A2 from free form (micelle/monomer) into liposome

Method

1. Liposomes containing 100µM FSL-A2 were prepared by LM, H and PS methods of preparation (method 2.2.2).
2. Immediately following synthesis each liposome dispersion was divided into three aliquots which were stored at 4°C, RT and 37°C.
3. An aliquot was removed from each sample at various time points EIA (see method below) was used to measure free FSL present.
4. Liposomes stored at 4°C and RT after 2 hours, 1, 3 and 7 days of storage. Due to reasons discussed previously samples stored at 37°C were only tested at time points 0 and 2 hours.
5. Liposomes containing no FSL were also included as a negative control, and FSL micelles dispersions (10, 50 and 100µM) were also tested at each time point.
6. Experiment was carried out in duplicate.

Results

Figure 74 shows the detection of monomer/micelle FSL-A2 after liposome dispersions were stored at different temperatures, 4°C, RT, and 37°C, after the addition of FSL-A2. The results are shown minus the blank and as a percentage of the (maximum) absorbance obtained by 100µM FSL-A2 micelle dispersions (run in parallel at each time point) to enable comparison between time points and correct for slight experimental variation/colour development between plates. PBS and blank liposome result averaged and used as the blank value.

LM liposomes showed almost no change in absorbance at all temperatures and time points. Absorbance was low (<5%) and very close to the results shown by the negative controls (PBS and blank liposomes). This indicates that LM liposome dispersions contain no or very little micelle/monomer FSL, as expected due to the method of FSL incorporation (FSL is incorporated into lipid film during first step of synthesis and consequently all FSL is integrated into the liposome membrane, see 2.2.2).

As seen with FSL-FLRO4 the incorporation of FSL-A2 into H and PS liposomes was temperature dependent, occurring most quickly at 37°C. PS and H liposomes stored at 37°C showed rapid decline of detected free micelle/monomer FSL within the liposome dispersion to <10% reactivity by 2 hours. These results show that the majority of micelle/monomer FSL present in H and PS liposome dispersions has become incorporated into the liposomes within 2 hours storage at 37°C.

H and PS liposomes stored at RT and 4°C also showed decrease in detected monomer/micelle FSL-A2 reaching maximum insertion within 24 and 72 hours respectively. Liposomes stored at 4°C took slightly longer than those stored at RT to reach maximum insertion. The maximum insertion point (shown by plateau) was approximately the same as the absorbance shown by the negative controls (blank liposomes and PBS). This suggests that the majority of monomer/micelle FSL has incorporated/associated with the liposomes.

a) Lipid Mix

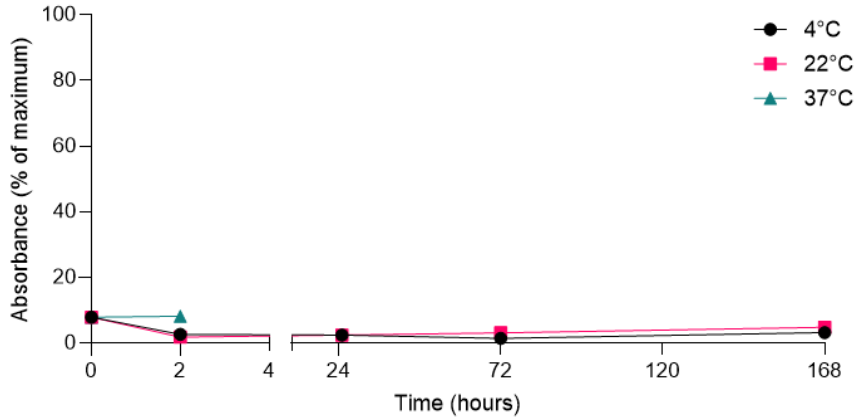

b) Hydration

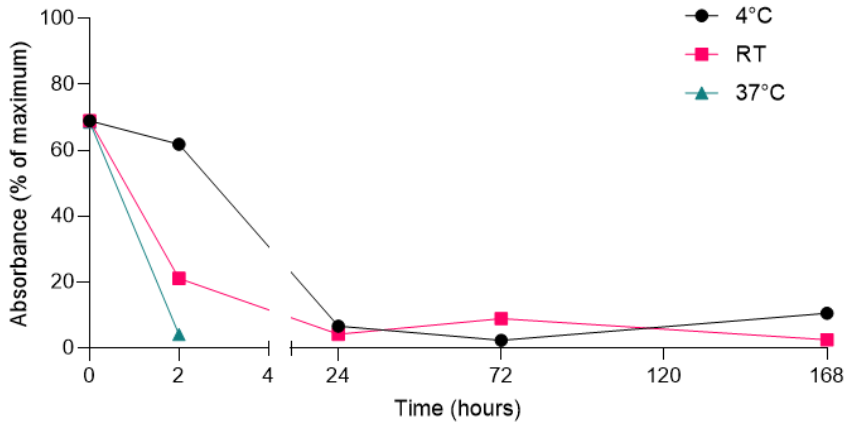

c) Post Synthesis

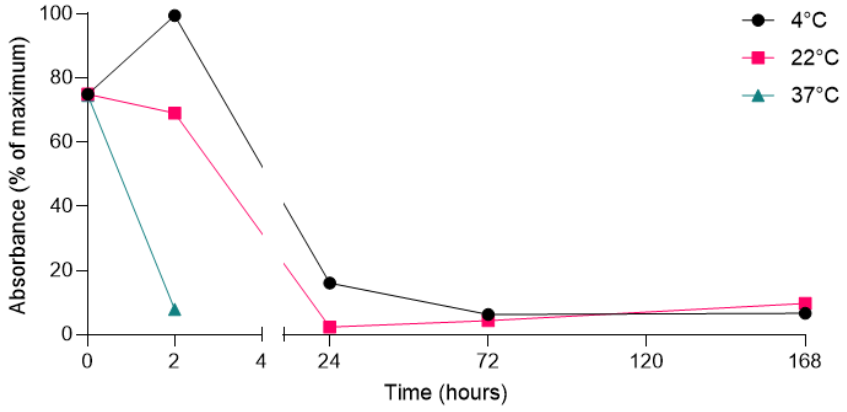

Figure 74 Detection of free FSL-A2 in 100 A2 liposome dispersions. Liposomes were prepared with 100µM FSL-A2 added by (**a**) LM, (**b**) H, and (**c**) PS methods and stored at 4°C and RT for one week, or 37°C for 2 hours. Free FSL-A2 decreased rapidly in both the PS and H liposome dispersions during the first 24 hours and maximum insertion was reached within 2 hours at 37°C, and between day 1-3 when stored at RT and 4°C. No free FSL-A2 was detected in LM liposomes. Results, minus the PBS blank, are shown as a percentage of the (maximum) absorbance obtained from the positive control 100µM FSL-A2 micelle dispersion carried out in parallel at each time point. Blank liposomes (with no FSL) and FSL micelle dispersions were tested in parallel (results not shown).

3.1.3 FSL-Biotin

The same experiment was attempted to be carried out with FSL-Biotin. The same method was followed as for FSL-A2 with the exception that FSL-Biotin was detected by the addition of streptavidin conjugated with alkaline phosphatase, rather than anti-A followed by anti-antibody conjugated with alkaline phosphatase.

Method

1. Wells (96 well culture plate, Greiner Bio-one, Cat# 650180, Mediray) were blocked with 2% BSA PBS for 1 hour at RT.
2. The liposome samples were diluted 1:3 in PBS and 50µL aliquots were added to the plate in duplicate and incubated for 30 minutes at RT.
3. The plate was washed three times with PBS and once with TBS.
4. 100µL of Streptavidin conjugated with alkaline phosphatase (Sigma, Cat#S2890-1MG) diluted to 1µg/mL in 2% BSA TBS was added to each well and incubated for 30 minutes at RT.
5. The plate was washed three times with TBS and then once with substrate buffer.
6. The substrate p-nitrophenylphosphate (pNPP) (Sigma Aldrich Cat# P7998-100ml) was added to plate and the absorbance was read at 405nm after 30 minutes incubation at RT.

Results

Unfortunately, when the initial trial was carried out, to compare FSL-biotin liposomes with FSL-biotin micelle/monomer dispersions (to determine if FSL-biotin liposomes were unable to bind to the plate) it was found that the FSL micelle/monomer dispersions did not result in good positive reactivity. Very little colour development occurred, even with 100µM FSL-biotin micelle dispersion, as shown in Figure 75. In addition, very little difference between liposomes, micelles, and PBS (negative control) was seen. It was decided that this differentiation was not sufficient to proceed.

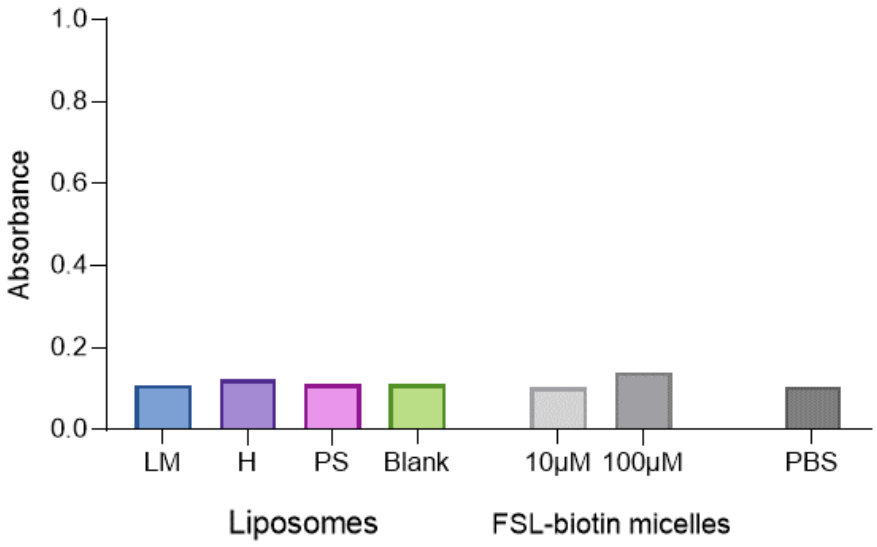

Figure 75 EIA detection of FSL-biotin liposomes and micelles. Liposomes were prepared containing 100µM FSL-biotin by LM, H and PS protocols. Blank liposomes containing no FSL were also tested as a negative control. 10µM and 100µM dispersions of FSL-biotin (labelled micelles but may also contain monomers) were tested. Very little colour development occurred, results showed very little difference between liposomes and micelles and PBS blank control.

A possible explanation for the very low reactivity shown by FSL-biotin micelle solutions is that FSL-biotin constructs have been shown to adopt a folded conformation when coated onto a surface and when in micelle formation [260]. Zalygin et al. predict using a combination of molecular dynamics simulation and experimental results that 99% of the FSL-biotin molecules coating a surface adopt a folded conformation, with only 1% fully extended (although the relative percentage of extended FSL-biotin could be affected by external factors such as temperature) [260]. The FSL-biotin construct can fold via the flexible hinge region in the CMG spacer, so that the hydrophobic biotin head groups are 'hidden' as shown in Figure 76. Therefore, at any one point in time only approximately 1% of the biotin residues are available for interaction with streptavidin. It is unknown whether there is a permanent presentation of only 1% of biotin residues, or whether it is a dynamic 'pop-up' process [260]. Because most of the biotin residues are hidden and unable to react with streptavidin this may be causing the lack of reactivity seen in EIA.

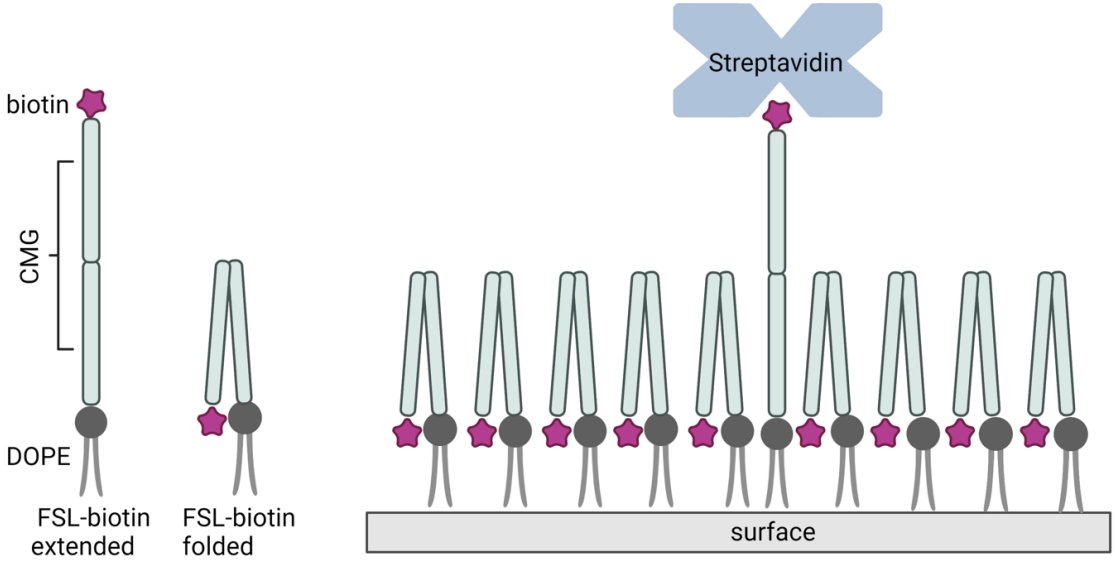

Figure 76 Predicted conformation of FSL-biotin constructs coating a surface. A monolayer of constructs forms, 99% of the FSL molecules are folded and only ≈1% adopt an extended conformation [253, 260]. The majority of the biotin head groups are unavailable to react with streptavidin. Adapted from [260]. Created with BioRender.com.

Summary

Free FSL was not detected in liposome dispersions prepared by LM protocol. In the LM protocol FSL is added to liposomes with the lipid ingredients before formation of the thin lipid film. Consequently, the FSL constructs are an integral part of liposome membrane (see 2.2.2) and there is no 'free' FSL micelles/monomers present in the liposome dispersion. Therefore, no change in fluorescence or free FSL was detected.

Incorporation of FSL-A2 and FSL-FLRO4 constructs into liposomes prepared by H and PS protocols was temperature and time dependent, occurring most quickly at 37°C and much more slowly at 4°C. Maximum FSL insertion was reached within 2 hours when liposome dispersions were incubated at 37°C, within 4 hours at RT, and after approximately 2 days when stored at 4°C.

There was no major difference detected in the rate of insertion between FSL-A2 and FSL-FLRO4, indicating that the functional head group and spacer did not significantly alter insertion kinetics.

3.2 Transfer of FSL between liposomes

Experiments were conducted to determine if FSL constructs could transfer between liposomes; A2 and Biotin liposomes were prepared and then 'liposome mix' samples composed of equal volumes of A2 liposomes and biotin liposomes were made. After incubation an EIA technique was used to determine if the FSL constructs were able to transfer from one liposome to another by detecting the formation of liposomes containing both FSL-A2 and FSL-biotin on their surface. The effect of incubation time and temperature and the method of liposome preparation on this transfer was investigated.

Possible transfer mechanisms are shown in Figure 77 and briefly described below;

a) transfer of free monomer/micelle FSL present in supernatant,
b) FSL monomer diffusion: FSL dissociates from liposome membrane and transfers to another liposome by diffusion through the aqueous space.
c) FSL transfer occurs during collision of liposomes
d) Fusion of liposomes

The exact mechanism of FSL integration into liposomes is unknown, as discussed previously depending on method of synthesis FSL constructs may be integrated into the liposome membrane, and/or FSL micelles could be adsorbed to the liposome surface. It is possible that FSL transfer will be affected by the method of FSL association (integration/adsorption) with the liposome.

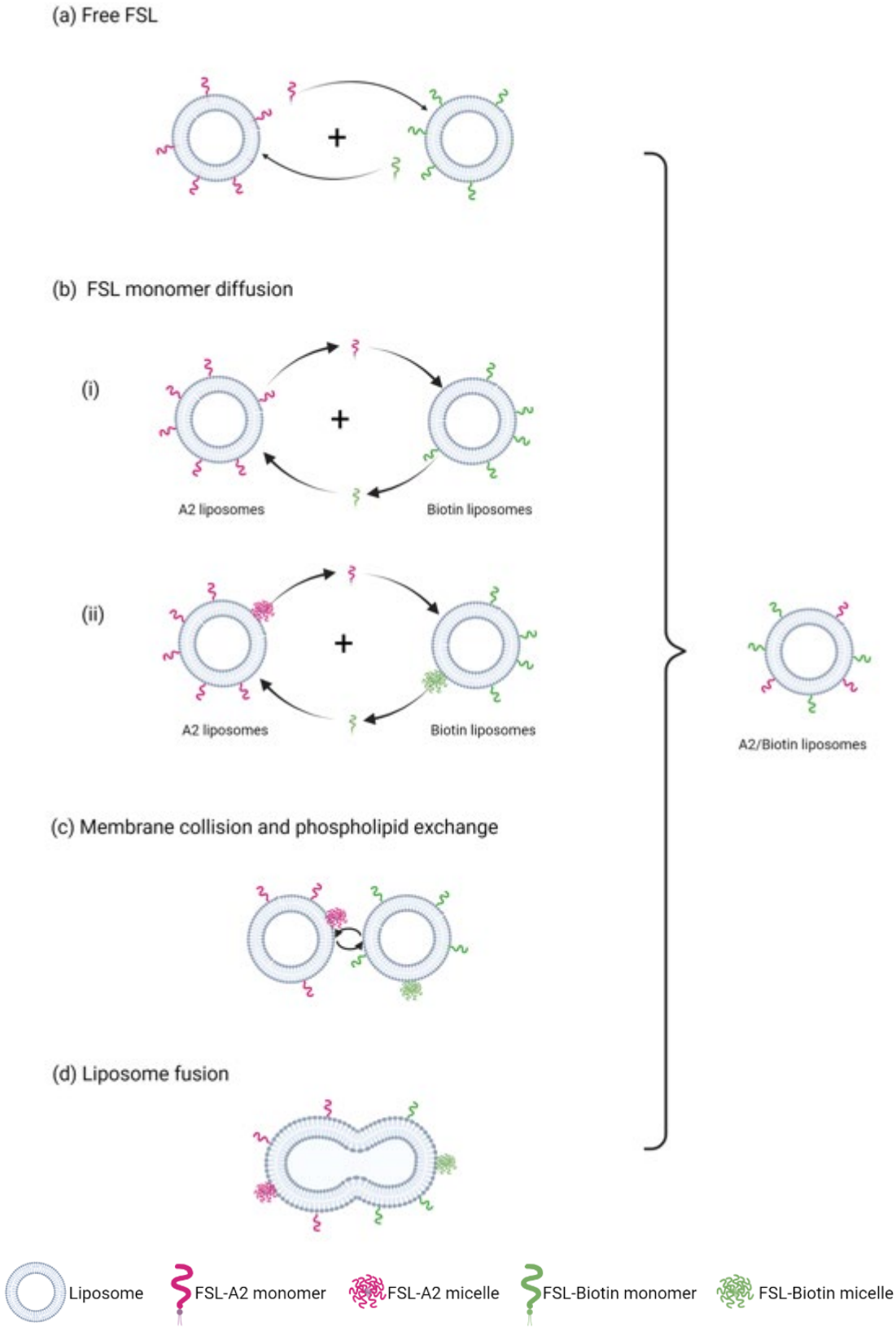

Figure 77 Theoretical mechanisms of FSL transfer between liposomes. (**a**) Free FSL present in liposome supernatant transfers to liposome. (**b**) FSL monomer diffusion: (**i**) FSL that was integrated into liposome membrane or (**ii**) FSL that was adsorbed to liposome surface disassociates and transfers to another liposome by diffusion through aqueous space (**c**) liposomes collide and FSL exhanges between liposome membranes during the collision (as in (b) FSL may be (i) integrated or (ii) adsorbed to liposome membrane) (**d**) Liposomes fuse together. Diagram not to scale. Created with BioRender.com.

Method Overview

Liposome 'mix' samples, containing equal volumes of A2 liposomes mixed with biotin liposomes, were prepared. These mix samples were then divided into three aliquots and incubated at either 4°C, RT or 37°C for up to 72 hours. An EIA technique using streptavidin coated microwell plates was used to detect if liposomes containing both FSL-A2 and FSL-biotin had been formed. Liposomes labelled with FSL-biotin bind to the streptavidin coating on the microwell surface. After washing to remove unbound liposomes an anti-A reagent followed by a secondary alkaline phosphatase labelled anti-immunoglobulin reagent was used to detect the presence of FSL-A2 on the liposomes which were bound (via FSL-biotin) to the streptavidin wells, see Figure 78. Only the liposomes which have both FSL-biotin and FSL-A2 on their surface result in a positive reaction. Therefore, a positive reaction indicated that the transfer of FSL between liposomes had occurred.

Method

1. Liposome dispersions containing 100µM FSL-A2 and liposome dispersions containing 100µM FSL-biotin were prepared by LM, H and PS protocols (see 2.2.2)
2. The liposome dispersions were then stored at 4°C for at least 3 days to ensure maximum FSL incorporation into the liposomes had occurred.
3. Equal volumes of FSL-A2 and FSL-biotin liposomes were mixed to form nine liposome mix samples, as detailed in Table 14.
4. Each of the nine liposome mixes were divided into three aliquots which were stored at 4°C, RT and 37°C for up to 24 hours.
5. Aliquots were removed from each liposome mix at various time points and analysed by EIA (method detailed below, Figure 78) to determine if liposomes containing both FSL-A2 and FSL-biotin had been formed. Once transfer of FSL was detected further time points were not tested.
6. Aliquots of the original unmixed liposome dispersions and blank liposomes were also incubated at 4°C, RT and 37°C and were tested in parallel as negative controls at each time point (results not shown).

Table 14 Description of liposome mix samples

Liposome Mix	Liposome description (1:1 v/v)		
	100 biotin	:	100 A2
1	LM	:	LM
2	LM	:	H
3	LM	:	PS
4	H	:	LM
5	H	:	H
6	H	:	PS
7	PS	:	LM
8	PS	:	H
9	PS	:	PS

EIA technique for the detection of FSL-A2

1. Blocking step: Microplate wells (Pierce™Streptavidin coated clear strip plates with Blocker™BSA, Cat# 151221 ThermoScientific USA) were washed four times with 100µL of 2% bovine serum albumin (Gibco, Cat# 30063-572, NZ) in phosphate buffered saline pH 7.4 (PBS).
2. Liposomes were diluted 1:4 with PBS and then 50µL aliquots were incubated for one hour at RT.
3. The microplate was washed four times with PBS.
4. Monoclonal anti-A (Immucor, Cat# 0006400) was diluted 1:4 in 2% BSA PBS and 50µL was added to all wells and incubated for thirty minutes.
5. The microplate was washed three times with PBS and then once with TBS.
6. The secondary antibody anti-mouse IgM/G/A conjugated to alkaline phosphatase (Chemicon Cat# AQ502A) was diluted 1:1000 in 2% BSA TBS and 50µL was added to each well and incubated for 30 minutes at RT.
7. The microplate was washed three times with TBS and once with substrate buffer (100mM Tris, 100mM NaCl, 50mM $MgCl_2$, pH=9.5).
8. The substrate, pNPP, was added to each well (50µL) for colour development of the assay
9. Absorbance was read at 405nm after 60 minutes.

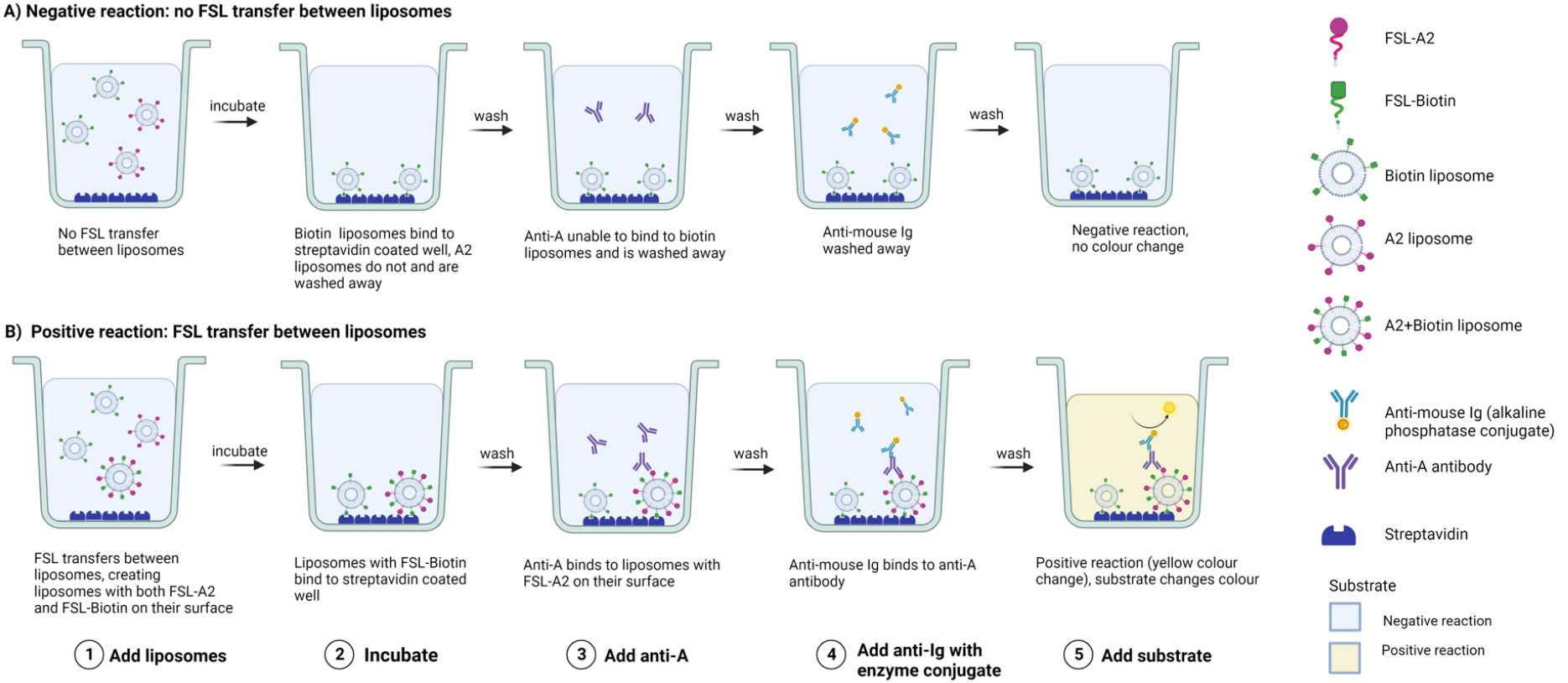

Figure 78 Diagram showing EIA method used to detect transfer of FSL between liposomes. (**a**) Negative reaction: (**1**) FSL does not transfer between liposomes. (**2**) Biotin liposomes bind to well via streptavidin and A2 liposomes washed away, (**3**) anti-A reagent unable to bind to liposomes as no FSL-A2 present. (**4**) Secondary anti-Ig (with enzyme conjugate) unable to bind and washed away. (**5**) No colour change when conjugate added as no enzyme present. (**b**) Positive reaction: (**1**) FSL transfers between liposomes resulting in liposomes labelled with both FSL-A2 and FSL-biotin. (**2**) A2/biotin liposomes bind to streptavidin coated wells. (**3**) Anti-A reagent binds to liposomes with A2 also on their surface, (**4**) secondary anti-antibody (with enzyme conjugate) binds to anti-A. (**5**) Substrate is added and due to presence of enzyme changes colour to yellow. (Note: anti-A shown as an IgG molecule in diagram but is actually IgM). Created with BioRender.com.

Results

The EIA results for each liposome mix are shown in Figure 79. Results are shown with the liposome mixes organised by increasing positive reactivity. A positive reaction indicated that liposomes containing both FSL-A2 and FSL-biotin on their surface were present within the dispersion and therefore indicated that FSL transfer between liposomes had occurred. Absorbances are shown minus baseline (time = 0) reactivity. As controls the unmixed liposome dispersions and blank liposomes (containing no FSL) were tested in parallel at each time point. These all gave expected negative reactions, results not shown.

The transfer of FSL was temperature dependent, occurring much faster at 37°C than 4°C. Transfer of FSL in liposomes stored at 37°C was detected in all samples after 4 hours incubation. When stored at RT transfer was detected after 24 hours, while those stored at 4°C did not show transfer in the time frame tested, with the exception of sample number 9 which showed weak positive reaction.

Variation in reactivity between mix samples was observed and no obvious pattern could be identified. Results are arranged by strength of positive reaction on graphs. In the samples stored at 37°C the highest reactivity was seen in the liposome mix samples which contained PS liposomes (samples 3, 6, 7, 8, and 9). PS liposome dispersions may still contain some residual free micelle/monomer FSL which could be contributing to this perceived increased in transfer. However, this same pattern was not seen with the liposome stored at RT. In this case liposomes mix 6, 7, and 8 were among the least reactive. No pattern could be discerned for the RT mix samples regarding method of FSL addition and transfer of FSL.

Of note is liposome mix 1 which was composed of liposomes that were both prepared by lipid mix method, meaning there was no micelle FSL present within this mix. FSL transfer in this case can not be due to mechanism (a) shown in Figure 77. The positive reaction observed from this sample (at both 37°C and RT) provides strong evidence that FSL transfer between liposome membranes is occurring and is not solely due to residual free FSL remaining in supernatant (although this may also occur).

From these results it can not be determined which of the transfer mechanisms shown in Figure 77 are occurring. However, mechanism (d) is considered unlikely as the liposome dispersions have been shown to be stable (for at least 8 weeks) with no significant change in liposome size observed (see 3.4.1). This indicates that significant liposome fusion/aggregation is not occurring.

a) 37°C

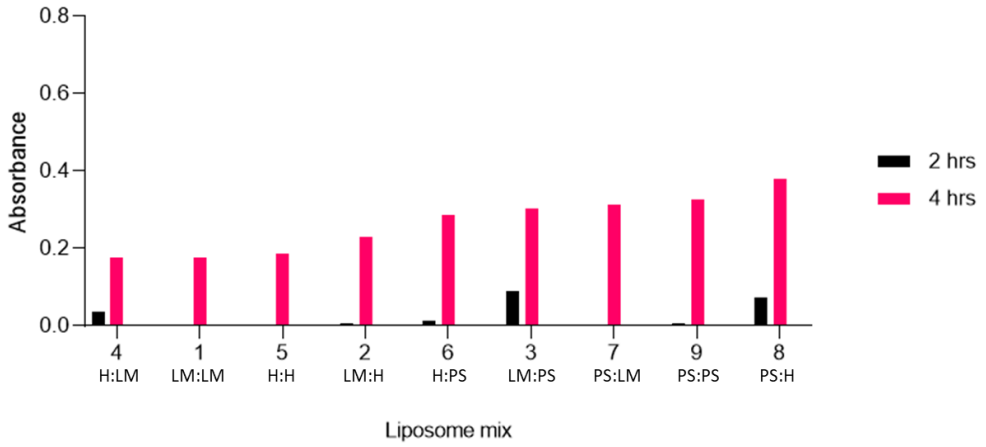

b) RT

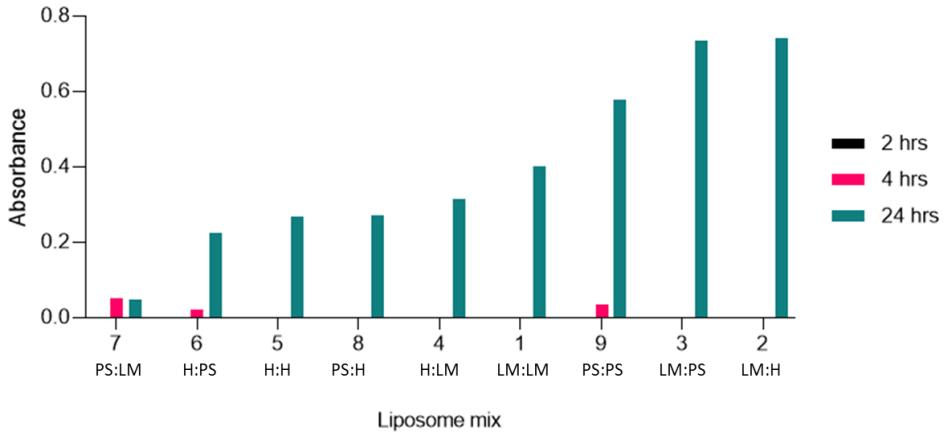

c) 4°C

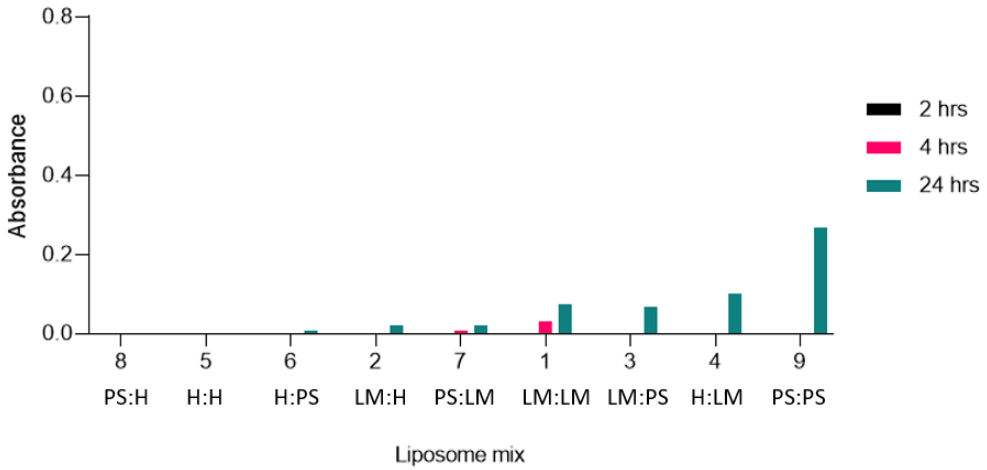

Figure 79 EIA results showing transfer of FSL constructs between liposomes. Results in each group are ranked in order of least to greatest absorbance. FSL transfer between liposomes was detected after 4 hours storage at 37°C and 24 hours at RT. Transfer was not detected in liposomes stored at 4°C, with the exception sample number 1, in the 24 hour time frame. No pattern in transfer relating to storage temperature and method of preparation was observed. Samples containing a mix of FSL-A2 liposomes and FSL-biotin liposomes were prepared and stored at (**a**) 37°C, (**b**) RT and (**c**) 4°C. EIA was used to detect the formation of liposomes with both FSL-A2 and FSL-biotin on their surface. Only liposomes with both constructs result in a positive reaction. Absorbance results are shown minus baseline (time =0) reactivity. Liposome mix number and liposome composition (biotin:A2) are shown on x axis. See Table 14 for full description.

Summary

FSL transfer between liposomes was observed. The transfer of FSL was temperature dependent, transfer occurred within 4 hours at 37°C and 24 hours at RT. Transfer was not observed at 4°C.

The transfer of FSL between liposomes did not appear to be significantly influenced by the method (LM, H, PS) in which FSL was originally incorporated into the liposomes.

3.3 Transfer of FSL from liposome to cells

The previous experiment showed that FSL constructs can transfer between liposome membranes. The next experiments were conducted to determine if FSL constructs also transfer from liposome to cell membranes, and if so to investigate the effects of various parameters on this transfer;

- liposome FSL concentration
- method of liposome synthesis
- liposome age
- incubation time and temperature (RBC + liposome)
- varying liposome constituents (cholesterol and charge).

RBC were used as a model cell membrane for these experiments. RBC were selected because they are easy to work with, they do not require maintenance, and simple techniques can be used to detect the presence of FSL on their surface. The presence of FSL-biotin and FSL-FLRO4 on RBC was measured by flow cytometry, while FSL-A2 was detected by reaction with standard blood grouping reagents, (monoclonal anti-A) which results in agglutination. The methods used for these experiments are detailed below in section 3.3.1.

There are several possible theoretical mechanisms of FSL transfer from liposome to RBC membrane as discussed in section 1.7 and shown in Figure 80. Liposomes may adsorb to the RBC surface or become entrapped within the glycocalyx by non-specific mechanisms such as electrostatic forces (glycocalyx not shown, see Figure 20 Different ways FSL constructs may associate with cell membranes.). Lipid transfer may occur between liposome and RBC by monomer diffusion or collision exchange. In addition, any free FSL (monomer/micelles) that remains in the liposome dispersion supernatant could also transfer to the RBC. The liposome could fuse with the RBC membrane. It is also possible for cells can take up liposomes by endocytosis, however this mechanism is not possible here as RBC can not carry out endocytosis [231].

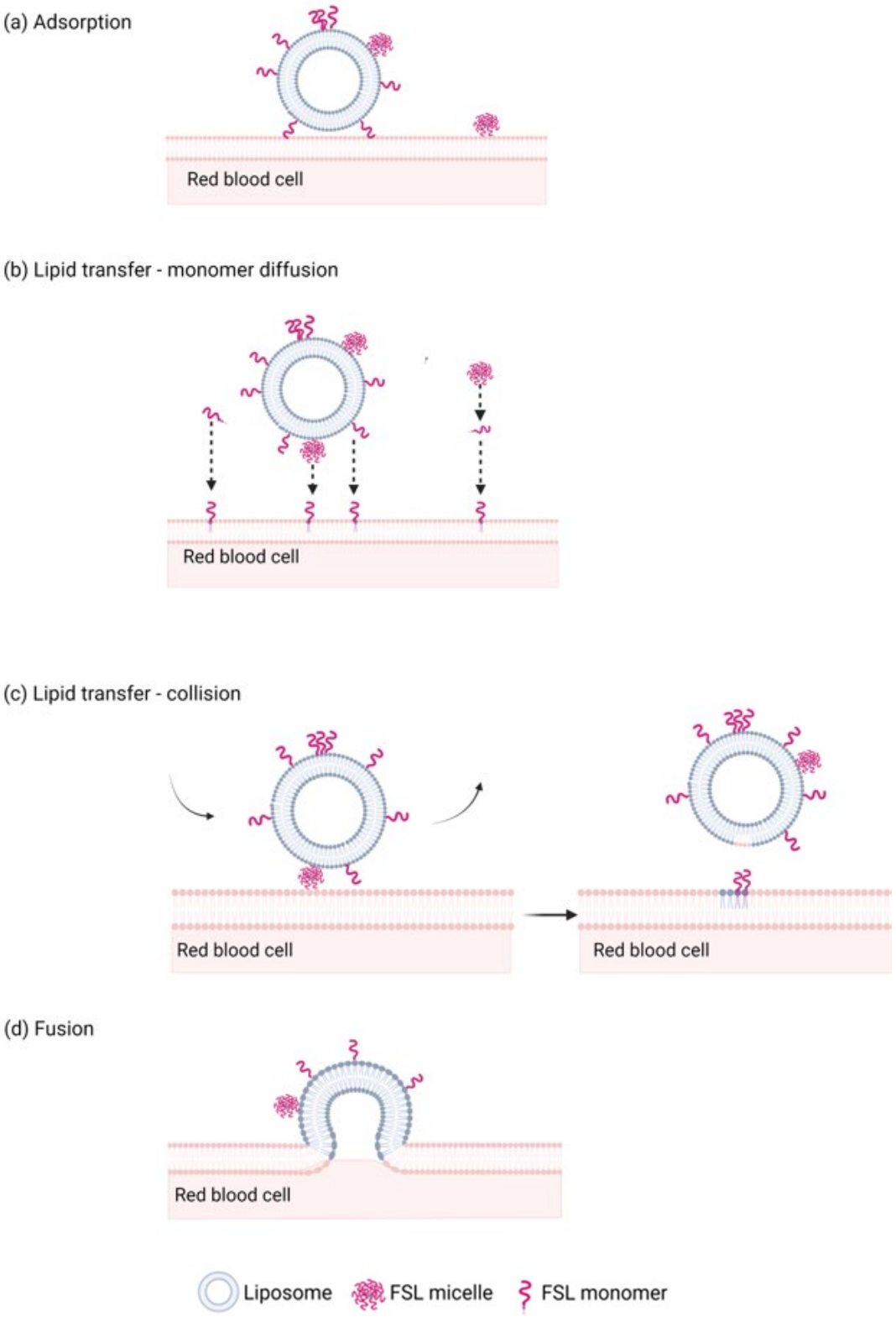

Figure 80 Theoretical mechansims of FSL transfer from liposomes to RBC membrane. (**a**) Liposomes may adsorb (by non-specific mechansims such as electrostatic forces, entrapment in glycocalyx) to the RBC membrane. (**b**) Lipid transfer may occur by monomer diffusion. FSL constructs disassociate from liposme membrane and diffuse to RBC membrane. Any free FSL constructs present in liposome supernatnat can also transfer to RBC membrane. (**c)** Lipid transfer may occur by collision, lipid exchange between liposome and RBC membrane when they collide together. (**d**) the liposome may fuse with RBC membrane. Diagram approximately to scale. Created with BioRender.com.

3.3.1 Methods

The methods used to investigate the transfer of FSL constructs to RBC and the methods subsequently used to detect and measure any FSL which had transferred to the RBC are detailed below.

a) Kodecyte preparation - transfer of FSL to RBC

FSL constructs have been shown to spontaneously and rapidly label cell membranes [56, 230, 244, 350]. Methodology for this is well established and involves incubating equal volumes of FSL solution with cells for two hours at 37°C. This two hour method has been shown to achieve approximately 80% (of the maximum observed) insertion, however insertion begins to occur immediately, and temperature and time of incubation can be varied [230, 261]. To determine if FSL could transfer from liposomes to RBC the same methodology was used; incubating equal volumes of packed RBC with liposome dispersion for 2 hours at 37°C.

1. Equal volumes of washed packed group O RBC (25µL) and liposomes (or a FSL micelle/monomer dispersion) were incubated together for 2 hours at 37°C.
2. The RBC were washed four times with PBS.
3. The presence of FSL on RBC was measured by flow cytometry for FSL-FLRO4 and FSL-biotin, and by haemagglutination for FSL-A2 (see below).

Note: RBC labelled with FSL are termed kodecytes. Kodecytes were prepared fresh as required and used immediately, unless otherwise noted. However, they could be stored if required, suspended 5% v/v in cell preservative solution ID-cellstab (Biorad, Cat# 005650) for up to 4 weeks.

b) Detection of FSL-FLRO4 on RBC (flow cytometry analysis)

1. The prepared RBC were diluted 1:5,000 v/v in PBS.
2. Flow cytometry measurements were carried using a Cytek Northern Lights spectral analyser with a 3 laser set up (blue, red and violet) and 24 measurement channels.
   10,000 events were recorded. Data was analysed using Kaluza Analysis software.

c) Detection of FSL-biotin on RBC (flow cytometry analysis)

Detection of FSL-biotin on RBC required the addition of a secondary fluorescent label, streptavidin Alexa Fluor™ 488™ 488, before analysis by flow cytometry.

1. 2µL of washed packed RBC were incubated with 10µL 20µg/mL streptavidin Alexa Fluor™ 488 (Invitrogen, Cat# S11223, ThermoFisher) in PBS for 30 minutes at RT.
2. The RBC were washed three times with PBS and then resuspended with 1mL PBS for analysis by flow cytometry.

3. Flow cytometry measurements were carried out using a Cytek Northern Lights spectral analyser with a 2 laser set up (blue and red) and 24 measurement channels.
   10,000 events were recorded. Data was analysed using Kaluza Analysis software.

d) Detection of FSL-A2 on RBC (column agglutination test)

FSL-A2 was detected using serological anti-A reagents and standard haemagglutination techniques. Haemagglutination is the clumping together of RBC to form a macroscopic aggregate+69. This can be caused by the specific binding of IgM antibody cross linking an antigen expressed on the surface of adjacent RBC. Haemagglutination can be used to identify the presence of an antigen on the surface of RBC (when a known specificity antibody is used), or to determine the specificity of an unknown antibody by using cells with known antigen expression.

The presence of FSL-A2 on the surface of RBC was detected using a monoclonal IgM anti-A reagent. If FSL-A2 was present on the surface of the RBC then the IgM anti-A reagent would bind to the RBC and cause agglutination. Group O RBC were always used for these transfer experiments as they do not have the A antigen.

Method

1. Neutral cards (Grifols DG Gel neutral cards, cat#210343, Spain) were used and 50µL of anti-A monoclonal antibody reagent (Anti-A series 1, Immucor, Cat# 0006400) was dispensed into each well.
2. 50µL of each RBC sample was diluted 3% v/v in ID-cellstab and then added to the appropriate well.
3. The cards were incubated for 15 minutes at 22°C and then centrifuged in the Grifols DG Spin Centrifuge at a pre-programmed speed for 10 minutes.
4. The reactions were graded for agglutination using the 0-4 grading system, described below. [351]

Agglutination Scoring

Scoring was assigned based on the position and pattern of cells in the well. A negative reaction (0), where no agglutination has occurred, results in a pellet of cells at bottom of the column, as shown in Figure 81. A strong positive reaction (4+) results in a band of cells which remain at the top of the gel. Agglutination reactions between these (3+, 2+, 1+) result in agglutinates which show characteristic patterns in the gel, as shown in Figure 81.

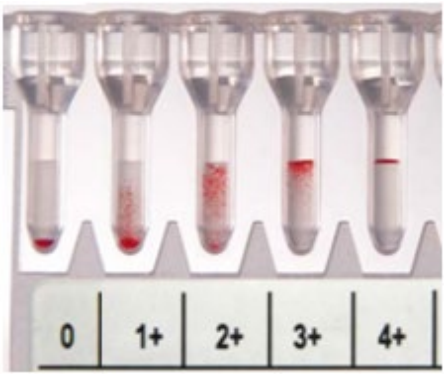

Score	Description
4+	Single sharp band at the top of column
3+	More diffuse band at top of column
2+	Cells spread out from top to bottom of column
1+	Diffuse bank at base of column
0	All cells at the base of column

Figure 81 Agglutination reactions and scoring system in CAT. A negative reaction is when all RBC pellet at the bottom of well. Positive reactions are graded on a scale from 1+ to 4+. Figure adapted from [352]

3.3.2 Kodecyte calibration curves

A preliminary experiment was carried out to first create a 'kodecyte standard curve' for each FSL construct. Kodecytes were prepared by incubating RBC with a range of different concentration FSL dispersions (method 3.3.1a). The FSL that transferred to the resulting kodecytes was then measured by agglutination or flow cytometry (methods 3.3.1 b, c, and d). These results could later be used to estimate the amount of FSL that had transferred to RBC from liposome dispersions (assuming that in this case, when FSL alone added to RBC, that almost all FSL added binds to the RBC (unpublished Prakash)). For FSL-biotin and FSL-FLRO4 PRISM GraphPad was used to interpolate FSL concentrations from the standard curves.

FSL-A2

Figure 82 shows the agglutination reactions of kodecytes prepared by incubating RBC with increasing concentration FSL-A2 micelle dispersions. The strength of agglutination (from 1+ to 4+) is semi quantitative. No agglutination shows that no or only a very small amount of FSL-A2 has transferred to the RBC.

Agglutination of the A2-kodecytes increased with the concentration of FSL between 1-10µM. FSL was not detected on the kodecytes incubated with FSL micelle/monomer at concentrations less than 1µM,therefore the minimum detectable FSL concentration is ≈1µM.

Maximum agglutination strength, 4+, was reached after incubation with approximately 8µM FSL-A2. Above this any increase in the amount of FSL-A2 present on RBC membrane cannot be distinguished.

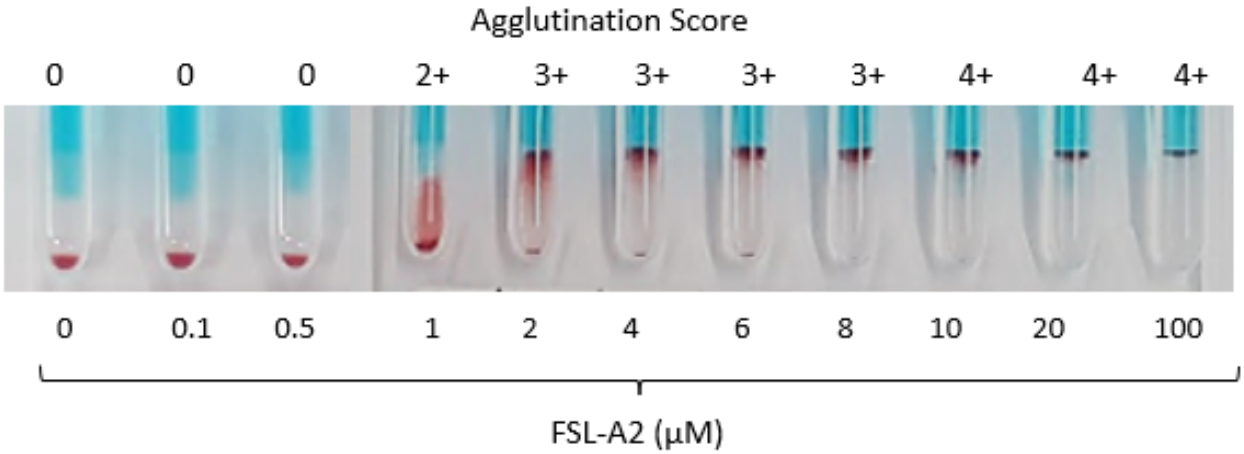

Figure 82 FSL-A2 kodecyte standard curve. Agglutination reactions of FSL-A2 kodecytes with anti-A reagent in gel cards is shown. Kodecytes were prepared by incubating RBC with varying concentration FSL-A2 dispersions. This calibration curve can be used to estimate the amount of free micelle/monomer FSL present in a liposome dispersion based on the detected transfer of FSL to RBC.

FSL-biotin and FSL-FLRO4

Figure 83 shows the fluorescence of kodecytes prepared by incubating RBC with increasing concentration FSL-biotin and FSL-FLRO4 micelle dispersions.

A notable difference between FSL-FLRO4 and FSL-Biotin was that FSL-biotin resulted in much greater RBC fluorescence than FSL-FLRO4. For example, 100 FLRO4 kodecytes had a mfi of 148 while 100 biotin kodecytes had mfi of 352. However, it is likely that this difference in fluorescence is due to the different performance characteristics of the fluorescent labels used (fluorescein with FSL-FLRO4 versus Alexa Fluor™ 488 for FSL-biotin) rather than an indication of greater transfer of FSL-biotin constructs compared to FSL-FLRO4.

The fluorescence of the FSL-FLRO4 and FSL-biotin kodecytes increased in a linear concentration-dependent manner up to ≈50µM FSL-FLRO4 and ≈75µM for FSL-biotin. Above these concentrations the increase in fluorescence flattened out to reach a plateau around ≈100µM (FSL-FLRO4) and ≈150µM (FSL-biotin). This plateau may be due to several factors:

- self-quenching of fluorophores, as the concentration of FSL within the RBC membrane increases self-quenching may occur (FSL constructs may cluster together within the membrane further contributing to this effect)

- the plateau region may occur after the concentration of the FSL constructs reaches CMC, above this point FSL constructs form micelles in the supernatant. FSL in micelle form may not transfer to RBC as readily as FSL monomers. Consequently, above CMC FSL transfer to RBC may be significantly reduced [195].

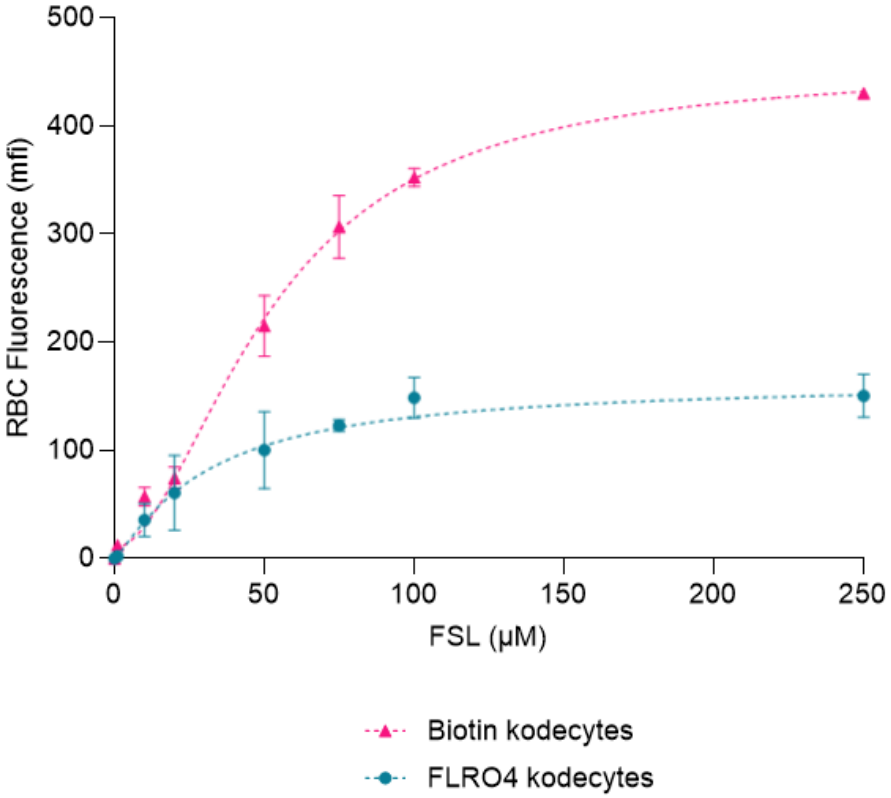

Figure 83 FSL-FLRO4 and FSL-biotin kodecyte standard curve. Graph showing the fluorescence of biotin and FLRO4 kodecytes prepared by incubating RBC with varying concentration of FSL-biotin or FSL-FLRO4 dispersions. FSL-biotin kodecytes required addition of Streptavidin Alexa Fluor™ 488 for detection. This calibration curve was used to estimate the amount of free micelle/monomer FSL present in a liposome dispersion based on the detected transfer of FSL to RBC. Mean ± standard deviation, n=2.

3.3.3 Effect of FSL concentration and method of liposome preparation

The aim of this experiment was to determine if transfer of FSL constructs from liposomes to RBC could be detected, and if so what effect, if any, the liposome preparation method (lipid mix, hydration, post synthesis) and FSL concentration would have on this transfer. Figure 84 shows possible mechanisms of FSL transfer to RBC from liposomes (prepared by LM, H and PS methods).

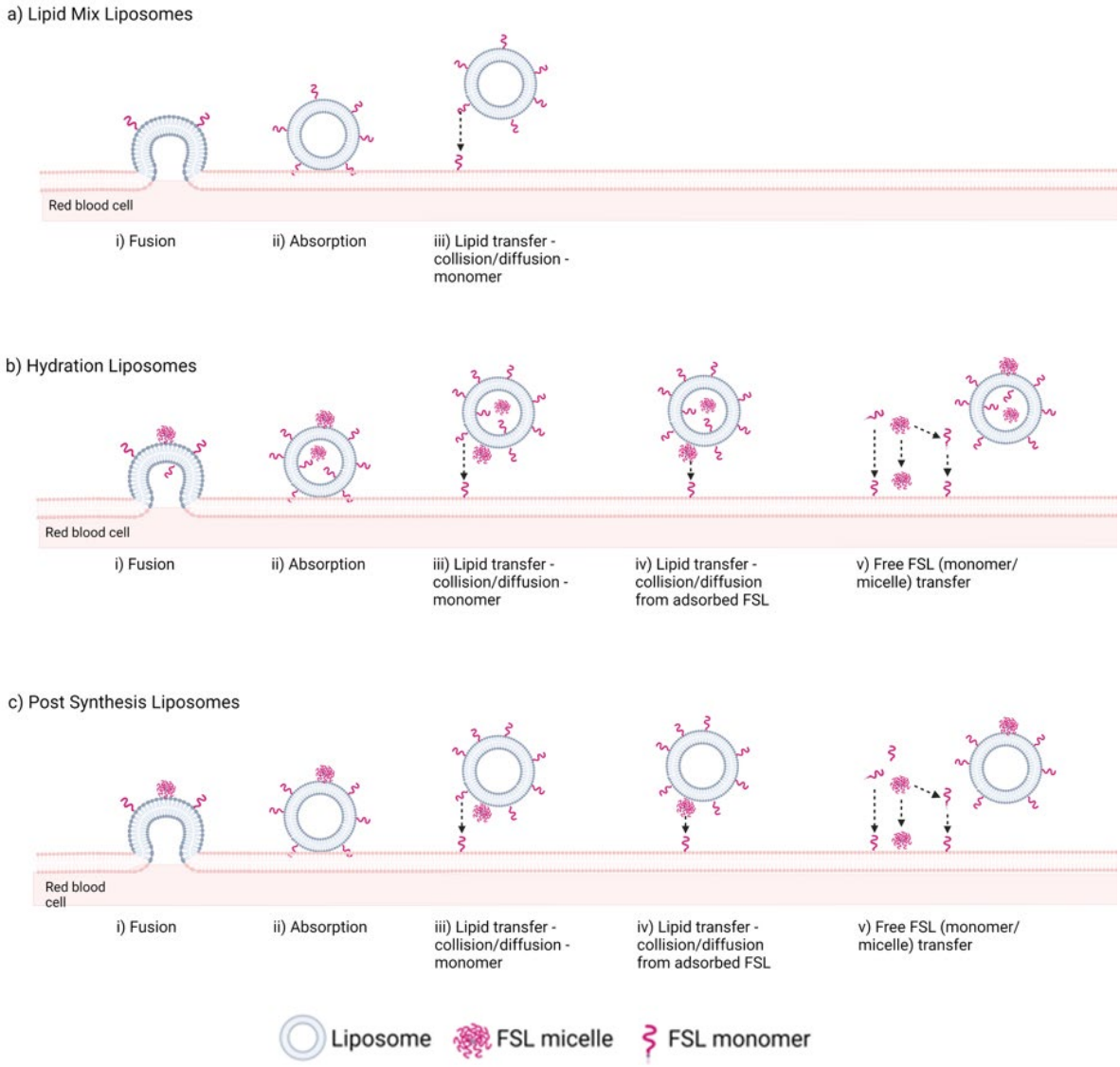

Figure 84 Possible mechanisms of FSL transfer from liposome to RBC. Transfer of FSL from liposomes prepared by (**a**) LM, (**b**) H and (**c**) PS methods are compared. Potential mechansims include that (**i**) liposomes may fuse with RBC membrane, (**ii**) liposomes may absorb onto RBC membrane without becoming integrated, (**iii**) FSL constructs may transfer to RBC membrane by exchange during collision between liposome and RBCs or FSL constructs may diffuse out of liposome membrane and then transfer to the RBC membrane or (**iv**) transfer from FSL micelles which have adsorbed to the surface of the liposome, and (**v**) unincorporated FSL (micelle/monomer) present in dispersion may transfer/adsorb to the RBC (independent of liposomes). Mechanism (**iv** and **v**) can only occur in liposomes prepared by H and PS methods as LM liposome dispersions contain no free micelle/monomer to adsorb to the surface of the liposome or to transfer RBC. Image approximately to scale, except size of liposome ≈60nm not 100nm. Created with BioRender.com.

Method

1. Liposome dispersions were prepared containing varying concentrations of FSL, inserted by LM, H and PS protocols (method 2.2.2).
2. Liposomes were stored for 72 hours at 4°C after addition of FSL to ensure maximum insertion of FSL into liposome had occurred.
3. An aliquot from each liposome dispersion was removed and incubated with an equal volume of washed packed RBC for 2 hours at 37°C.
4. Transfer of FSL to RBC was then detected by flow cytometry (FSL-FLRO4 and FSL-biotin) or haemagglutination (FSL-A2) (methods 3.3.1 b, c, and d).
5. RBC were also incubated with FSL micelle dispersions (labelled micelle although would have contained both micelles and monomers) for comparison, and with blank liposomes (containing no FSL) as a negative control.

Results

FSL-FLRO4

The mean fluorescence intensity of RBCs (termed kodecytes) after incubation with FLRO4 liposomes and dispersions of FSL-FLRO4 alone (labelled micelles) are shown in Figure 85.

PS and H liposome dispersions showed very similar transfer of FSL to RBC e.g. PS liposomes containing 100µM FSL-FLRO4 resulted in RBC fluorescence of 1.7 mfi, while H liposomes containing 100µM FSL-FLRO4 resulted in RBC fluorescence of only 1.5 mfi. Transfer of FSL from H and PS liposomes to RBC was concentration dependent (detected levels of FSL on RBC increased with increasing FSL concentration in the liposome dispersion) and remained approximately linear in the concentration ranges tested.

Very little/no transfer of FSL was observed from LM liposomes to RBC. RBC fluorescence was ≤0.4mfi even after incubation with all concentration FSL-FRO4 liposomes.

The transfer of FSL from FSL-FLRO4 micelle dispersions resulted in much greater transfer of FSL than liposome dispersions containing the equivalent concentration of FSL. For example, RBC incubated with 100µM FSL-FLRO4 micelle/monomer dispersion resulted in RBC fluorescence of 148 mfi. While RBC incubated with PS/H liposomes containing 100µM FSL-FLRO4 resulted in RBC fluorescence of ≈2mfi. This transfer from liposome dispersion was approximately 1% of transfer from micelle transfer.

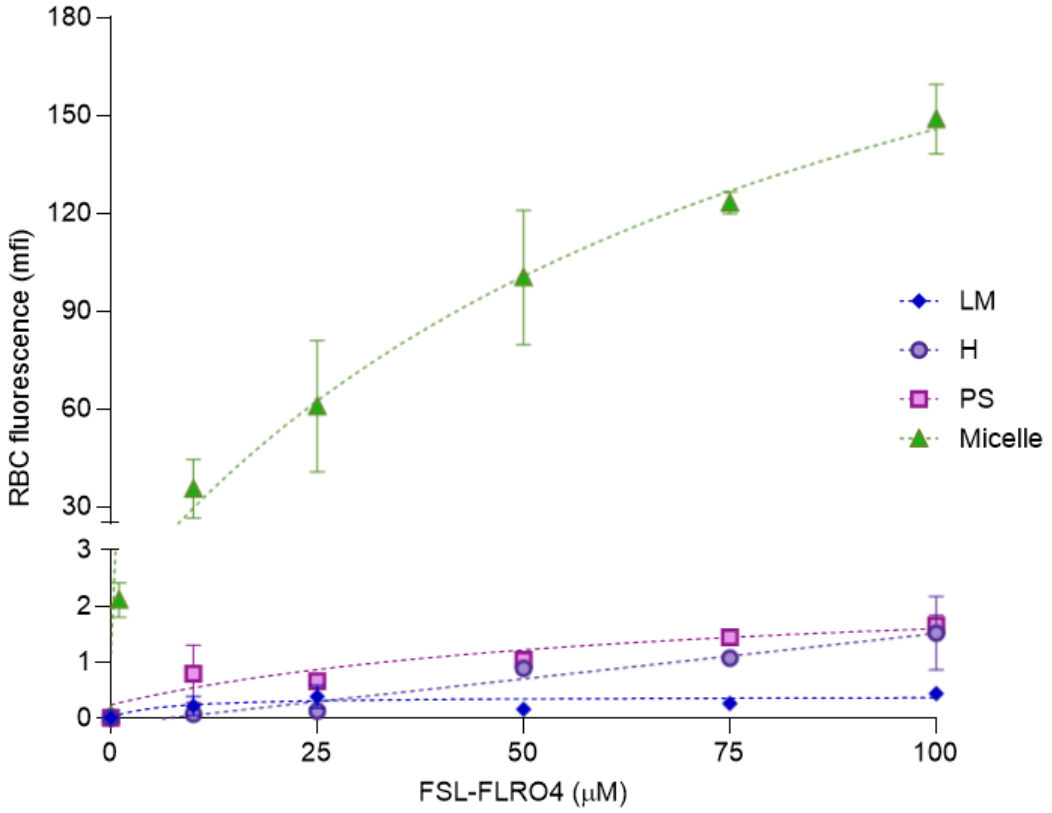

Figure 85 Transfer of FSL-FLRO4 from liposomes to RBC. RBC were incubated with varying concentration FLRO4 liposomes (prepared by LM, H, and PS protocols) and FSL-FLRO4 dispersions (labelled micelles) for 2 hours at 37°C. FSL-FLRO4 was detected on RBC after incubation with H and PS, but not LM liposomes. Much greater levels of FSL was detected on RBC after incubation with FSL-FLRO4 dispersions (labelled micelles). Transfer of FSL from H and PS liposomes to RBC was concentration dependent. Note change in scale after break in Y axis. Results show mean ± SD, n=2

By comparing the fluorescence of RBC after incubation with liposomes with the fluorescence of RBC incubated with micelle FSL (kodecyte standard curve, Figure 83), the amount of FSL that transferred from liposomes to RBC could be estimated (values interpolated using PRISM GraphPad). For example, RBC incubated with 100μM FSL-FLRO4 liposome dispersion (PS) resulted in an mfi of 1.7. By comparing to the micelle curve, this level of fluorescence is equivalent to transfer seen from 0.7μM FSL-FLRO4 micelle (assuming that the majority of FSL inserts into RBC when added alone). Therefore, it was estimated that approximately 0.7μM FSL transferred from liposome dispersion to RBC, which was 0.7% of the 100μM FSL present in liposome dispersion.

Table 15 shows the fluorescence of RBC after incubation with FLRO4 liposome dispersions and the calculated percentage transfer of FSL from liposome to RBC. Transfer from H/PS liposomes was estimated to be approximately 1% of FSL present in liposome dispersion at all concentrations. Transfer from LM liposomes were very low, in all cases kodecyte fluorescence was <0.4 mfi, equating to ≤0.3μM FSL concentration, and <1% of FSL originally present.

Table 15 Estimated percentage transfer of FSL-FLRO4 from liposomes to RBC

Liposome		Kodecyte fluorescence	Calculated FSL on kodecyte	Estimated FSL transfer
Method of preparation	FSL- FLRO4 µM	mfi	µM	%
LM	25	0.2	0.2	0.8%
	50	0.2	0.2	0.4%
	75	0.3	0.2	0.2%
	100	0.4	0.3	0.3%
H	25	0.1	0.2	0.8%
	50	0.9	0.4	0.8%
	75	1.1	0.5	0.6%
	100	1.5	0.6	0.6%
PS	25	0.7	0.3	1.2%
	50	1.1	0.5	1.0%
	75	1.5	0.6	0.8%
	100	1.7	0.7	0.7%

FSL-biotin

The mean fluorescence intensity of RBC after incubation with biotin liposomes and FSL-biotin monomer/micelle dispersion, are shown in Figure 86. Results show the same pattern of transfer as seen with the FSL-FLRO4;

- Negligible transfer from LM liposomes.
- Transfer was detected after incubation with PS and H liposomes.
- Transfer from P and H liposomes was concentration dependent.
- PS liposomes showed greater transfer of FSL to RBC compared to H liposomes.
- FSL micelles resulted in significantly greater transfer to RBC.

As observed with FSL-FLRO4 transfer of FSL-biotin from H and PS liposomes to RBC was concentration dependent (detected levels of FSL on RBC increased with increased FSL concentration in the liposome dispersion) and remained approximately linear in the concentration ranges tested.

PS liposomes resulted in slightly greater transfer of FSL-biotin to RBC compared to H liposomes, for example PS liposomes containing 100µM FSL-biotin resulted in RBC fluorescence of 55 mfi, while H liposomes resulted in RBC fluorescence of 22mfi.

FSL-biotin micelle/monomer dispersions resulted in much greater transfer of FSL to RBC compared to liposome dispersion. For example, RBC incubated with 100µM FSL-biotin micelle/monomer dispersion resulted in mean fluorescence intensity of 352, while RBC incubated with 100µM liposomes PS/H resulted in mean fluorescence intensity of 55/22 which was 16%/6% (of micelle transfer) respectively.

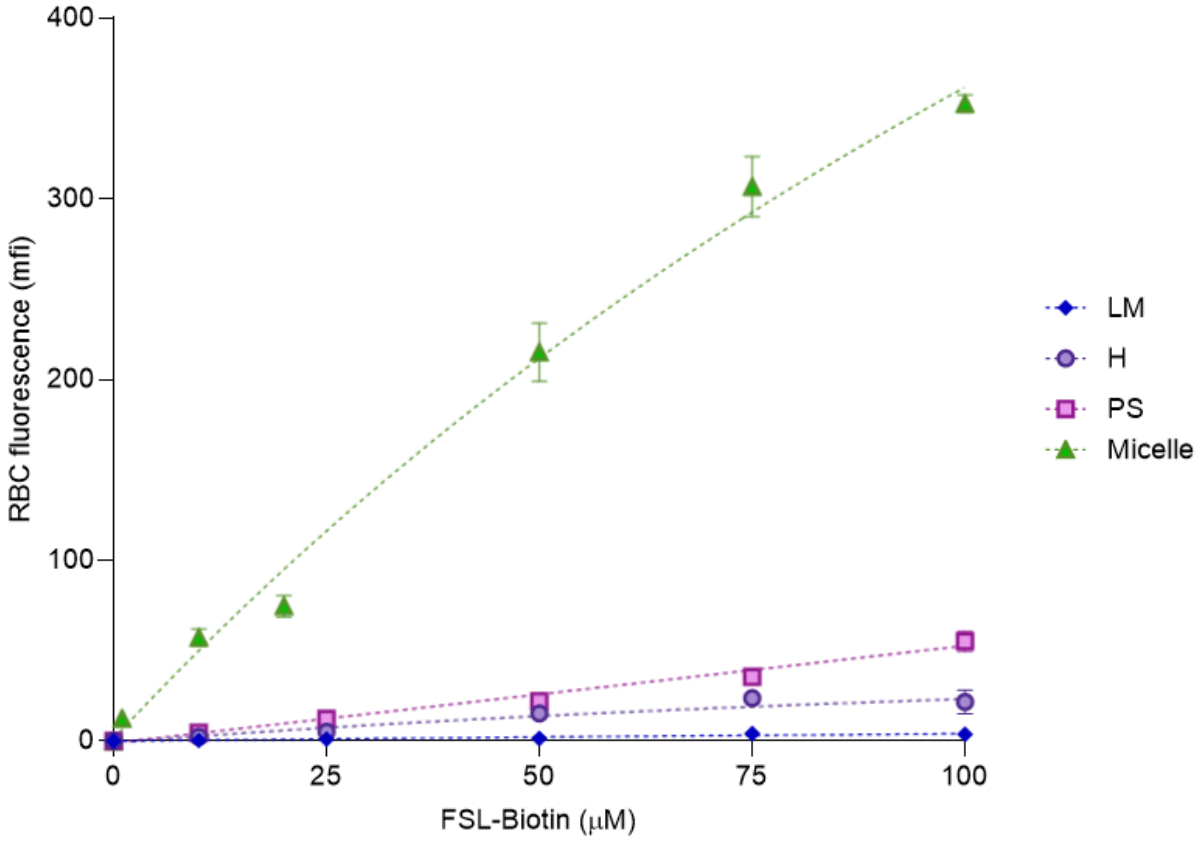

Figure 86 Transfer of FSL-biotin from liposomes to RBC. RBC were incubated with varying concentration biotin liposomes (prepared by LM, H, and PS protocol) and FSL-biotin dispersions (labelled micelles) for 2 hours at 37°C. The presence of FSL-biotin on the RBC was detected using streptavidin Alexa Fluor™ 488. FSL-biotin was detected on RBC after incubation with H and PS, but not LM liposomes. Much greater levels of FSL was detected on RBC after incubation with FSL-biotin dispersions. Transfer of FSL from H and PS liposomes to RBC was concentration dependent. Results show mean ± SD, n=2

Table 16 shows the kodecyte fluorescence obtained after incubation with liposomes, and the calculated percentage of FSL that transferred from liposome dispersion to RBC (from comparison with standard curve Figure 83, results interpolated using PRISM GraphPad).

Using these calculations, it was estimated that approximately 5-9% of FSL-biotin transferred from H liposomes, and approximately 12-15% from PS liposome dispersions 50-100uM liposomes. FSL-biotin values could not be calculated for 10 and 25µM liposomes (PS/H) and all concentration LM liposomes as they were too low (in all cases kodecyte fluorescence was <12 mfi, equating to <1µM FSL-biotin concentration, which was <1% of FSL originally present).

Table 16 Estimated percentage transfer of FSL-biotin from liposomes to RBC

Liposome FSL-biotin µM	Liposome method of preparation					
	H			PS		
	Kodecyte fluorescence mfi	Calculated micelle µM	% FSL	Kodecyte fluorescence mfi	Calculated micelle µM	% FSL
10	3	<1	<1%	4	<1	<1%
25	5	<1	<1%	12	<1	<1%
50	15	2.4	5%	22	5.9	12%
75	24	6.6	9%	35	9.9	13%
100	22	5.9	6%	55	14.7	15%

FSL-A2

The agglutination score of RBCs (termed kodecytes) after incubation with varying concentration A2 liposomes and FSL-A2 micelle/monomer dispersions are shown in Table 17. Images of gel cards and agglutination reactions are shown in Figure 87. Natural RBC (group A, B and O) and blank liposomes (with no FSL) were tested in parallel as controls and expected reactions obtained, results not shown.

Table 17 Agglutination scores of A2 kodecytes

Sample		**Agglutination Score**					
		Liposome FSL-A2 concentration µM					
		10	25	50	75	100	150
RBC + Liposomes	LM	0	0	0	0	0	0
	H	0	0	2+	2+	2+	3+
	PS	0	0	2+	3+	3+	4+
RBC + FSL micelles		4+	4+	4+	4+	4+	4+

Agglutination of the kodecytes indicates that FSL-A2 is present on the RBC membrane. No agglutination shows that no or only a very small amount of FSL-A2 has transferred to the RBC.

Strong agglutination (3+ and 4+) was observed after incubation with H and PS liposomes containing ≥25µM FSL-A2, RBC incubated with LM liposomes showed no agglutination, indicating that FSL-A2 did not

transfer from these liposomes to RBC. RBC incubated with all concentrations (10-250µM) FSL-A2 dispersions showed strong 3+ or 4+ agglutination. Transfer of FSL-A2 from PS/H liposomes to RBC showed the same pattern as that seen for FSL-FLRO4 and FSL-biotin.

- Negligible transfer from LM liposomes
- Transfer from 25-250µM PS/H liposome dispersions was observed and was concentration dependent.
- PS liposomes showed slightly greater transfer of FSL to RBC compared to H liposomes. Transfer was detected from 50-250µM PS liposomes, strength of agglutination reactions increased from 2+ to 4+. Transfer of FSL was detected from 100 and 250µM H liposomes, strength of agglutination reaction was 2+ to 3+.
- Micelle/monomer FSL dispersions resulted in the greatest transfer of FSL to RBC (FSL-A2 transfer from all concentrations 10-250µM was observed and strength of agglutination 3+ and 4+).

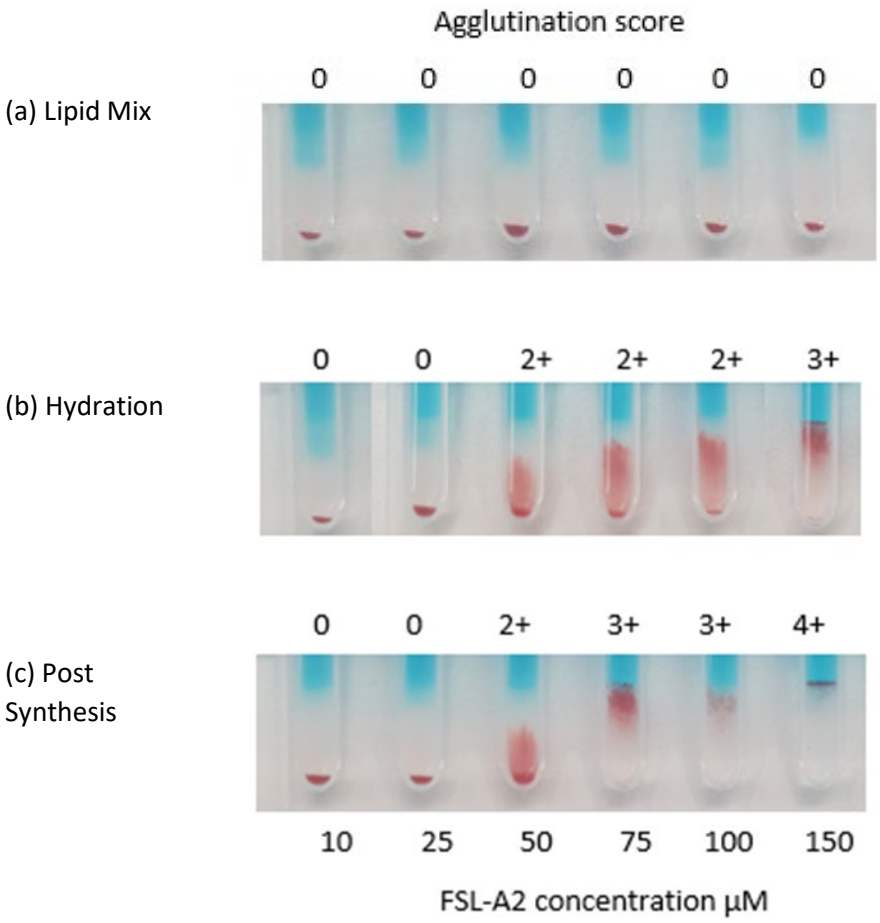

Figure 87 Agglutination reactions of A2 kodecytes. Kodecytes were prepared by incubating RBC with A2 liposomes prepared by (**a**) LM, (**b**) H, and (**c**) PS methods containing varying concentrations of FSL-A2 (10, 25, 50, 75, 100 and 250µM). No transfer of FSL-A2 was seen from LM liposomes to RBC (no agglutination observed). FSL-A2 transfer from PS and H liposomes showed a clear correlation to concentration of FSL in the liposome dispersions.

By comparing the kodecyte (RBC incubated with liposomes) agglutination strength obtained in this experiment against the kodecyte (RBC incubated with FSL micelles) standard curve curves (Figure 82) the amount of FSL-micelle/monomers remaining in the liposome dispersions could be estimated. For example, the RBC incubated with 100µM FSL-A2 liposome dispersion (PS) showed 3+ agglutination. The kodecyte standard curve shows that 3+ agglutination results from incubation of RBC with 2-6µM FSL-A2 micelles. Therefore approximately 2-6µM FSL-A2 transferred from liposome dispersion to RBC. This equates to approximately 2-6% of the FSL (100µM) added to the original liposome dispersion. Table 18 shows calculations from 50-100µM liposome dispersions.

Table 18 Estimated percentage transfer of FSL-A2 from liposomes to RBC

Liposome FSL A2 µM	Method of FSL addition to liposomes					
	H			PS		
	Agglutination	Calculated micelle µM	% FSL	Agglutination	Calculated micelle µM	% FSL
50	2+	1	2%	2+	1	2%
75	2+	1	1.5%	3+	2-6	3-8%
100	2+	1	1%	3+	2-6	2-6%
150	3+	2-6	1-4%	4+	≥8	≥5%

Approximately 2-8% of the FSL transfers from PS liposome dispersion to RBC, and 2% from H liposomes dispersions.

Summary

All three FSL constructs showed the same pattern of reactivity:

Transfer to RBC was dependent on method of liposome preparation;

- No/negligible transfer of FSL from LM liposomes was observed.
- Transfer of FSL from PS and H liposome dispersions to RBC was observed.
- Greater transfer was seen from PS liposomes than H liposomes, particularly evident for FSL-biotin e.g. RBC incubated with 100µM FSL biotin liposomes resulted in 67mfi (PS) and only 20mfi (H), RBC incubated with 150µM FSL-A2 liposomes resulted in 4+ (PS) and 3+ (H) agglutination scores.

Transfer of FSL from H and PS liposome dispersions to RBC was concentration dependent, greater transfer was observed from liposome dispersions containing higher concentrations of FSL

Incubation with dispersions of FSL alone (labelled micelle on graphs) resulted in much higher transfer of FSL to RBC than seen from liposome to RBC (transfer of FSL-FLRO4 from liposome dispersions was less than 1% of micelle transfer, and ≤16% for FSL-biotin).

Comment

A significant difference in the transfer of FSL to RBC was observed between the three methods of liposome preparation. Negligible FSL transfer was observed from LM liposomes, but a small amount of transfer was observed from H and PS liposomes.

Because there was no observed transfer from LM dispersions, several mechanisms of FSL transfer to RBC can be excluded; significant transfer is probably not occurring by liposome adsorption/fusion to the RBC or transfer of FSL monomers which have integrated into the liposome membrane, Figure 88.

An important difference between LM and PS/H liposome dispersions is that the H and PS liposome dispersions (in which FSL constructs are added as a micelle dispersion during liposome synthesis and the liposome dispersion are not subsequently washed) may contain some micelle/monomer FSL remaining in the liposome dispersion (which has not bound to the liposomes). In addition, it is possible that some FSL may have adsorbed to the surface of PS/H liposomes (rather than integrating into the membrane). In contrast LM liposome dispersions, due to their method of synthesis (see 2.2.3) contain no free FSL and all FSL is integrated into the liposome membrane.

Therefore, it is hypothesised that the observed transfer of FSL to RBC from H/PS liposomes is due to either

- unincorporated micelle/monomer FSL present in the PS/H liposome dispersions (which has been shown to transfer to RBC very well, see 3.1). A dynamic equilibrium may form between FSL monomers, FSL micelles and FSL on liposome.
- FSL which has adsorbed to the surface of the H/PS liposomes (but not integrated into the liposome membrane). This adsorbed FSL may be able to transfer to RBC.

Transfer may be due to one or both of these mechanisms.

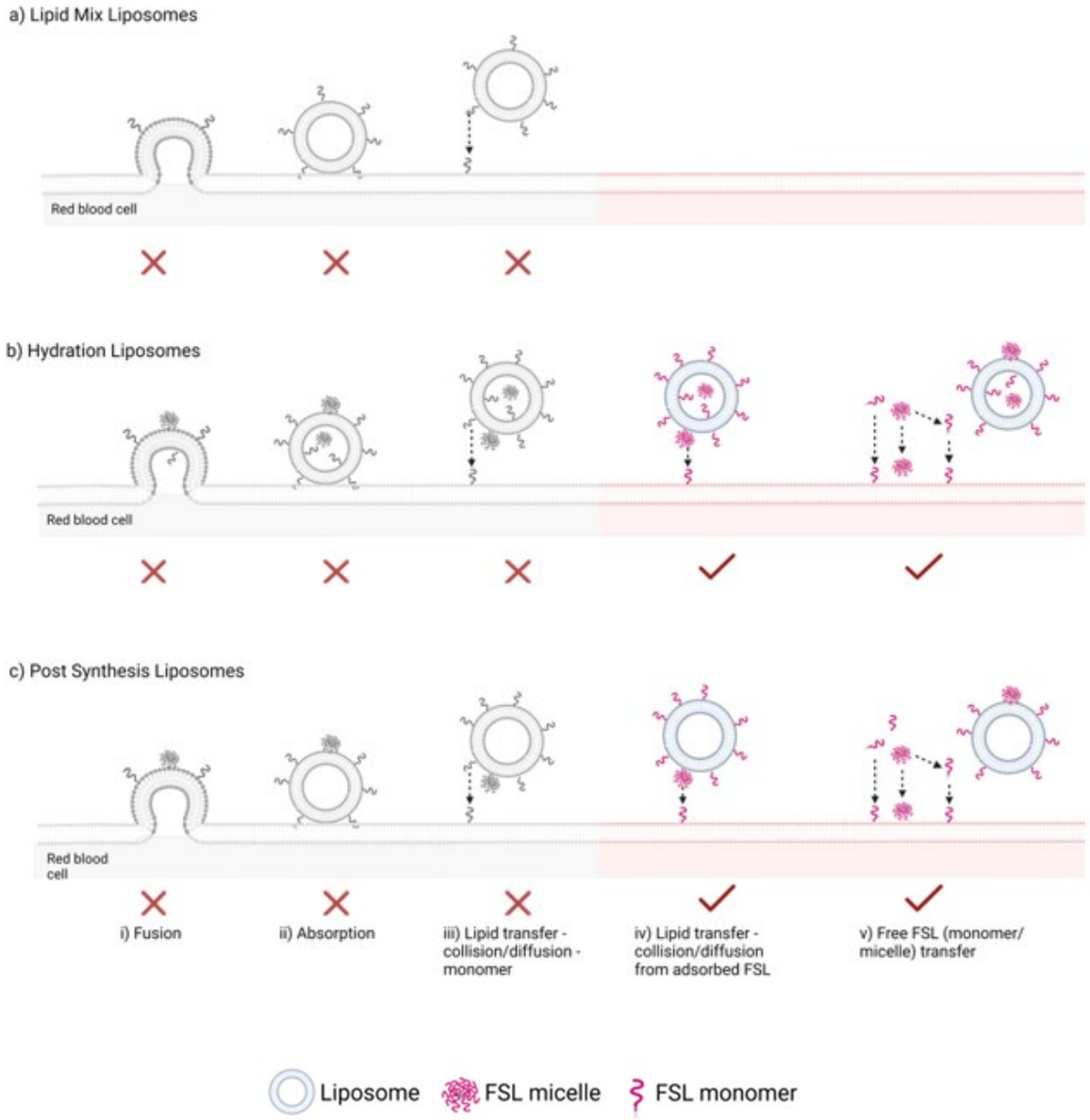

Figure 88 Speculated mechanism of transfer of FSL from liposomes to RBC based on results. Because FSL transfer was not observed from (**a**) LM liposomes to RBC, these results suggest that transfer via mechanisms (**i**) (**ii**) and (**iii**) did not occur (or were very minimal). It is therefore hypothesised that the observed labelling of RBC with FSL from (**b**) H and (**c**) PS liposome dipsersions is due to either mechanism (**iv**) transfer of FSL adsorbed to the surface of liposomes, or (**v**) the presence of free micelle/monomer FSL remaining in these dispersions, rather than transfer of FSL from liposome membrane to RBC membrane. Image approximately to scale, except liposmes shown ≈60nm in diameter, not 100nm as used in this study. Created with BioRender.com.

3.3.4 Preparation of washed liposomes

The previous experiments show that a small amount of FSL transfer occurs from liposomes labelled with FSL by PS and H methods. It is not possible from these results to determine whether the transfer of FSL from PS and H liposome dispersions is due to free FSL remaining in the supernatant, or FSL which has adsorbed to the surface of these liposomes. No evidence of this second mechanism was observed in the TEM images.

In order to distinguish which of these two mechanisms is occurring it is necessary for the PS/H liposome dispersions to be washed. The removed supernatant could then be analysed to determine if free FSL was present, and the washed liposomes could be used to determine if FSL transfer to RBC was affected by washing/removal of supernatant).

In the absence of access to an ultra-high centrifuge an attempt was made to wash liposomes using centrifugal filtration methods. An Amicon centrifugal filter (Amicon ultra-0.5 centrifugal 30K filter device (Merck, Cat # UFC503024, Ireland) was trialled. Unfortunately, this experiment was unsuccessful. It was found that the liposome dispersions blocked the membranes. Trials of additional filters with larger molecular weight cut offs could be explored to overcome this issue. However, this was not able to be actively pursued, nor was it a focus for this research.

3.3.5 Effect of liposome age – 1 week

In the previous experiment (3.3.3) transfer of FSL from liposome dispersions to RBC differed depending on the method of liposome preparation. Transfer of FSL from H and PS liposome dispersions to RBC was observed, in contrast very little/no transfer of FSL to RBC from LM liposomes occurred. It is hypothesised that the observed FSL transfer from H and PS liposome dispersions is due to the presence of free monomer/micelle FSL in the H and PS dispersions (rather than transfer of FSL from liposome membrane to RBC membrane) (mechanism (iv) shown in Figure 84).

Results from earlier experiments (section 3.1 FSL incorporation into liposomes) showed that free FSL-FLRO4 and FSL-A2 is detectable in the supernatant of PS and H liposome dispersions for several days after synthesis (see 3.1.1 and 3.1.2 FSL incorporation into liposomes).

Therefore, to test this hypothesis transfer of FSL from liposome dispersion to RBC was measured at various time points after liposome synthesis. If this hypothesis is correct then transfer of FSL to the RBC from H and PS liposome dispersions should decrease during days 1-3 after synthesis (corresponding to observed increased FSL incorporation/association with liposomes). Transfer should then reach a plateau around day 3, as shown in Figure 89. While transfer from LM liposomes should remain low/negligible as all FSL is incorporated into the liposome membrane during synthesis, therefore there is no movement of FSL after synthesis, Figure 90. The following experiment was carried out to establish if this decrease in FSL transfer to RBC could be detected.

Method

1. Liposomes containing 100µM FSL were prepared by all three methods of FSL insertion. The liposomes were then immediately divided into two aliquots and stored at RT and 4°C for seven days.
2. Aliquots (30µL) were removed from the liposome dispersions on days 1, 3 and 7 and incubated together with RBC for 2 hours at 37°C (kodecyte preparation method 3.3.1 a).
3. The presence of FSL on the RBC was then measured by flow cytometry (FSL-FLRO4, FSL-biotin) or haemagglutination (FSL-A2) (see 3.3.1 b, c, and d).

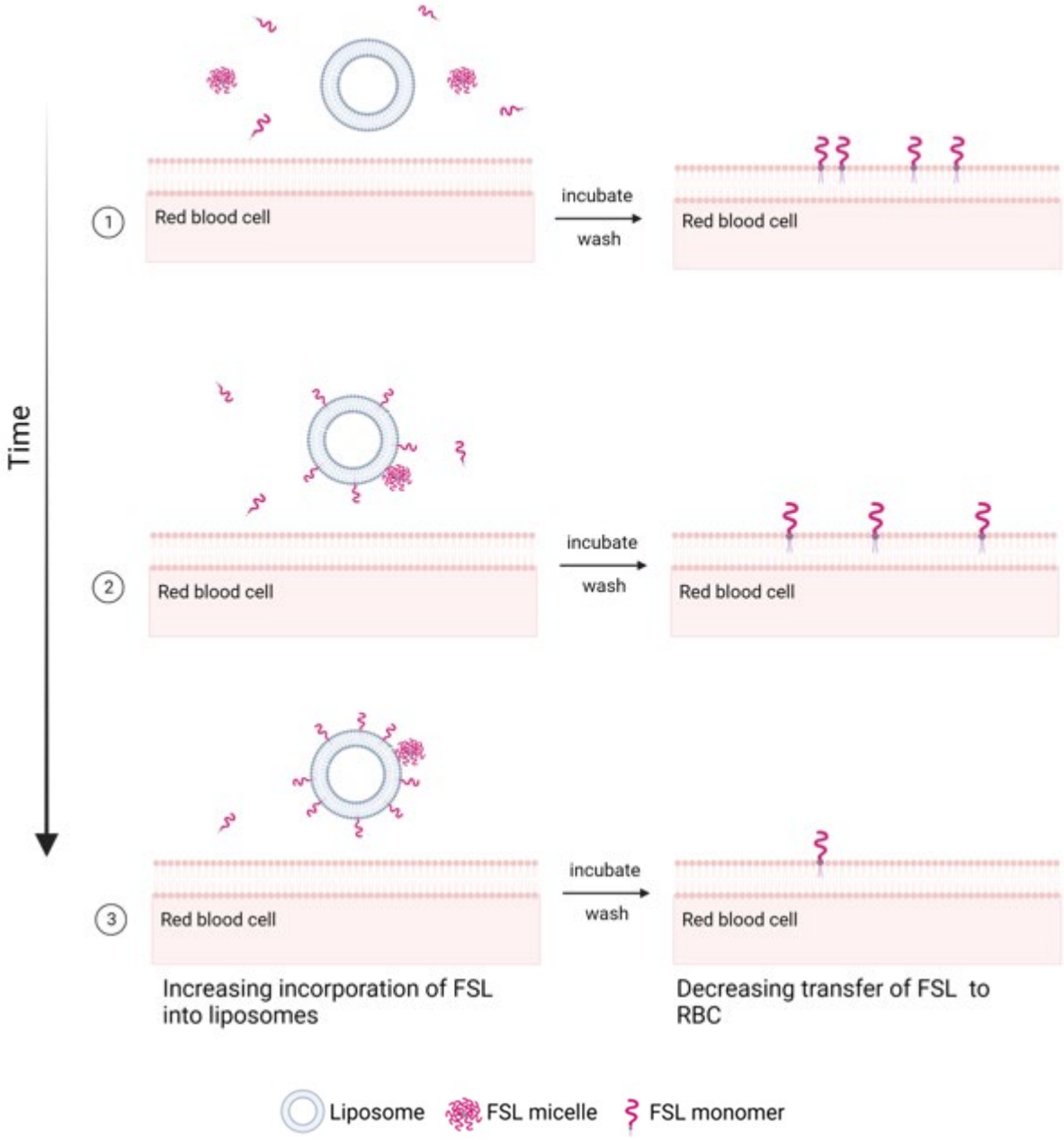

Figure 89 Proposed mechanism for transfer of FSL to RBC from a (PS) liposome dispersion, showing change in transfer over time. (**1**) Immediately following addition of FSL to blank lipsoomes there is a high concentration of FSL micelles/monomers in supernatant available to bind to RBC. (**2**) After liposome dispersion has been incubated with FSL constructs for some time (i.e. 1 hour) more FSL constructs have incorporated into the liposomes. The concentration of FSL micelle/monomer in supernatant has decreased, and when added to RBC there is less FSL available to transfer to the RBC. (**3**) After further incubation of liposme dipserion maximum FSL insertion into liposomes has occurred, and very little FSL remians in the liposme supernatnat. When added to RBC very little transfer of FSL to RBC is seen. Diagram approximately to scale, except liposmes shown only ≈60nm in diameter not 100nm as synthesised in this study. Created with BioRender.com.

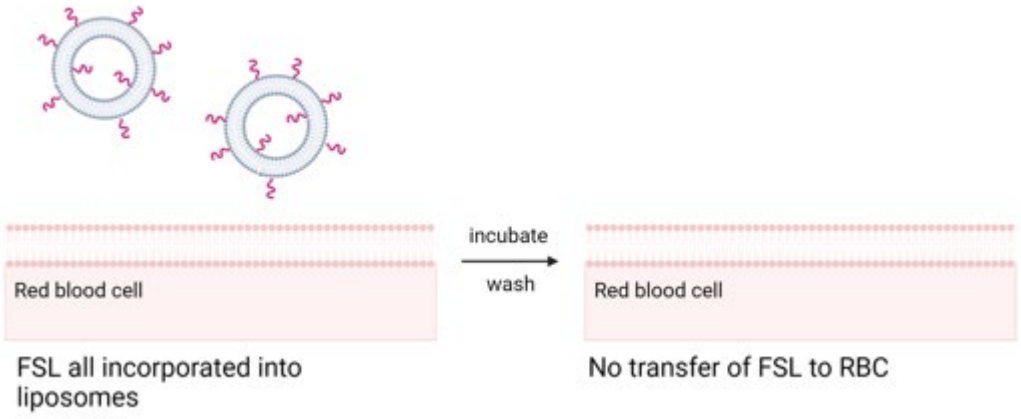

Figure 90 Theoretical transfer of FSL from LM liposome dispersion to RBC. LM liposome dispersion contains no micelle/monomer FSL. All of the FSL is incorporated into the liposome membrane during synthesis. There is no movement of FSL from monomer/micelle in supernatant into liposomes, so fluorescence of liposome dispersion does not change with time. Because there is no micelle/monomer FSL present in liposome dispersion there is no observed transfer of FSL-FLRO4 to the RBC at all time points. Diagram approximately to scale, except liposmes shown only ≈60nm in diameter not 100nm as synthesised in this study. Created with BioRender.com.

Results – 7 days storage

Graphs comparing the mean fluorescence intensity of RBC after incubation with 100 FLRO4 liposomes and 100 biotin liposomes are shown Figure 91 and Figure 92.

The transfer of FSL-biotin and FSL-FLRO4 from liposome dispersions to RBC showed similar patterns of reactivity;

- Transfer of FSL from LM liposomes to RBC was not observed.
- Transfer of FSL from PS liposomes (both FLRO4 and biotin) that were stored at 4°C, to RBC declined between day 1 and day 3 and then remained constant. This reduction in transfer is likely due to the increasing incorporation of FSL into liposome during days 1-3, leaving less micelle/monomer FSL available in liposome supernatant to label the RBC. After day three maximum FSL insertion/adsorption with liposome has been reached (see 3.1).
- Transfer of FSL from the PS and H liposomes that were stored at RT, was very low. This is most likely because incorporation of FSL into liposome occurs much faster at RT (than 4°C), maximum insertion/adsorption has been reached within 24 hours (section 3.1 FSL incorporation into liposomes). Very little free FSL micelle/monomer remains in these liposome dispersions to label the RBC. The correlation between increasing FSL association with liposomes (results from 3.1) and declining transfer of FSL to RBC (this experiment) is shown in Figure 93.

.

FSL-FLRO4

a) Lipid Mix

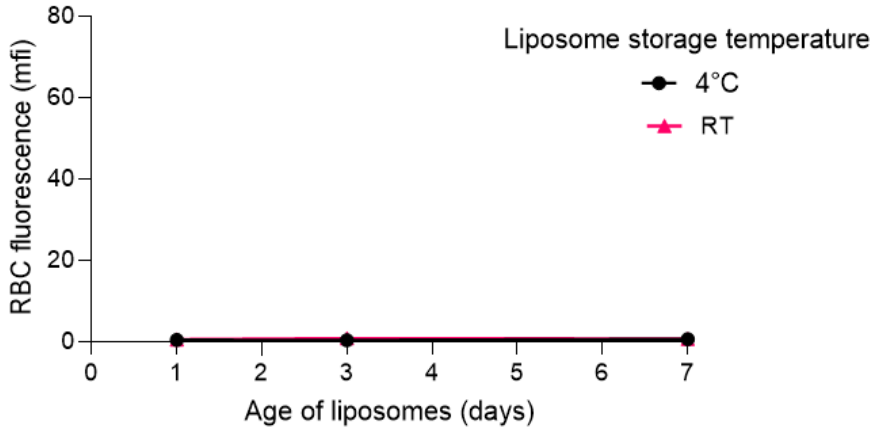

b) Hydration

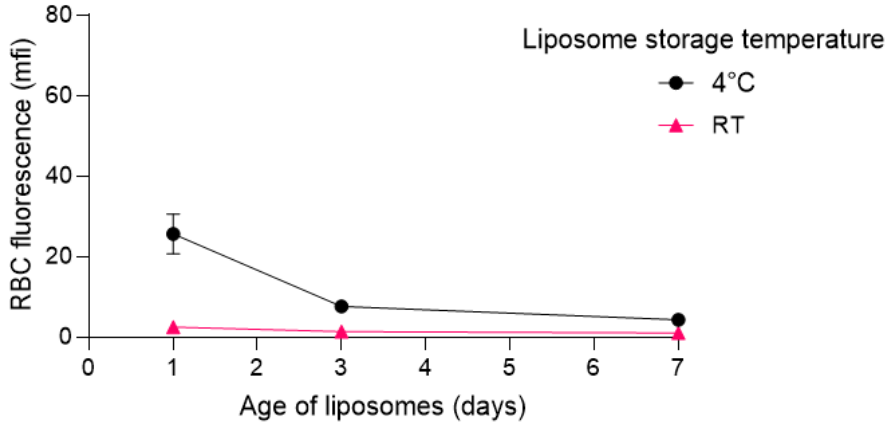

c) Post Synthesis

Figure 91 Effect of liposome age on FSL-FLRO4 transfer. Graphs showing the effect of liposome storage time and temperature on transfer of FSL-FLRO4 from liposome to RBC. Liposomes were prepared with 100µM FSL-FLRO4 added by (**a**) LM, (**b**) H and (**c**) PS method. Transfer of FSL-FLRO4 to RBC from H and PS liposomes which had been stored at 4°C decreased between day 1 and day 3. No or very little transfer was seen from LM liposomes (both storage temperatures), or H and PS liposomes that were stored at RT.

FSL-biotin

a) Lipid Mix

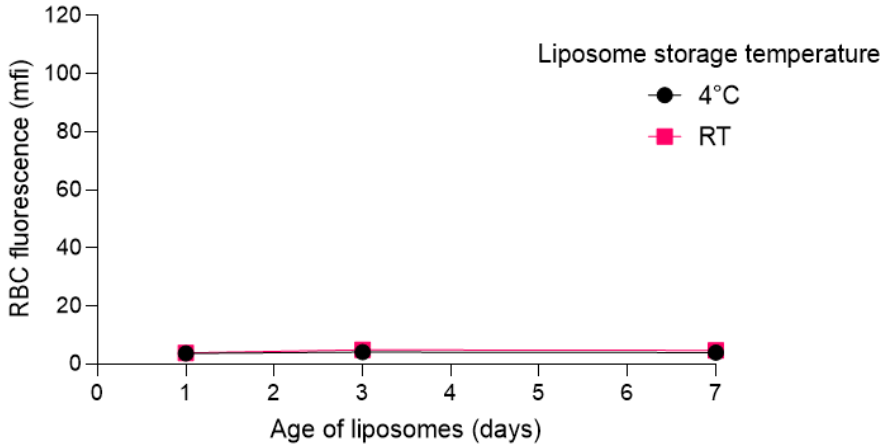

b) Hydration

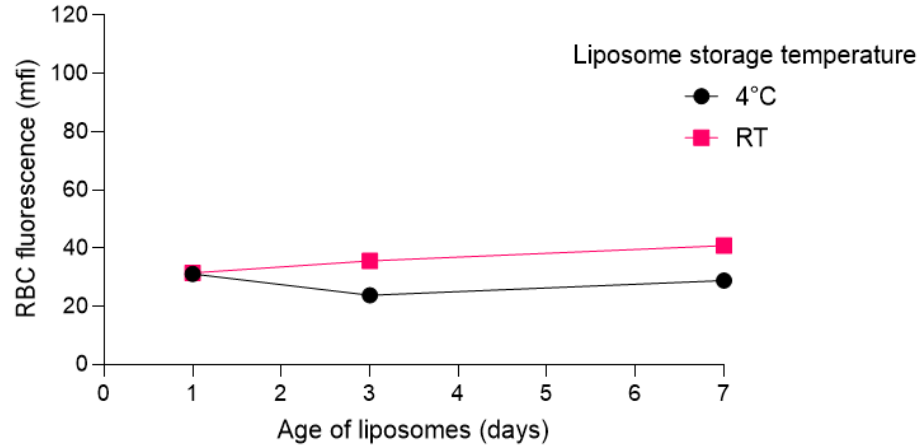

c) Post Synthesis

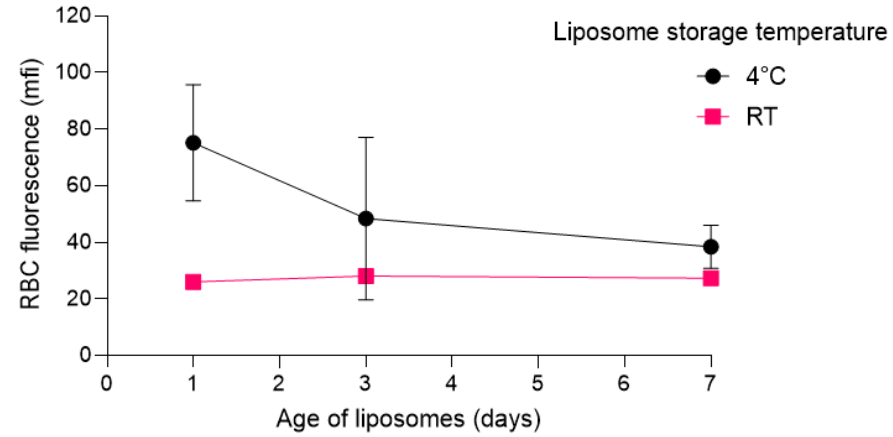

Figure 92 Effect of liposome age on FSL-biotin transfer. Graphs showing the effect of liposome storage time and temperature on transfer of FSL-biotin from liposome to RBC. Liposomes were prepared with 100µM FSL-biotin added by (**a**) LM, (**b**) H and (**c**) PS method. Transfer of FSL to RBC from H and PS liposomes that had been stored at 4°C decreased between day 1 and day 3. No or very little transfer was seen from LM liposomes stored at both temperatures, and H and PS liposomes that had been stored at RT. (Biotin was detected using streptavidin Alexa Fluor™ 488).

Overlay graphs, Figure 93, show the correlation between the observed decrease in FSL transfer to RBC (this experiment) and the observed decrease in free FSL micelle/monomer present in liposome dispersions (results from 3.1.1).

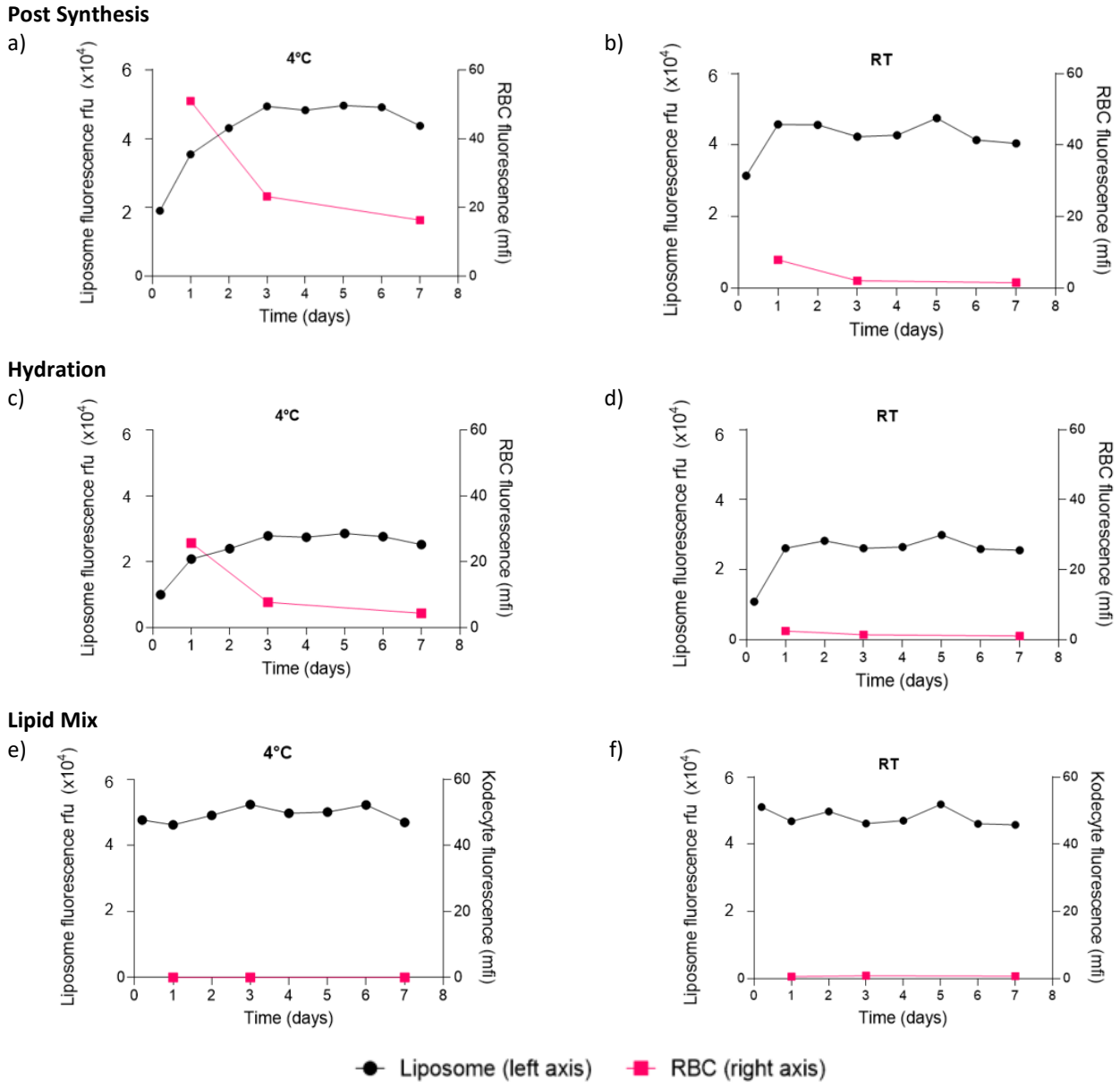

Figure 93 FSL-FLRO4 overlay graphs. Graphs showing the change in fluorescence of 100 FLRO4 liposome dispersions ( ) and fluorescence of RBC ( ) after incubation with liposomes. As fluorescence of H and PS liposome dispersions increases (indicating increased FSL incorporation into the liposome), transfer of FSL from the liposome dispersion to RBC decreases. LM liposomes showed no change in fluorescence and no FSL transfer to RBC. This correlation shows that as free FSL incorporates into liposome transfer to RBC decreases.

FSL-A2

Table 19 shows the agglutination scores of RBCs after incubation with 100 A2 liposomes (LM, H and PS). Agglutination of the kodecytes indicates that FSL-A2 is present on the RBC membrane.

Table 19 Agglutination reactions of A2 kodecytes.

Sample			**Agglutination Reaction**			
		Liposome storage temp*	Liposome storage time (days)*			
			2 hours	1	3	7
RBC + liposome	LM	4°C	0	0	0	0
	H		4+	2+	2+	2+
	PS		4+	4+	3+	3+
	LM	RT	0	0	0	0
	H		4+	2+	2+	2+
	PS		4+	3+	3+	3+

* Temperature and length of time that liposomes were stored (after their synthesis) before being used to prepare the kodecytes.

A similar pattern of reactivity to FSL-biotin/FSL-FLRO4 was observed;

- Transfer of FSL from LM liposomes to RBC was not observed (both temperatures and all time points).
- Transfer of FSL from PS liposomes to RBC declined between day 1 and day 3 and then remained constant.
- Transfer of FSL from H liposomes to RBC declined between 2 hours and day 1 then remained constant.

As with FSL-FLRO4 liposomes, the decrease in agglutination strength correlated well with the results observed in experiment 3.1.2 FSL incorporation into liposomes. As detected levels of free FSL-A2 in PS and H liposome dispersions decrease (experiment 3.1.2) the transfer of FSL to RBC also decreased (this experiment). Overlay graphs are shown in Figure 94. This correlation shows that as FSL incorporates/associates with liposome membrane transfer to RBC decreases.

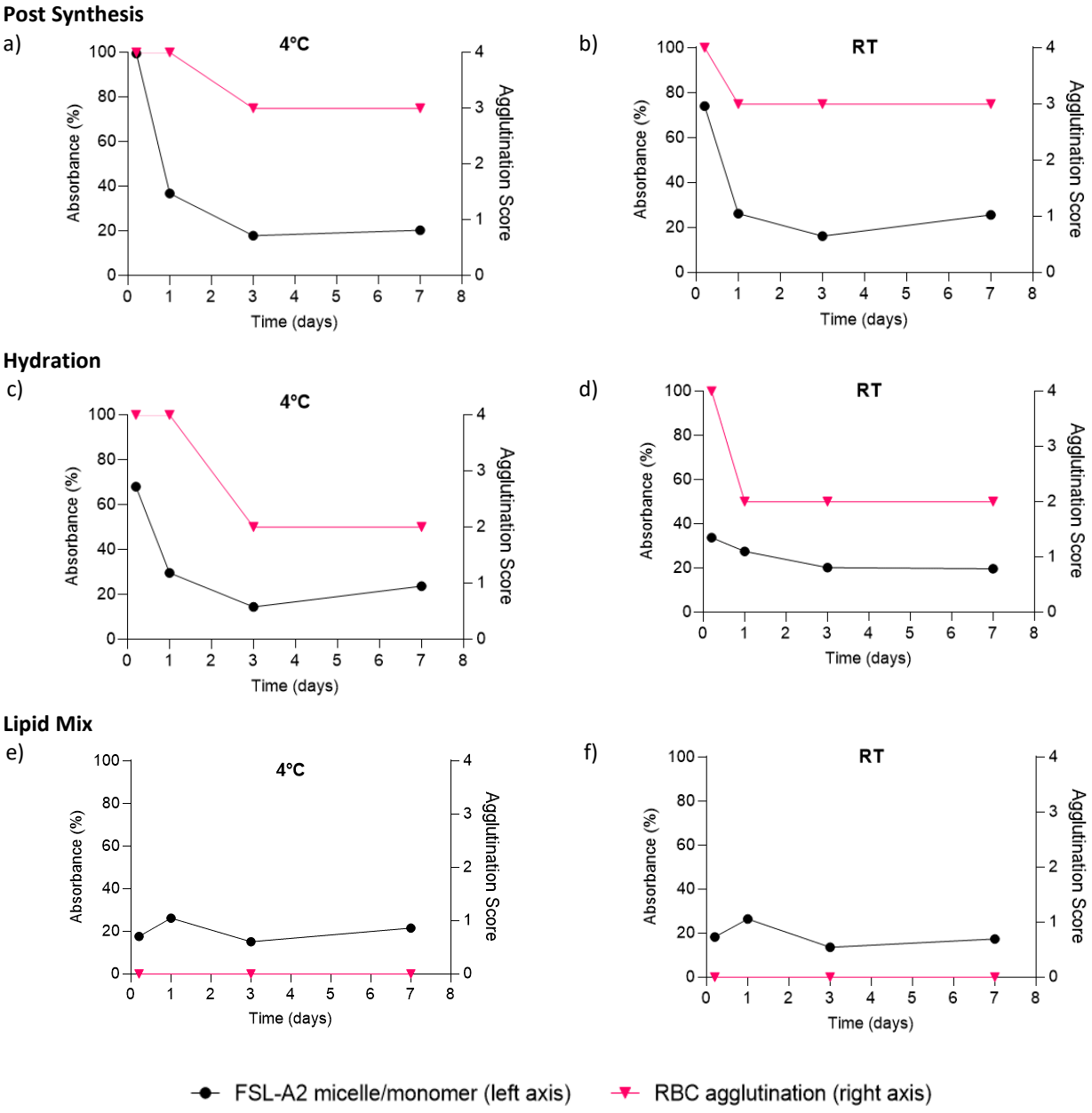

Figure 94 FSL-A2 overlay graphs. Graphs showing the level of micelle/monomer present in 100 A2 liposome dispersion (●) and agglutination of kodecytes (▼) formed after incubation with liposomes. A corresponding decrease in free FSL detected in H and PS liposome dispersions and decrease in agglutination of kodecytes (showing decreased transfer of FSL-A2 to RBC) can be seen. Very little free FSL was detected in LM liposomes, and no FSL transfer to RBC from LM liposomes was observed. This correlation shows that as free FSL incorporates into liposome transfer to RBC decreases.

Summary

Results show that as FSL incorporates into the liposomes transfer of FSL to RBC declines.

FSL was only detected on RBC after incubation with H and PS liposome dispersions. The amount of FSL that transferred to the RBC from H and PS liposome dispersions decreased with increasing age of the liposomes. This reduction in transfer occurred more slowly when liposomes were stored at 4°C than when they were stored at RT. The reduction in labelling of RBC correlated well (as shown in overlay graphs Figure 93 and Figure 94) with previous experiments (section 3.1.1 and 3.1.2) that showed increasing FSL-A2 and FSL-FLRO4 incorporation into liposomes. As FSL in the supernatant (micelle/monomer) incorporates into the liposome there is less available to bind to the RBC (Figure 91). After incubation for 24 hours at RT and ≈3 days at 4°C a plateau was reached after which no further change was observed (i.e. maximum FSL insertion has been reached).

FSL constructs were not observed to transfer from LM liposomes to RBC. Earlier results suggest LM liposome dispersions contain no 'free' micelle/monomer FSL (see 2.2.1), therefore movement of FSL from free micelle form to liposome is not observed (e.g. fluorescence of liposome dispersion does not change with time), and no transfer of FSL to RBC occurs (Figure 90). It is therefore hypothesised that FSL which has integrated into the liposome membrane does not readily transfer to RBC (under conditions tested, 2 hours at 37°C).

Although the labelling of RBC with FSL from H and PS liposomes decreased with time, it did not reduce to the very low levels seem with LM liposomes. This suggests that a small amount of FSL remains available to transfer to RBC in these dispersions. The FSL which is able to transfer to RBC may have remained in supernatant as 'free' micelle/monomers, or alternatively it may be that some FSL adsorbs to the surface of liposomes (rather than fully integrating into the membrane) and it is this adsorbed FSL which can transfer to RBC.

3.3.6 Effect of liposome age – 12 weeks

The previous experiment was then repeated and extended for 12 weeks. This was to determine if the amount of FSL that transferred to the RBC would change over time. By monitoring the transfer of FSL to RBC (kodecyte preparation) and comparing these results over time this method was used to indirectly determine if the FSL constructs were retained in the liposome membrane. If they were not, then it was expected that micelle/monomer FSL in the liposome dispersion would increase, and consequently the transfer of FSL to RBC would also increase.

Method

The method used was the same as detailed in the previous experiment (3.3.4), except liposomes were stored at 4°C only for 12 weeks. Aliquots were removed to prepare kodecytes at various time points and the transfer of FSL to RBC measured by agglutination or flow cytometry (see 3.3.1 for methods).

Note: the size, PDI, and zeta potential of the liposome dispersions were also measured at each time point and found to be stable (results shown in 3.4).

Results

FSL-A2

Table 20 shows the agglutination scores of RBCs after incubation with 100µM FSL-A2 liposome dispersions. Natural RBC and blank liposomes were tested in parallel as controls, expected reactions obtained, results not shown.

Table 20 FSL-A2 transfer from liposome to RBC after 12 weeks storage at 4°C.

Sample		**Agglutination score**				
		Liposome storage time (weeks)				
		1	**2**	**4**	**8**	**12**
RBC + 100µM A2 liposomes	LM	0	0	0	0	0
	H	2+	2+	2+	2+	2+
	PS	3+	3+	3+	3+	3+

RBC incubated with LM liposomes showed no agglutination with anti-A at all time points indicating that no detectable transfer of FSL-A2 from LM liposomes to RBC occurred.

In contrast, transfer of FSL-A2 was detected when RBC were incubated with PS and H liposomes. RBC incubated with H liposomes showed 2+ agglutination, and those with PS liposomes showed 3+ agglutination. The strength of agglutination remained unchanged over the 12 weeks. This indicates that the amount of free (micelle/monomer) FSL present in the liposome dispersions did not change.

By comparing with the standard kodecyte results (Figure 82) it can be seen that 3+ agglutination occurs when RBC are incubated with 4-10µM micelle FSL-A2. Incubation with ≥10µM FSL-A2 results in RBC showing strong 4+ agglutination. Therefore, it was determined that the equivalent of ≈4-10µM FSL-A2 had transferred from the 100 A2 PS and H liposome dispersion to the RBC. This is approximately 5-10% of the amount of FSL (100µM) originally added to the liposome dispersion. Therefore, it appears that

approximately 5-10% of FSL-A2 added to the liposomes was able to transfer to RBC. This FSL may have remained in the liposome dispersion as free FSL in the supernatant, even after 12 weeks. Or alternatively it may be due to FSL which has adsorbed to the surface of liposome (rather than integrating into the membrane).

These results show that majority of FSL-A2 is incorporated/associated with the liposomes and was then retained for the 12 weeks (when stored at 4°C in PBS).

FSL-biotin

Figure 95 shows RBC fluorescence after incubation with FSL-biotin liposome dispersions which had been stored for up to 12 weeks at 4°C (detected via addition of streptavidin Alexa Fluor™ 488).

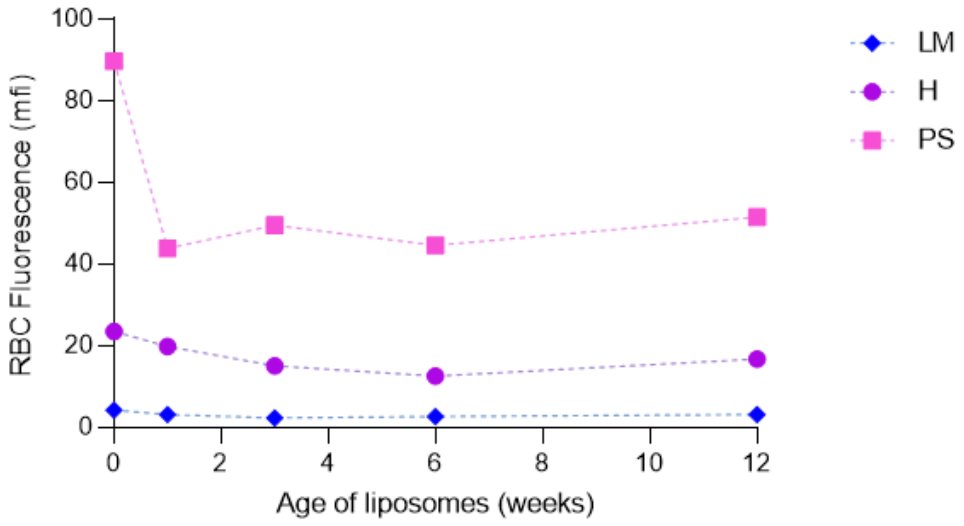

Figure 95 Transfer of FSL-biotin to RBC. Graph showing the transfer of FSL to RBC after incubation (2hours, 37°C) with 100 biotin liposomes. Liposomes containing 100µM FSL-biotin were prepared by LM, H and PS methods and stored for 12 weeks at 4°C. Aliquots were removed at various time ponts and incubated for 2 hours at 37°C with RBC, and FSL transfer to RBC measured. Transfer from PS and H liposomes showed an initial decrease during first week, then remained unchanged for following 11 weeks. No transfer was seen from LM liposomes. FSL-biotin was detected using streptavidin Alexa Fluor™ 488. After insertion FSL constructs appear to retained by liposomes.

Transfer of FSL-biotin from LM liposomes was very low at all time points and did not change over the 12 week period.

Transfer from H and PS liposomes decreased from week 0 to week 1 and then remained constant for the following 11 weeks. The fluorescence of these RBC (weeks 1-12) was quite high, 40 mfi after incubation with PS liposomes and 20 mfi after incubation with H liposomes. By comparing with the biotin kodecyte standard curve, Figure 83, an estimate of the amount of FSL-biotin that transferred to RBC was calculated, 40 mfi is equivalent to ≈10µM FSL-biotin, and 20mfi correlates to ≈4µM FSL-biotin. That is approximately 10% and 4% of the FSL originally added to these liposome dispersions(100µM) transferred to RBC.

These results show that majority of FSL-biotin was incorporated/associated with the liposomes and was then retained for the 12 weeks (when stored at 4°C in PBS).

FSL-FLRO4

Figure 96 shows RBC fluorescence after incubation with FSL-FLRO4 liposome dispersions which had been stored for up to 12 weeks at 4°C.

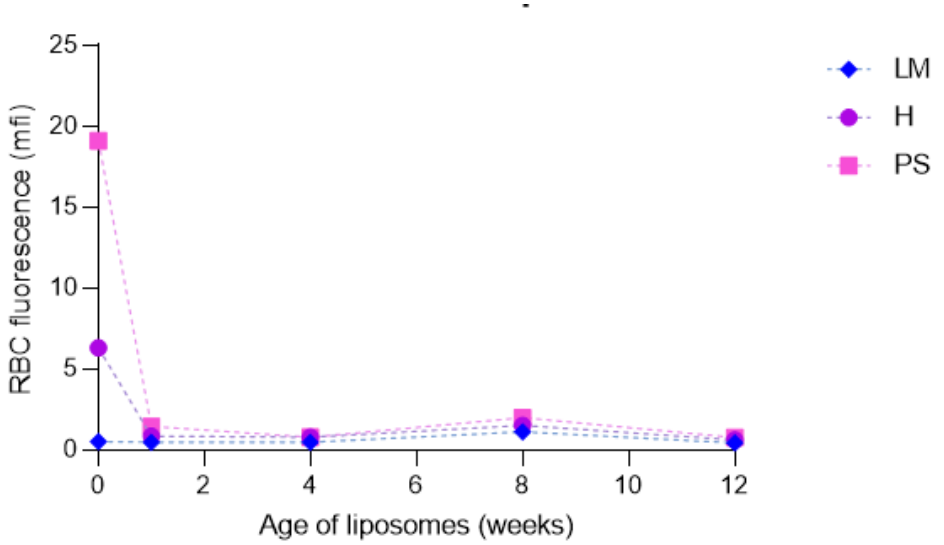

Figure 96 Transfer of FSL-FLRO4 to RBC. Graph showing the transfer of FSL to RBC after incubation (2hours, 37°C) with 100 FLRO4 liposomes. Liposomes contining 100µM FSL-FLO4 were prepared by LM, H and PS methods and stored for 12 weeks at 4°C. Aliquots were removed at various time ponts and incubated for 2 hours at 37°C with RBC, and FSL transfer to RBC measured. After an initial decrease in FSL transfer from PS and H liposomes during first week 1, transfer remained unchanged for following 11 weeks. Negligble transfer was seen from LM liposomes. After insertion FSL constructs appear to be retained by liposome.

Very little/no transfer of FSL-FLRO4 from LM liposomes to RBC was observed, even after extended 12 week storge.

Transfer of FSL from PS and H liposomes to RBC declined during the first week of storage. After 1 week, the amount of FSL detected on RBC was very low (<1.5mfi) and did not change during the remaining 11 weeks.

The fluorescence of RBC after incubation with liposomes from week 1-12 was <1.5 mfi. The amount of FSL micelle/monomer present in liposome dispersion was estimated to be <1µM by comparing with the FSL-FLRO4 kodecyte standard curve, section Figure 83.

These results show that almost all of FSL-FLRO4 was incorporated/associated with the liposomes and was retained for the 12 weeks (when stored at 4°C in PBS).

Summary

No transfer of FSL from LM liposome dispersions to RBC was observed at all time points.

A small amount of FSL transfer from FSL-biotin and FSL-A2 liposomes, prepared by H and PS methods, to RBC was observed. After an initial decrease during week 1, the amount of FSL transferred to RBC remained the same between weeks 1-12. This shows the amount of FSL micelle/monomers present within these liposome dispersions did not change during this time. After incorporation into liposome during week 1 the FSL constructs appeared to be retained by the liposomes during the remaining 12 week period.

By comparing transfer of FSL with kodecyte standard curves, it was estimated that approximately 5-10% of FSL-A and FSL-biotin added to liposome dispersions transferred to RBC (during week 1-12). This FSL may have remained as free micelle/monomer FSL within liposome supernatant, or it may have adsorbed to the surface of liposomes, without integrating into the membrane.

In contrast to FSL-A2 and FSL-biotin, very little transfer of FSL-FLRO4 (all three methods of preparation H, PS and LM) to RBC was observed. This appears to show that most of the FSL-FLRO4 constructs integrate into the liposome membrane and are therefore unable to transfer to the RBC.

A possible explanation for this difference between FSL-A2/FSL-biotin (in which 10% FSL remained available to transfer to the RBC) and FSL-FLRO4 (<1% FSL transfer) is that FSL-FLRO4 constructs show increased insertion into the liposome membrane, leaving almost no FSL-FLRO4 micelles/monomers remaining in the dispersion available to label the RBC, or adsorbed to the liposome surface.

FSL-FLRO4 has a short adipate spacer while FSL-A2 and FSL-biotin both have the much larger and more hydrophilic CMG(2) spacer. This difference may result in different behaviour of the FSL-FLRO4 molecules and effect their insertion characteristics. The CMG(2) spacer improves the hydrophilicity of FSL-A2 and FSL-biotin which may favour slightly increased concentration of FSL-A2 and FSL-biotin remaining as micelle/monomer form within the liposome dispersion.

Another contributing factor could be the CMC of the FSL constructs. The earlier CMC results suggested that FSL-FLRO4 has a much higher CMC (100-130µM) than the other two constructs (≈50µM) (see 2.1.3

Critical micelle concentration). This may also affect insertion behaviour. In this experiment FSL constructs were used at 100µM concentration, this is above the CMC of FSL-A2 and FSL-biotin, and at or slightly below the CMC of FSL-FLRO4.

Alternatively, the detection of small quantities of FSL-FLRO4 may be less sensitive than detection of FSL-biotin (detected via fluorescence of streptavidin-Alexa Fluor™ 488) and FSL-A2 (haemagglutination by anti-A). Fluorescein, the fluorescence head group of FSL-FLRO4, is well known to quench and photo bleach.

3.3.7 Effect of incubation time and temperature

In the previous experiments investigating transfer of FSL between liposomes and cells, contact time between liposomes and RBC was 2 hours at 37°C, see method 3.3.1a. This method was chosen based on the established method to prepare kodecytes [56]. The following experiment was carried out to determine if longer contact times between liposomes and RBC would affect FSL transfer. Liposomes and RBC were incubated together for up to 6 hours at 4°C or 37°C. Aliquots were removed at various time points and the amount of FSL on RBC was measured.

Method

1. Liposome dispersions were prepared containing 100µM FSL incorporated by LM, H and PS protocols (method 2.2.2). The liposome dispersions were stored at 4°C for 4 days to ensure maximum FSL insertion into the liposomes had occurred and that minimal micelle FSL remained in H and PS dispersions.
2. Equal volumes of packed RBC and liposomes were mixed together. This mixture was then divided into two, one aliquot was stored at 37°C and the other at 4°C.
3. Aliquots were removed after 1, 2, 4, and 6 hours incubation. The resulting RBC (kodecytes) were analysed by flow cytometry (FSL-FLRO4 and FSL-biotin) or by haemagglutination (FSL-A2) to detect the presence of FSL on the kodecytes (see 3.3.1 for methods).
4. FSL micelles and blank liposomes (containing no FSL) were tested in parallel.

Results

Graphs showing the fluorescence of RBC after incubation with FSL-FLRO4 and FSL-biotin liposomes are shown in Figure 97 and Figure 98.

FSL-FLRO4

RBC incubated with FLRO4 liposomes continued to increase in fluorescence over the 6 hour incubation period at both 4°C and 37°C. This occurred with all three types of liposomes, PS, H and LM. However, in all cases the level of FSL detected on RBC remained low (<6 mfi) even after 6 hours incubation at 37°C and was less than 2% of the fluorescence shown by RBC incubated with micelle/monomer FSL.

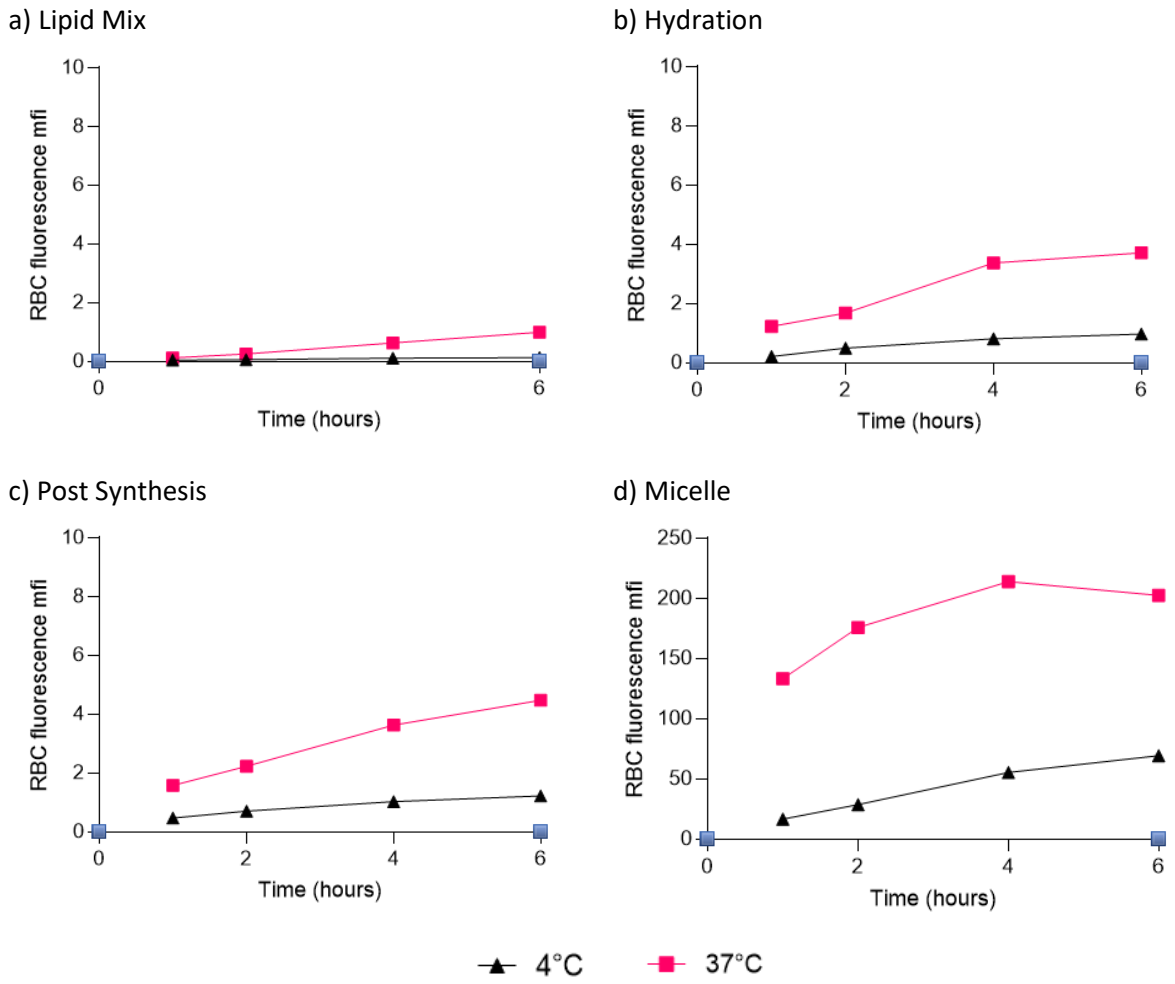

Figure 97 Effect of incubation time and temperature on transfer of FSL-FLRO4 from liposome to RBC. Note: different Y axis scale of graph (d). RBC were incubated with (**a, b, c**) 100 FLRO4 liposomes or (**d**) 100µM FSL-FLRO4 monomer/micelle dispersion at 4°C and 37°C for up to 6 hours. Transfer of FSL-FLRO4 from liposomes to RBC increased with increased incubation time, and was greater at 37°C than 4°C. However, despite this increase the actual transfer of FSL from liposomes to RBC remained very low (<10mfi in all cases) and was less than 2% of the transfer observed from FSL micelle dispersion (200mfi).

FSL-biotin

Graphs showing the fluorescence of RBC after varying length incubations with liposomes (a, b, c) or FSL micelle/monomer dispersions (d), at 4°C or 37°C are shown in Figure 98. FSL-biotin was detected by addition of streptavidin Alexa Fluor™ 488. Transfer of FSL-biotin to RBC increased with increased incubation time, and was greater at 37°C than 4°C.

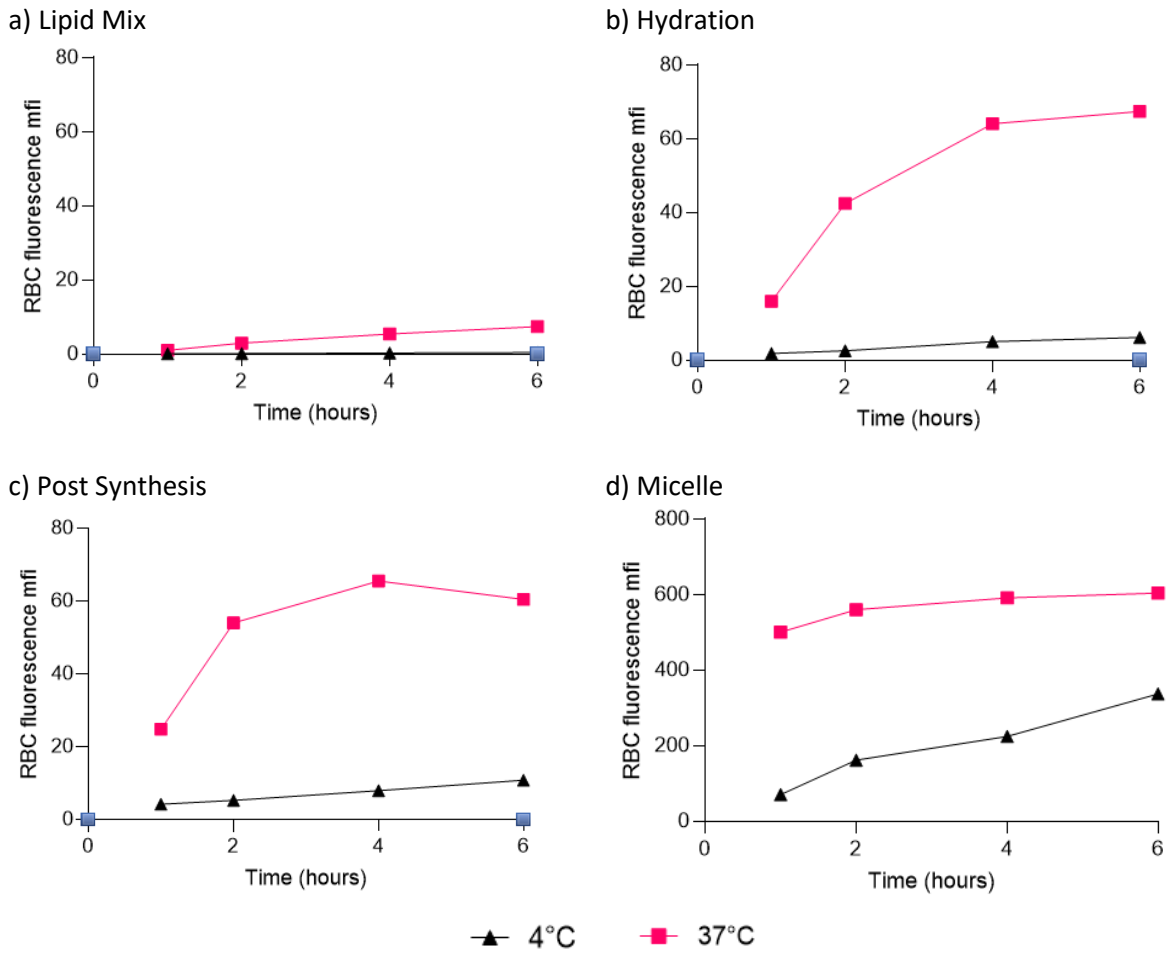

Figure 98 Effect of incubation time and temperature on transfer of FSL-biotin from liposomes to RBC. Note: different Y axis scale on graph (d), 100x greater). RBC were incubated with (**a, b, c**) 100 FLRO4 liposomes or (**d**) 100µM FSL-FLRO4 monomer/micelle dispersion at 4°C and 37°C for up to 6 hours. Transfer of FSL-FLRO4 from liposomes to RBC increased with increased incubation time, and was greater at 37°C than 4°C. Maximum fluoresence was seen around 6 hours incubation, after which fluorescence remained constant or decreased. FSL transfer from liposome dispersion to RBC was less than 10% of transfer seen from FSL micelle/monomer dispersion (600mfi).

Almost no transfer of FSL from LM liposomes to RBC, at both 4°C and 37°C, was observed. RBC fluorescence reached a maximum of 0.53 mfi after 6 hours at 4°C, and 7mfi after 6 hours incubation at 37°C This was 0.1% and 1% of the RBC fluorescence seen after incubation with FSL micelle/monomer dispersions at 4°C and 37°C respectively.

RBC incubated with H and PS liposomes at 4°C showed a small increase in FSL transfer with time, increasing from 2mfi to 6mfi (H) and from 4mfi to 10mfi (PS). This was ≈2-3% of the transfer shown by FSL micelle/monomer dispersion.

RBC incubated with H and PS liposomes at 37°C showed an increase in fluorescence during the first four hours, after which the fluorescence appeared to plateau. This suggests maximum FSL-biotin insertion has been achieved after 4-6 hours incubation at 37°C. The fluorescence of kodecytes prepared with H liposomes increased from 16 to 64mfi, and those prepared with PS liposomes increased from 24 to 65 mfi. This was approximately 5-10% of micelle/monomer transfer.

FSL-A2

The agglutination scores of RBC after varying length incubations with A2 liposomes or FSL-A2 micelle dispersions at 4°C and 37°C are shown in Table 21.

Table 21 A2 kodecyte agglutination scores. Comparison of different incubation times and temperatures used to prepare kodecytes.

Sample			**Agglutination Score**			
		Incubation temp (°C)	Incubation time (hours)			
			1	2	4	6
Kodecyte	LM	4	0	0	0	0
	H		0	0	0	0
	PS		0	0	0	0
	Micelle		4+	4+	4+	4+
	LM	37	0	0	0	0
	H		0	3+	3+	3+
	PS		0	3+	3+	3+
	Micelle		4+	4+	4+	4+

No transfer of FSL was observed from LM liposomes at both 4°C and 37°C and all incubation times.

Very little transfer was observed when RBC and liposomes were incubated together at 4°C. RBC incubated with the FSL micelle dispersion at 4°C showed strong agglutination (4+) after just 1 hour incubation.

FSL transfer was observed from H and PS liposomes incubated with RBC at 37°C for 2 hours or more. The strength of agglutination (3+) did not change, indicating maximum transfer had occurred within first two hours of incubation. Transfer from PS and H liposome dispersions was much less than from micelle/monomer dispersions (≈2-10% of micelle/monomer transfer).

Summary

FSL transfer from liposome dispersions was considerably less (<10%) than seen from FSL micelle dispersions. As observed in previous experiments FSL transfer depended on method of liposome preparation.

Transfer of FSL from PS and H liposomes was observed to be time and temperature dependent; very little/no FSL transfer was seen when liposomes and RBC were incubated together at 4°C. Transfer of FSL-FLRO4 and FSL-biotin to RBC was observed after 1 hour incubation at 37°C, and FSL-A2 after 2 hours at 37°C.

Maximum transfer of both FSL-FLRO4 and FSL-biotin from liposomes to RBC was reached after 4 hours incubation at 37°C, after this transfer did not increase any further. While FSL-A2 had reached maximum insertion within 2 hours at 37°C.

Transfer of FSL-A2 and FSL-biotin from liposome dispersion to RBC was approximately 5-10% of transfer seen from FSL micelle/monomer dispersions to RBC, while transfer of FSL-FLRO4 was just 2% of micelle/monomer transfer.

3.3.8 Effect of liposome composition – cholesterol and charge

A final experiment was conducted to investigate if altering the lipid composition of the liposome would affect the transfer of FSL from liposomes to RBC. Two additional lipid components were added – cholesterol and an FSL construct with a positive charge

Cholesterol is a dominant lipid in cell membranes and is very commonly included in liposomes. It reduces the fluidity of the liposome membrane and improves liposome stability and permeability characteristics. Because cholesterol is so commonly included in liposome compositions, an experiment was conducted to investigate if the presence of cholesterol would alter size, charge or transfer of FSL-FLRO4. Cholesterol was added to liposomes along with FSL-FLRO4 and then compared with liposomes without cholesterol to determine if the characteristics of FSL transfer would be altered by its addition. Presence of 30-40% cholesterol has been shown to cause domain formation in vesicles composed of PC/Chol [341] and cholesterol content has been shown to significantly alter post insertion of a PEG-lipid conjugate into liposomes [196].

Liposome interaction with RBC is influenced by charge. RBC are negatively charged, and all previously used liposomes in this project have also been negatively charged (see 2.2.4). An FSL construct,

FSL-$(Me_3N^+)_2$ referred to as FSL-(+), was used to synthesise liposomes with a net positive charge. FSL-(+) (GlycoNZ, New Zealand) has a positively charged functional head group, due to presence of a quaternary ammonium ion (more precisely, two such groups in one molecule - one compensates for the negative charge of phosphate, and the second actually introduces an additional positive charge), shown in Figure 99 [253]. FSL-(+) is composed of a DOPE tail with an adipate spacer.

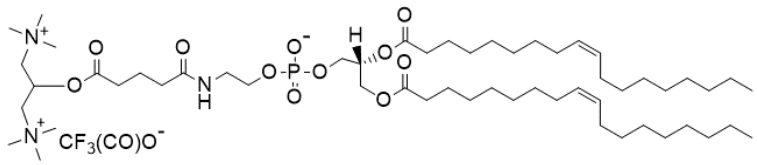

Figure 99 Chemical formula of FSL-$(Me_3N^+)_2$ (referred to as FSL-(+))

Positively charged liposomes were synthesised by including FSL-(+) in their composition-to determine what effect charge would have on the FSL transfer characteristics. Because RBC are negatively charged, it was hypothesised that positive charged liposomes might enable closer contact/adsorption between liposome and RBC membrane (via electrostatic interaction) and facilitate increased FSL transfer.

Method

1. Liposomes were prepared composed of combinations of egg phosphatidylcholine (EPC), FSL-FLRO4, cholesterol and FSL-(+) as shown in Table 22. The proportions of lipid are also shown in Table 22 and were chosen to maintain the ratio of FSL-FLRO4 to total lipid at 120:1.
2. Cholesterol (20 mol% of total lipid) and 1000µM FSL-(+) were added to the liposomes during the lipid mix stage of liposome preparation.
3. The FSL-FLRO4 constructs (100µM) were added to the liposomes by LM, H, or PS methods (method 2.2.2).
4. The size and zeta potential of the liposomes were measured by DLS analysis
5. The prepared liposomes were then incubated with RBC for 2 hours at 37°C and the RBC were subsequently analysed for presence of FSL-FLRO4 by flow cytometry (using methods described in 3.3.1).
6. Experiment was carried out on two separate occasions, mean results shown.

Table 22 Liposome lipid ratios

Abbreviation	Lipid Ratio	Lipid components			
		Egg Phosphatidylcholine (E)	FSL-FLRO4 (F)	Cholesterol (C)	FSL-(+) (+)
E:F	120 :1	120	1		
E:F:C	100:20:1	100	1	20	
E:F:(+)	110:10:1	110	1		10
E: F:C: (+)	90:20:10:1	90	1	20	10

Results

Size

The mean size and zeta potential of liposomes containing different lipid components are shown in Figure 100 and Figure 101 respectively. The mean polydispersity of the liposomes is shown in Table 23.

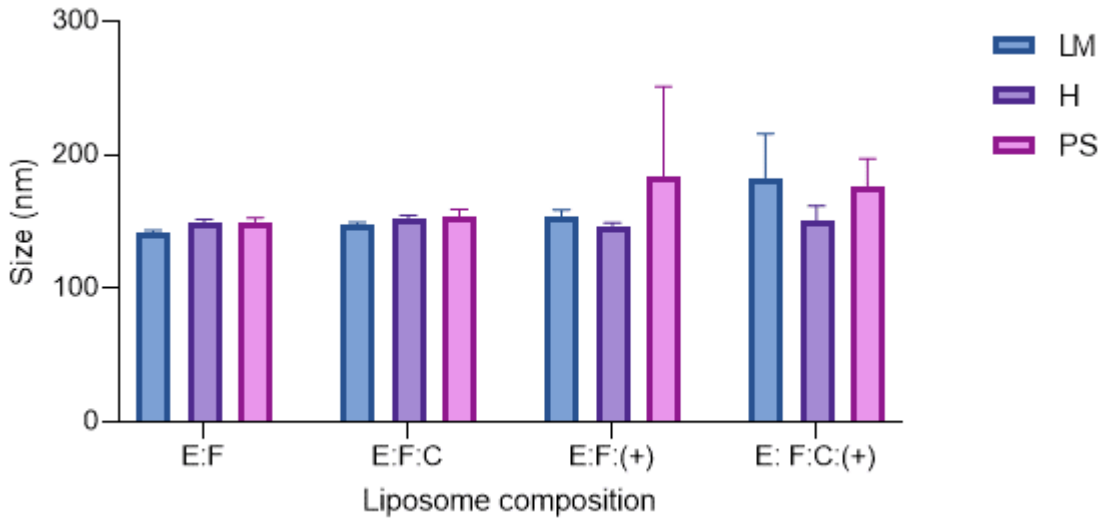

Figure 100 Size of 100 FLRO4 liposomes with different lipid compositions. Liposomes were composed of egg phosphatidylcholine (E), FSL-FLRO4 (F), and FSL-(+) (+), lipid ratios are detailed in Table 19. 100µM FSL-FLRO4 was added to liposomes by LM, H, and PS methods. Mean ± SD, n=2

No significant variation in size of the liposomes was observed in liposomes composed of EPC and FSL-FLRO4 (E:F) and EPC, FSL-FLRO4 and cholesterol (E:F:C). Much greater variation was seen in size of liposomes containing FSL-(+).

The PDI of the positively charged liposomes were also slightly increased (and greater than 0.1). This may reflect an increased tendency of the positively charged liposomes to aggregate. Alternatively, the

presence of FSL-(+) may alter the way FSL-FLRO4 associates/incorporates into the liposomes, and/or the binding of ions to the surface of the liposome which could alter the observed hydrodynamic size of the liposome.

Table 23 PDI comparison of FLRO4 liposomes with different lipid compositions.

Liposome composition	**Mean Poly-dispersity Index (PDI)**		
	Liposome Preparation Method		
	Lipid Mix	Hydration	Post Synthesis
E:F	0.08	0.08	0.09
E:F:C	0.07	0.07	0.07
E:F:(+)	0.14	0.13	0.29
E: F:C: (+)	0.20	0.15	0.26

n=2

Charge

The liposomes containing FSL-(+) (E:C:+ and E:F:C:+) were positively charged. The liposomes without FSL-(+) (E:F and E:F:C) were negatively charged.

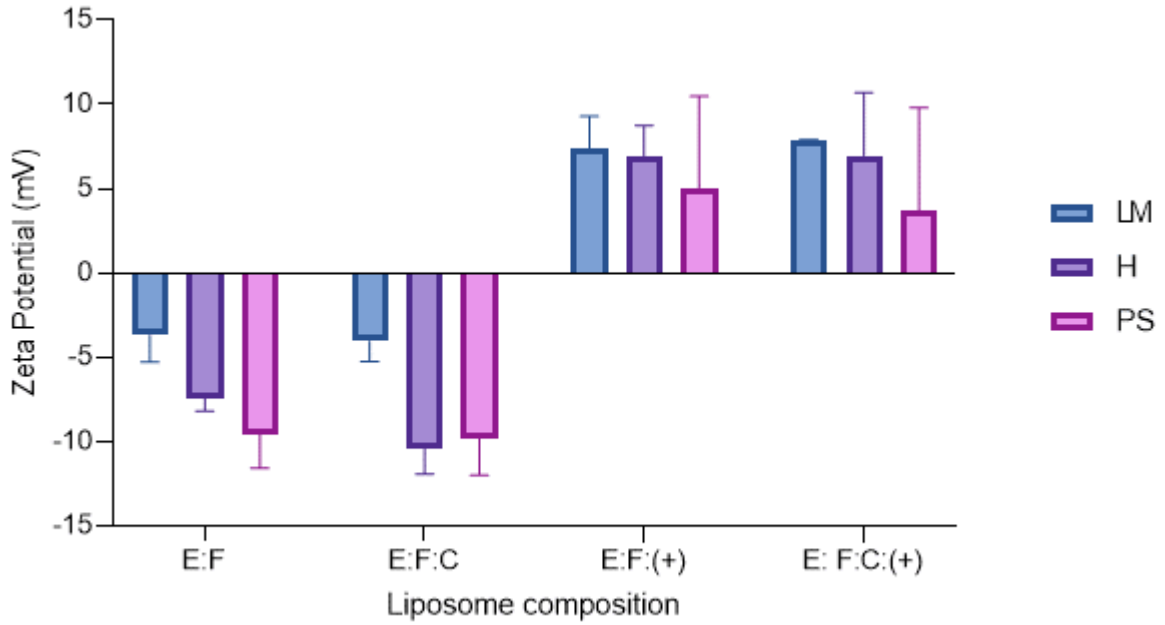

Figure 101 Zeta potential of FLRO4 liposomes with different lipid compositions . Liposomes containing FSL-(+) were positively charged, liposomes without were negatively charged. Liposomes were composed of egg phosphatidylcholine (E), FSL-FLRO4 (F), and FSL-(+) (+), lipid ratios are detailed in Table 19. 100µM FSL-FLRO4 was added to liposomes by LM, H, and PS methods. Results shown are mean ± SD, n=2

FSL-FLRO4 transfer to RBC - effect of cholesterol

The transfer of FSL-FLRO4 from liposomes containing 20 mol% cholesterol was compared to transfer from liposomes without cholesterol, results are shown in Figure 102.

The transfer of FSL-FLRO4 from liposomes containing cholesterol (E:F:C) was compared with transfer from liposomes without cholesterol (E:F). No significant difference was observed. Slightly reduced levels of FSL-FLRO4 labelling of RBC was seen from PS liposomes containing cholesterol compared with PS without cholesterol. However, this variation was within experimental variation. Alternatively cholesterol could be altering the fluidity of the liposome membrane and could also cause formation of domains/phase separation within the liposome membrane (see 1.5.3 Lamellar bilayer phases (thermotropic phase behaviour of membranes) and 1.5.5 Lateral phase separation) and this could effect FSL insertion/retention/transfer characteristics.

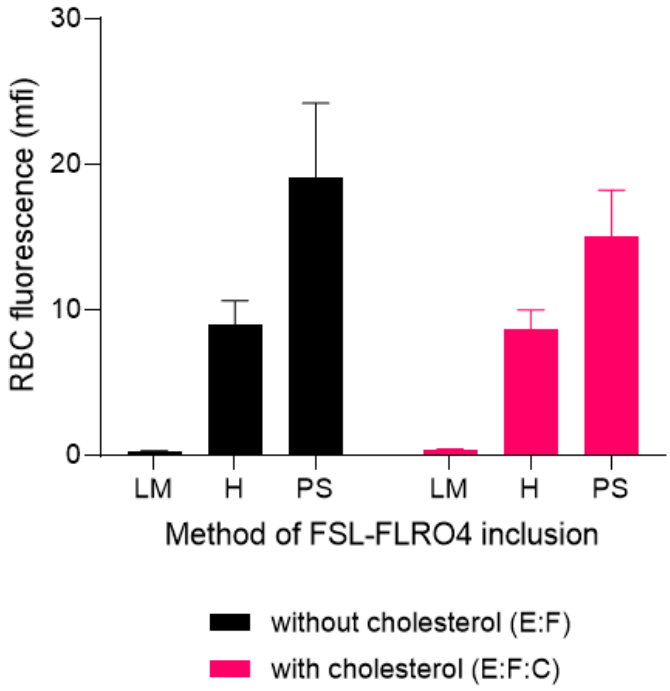

Figure 102 Effect of cholesterol on the transfer of FSL-FLRO4 from liposome to RBC. Cholesterol did not appear to significantly change transfer characteristics of FSL-FLRO4 from liposome to RBC. Liposomes containing 100µM FSL-FLRO4 were prepared with and without the addition of cholesterol, lipid ratios are detailed in Table 19. FSL-FLRO4 was added by LM, H and PS protocols. Liposomes were incubated with RBC and transfer of FSL to RBC measured by flow cytometry. Results shown are mean ± SD, n=2

FSL-FLRO4 transfer to RBC - effect of positive charge

Figure 103 compares the effect of charge on transfer of FSL-FLRO4 from liposome to RBC. Liposomes, composed of egg phosphatidylcholine and FSL-FLRO4 only, were negatively charged. The liposomes containing FSL-(+) were positively charged (Figure 101). Unlike previous experiments, liposomes which were positively charged resulted in almost no transfer of FSL-FLRO4 to the RBC.

As discussed previously the observed 'transfer' of FSL from H and PS liposome dispersions may be due to the presence of micelle FSL remaining in supernatant, or FSL adsorbed to the surface of the liposome. It is probably this FSL which labels/transfers to the RBC, rather than transfer of FSL that has integrated into the liposome membrane to RBC membrane. Therefore, a possible explanation for these results is that the positively charged liposome dispersions has increased the incorporation of the negatively charged FSL-FLRO4 into the liposome. Either by increasing the insertion of FSL into liposome and consequently decreasing free micelle/monomer FSL remaining in the supernatant, or by increasing the adsorption of FSL to surface of liposome.

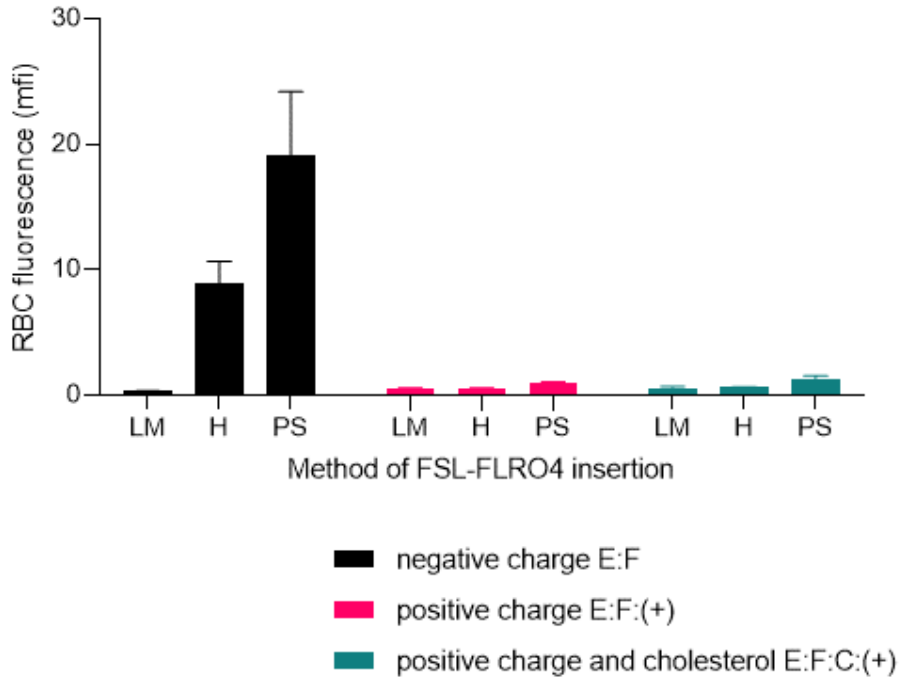

Figure 103 Effect of liposome charge on the transfer of FSL-FLRO4 from liposome to RBC. Liposomes containing FSL-(+) were positively charged and showed reduced transfer of FSL-FLRO4 to RBC (compared with negatively charged liposomes containing EPC and FSL-FLRO4). Liposomes were composed of egg phosphatidylcholine (E), FSL-FLRO4 (F), and FSL-(+) (+), lipid ratios are detailed in Table 19. 100µM FSL-FLRO4 was added to liposomes by LM, H, and PS methods. Results shown are mean ± SD, n=2.

Summary

No significant difference was observed in the transfer of FSL-FLRO4 to RBC between liposomes containing cholesterol and those without cholesterol.

Interestingly, liposomes (PS and H) with a positive charge showed reduced transfer of FSL-FLRO4 to RBC compared with negatively charged liposomes. No difference was observed for LM liposomes (no transfer observed from both negatively and positively charged liposomes).

Earlier results suggest that the transfer of FSL to RBC from PS and H liposome dispersions may be due to either residual micelle/monomer FSL which remains in the liposome dispersion or FSL adsorbed to the liposome surface, rather than transfer of FSL that has integrated into the liposome membrane to RBC membrane (see 3.3.4). Reduced transfer to RBC therefore could be caused by reduced levels of FSL micelle/monomer in the liposome supernatant or increased adsorption to liposome surface. Therefore, a possible explanation for these results is that the positive charge has increased FSL-FLRO4 incorporation/association with liposome which decreases the transfer to RBC.

3.4 Stability of FSL modified liposomes

To determine if the inclusion of FSL constructs had any effect (positive or negative) on the stability of liposomes a 12 week experiment was designed.

Liposomes dispersions containing 10 and 100µM of each FSL construct (FSL-A2, FSL-biotin and FSL-FLRO4) were prepared and stored at 4°C for 12 weeks. At various time points aliquots were removed and the size and zeta potential of the liposomes was measured to determine if addition of FSL effected liposomes stability.

The removed liposome aliquots were also incubated with RBC to measure the transfer of FSL from liposome to RBC. This aim of this was to measure the retention of the FSL within the liposomes. As labelling of RBC is postulated to be due to free FSL within the liposome dispersion (rather than transfer of FSL out of liposome membrane), by measuring transfer of FSL to RBC from the liposome dispersion over time can observe if the levels of free micelle/monomer FSL within the dispersion change with time and detect if FSL is remaining incorporated into liposome membrane.

Method

1. Liposomes were prepared containing 10 and 100µM FSL, added by all three insertion protocols (LM, H, PS) method 2.2.2.
2. Blank liposomes, composed of egg phosphatidylcholine alone, were tested in parallel.
3. The liposome dispersions were stored at 4°C for 12 weeks.
4. At various timepoints a 200µL aliquot was removed from each liposome dispersion and the size, charge and transfer of FSL to RBC was measured;
    a) 150µL was diluted to 1.5mL with PBS for size and charge analysis by DLS.
    b) 25µL was incubated with an equal volume of washed packed RBC for 2 hours at 37°C, and transfer of FSL to RBC was then measured by flow cytometry or haemagglutination (method 3.3.1).

Statistical analysis of size was carried out using PRISM GraphPad. To determine if size of liposomes altered significantly over time, mean size measurements were compared to the size result from time = 0. Two way ANOVA and post hoc Tukey's test were used. The polydispersity index (PDI) is a measure of sample homogeneity, values <0.2 are considered acceptable and indicate a homogenous liposome dispersion. Each measurement was repeated three times and the mean and standard deviation reported below.

This experiment was repeated on two separate occasions, with similar patterns of results seen.

3.4.1 Size

The results obtained from all three constructs (both 10 and 100µM) showed no significant differences, between construct and concentration. Therefore, representative size (Figure 103) and PDI (Table 24) results from 100µM FSL-biotin only are shown.

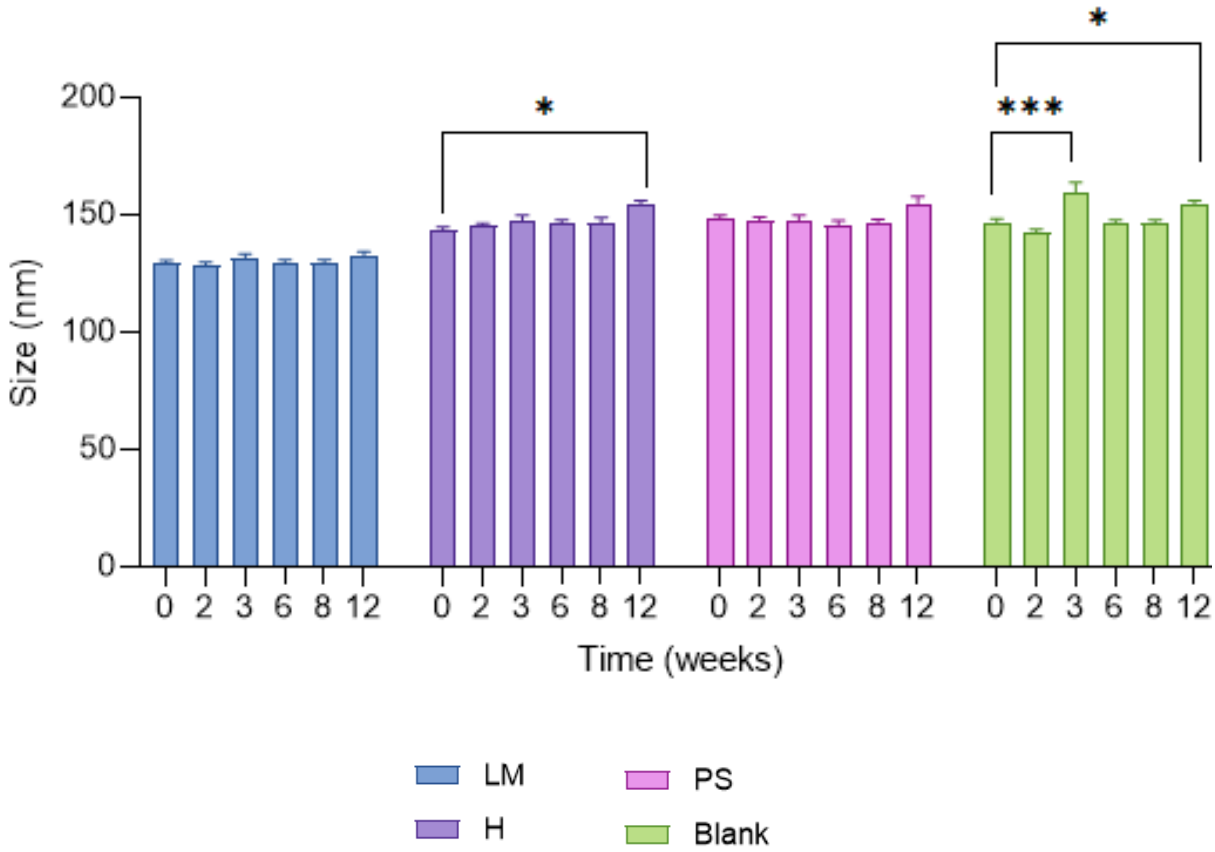

Figure 104 Size of FSL-biotin liposomes over 12 weeks. Liposomes were prepared containing 100µM FSL-biotin added by LM, H and PS methods. A very small increase in liposome size, less than 8%, was seen at week 12 in 10µM LM and H and all three 100µM liposomes. Results shown are mean ± standard deviation, n=3. * P>0.05 **P>0.01

Table 24 PDI values of FSL-biotin (100µM) and blank lipoosmes stored for 12 weeks at 4°C

Time (weeks)	Polydispersity Index (PDI)			
	Liposome			
	Blank	LM	H	PS
0	0.08	0.06	0.10	0.08
2	0.09	0.09	0.10	0.08
3	0.10	0.08	0.11	0.09
6	0.10	0.09	0.07	0.10
8	0.09	0.10	0.08	0.08
12	0.10	0.10	0.05	0.08

The size of the liposomes did not change during first 8 weeks of storage. There was also no change in PDI observed within this time. At week 12 a slight increase in liposome size was observed in several of the liposomes containing FSL and one blank liposome sample. This increase in size did not appear to be related to FSL concentration or method of FSL insertion. Across the two repeats and between different constructs it was observed in blank liposome samples (containing no FSL), liposomes containing FSL inserted by all three methods (LM, H, PS) and both 10 and 100µM concentrations of FSL.

Although statistically significant the observed increase in size was very small (between 1-8% in all cases). The same trend was seen when the experiment was repeated; no change in size for first 8 weeks and then a slight increase in size in some samples (although which liposomes increased in size varied between repeats). Because the increase in size was also observed in blank liposome samples (which contained no FSL) this slight increase is considered unlikely to be due to FSL.

The PDI values also showed no significant change over the 12 weeks. This indicates that the liposome dispersions remained monodisperse and did not aggregate and supports the size data that the liposome dispersions were stable for at least the first 8 weeks of storage.

Summary

The addition of FSL-A2, FSL-biotin and FSL-FLRO4 did not cause any change to liposome size during first 8 weeks of storage. After this time point, a slight variation in liposome size was observed, but did not appear to be related to FSL construct inclusion.

3.4.2 Zeta Potential

The following figures, Figure 105-107, show the zeta potential of FLRO4 liposomes, biotin liposomes and A2 liposome dispersions stored for 12 weeks at 4°C.

FSL-FLRO4

(a) 10µM FSL-FLRO4 liposomes

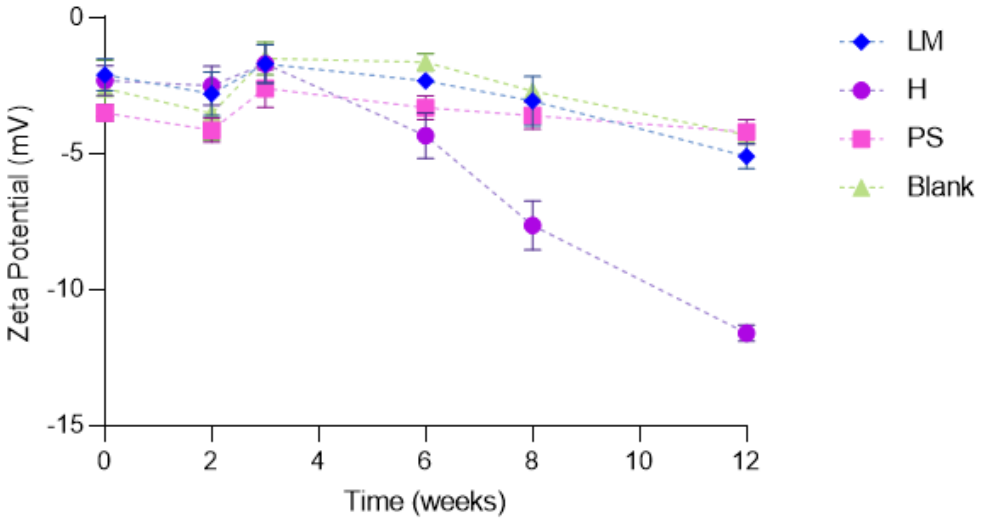

(b) 100µM FSL-FLRO4 liposomes

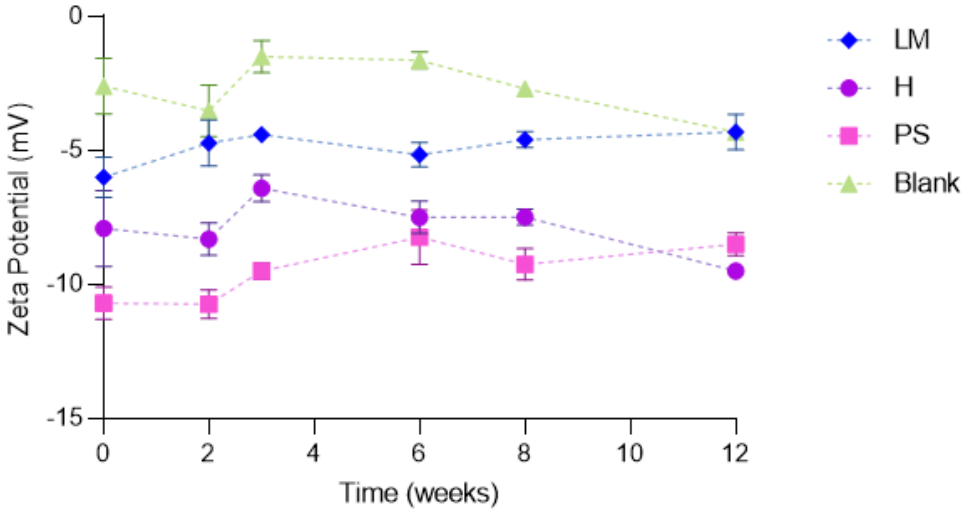

Figure 105 Zeta potential of FSL-FLRO4 liposomes stored for 12 weeks at 4°C. Liposomes were prepared containing (**a**) 10µM FSL-FLRO4 or (**b**) 100µM FSL-FLRO4. FSL was added by LM, H and PS methods. Liposomes containing 10µM FSL showed slight increase in negative charge after week 3 (except H sample, which showed significant increase in negative charge). Liposomes containing 100µM LM and PS showed no significant change in zeta potential.

The FSL-FLRO4 liposomes were all negatively charged. The zeta potential of the liposomes containing 10µM FSL-FLRO4 remained unchanged, except for the hydration liposomes (Figure 105b), which showed

a small increase in negative charge after week 3, increasing from negative 2.5mV to negative 11.6mV at week 12. The cause of this increase in negative charge is unknown and could be due to experimental error, bacterial contamination, lipid hydrolysis and/or oxidation [353]. The zeta potential of the liposomes containing 100µM FSL-FLRO4 did not change significantly over the 12 week period.

FSL-biotin

(a) 10µM FSL-biotin liposomes

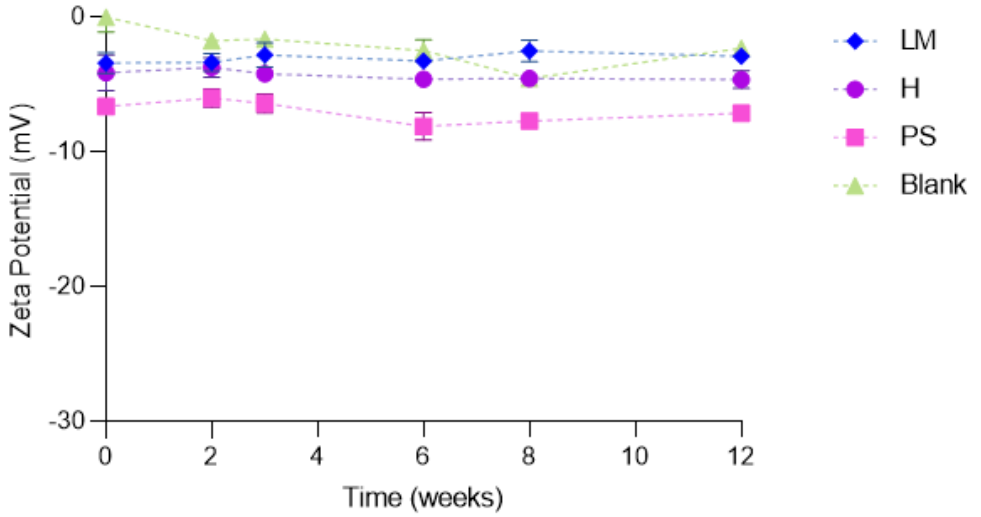

(b) 100µM FSL-biotin liposomes

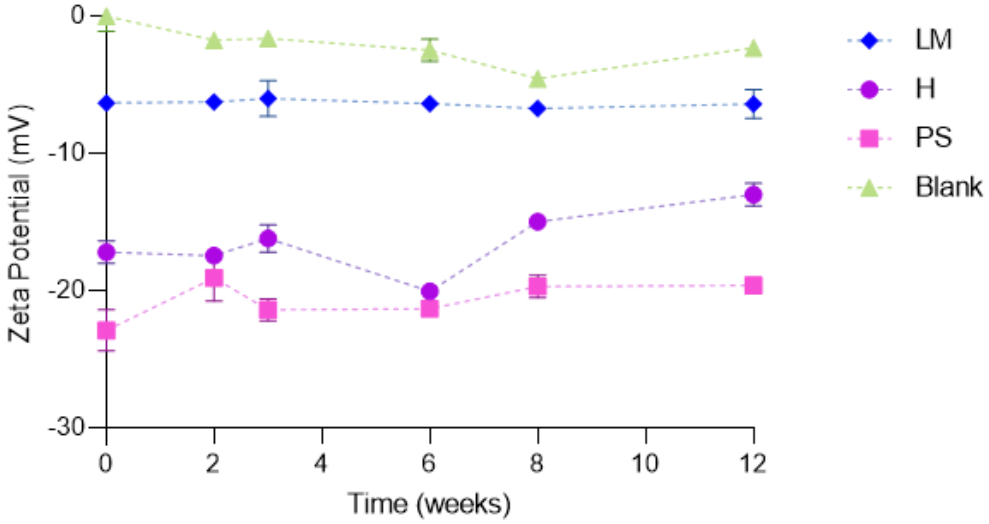

Figure 106 Zeta potential of FSL-biotin liposomes stored for 12 weeks at 4°C. Liposomes were prepared containing (**a**) 10µM FSL-biotin or (**b**) 100µM FSL-biotin. FSL was added by LM, H and PS methods. No change is zeta potential was seen.

The FSL-biotin liposomes were negatively charged, and their zeta potential did not change significantly over the 12 weeks.

FSL-A2

(a) 10µM FSL-A2 liposomes

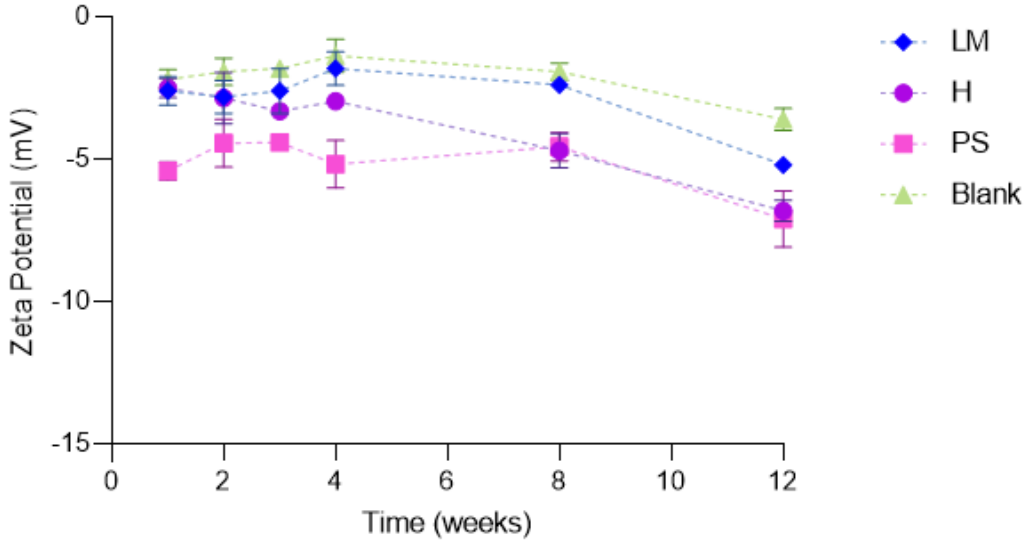

(b) 100µM FSL-A2 liposomes

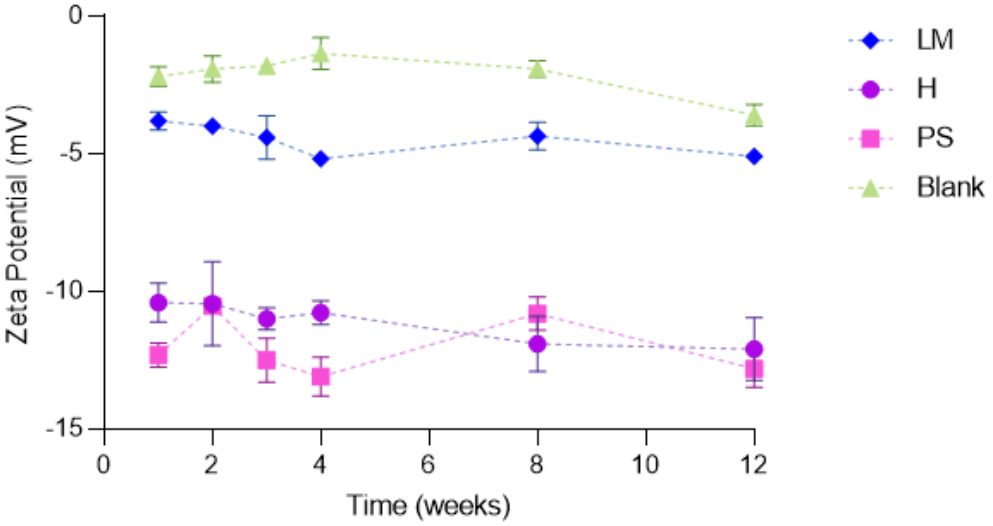

Figure 107 Zeta Potential of FSL-A2 liposomes stored for 12 weeks at 4°C. Liposomes were prepared containing (**a**) 10µM FSL-A2 or (**b**) 100µM FSL-A2. FSL was added by LM, H and PS methods. Liposomes containing 10µM FSL showed slight increase in negative charge after week 8. Liposomes containing 100µM FSL showed no significant change in zeta potential.

The FSL-A2 liposomes were negatively charged. The zeta potential of these liposomes remained relatively constant over the 12 week period. The liposomes containing 10µM FSL-A2, including the blank liposomes containing no FSL, a small increase in negative charge was seen after week 8 (Figure 107a). However, this increase was very small, each sample increasing in charge by only approximately -2mV

The liposomes containing 100µm FSL-A2 (Figure 107b) showed no significant change in zeta potential.

Summary

The zeta potential of liposomes was very stable over the 12 weeks, with the exception of one sample, FSL-FLRO4 hydration liposomes, which showed an increase in negative charge from -2.3mV to -11.6mV. The cause of this increased negative charge is unknown. Similar increases in negative charge, after more than four weeks storage was seen with other samples during the repeat experiment. Possible explanations include lipid oxidation/hydrolysis or possible bacterial contamination of the samples.

Chapter 4 Discussion

A wide variety of molecules can be conjugated to the surface of liposomes for a range of reasons, including to enable specific and targeted binding of liposomes to receptor molecules on specific cells [152], to facilitate endocytosis and intracellular delivery of bioactive molecules, to enable triggered release of cargo at a desired site, to reduce opsonisation and rapid removal by reticuloendothelial system and complement mediated destruction [73, 129]. Examples of binding ligands include antibodies, aptamers, carbohydrates, proteins/peptides, and small molecules such as vitamins [129].

Currently there are 25 clinical liposome products approved by FDA and EMA [16, 23, 24]. None of these so far are capable of active targeting and binding to specific target cells, instead rely on passive mechanisms of accumulation, such as the EPR effect [148]. While considerable success has been achieved *in vitro* with active targeting of liposomes, this has not, to date, led to the same level of success in developing clinical products. *In vivo* studies have shown that labelled liposomes result in very little increase to liposome efficacy compared to unlabelled liposomes [22]. Likely explanations include difficulties with scale up, poor correlation between animal models and humans, variation between patients and cancers, difficulties ensuring uniform production, and increased production costs [21, 133]. In addition, limitations associated with conjugation strategies [73] may also contribute to this lack of clinical success.

Kode technology is a rapid surface labelling technology that has been successfully used to modify and functionalise a range of biological and synthetic surfaces, e.g. cells, stainless steel, nanofibers, nitrocellulose [253]. Kode technology uses function-spacer-lipid (FSL) constructs to attach a range of bioactive functional groups, such as biotin, fluorophores, proteins, onto surfaces without the need for complex modification reactions. Due to similarities between natural cell membranes and liposome membranes it was anticipated that Kode technology could be used as a novel approach to label the surface of liposomes.

Prior to this research while FSL constructs had been successfully used to modify a range of cells and viruses, their use to modify liposomes had not been investigated. Therefore, an opportunity existed to explore the possible use of Kode constructs to modify the surface of liposomes. During this study several groups published studies utilising liposomes modified with Kode constructs [39, 354-360], however this research project explores in detail the interaction dynamics of FSL constructs with liposomes and consequences of different labelling methods.

The aim of this research was to investigate modification of unwashed liposomes with FSL constructs. This included developing methods to label liposomes with FSL constructs, synthesis and characterisation of FSL modified liposomes (size, charge, morphology) and evaluation of FSL insertion dynamics comparing effect of synthesis method, FSL type, retention and stability.

The conclusions of this research were positive, the results demonstrated successful modification of liposomes with Kode technology. Three methods of FSL addition to liposomes were evaluated, all three were successful. FSL modification of liposomes did not have any significant detrimental effects to liposome stability or morphology. Proof of concept that FSL constructs could be used as a method to modify the surface of liposomes was established. However, there were differences in dynamics of insertion detected between FSL constructs and dependent on method of FSL incorporation.

1. FSL construct characterisation

Kode technology utilises function-spacer-lipid (FSL) constructs to modify biological and non-biological surfaces. FSL constructs are amphiphilic molecules which are able to disperse in water and self-assemble onto biological surfaces, such as cell membranes, and non-biological surfaces such as stainless steel, nanofibers [240]. FSL constructs are composed of a functional head group (F) which is attached via a spacer (S) to a lipid tail group (L) [253]. Modification with these constructs is simple and is achieved by contact between an FSL dispersion and the surface/cell to be modified [56]. Modification is rapid, occurring in seconds for non-biological surfaces [241] or between 30-120 minutes at 37°C for biological surfaces. [57, 242]. Insertion of FSL constructs into cell membranes is believed to be due to hydrophobic forces (the hydrophobic lipid tail inserts into the cells phospholipid bilayer membrane) [253].

Three FSL constructs were used in this project; FSL-A2, FSL-biotin and FSL-fluorescein (FSL-FLRO4). These were selected to have different functional head groups; glycan (FSL-A2), vitamin (FSL-biotin), and a fluorophore (FSL-FLRO4), and two different spacer molecules, long CMG(2) (FSL-A2 and FSL-biotin) and short adipate (FSL-FLRO4). By using different functional head groups and spacer moieties it was hoped that any difference in interaction with liposomes caused by variation of these structures could be detected.

These three FSL constructs have been well studied previously and can be detected and measured using a variety of relatively simple laboratory techniques such as flow cytometry, fluorescent microscopy, immunoassay, and haemagglutination [230, 240, 246, 253]. These constructs were used to gain an understanding of the interaction between liposomes and FSL constructs (proof of concept) in order to determine how FSL constructs can be most suitability applied to liposome modification. Once this proof

of concept was established it was hoped that in the future FSL constructs could be developed with new functional head groups specifically designed to facilitate targeted binding of liposomes to target receptors/cells.

The primary methods used to detect and measure liposomes (and FSL constructs) in this project were dynamic light scatter (zetasizing) and transmission electron microscopy. For the detection and measurement FSL movement between liposomes and cells additional techniques such as flow cytometry, enzyme immunoassay, and serological haemagglutination techniques were used.

The liposomes were used unwashed because the objective outcome was to design a simple labelling method using FSL constructs as a post synthesis addition to liposomes. Therefore, unwashed liposomes were used so that insertion dynamics of FSL constructs could be fully understood, and the advantages/limitations of this methodology determined.

The FSL modified liposome prepared in this research were used without an additional wash/purification step after the addition of FSL constructs. It was hoped that FSL constructs could be applied as an 'add on' addition to fully formed liposomes without the need for additional purification (washing steps). Purification (washing) can be time consuming and can negatively impact the quality of final produce (dilution, loss of product, leakage of encapsulated materials). Therefore, the characteristics of unwashed liposomes were investigated and determined.

FSL characterisation

In order to understand liposomal labelling, it was first necessary to understand solution phase FSLs i.e. micelles. The initial research aim was to characterise FSL constructs in aqueous solutions, particularly to determine if they form micelles, and if so their size, charge and critical micelle concentration. Previously, except for the work of Zalygin et al. [260] and Ilyushina et al. [244], these properties of FSL constructs had not been thoroughly investigated. By determining the behaviour of FSL constructs in aqueous solution it was hoped this would provide insight into their interaction with liposomes, particularly in the two methods where FSL constructs were added to liposomes dispersed in aqueous solution.

When measured by dynamic light scatter nanoparticles (referred to as micelles) were detected in dispersions of all three FSL constructs (dispersed in PBS pH 7.4), from concentrations as low as 5µM. Increased concentration of FSL did not lead to increased micelle size, but rather an increase in the number of micelles present (in the concentration ranges tested 0-100µM). The micelles of all three constructs were found to have a negative zeta potential.

The size of the observed micelles varied between construct, FSL-A2 and FSL-biotin micelles had a diameter of approximately 15nm, and FSL-FLRO4 micelles 7nm. Fully extended FSL-A2 and FSL-biotin constructs measure approximately 9nm [260]. Because the size of micelles measured by DLS were 14/15nm in diameter, this suggests that FSL constructs are not in a fully extended linear end-to-end conformation (as the micelles would then have a greater diameter), but must instead adopt a folded conformation, as shown in Figure 108 [260]. The FSL-biotin results obtained in this study were in good agreement with the literature, Zalygin et al. [260] report the detection of FSL-biotin micelles (dispersed in PBS at a concentration of 100µM) of approximately 10-12nm when measured by DLS, atomic force microscopy and small angle X-ray scattering. The analysis of FSL-A2 and FSL-biotin micelles had not been previously reported.

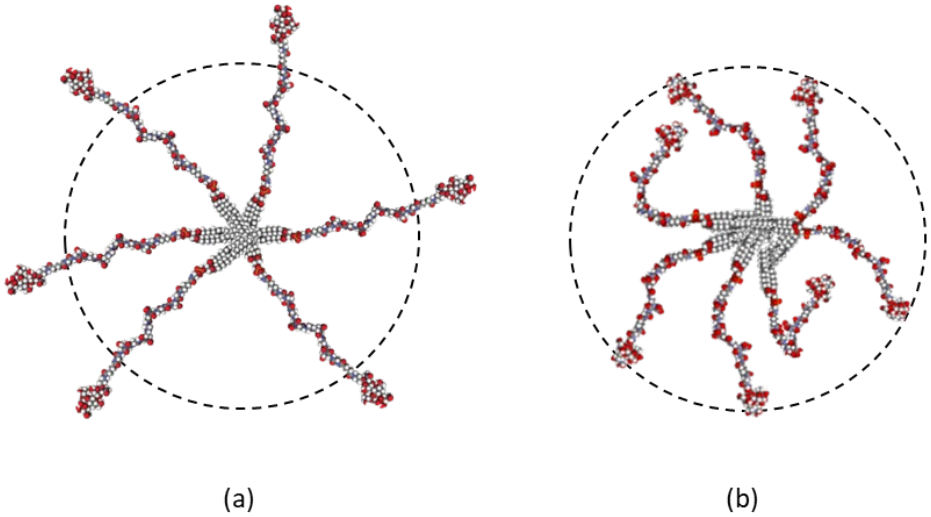

Figure 108 Schematic diagram of FSL-biotin micelles. Potential conformation of FSL constructs are shown; (**a**) fully extended or (**b**) possible folded/bent conformation. Dotted line shows measured diameter (≈15nm) of the micelles [253].

CMC

Following detection of FSL micelles, the critical micelle concentration (the concentration where micelles begin to form [305]) of the three FSL constructs was investigated. CMC was of particular interest as it has been reported in literature that transfer of lipid linked labelling molecules (likely to have similar mechanism of insertion as FSL constructs) to liposomes is reduced when molecules are in micelle conformation compared to monomers [195].

Determining the CMC proved to be challenging. Variation was seen between constructs and between results obtained by the different methods. While the DLS size data showed that micelles were detectable in dispersions of all three constructs from concentrations as low as 5µM, the calculated CMC results ranged between 3µM to 130µM. Several factors likely contribute to this wide variation; in reality CMC is

not a sharply defined point, but actually occurs over a range of concentrations. The measured CMC is dependent on the chosen method (different methods measure very different physical properties) and interpretation of the obtained data. No single approach is universally applicable and there is no universally accepted method for how to interpret experimental data to determine the CMC point [62]. In addition, this research was limited to performing techniques using equipment that was available.

CMC may be measured by a variety of methods including surface tension (Wilhelmy Plate, Du Nouy ring, Pendant drop methods)[306], electrical conductivity [307], calorimetry [308], static and dynamic light scattering [309, 310], and fluorescence (quenching) spectroscopy [62, 311].

In this study multiple techniques were used, these included surface tension (pendant drop technique) [314, 315], fluorescent spectroscopy technique (pyrene I/II method) [320]), and dynamic light scatter [310]. For FSL-FLRO4 an additional method, measuring the emitted fluorescence was also carried out (based on concept that fluorescein self-quenches when in the molecules are close contact, such as when they are in a micelle configuration).

The first techniques used was the pendant drop technique, this measures the surface tension of a liquid by analysing the shape of a drop of liquid suspended from a needle [314, 315]. This method was found to be unsuitable as there was no detectable change in surface tension of the FSL dispersions.

The next method employed was a fluorescence spectroscopy technique (pyrene I/II method)[62]. Pyrene emits a characteristic fluorescent spectra in solution, (Figure 29) which is dependent on the solvent environment surrounding the pyrene molecule [320]. When the solution is below the surfactant CMC, the surfactant molecules are present as monomers and pyrene is exposed to the polar environment of water. Above CMC, micelles form, and the pyrene molecules preferentially bind to the hydrophobic interior of the micelles which alters the emitted spectra [305].

The CMC results obtained from this method were 48µM and 28µM for FSL-A2 and FSL-biotin respectively. The result for FSL-FLRO4 was considerably higher at 130µM. However, this higher result was supported by the analysis of FSL-FLRO4 fluorescence; increasing concentration FSL-FLRO4 dispersions showed increased fluorescence until ≈100µM, above this concentration fluorescence did not change. This result suggests that above this concentration (≈100µM) all additional FSL constructs form micelles (which are quenched and hence contribute no fluorescence).

CMC can also be determined by analysis of the count rate data (measured number of micelles present in FSL dispersions of increasing concentration) obtained from DLS measurements. This method resulted in a very similar CMC result for all three constructs, with calculated values falling between 14-20µM.

However, this result for FSL-FLRO4 was significantly less than that calculated by the fluorescent spectroscopy pyrene I/III technique (130µM).

The calculated CMC of FSL-biotin (28µM by pendant drop, 14 µM by DLS) were in good agreement with Zalygin et al. [260] who reported CMC for FSL-biotin of 13µM in PBS measured by pyrene method. In contrast, Ilyushin et al. [244] reported considerably lower CMC results for FSL-biotin and FSL-FLRO4 of 5µM in aqueous solution, however the methodology and diluent details were not provided so comparison to these results is not possible.

In summary, although a wide range of results were obtained by the various methods (particularly for FSL-FLRO4) the CMC of FSL-A2 probably lies within the range 20-50µM, FSL-biotin within the range of 14-30µM, and FSL-FLRO4 in the range of 100-130µM.

However, the results also showed that micelles were detected in dispersions of all three constructs from concentrations as low as 5µM, meaning in the concentrations used in this study at least some micelles (alongside monomers) were present in the FSL dispersions.

2. Liposome synthesis and characterisation

Liposome Synthesis

The primary aim of this research was to establish methods to label liposomes with Kode constructs. Three methods for incorporating FSL constructs into liposomes were evaluated. Liposomes in this study were prepared by the thin lipid film hydration method [286], followed by extrusion to form liposomes of a uniform size and lamellarity [4, 287]. This approach was selected because it is a well-established, simple, and reproducible method which requires relatively inexpensive and simple laboratory equipment. It is one of the most widely used methods (at laboratory scale) for liposome preparation [81, 279]. It consists of three steps, thin lipid film formation, lipid film hydration and extrusion, as shown in Figure 23 Liposome preparation via thin film hydration. Liposomes were not washed after the addition of FSL constructs.

Liposomes were primarily composed of EPC. FSL constructs were added so they accounted for approximately one percent of the total lipid (in moles). EPC was selected because it has a very low T_m, meaning that the liposome membranes were in a liquid disordered state at all temperatures utilised in this study. This was considered advantageous as it allows for free movement of FSL within the liposome membrane. It was also hoped it would enable optimal insertion of FSL constructs, Eliasen et al. [174] showed that insertion of a lipid based label was increased in liposomes with more fluid membrane (i.e. composed of unsaturated lipids) compared to more densely packed membrane (composed of

saturated lipids). It was also advantageous from a technical perspective in that all procedures including extrusion could be carried out at RT without the need for heating.

The FSL constructs were incorporated into liposome by three methods, referred to as LM, H and PS. In the LM method FSL constructs were added together with other lipid constituents before formation of lipid membrane. In the H method FSL constructs were dispersed in the aqueous solution used to hydrate the dried lipid films, and finally for the PS method FSL dispersed in aqueous solution was added to preformed liposomes. LM and PS methods are commonly used methods to incorporate lipid linked molecules into liposomes [174, 195, 196, 361].

It was hypothesised that the addition FSL by the three methods could result in different FSL distributions within the liposomes. The liposomes prepared by LM method are synthesised with FSL as an integral part of the liposome membrane. Therefore, FSL constructs may be expressed on both interior and exterior of liposome and may or may not be evenly disturbed in the lipid membrane. The drying down process can lead to de-mixing resulting in uneven distribution of FSL. Liposomes prepared by H method may have FSL on both internal and external membrane, FSL is added during formation of liposome vesicles and therefore will be encapsulated within the liposome interior. Liposomes prepared by PS method can only have FSL on their exterior surface. FSL is added to fully formed liposomes in this method so can not be present in the liposome interior. The liposomes prepared in this research were used unwashed, therefore the H and PS liposome preparations could also contain free FSL remaining in the supernatant which has not incorporated with the liposomes.

It was unknown how FSL constructs would interact with liposomes, particularly when added by PS and H methods. Possibilities included that FSL constructs would not interact (no evidence was seen of this), or they could associate with liposomes by integrating into the liposome membrane or by adsorbing to the liposome surface. It was also unknown if all of the FSL would associate with liposomes or if some would remain unincorporated in the liposome dispersion. Literature shows that post insertion efficiency may less than 100% [147, 174, 196]. In addition, Eliasen et al. [174] reported considerable intra-batch heterogeneity of labelling of liposomes, including presence of approx. 10% liposomes with almost no label.

Table 25 summarises the theoretical locations of FSL after addition to liposomes by the three different protocols: lipid mix, hydration and post synthesis.

Table 25 Theoretical distribution of FSL constructs in liposomes prepared by LM, H and PS methods.

Liposome FSL label characteristic		Method of Liposome Preparation				
		Lipid Mix			Post Synthesis	Hydration
		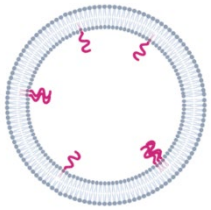	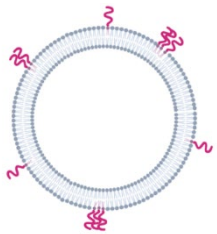	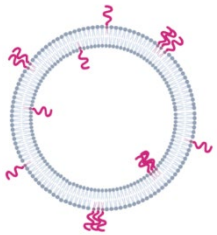	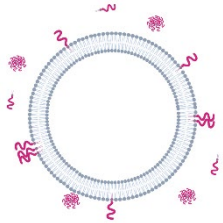	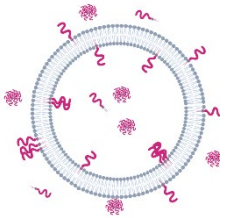
Integrated	internal leaflet	✓	-	✓	-	✓
	external leaflet	-	✓	✓	✓	✓
Adsorbed	internal leaflet	-	-	-	-	✓
	external leaflet	-	-	-	✓	✓
Free	external	-	-	-	✓	✓
	internal	-	-	-	-	✓

Characterisation of FSL modified liposomes

An additional aim of this research was to characterise FSL modified liposomes, specifically regarding liposome size, charge, and morphology.

Liposomes were synthesised with FSL added by the three methods (LM, H and PS) and their physical characteristics (size, charge and morphology) were measured. The synthesised liposomes were found to be mostly small unilamellar liposomes approximately 100nm in size. The addition of FSL was not found to cause any significant alteration to liposome size, lamellarity or stability, but did cause an increase in negative charge.

The addition of FSL constructs at concentrations less than 100µM had no effect on liposome size. Addition of greater concentrations (250µM) of FSL-A2 and FSL-biotin caused slight variation in liposome size. Notably, variations in liposome size were more pronounced when FSL was added using the post-synthesis method. However, this was not unexpected behaviour as in both the H and LM methods the sizing of the liposomes occurs after FSL has been incorporated into the liposome. Therefore, the sizing process adjusts the liposome size, including the FSL constructs, to 100nm. In contrast, when prepared by PS method FSL is added to fully synthesised liposomes after they have already been sized/extruded (to 100nm). This effect has been observed by other groups [361].

The addition of FSL-FLRO4 did not alter liposome size at all concentrations tested. FSL-FLRO4 is a smaller construct than the other two FSL constructs (≈5nm compared to ≈9nm) for FSL-A2 and FSL-biotin, see Figure 33 Schematic diagram comparing size of FSL-A2, FSL-biotin and FSL-FLRO4. [253]).

The addition of all three constructs resulted in an increased negative zeta potential of the liposomes in a concentration dependent manner. Addition of FSL by the PS method resulted in the greatest increase in zeta potential for all three constructs, possibly due to the higher surface density of FSL on the exterior of liposomes prepared by this method.

TEM analysis confirmed that the majority of liposomes were small unilamellar liposomes, with a mean size of approximately 100nm, although quite a wide variation in size was observed (12-320nm). Addition of FSL, regardless of the FSL construct or method of insertion, did not cause any detectable alteration to the morphology or membrane organisation of the liposomes.

To confirm that the functional head group of the FSL constructs remained biologically active and had not been negatively impacted as a result of incorporation into the liposome an EIA technique was used to detect FSL-A and FSL-biotin, and the fluorescence of FSL-FLRO4 was measured by spectrophotometry.

The results confirmed that the constructs remained biologically active, in addition several important observations were made.

Firstly, of particular importance, it was observed that dispersions of FSL-FLRO4 alone (micelles/monomer) exhibited significantly lower levels of fluorescence (<4%) than FSL-FLRO4 liposome dispersions (see section 2.2.7 and Figure 64 Fluorescence of FSL-FLRO4 liposomes.). This is most likely because dispersions of FSL alone (concentrations greater than 5µM) contain both FSL monomers and micelles. The FSL-FLRO4 constructs in micelle formation probably self-quench due to their close proximity to each other. It is well known that fluorophores can 'self-quench' when the fluorophore molecules are present in high concentration or in an aggregate state (i.e. micelle) due to their close proximity [332, 348]. This key observation was utilised in several later experiments to monitor the integration of FSL-FLRO4 into liposomes by measuring changes in fluorescence.

Secondly, it was observed that the fluorescence of the FSL-FLRO4 liposome dispersions was dependent on the method by which FSL had been added, i.e. LM, H or PS (see 3.1.1 FSL incorporation into liposomes FSL-FLRO4). LM liposome dispersions showed significantly greater fluorescence (5 $x10^4$ rfu) than the PS and H liposome dispersions (≈3-3.5 $x10^4$ rfu). A proposed explanation for this difference in fluorescence was that LM liposome dispersions contain no micelles. Because there are no micelles the dispersion has a higher fluorescence than H and PS liposome dispersions, which may contain some residual FSL micelles remaining in the liposome supernatant or adsorbed to the surface of liposomes. The FSL micelles are quenched, and hence the H/PS dispersions show slightly less fluorescence.

The increase in fluorescence of H and PS FSL-FLRO4 liposome dispersions was observed to be concentration dependent until approximately 100µM. Above this concentration fluorescence plateaued and no longer increased. Interestingly, this corresponds with the calculated CMC of FSL-FLRO4 (2.1.3 Critical micelle concentration). It is possible that above this concentration all additional FSL constructs adopt a micelle conformation. Possible explanations include that FSL transfer to the liposomes is reduced from micelles compared to monomer in solution, or alternatively some of the micelles themselves may be adsorbing to liposome. This phenomenon has been reported in literature, where post synthesis labelling of liposomes is influenced by the CMC of the labelling molecules, transfer is reduced above CMC of the labelling molecule [195].

3. Dynamics of liposome modification

The next aim of this project was to measure the dynamics of FSL liposome modification. This included measuring the incorporation of FSL constructs into liposomes (primarily when added by H and PS methods) and also the retention of FSL constructs in liposome membrane after incorporation.

All three methods were shown to successfully label liposomes with FSL constructs. Maximum insertion of FSL constructs (into H/PS liposomes) occurred within 2 hours incubation at 37°C, 24 hours at RT and up to 3 days at 4°C. Experiments indicate that majority of FSL is incorporated into the liposome.

Incorporation of FSL

FSL added by LM method results in 100% incorporation (due to method of synthesis, all FSL is integrated into liposome during formation of membrane). While incorporation of FSL into liposomes (after addition by PS and H methods) was found to be temperature and time dependent. Results indicate that the majority of FSL becomes associated/incorporated into the liposomes.

Incorporation of FSL-A2 was measured using an EIA technique, which detected free FSL in the liposome dispersion. Free FSL-A2 was shown to bind to the surface to microplate surface while FSL-A2 liposomes did not. The presence of FSL-A2 was then detected using anti-A followed by a secondary anti-antibody enzyme conjugate. A similar EIA technique (utilising streptavidin-alkaline phosphatase) was attempted for FSL-biotin but was unsuccessful. Free FSL-A2 decreased rapidly in both the PS and H liposome dispersions during the first 24 hours and maximum insertion was reached within 2 hours at 37°C, and between day 1-3 when stored at RT and 4°C. Free FSL levels declined to almost nothing, which indicates that almost all of the FSL incorporates into the liposomes. No free FSL-A2 was detected in LM liposome dispersions.

Incorporation of FSL-FLRO4 was measured by observing the change in fluorescence of the liposome dispersion after the addition of FSL-FLRO4. As FSL-FLRO4 moved from (quenched) micelle conformation in supernatant into the liposome membrane, where it could move further apart and become unquenched, the fluorescence of dispersion increased. Similar results to FSL-A2 were observed, maximum insertion occurred within 2 hours at 37°C, 4 hours at RT and 24-48 hours at 4°C. LM liposomes showed no change in fluorescence and a much higher fluorescence (≈50,000 rfu) than maximum fluorescence of PS/H liposomes (≈30,000 rfu). A possible explanation for this difference in fluorescence is that a small amount of FSL remains as micelles in PS/H liposome dispersions. Because micelles are quenched the total fluorescence of the dispersion is less than LM liposome dispersions where all FSL is integrated into the liposome membrane. The micelles may remain in the supernatant of liposome dispersion and/or they

could adsorb to the external surface of the liposomes (without integrating into the membrane, and hence remain quenched).

Similar insertion dynamics were observed for both FSL-A2 and FSL-FLRO4 constructs, suggesting that spacer and head group did not significantly affect FSL insertion into liposomes. Maximum FSL insertion occurred within 2 hours at 37°C, 24 hours at RT and took up to three days at 4°C. These results were in good agreement with literature where similar incorporation rates are reported for other types of phospholipid anchored labels added to liposomes by similar post synthesis methodology [174, 361, 362].

These results are similar to those previously observed for FSL insertion into cells [230, 240, 253]. Rapoport et al. [230] observed slightly slower incorporation of FSL-A2 into cells compared with FSL-FLRO4. This was not observed in this study; however, this may be due to differences in sensitivity of the EIA technique used in this study compared with flow cytometry method used by Rapoport. It could also reflect differences in insertion kinetics between natural cell membranes and artificial liposome membranes. Phospholipid transfer between liposomes has been shown to occur much faster than exchange rate with cell membranes [197].

Retention of FSL labelling

Phospholipids have been shown to spontaneously elute from liposome membranes and transfer to other liposomes [120-122]. The rate of transfer is dependent on a number of factors including temperature, phospholipid structure (fatty acid chain length and unsaturation), phase of liposome membrane and vesicle concentration [121, 123]. To investigate the retention of FSL constructs their transfer between liposomes and from liposome to cell membranes was investigated.

Lipid such as phospholipids and cholesterol (and likely FSL constructs) can transfer between membranes by several mechanisms; membrane fusion, lipid exchange during collision, lipid exchange by diffusion – lipid dissociates from donor membrane and diffuses through aqueous supernatant to new membrane. In addition, it is important to note than in this research because unwashed liposomes were used any FSL which remained in liposome supernatant (unincorporated with the liposomes) could also 'transfer' to new liposome/cell membrane.

Transfer between liposomes

An EIA method was used to detect transfer of FSL between liposomes. FSL-A liposomes and FSL-biotin liposomes were incubated together and then an EIA technique used then used to detect liposomes that expressed both FSL-A2 and FSL-biotin on their surface. Liposomes containing FSL-biotin were then captured by binding to streptavidin coated microplate (via FSL-biotin), then the presence of FSL-A2 was

detected using anti-A. Only the presence of liposomes with both constructs on their surface would cause a positive EIA reaction.

Transfer between liposomes was observed and was found to be temperature and time dependent [120]. Transfer was observed after 4 hours incubation at 37°C and 24 hours at RT. Significant transfer was not observed at 4°C in the time frame tested (24 hours). Contrary to expectation, transfer of FSL between liposomes did not appear to be influenced by the method (LM, H, PS) in which FSL was originally incorporated into the liposomes.

Transfer between liposomes and RBC

FSL transfer from liposomes to RBC was found to be dependent on method of liposome preparation. Negligible transfer (<1%) was observed from LM liposomes to RBC, while up to 10% transfer was observed from H and PS liposomes.

RBC were used as a model cell membrane for these experiments. RBC were selected because they are easy to work with, they do not require maintenance, and simple techniques can be used to detect the presence of FSL on their surface. The presence of FSL-biotin and FSL-FLRO4 on RBC was measured by flow cytometry, while FSL-A2 was detected by reaction with standard blood grouping reagents, (monoclonal anti-A) which results in agglutination.

Differences in amount of transfer was observed between FSL constructs. It was observed that approximately 5-10% of FSL-A2 and FSL-biotin transferred from PS/H liposomes to RBC, while just 2% of FSL-FLRO4 transferred. Transfer was temperature dependent, occurring much faster at 37°C than 4°C. Transfer of FSL-FLRO4 and FSL-biotin reached a maximum after 4 hours at 37°C, while FSL-A2 reached maximum transfer within 2 hours. Holovati et al. [224] reported a 12% greater uptake by RBC of liposomes after 2 hours at 37°C than RT, and no uptake in same time period at 4°C. Increased temperature likely increases the increase collision rate between RBC and liposomes and would also increase the fluidity of cell/liposome membranes which may create more favourable conditions for lipid transfer and/or membrane fusion to take place.

Increased contact time between liposomes and RBC did not result in significant increases to this transfer, once maximum was reached this remained unchanged even after extended storage up to 12 weeks at 4°C and 6 hours at 37°C. An important note here is that the PS and H liposome dispersions were used unwashed, and therefore any FSL remaining in supernatant could account for the apparent transfer of FSL to the RBC.

Because FSL transfer did not occur from LM liposomes, even after extended incubation times, this shows that FSL transfer to RBC is not caused by liposome/RBC fusion, or transfer of FSL which is integrated into the liposome membrane. This observation is supported by literature, studies show liposomes composed of EPC alone do not readily induce cell/liposome fusion [51, 221, 363].

Therefore, it was hypothesised that the observed transfer of FSL from H/PS liposomes was most likely due to either

- free unincorporated FSL that has remained within the liposome dispersion. This was in agreement with literature where Mare et al. [196], Eliason et al. [174] and Nag et al. [147] observed approximately 80% efficiency of post insertion.

  Monomers, micelles, small and/or large aggregates are known to coexist in thermodynamic equilibrium with each other [84, 85]. It is possible that FSL monomers, micelles and FSL labelled liposomes form a dynamic equilibrium and once this equilibrium has been reached the distribution of FSL remains unchanged (unless additional factors added to the system such as new membrane).
- Alternatively, FSL added by PS/H methods may adsorb to the surface of the liposomes but does not become fully integrated. It is this adsorbed FSL on the external surface of the liposome which is able to transfer to RBC.

It is also possible that a combination of these mechanisms is occurring. Without access to an ultra-high centrifuge the experimental results were unable to determine which of these two mechanisms were occurring. Further research to establish the exact mechanism is required.

FSL transfer was not altered by the presence of cholesterol in the liposomes but was affected by varying liposome charge. The use of charged lipids can increase electrostatic attraction between oppositely charged membranes/vesicles which can help to increase lipid transfer [71, 72]. However, it was found that the addition of positively charged FSL into liposome reduced FSL-FLRO4 transfer to RBC. It is possible that the positive charge helped to increase incorporation/adsorption of the (negatively charged) FSL construct with the liposome, which resulted in reduced transfer to RBC.

4. Stability

The final aim of this research was to determine the stability of FSL modified liposomes. The effect of FSL constructs on stability was assessed by preparing FSL labelled liposomes and storing them at 4°C for 12 weeks. Aliquots were removed at various intervals and the size and zeta potential of the liposomes was

measured. This showed that the FSL modified liposomes were very stable, their size and charge did not significantly change during the first 8 weeks of storage. At the 12 week time point some small variations in liposome size were observed, however this also occurred in the blank liposomes (containing no FSL) so was not a result of FSL modification.

Transfer of FSL from liposome to RBC was also measured over the 12 weeks. Earlier experiments established that FSL which is integrated into membrane (i.e. LM liposomes) does not readily transfer to RBC. FSL transfer to RBC therefore provided an indirect method to measure the dissociation of FSL from liposome. If FSL was retained by the liposome over time the transfer of FSL to RBC would remain constant. Any increase in transfer would indicate dissociation of FSL from liposome membrane. This was not observed, after an initial decline during first 3 days, the transfer to FSL remained constant for the 12 weeks tested. This indicates that the FSL was retained by liposome throughout the 12 week incubation.

A caveat of these results is that in this research the liposomes were stored in PBS. Therefore, these results may not reflect retention characteristics in the presence of serum lipids and proteins. Münter et al. [121] show that dissociation of a range of fluorescent lipid labels was significantly increased in the presence of plasma (up to 75% increase in dissociation from liposome) compared to PBS.

During this study several groups published studies using a variety of FSL constructs to label liposomes. In all cases, the FSL was added to liposomes by LM methodology [39, 354-360]. FSL constructs were used to study lectin binding or to tether liposomes to streptavidin surfaces to enable further studies. Interestingly, FSL constructs were demonstrated to facilitate liposome fusion (with liposomes and cells) and uptake (into H1299 cells) via lectin mediated binding [354].

5. Limitations of Kode constructs and future research

FSL constructs were successfully used to modify the surface of liposomes in this study. It was found that they are well suited to this purpose (under the condition used in this study) and no significant detrimental effects were identified. Several limitations of this research have been identified and are discussed below. Further work is required to fully characterise the behaviour of FSL constructs within the liposome membrane and particularly their behaviour in systems containing plasma. This will help to further determine the suitability of Kode technology for use labelling liposomes intended for use as a therapeutic product.

The primary limitation of using Kode constructs to modify the surface of liposomes is that the conjugation is a non-covalent method, therefore under certain circumstances, e.g. temperature, presence of serum

lipids/proteins, FSL constructs may dissociate from the liposome surface. This is of particular concern for *in vivo* applications where presence of serum lipids/proteins could impact retention of FSL constructs in liposome membrane. All investigations in this project were performed in PBS and therefore more investigation is required to determine how the presence of serum (lipids and proteins) affects the behaviour and characteristics of FSL modified liposomes, with particular regard to retention.

Despite this potential limitation, Kode labelling showed good modification characteristics in this research. Kode modification of liposomes appeared to be very stable, remaining unchanged for up to 12 weeks storage at 4°C. Transfer of the FSL constructs from liposomes to RBC was low, only approximately 2-5% transfer to cells after two hours incubation was observed. This is similar to the previously observed *in vivo* elution of Kode constructs from Kode red blood cells, Oliver et al observed *in vivo* elution rates of 1% per hour [364] or 20% loss per day [266]. It should be noted that liposome survival *in vivo* is usually limited to just minutes or hours (depending on their composition) rather than days [48, 365]. Therefore, these observed elution rates, are unlikely to present a significant problem in the short time frame of liposome survival *in vivo*.

A further potential limitation is the effect of FSL constructs on membrane stability and importantly retention of encapsulated materials within the liposome. For FSL constructs to be an effective tool for labelling liposomes it is necessary that retention is not significantly reduced. These factors were not investigated in this project. Further work to determine if the addition of FSL to liposomes alters retention characteristics is needed.

The effect of using different liposome lipid compositions should also be studied. In this study egg phosphatidylcholine was the primary phospholipid used to form liposomes. Preparing liposomes using other phosphatidylcholine phospholipids should be investigated, particularly the use of phospholipids which have a phase transition temperature above 37°C, such as DPPC or DSPC. This is of interest as the resultant liposome membrane would be in a solid ordered state at 37°C (as opposed to fluid disordered state) which could significantly alter FSL retention and transfer properties.

In this study retention of FSL was investigated by observing transfer of FSL from liposome to RBC and between liposomes. Future research should extend these experiments to include additional types of cells, this would include evaluation of their interaction with such cells and would also be impacted by liposome stability in presence of other lipids and proteins (present in cell culture medium).

The exact binding mechanisms and distribution of FSL constructs within the liposomes are unknown. Possibilities include incorporation of lipid tail into membrane or adsorption to the RBC without integration. Further studies are required to resolve this question. This could be achieved by washing FSL modified liposomes to determine if this alters FSL transfer to RBC. Further electron microscopy studies and confocal microscopy could also be employed to help determine the distribution of FSL in liposomes.

The results of this initial proof of concept study are promising. Kode technology is a rapid and simple method that has shown good labelling characteristics of liposomes *in vitro*. Further research is necessary to determine the properties and characteristics of Kode modified liposomes *in vivo*. Several limitations discussed above also require further investigation. However, the current results and knowledge support the potential suitability of Kode technology to be used to develop therapeutic liposomes.

6. Conclusions

This research clearly demonstrated the ability of Kode constructs to modify the surface of liposomes without significantly altering their size, morphology or stability.

FSL constructs were added to liposomes by three methods; lipid mix (added along with together with the other lipid components before formation of thin lipid film), hydration (added with aqueous solution used to hydrate thin lipid films), and post synthesis (added to fully formed liposomes, after extrusion). The method of addition was not observed to have any effect on liposome size and morphology. However, likely resulted in differences to FSL distribution within the liposome.

LM and PS methods are recommended as most suitable. LM has advantage that all FSL is integrated into the liposome membrane (so no washing is needed to remove unincorporated FSL). However, FSL is distributed on both the interior and exterior of liposome membrane leading to reduced density on the exterior surface of liposome and can reduce encapsulation capacity. This method also exposes functional head group to solvent during synthesis which may not be suitable for all molecules.

PS method has advantage that only the liposome exterior is labelled so can result in highest density of labelling, in addition this method does not expose the functional head group to solvent. When added by this method a small amount of FSL either remains as free FSL in liposome supernatant or adsorbed to liposome surface. This unincorporated FSL can transfer to other cell membranes. The amount varied depending on FSL construct (1% for FSL-FLRO4, ≈10% FSL-biotin and FSL-A2). Insertion of FSL into liposomes was time and temperature dependent, maximum insertion of FSL constructs occurred within 2 hours incubation at 37°C, 24 hours at RT and up to 3 days at 4°C.

This research demonstrated successful proof of concept that FSL constructs can be used to label liposomes. This research could be extended to synthesise new FSL constructs with functional head groups selected to enable binding to specific receptors to facilitate binding of liposomes to target cells/tissues (active targeting).

References

1. Kim BY, Rutka JT, Chan WC. Nanomedicine. New England Journal of Medicine. 2010;363(25):2434-43.
2. Leung AWY, Amador C, Wang LC, Mody UV, Bally MB. What Drives Innovation: The Canadian Touch on Liposomal Therapeutics. Pharmaceutics. 2019;11(3):124.
3. Anselmo AC, Mitragotri S. Nanoparticles in the clinic: An update post COVID-19 vaccines. Bioengineering & translational medicine. 2021:e10246.
4. Bangham AD, Horne RW. Negative staining of phospholipids and their structural modification by surface-active agents as observed in the electron microscope. Journal of Molecular Biology. 1964;8(5):660-IN10.
5. Sessa G, Weissmann G. Phospholipid spherules (liposomes) as a model for biological membranes. J Lipid Res. 1968;9(3):310-8.
6. Weissig V. Liposomes Came First: The Early History of Liposomology. Methods in molecular biology (Clifton, NJ). 2017;1522:1-15.
7. Bangham AD, Hill MW, Miller N. Preparation and use of liposomes as models of biological membranes. Methods in membrane biology: Springer; 1974. p. 1-68.
8. Sessa G, Weissmann G. Incorporation of lysozyme into liposomes: a model for structure-linked latency. Journal of Biological Chemistry. 1970;245(13):3295-301.
9. Gregoriadis G, Ryman BE. Lysosomal localization of -fructofuranosidase-containing liposomes injected into rats. Biochem J. 1972;129(1):123-33.
10. Trosper T, Raveed D, Ke B. Chlorophyll a-containing liposomes. Biochimica et Biophysica Acta (BBA)-Bioenergetics. 1970;223(2):463-5.
11. Gregoriadis G, Ryman B. Liposomes as carriers of enzymes or drugs: a new approach to the treatment of storage diseases. Biochemical Journal. 1971;124(5):58P-P.
12. Gregoriadis G, Buckland RA. Enzyme-containing liposomes alleviate a model for storage disease. Nature. 1973;244(5412):170-2.
13. Allison A, Gregoriadis G. Liposomes as immunological adjuvants. Nature. 1974;252(5480):252-.
14. Papahadjopoulos D. Fate of liposomes in vivo: a brief introductory review. Journal of liposome research. 1996;6(1):3-17.
15. Klibanov AL, Maruyama K, Torchilin VP, Huang L. Amphipathic polyethyleneglycols effectively prolong the circulation time of liposomes. FEBS letters. 1990;268(1):235-7.
16. Thi TTH, Suys EJ, Lee JS, Nguyen DH, Park KD, Truong NP. Lipid-Based Nanoparticles in the Clinic and Clinical Trials: From Cancer Nanomedicine to COVID-19 Vaccines. Vaccines. 2021;9(4):359.
17. Gregoriadis G. Targeting of drugs. Nature. 1977;265(5593):407-11.
18. Heath TD, Fraley RT, Papahdjopoulos D. Antibody targeting of liposomes: cell specificity obtained by conjugation of F (ab') 2 to vesicle surface. Science. 1980;210(4469):539-41.

19. Leserman LD, Barbet J, Kourilsky F, Weinstein JN. Targeting to cells of fluorescent liposomes covalently coupled with monoclonal antibody or protein A. Nature. 1980;288(5791):602-4.

20. Torchilin V, Goldmacher V, Smirnov V. Comparative studies on covalent and noncovalent immobilization of protein molecules on the surface of liposomes. Biochemical and biophysical research communications. 1978;85(3):983-90.

21. Belfiore L, Saunders DN, Ranson M, Thurecht KJ, Storm G, Vine KL. Towards clinical translation of ligand-functionalized liposomes in targeted cancer therapy: Challenges and opportunities. Journal of controlled release. 2018;277:1-13.

22. Xu Y, Fourniols T, Labrak Y, Préat V, Beloqui A, des Rieux A. Surface modification of lipid-based nanoparticles. ACS nano. 2022;16(5):7168-96.

23. Yan W, Leung SS, To KK. Updates on the use of liposomes for active tumor targeting in cancer therapy. Nanomedicine. 2020;15(3):303-18.

24. Mohamed NA, Marei I, Crovella S, Abou-Saleh H. Recent developments in nanomaterials-based drug delivery and upgrading treatment of cardiovascular diseases. International Journal of Molecular Sciences. 2022;23(3):1404.

25. Xia Y, Xu C, Zhang X, Ning P, Wang Z, Tian J, et al. Liposome-based probes for molecular imaging: from basic research to the bedside. Nanoscale. 2019;11(13):5822-38.

26. Luiz MT, Dutra JAP, Tofani LB, de Araújo JTC, Di Filippo LD, Marchetti JM, et al. Targeted liposomes: a nonviral gene delivery system for cancer therapy. Pharmaceutics. 2022;14(4):821.

27. Laouini A, Jaafar-Maalej C, Limayem-Blouza I, Sfar S, Charcosset C, Fessi H. Preparation, Characterization and Applications of Liposomes: State of the Art. Journal of Colloid Science and Biotechnology. 2012;1(2):147-68.

28. Bulbake U, Doppalapudi S, Kommineni N, Khan W. Liposomal formulations in clinical use: an updated review. Pharmaceutics. 2017;9(2):12.

29. Ahmadi Ashtiani HR, Bishe P, Lashgari N, Nilforoushzadeh MA, Zare S. Liposomes in Cosmetics. J Skin Stem Cell. 2016;3(3):e65815.

30. Kheadr EE, Vuillemard JC, El Deeb SA. Accelerated Cheddar cheese ripening with encapsulated proteinases. International journal of food science & technology. 2000;35(5):483-95.

31. Huang L, Teng W, Cao J, Wang J. Liposomes as delivery system for applications in meat products. Foods. 2022;11(19):3017.

32. Karny A, Zinger A, Kajal A, Shainsky-Roitman J, Schroeder A. Therapeutic nanoparticles penetrate leaves and deliver nutrients to agricultural crops. Scientific Reports. 2018;8(1):7589.

33. Mallick S, Choi JS. Liposomes: versatile and biocompatible nanovesicles for efficient biomolecules delivery. Journal of nanoscience and nanotechnology. 2014;14(1):755-65.

34. Alfayez M, Kantarjian H, Kadia T, Ravandi-Kashani F, Daver N. CPX-351 (vyxeos) in AML. Leukemia & lymphoma. 2020;61(2):288-97.

35. Cipolla D, Wu H, Gonda I, Chan H-K. Aerosol performance and stability of liposomes containing ciprofloxacin nanocrystals. Journal of aerosol medicine and pulmonary drug delivery. 2015;28(6):411-22.

36. Salehi B, Mishra AP, Nigam M, Kobarfard F, Javed Z, Rajabi S, et al. Multivesicular liposome (Depofoam) in human diseases. Iranian Journal of Pharmaceutical Research: IJPR. 2020;19(2):9.

37. Chen J, Ma Y, Tao Y, Zhao X, Xiong Y, Chen Z, et al. Formulation and evaluation of a topical liposomal gel containing a combination of zedoary turmeric oil and tretinoin for psoriasis activity. Journal of liposome research. 2021;31(2):130-44.

38. Wang Y, Grainger DW. Lyophilized liposome-based parenteral drug development: Reviewing complex product design strategies and current regulatory environments. Advanced drug delivery reviews. 2019;151:56-71.

39. Tretiakova D, Vodovozova E. Liposomes as adjuvants and vaccine delivery systems. Biochemistry (Moscow), Supplement Series A: Membrane and Cell Biology. 2022;16(1):1-20.

40. Ramos GS, Vallejos VM, Borges GS, Almeida RM, Alves IM, Aguiar MM, et al. Formulation of amphotericin B in PEGylated liposomes for improved treatment of cutaneous leishmaniasis by parenteral and oral routes. Pharmaceutics. 2022;14(5):989.

41. López-Cano JJ, González-Cela-Casamayor MA, Andrés-Guerrero V, Herrero-Vanrell R, Molina-Martínez IT. Liposomes as vehicles for topical ophthalmic drug delivery and ocular surface protection. Expert opinion on drug delivery. 2021;18(7):819-47.

42. Souto EB, Macedo AS, Dias-Ferreira J, Cano A, Zielińska A, Matos CM. Elastic and ultradeformable liposomes for transdermal delivery of active pharmaceutical ingredients (APIs). International Journal of Molecular Sciences. 2021;22(18):9743.

43. Wang A, Yang T, Fan W, Yang Y, Zhu Q, Guo S, et al. Protein corona liposomes achieve efficient oral insulin delivery by overcoming mucus and epithelial barriers. Advanced healthcare materials. 2019;8(12):1801123.

44. He H, Lu Y, Qi J, Zhu Q, Chen Z, Wu W. Adapting liposomes for oral drug delivery. Acta pharmaceutica sinica B. 2019;9(1):36-48.

45. Khan O, Chaudary N. The use of amikacin liposome inhalation suspension (Arikayce) in the treatment of refractory nontuberculous mycobacterial lung disease in adults. Drug design, development and therapy. 2020:2287-94.

46. Rudokas M, Najlah M, Alhnan MA, Elhissi A. Liposome delivery systems for inhalation: a critical review highlighting formulation issues and anticancer applications. Medical principles and practice. 2016;25(Suppl. 2):60-72.

47. Khan A, Allemailem K, Almatroodi S, Almatroudi A, Rahmani A. Recent strategies towards the surface modification of liposomes: an innovative approach for different clinical applications. 3 Biotech. 2020;10.

48. Woodle MC. Controlling liposome blood clearance by surface-grafted polymers. Advanced drug delivery reviews. 1998;32(1-2):139-52.

49. Immordino ML, Dosio F, Cattel L. Stealth liposomes: review of the basic science, rationale, and clinical applications, existing and potential. International journal of nanomedicine. 2006;1(3):297.

50. Anarjan FS. Active targeting drug delivery nanocarriers: Ligands. Nano-Structures & Nano-Objects. 2019;19:100370.

51. Imam ZI, Kenyon LE, Ashby G, Nagib F, Mendicino M, Zhao C, et al. Phase-separated liposomes enhance the efficiency of macromolecular delivery to the cellular cytoplasm. Cellular and molecular bioengineering. 2017;10:387-403.

52. Antoniou AI, Giofrè S, Seneci P, Passarella D, Pellegrino S. Stimulus-responsive liposomes for biomedical applications. Drug discovery today. 2021;26(8):1794-824.

53. Vieira DB, Gamarra LF. Getting into the brain: liposome-based strategies for effective drug delivery across the blood–brain barrier. International journal of nanomedicine. 2016;11:5381.

54. Scherphof G, Roerdink F, Waite M, Parks J. Disintegration of phosphatidylcholine liposomes in plasma as a result of interaction with high-density lipoproteins. Biochimica et biophysica acta. 1978;542(2):296-307.

55. Tomnikova A, Orgonikova A, Krizek T. Liposomes: preparation and characterization with a special focus on the application of capillary electrophoresis. Monatshefte für Chemie-Chemical Monthly. 2022;153(9):687-95.

56. Blake DA, Bovin NV, Bess D, Henry SM. FSL constructs: a simple method for modifying cell/virion surfaces with a range of biological markers without affecting their viability. Journal of visualized experiments: JoVE. 2011(54).

57. Williams E, Barr K, Korchagina E, Tuzikov A, Henry S, Bovin N. Ultra-fast glyco-coating of non-biological surfaces. International journal of molecular sciences. 2016;17(1):118.

58. Created with BioRender.com.

59. Vakili-Ghartavol R, Rezayat SM, Faridi-Majidi R, Sadri K, Jaafari MR. Optimization of docetaxel loading conditions in liposomes: proposing potential products for metastatic breast carcinoma chemotherapy. Scientific reports. 2020;10(1):5569.

60. Xu Q, Tanaka Y, Czernuszka JT. Encapsulation and release of a hydrophobic drug from hydroxyapatite coated liposomes. Biomaterials. 2007;28(16):2687-94.

61. van Swaay D, deMello A. Microfluidic methods for forming liposomes. Lab on a Chip. 2013;13(5):752-67.

62. Aguiar J, Carpena P, Molina-Bolıvar J, Ruiz CC. On the determination of the critical micelle concentration by the pyrene 1: 3 ratio method. Journal of Colloid and Interface Science. 2003;258(1):116-22.

63. Tenchov R, Bird R, Curtze AE, Zhou Q. Lipid Nanoparticles—From Liposomes to mRNA Vaccine Delivery, a Landscape of Research Diversity and Advancement. ACS nano. 2021.

64. Joseph M, Trinh HM, Mitra AK. Peptide and protein-based therapeutic agents. Emerging nanotechnologies for diagnostics, drug delivery and medical devices: Elsevier; 2017. p. 145-67.

65. Guimarães D, Cavaco-Paulo A, Nogueira E. Design of liposomes as drug delivery system for therapeutic applications. International journal of pharmaceutics. 2021;601:120571.

66. Hianik T. Structure and physical properties of biomembranes and model membranes. Acta Physica Slovaca. 2006;56(6):687-805.

67. Avanti Polar Lipids. Egg PC [Available from: https://avantilipids.com/product/840051.

68. Eroğlu İ, İbrahim M. Liposome–ligand conjugates: a review on the current state of art. Journal of drug targeting. 2020;28(3):225-44.

69. Liu C, Zhang L, Zhu W, Guo R, Sun H, Chen X, et al. Barriers and strategies of cationic liposomes for cancer gene therapy. Molecular Therapy-Methods & Clinical Development. 2020;18:751-64.

70. Large DE, Abdelmessih RG, Fink EA, Auguste DT. Liposome composition in drug delivery design, synthesis, characterization, and clinical application. Advanced Drug Delivery Reviews. 2021;176:113851.

71. Marchi-Artzner V, Jullien L, Belloni L, Raison D, Lacombe L, Lehn J-M. Interaction, lipid exchange, and effect of vesicle size in systems of oppositely charged vesicles. The Journal of Physical Chemistry. 1996;100(32):13844-56.

72. Zhu T, Jiang Z, Ma Y. Lipid exchange between membranes: Effects of membrane surface charge, composition, and curvature. Colloids and Surfaces B: Biointerfaces. 2012;97:155-61.

73. Allen TM, Cullis PR. Liposomal drug delivery systems: from concept to clinical applications. Advanced drug delivery reviews. 2013;65(1):36-48.

74. Zhi D, Zhang S, Wang B, Zhao Y, Yang B, Yu S. Transfection efficiency of cationic lipids with different hydrophobic domains in gene delivery. Bioconjugate chemistry. 2010;21(4):563-77.

75. Kajiwara E, Kawano K, Hattori Y, Fukushima M, Hayashi K, Maitani Y. Long-circulating liposome-encapsulated ganciclovir enhances the efficacy of HSV-TK suicide gene therapy. Journal of controlled release. 2007;120(1-2):104-10.

76. Senior J, Gregoriadis G. Is half-life of circulating liposomes determined by changes in their permeability? FEBS letters. 1982;145(1):109-14.

77. Anderson M, Omri A. The effect of different lipid components on the in vitro stability and release kinetics of liposome formulations. Drug delivery. 2004;11(1):33-9.

78. Juszkiewicz K, Sikorski AF, Czogalla A. Building blocks to design liposomal delivery systems. International Journal of Molecular Sciences. 2020;21(24):9559.

79. Farhood H, Serbina N, Huang L. The role of dioleoyl phosphatidylethanolamine in cationic liposome mediated gene transfer. Biochimica et Biophysica Acta (BBA)-Biomembranes. 1995;1235(2):289-95.

80. Briuglia M-L, Rotella C, McFarlane A, Lamprou DA. Influence of cholesterol on liposome stability and on in vitro drug release. Drug delivery and translational research. 2015;5:231-42.

81. Lombardo D, Kiselev MA. Methods of Liposomes Preparation: Formation and Control Factors of Versatile Nanocarriers for Biomedical and Nanomedicine Application. Pharmaceutics. 2022;14(3):543.

82. Eloy JO, de Souza MC, Petrilli R, Barcellos JPA, Lee RJ, Marchetti JM. Liposomes as carriers of hydrophilic small molecule drugs: strategies to enhance encapsulation and delivery. Colloids and surfaces B: Biointerfaces. 2014;123:345-63.

83. Avanti Polar Lipids. Cholesterol [9/5/2023]. Available from: https://avantilipids.com/product-category/natural-lipids/cholesterol.

84. Lombardo D, Kiselev M, magazù S, Calandra P. Amphiphiles Self-Assembly: Basic Concepts and Future Perspectives of Supramolecular Approaches. Advances in Condensed Matter Physics. 2015;2015:1-22.

85. Israelachvili JN. Intermolecular and Surface Forces : Revised Third Edition. San Diego, UNITED STATES: Elsevier Science & Technology; 2011.

86. Koynova R, Tenchov B. Phase transitions and phase behavior of lipids. Encyclopedia of Biophysics. 2013:1841-54.

87. Israelachvili J, Marčelja S, Horn RG. Physical principles of membrane organization. Quarterly reviews of biophysics. 1980;13(2):121-200.

88. Khandelia H, Vattulainen I. Lipid Organization, Aggregation, and Self-assembly. In: Roberts GCK, editor. Encyclopedia of Biophysics. Berlin, Heidelberg: Springer Berlin Heidelberg; 2013. p. 1273-80.

89. Balazs DA, Godbey W. Liposomes for use in gene delivery. Journal of drug delivery. 2011;2011:326497.

90. Bailey AL, Cullis PR. Liposome fusion. Current topics in membranes, Volume 44: Elsevier; 1997. p. 359-73.

91. Cullis PR, Hope MJ, Tilcock CP. Lipid polymorphism and the roles of lipids in membranes. Chemistry and physics of lipids. 1986;40(2-4):127-44.

92. Koltover I, Salditt T, Rädler JO, Safinya CR. An inverted hexagonal phase of cationic liposome-DNA complexes related to DNA release and delivery. Science. 1998;281(5373):78-81.

93. Mouritsen OG. Life-as a matter of fat: Springer; 2005.

94. London E. Membrane Structure–Function Insights from Asymmetric Lipid Vesicles. Accounts of chemical research. 2019;52(8):2382-91.

95. Mozafari MR, Thompson AK, Reed CJ, Rostron C. Nanoliposomes. From fundamentals to recent developments. Victoria, Canada: Trafford Publishing; 2005. 237 p.

96. Eeman M, Deleu M. From biological membranes to biomimetic model membranes. Biotechnologie, Agronomie, Société et Environnement. 2010;14.

97. Charrois GJ, Allen TM. Drug release rate influences the pharmacokinetics, biodistribution, therapeutic activity, and toxicity of pegylated liposomal doxorubicin formulations in murine breast cancer. Biochimica et Biophysica Acta (BBA)-Biomembranes. 2004;1663(1-2):167-77.

98. Liu Y, Bravo KMC, Liu J. Targeted liposomal drug delivery: a nanoscience and biophysical perspective. Nanoscale Horizons. 2021;6(2):78-94.

99. Wu L, Ding H, Qu X, Shi X, Yang J, Huang M, et al. Fluidic multivalent membrane nanointerface enables synergetic enrichment of circulating tumor cells with high efficiency and viability. Journal of the American Chemical Society. 2020;142(10):4800-6.

100. Takechi-Haraya Y, Goda Y, Sakai-Kato K. Control of liposomal penetration into three-dimensional multicellular tumor spheroids by modulating liposomal membrane rigidity. Molecular pharmaceutics. 2017;14(6):2158-65.

101. Abumanhal-Masarweh H, da Silva D, Poley M, Zinger A, Goldman E, Krinsky N, et al. Tailoring the lipid composition of nanoparticles modulates their cellular uptake and affects the viability of triple negative breast cancer cells. Journal of controlled release. 2019;307:331-41.

102. Amarandi R-M, Ibanescu A, Carasevici E, Marin L, Dragoi B. Liposomal-Based Formulations: A Path from Basic Research to Temozolomide Delivery Inside Glioblastoma Tissue. Pharmaceutics. 2022;14(2):308.

103. Li J, Wang X, Zhang T, Wang C, Huang Z, Luo X, et al. A review on phospholipids and their main applications in drug delivery systems. Asian journal of pharmaceutical sciences. 2015;10(2):81-98.

104. Heberle FA, Feigenson GW. Phase separation in lipid membranes. Cold Spring Harbor perspectives in biology. 2011;3(4):a004630.

105. Simons K, Ikonen E. Functional rafts in cell membranes. nature. 1997;387(6633):569-72.

106. Vu TQ, Sant'Anna LE, Kamat NP. Tuning Targeted Liposome Avidity to Cells via Lipid Phase Separation. Biomacromolecules. 2023.

107. Larsen J, Hatzakis NS, Stamou D. Observation of inhomogeneity in the lipid composition of individual nanoscale liposomes. Journal of the American Chemical Society. 2011;133(28):10685-7.

108. Schram V, Lin H-N, Thompson TE. Topology of gel-phase domains and lipid mixing properties in phase-separated two-component phosphatidylcholine bilayers. Biophysical journal. 1996;71(4):1811-22.

109. Baumgart T, Hammond AT, Sengupta P, Hess ST, Holowka DA, Baird BA, et al. Large-scale fluid/fluid phase separation of proteins and lipids in giant plasma membrane vesicles. Proceedings of the National Academy of Sciences. 2007;104(9):3165-70.

110. Kaiser H-J, Lingwood D, Levental I, Sampaio JL, Kalvodova L, Rajendran L, et al. Order of lipid phases in model and plasma membranes. Proceedings of the National Academy of Sciences. 2009;106(39):16645-50.

111. Escribá PV. Membrane-lipid therapy: a new approach in molecular medicine. Trends in molecular medicine. 2006;12(1):34-43.

112. Lasic DD. Novel applications of liposomes. Trends in biotechnology. 1998;16(7):307-21.

113. Makhani EY, Zhang A, Haun JB. Quantifying and controlling bond multivalency for advanced nanoparticle targeting to cells. Nano Convergence. 2021;8(1):38.

114. Alkilany AM, Zhu L, Weller H, Mews A, Parak WJ, Barz M, et al. Ligand density on nanoparticles: A parameter with critical impact on nanomedicine. Advanced Drug Delivery Reviews. 2019;143:22-36.

115. Pomorski TG, Menon AK. Lipid somersaults: Uncovering the mechanisms of protein-mediated lipid flipping. Progress in lipid research. 2016;64:69-84.

116. Mouritsen OG, Bagatolli LA. Lipids in Bilayers—A Stress-Full and Busy Life. LIFE-AS A MATTER OF FAT: Springer; 2016. p. 85-93.

117. Contreras F-X, Sánchez-Magraner L, Alonso A, Goñi FM. Transbilayer (flip-flop) lipid motion and lipid scrambling in membranes. FEBS letters. 2010;584(9):1779-86.

118. Marquardt D, Heberle FA, Miti T, Eicher B, London E, Katsaras J, et al. 1H NMR shows slow phospholipid flip-flop in gel and fluid bilayers. Langmuir. 2017;33(15):3731-41.

119. Homan R, Pownall HJ. Transbilayer diffusion of phospholipids: dependence on headgroup structure and acyl chain length. Biochimica et Biophysica Acta (BBA)-Biomembranes. 1988;938(2):155-66.

120. Silvius JR, Leventis R. Spontaneous interbilayer transfer of phospholipids: Dependence of acyl chain composition. Biochemistry. 1993;32(48):13318-26.

121. Münter R, Kristensen K, Pedersbæk D, Larsen JB, Simonsen JB, Andresen TL. Dissociation of fluorescently labeled lipids from liposomes in biological environments challenges the interpretation of uptake studies. Nanoscale. 2018;10(48):22720-4.

122. Ahmed A, Heldt N, Slack G, Li Y. Lipid Exchange Rates of Conventional and Polymer Stabilized Liposomes. MRS Online Proceedings Library (OPL). 2002;724:N8. 2.

123. Jones J, Thompson TE. Spontaneous phosphatidylcholine transfer by collision between vesicles at high lipid concentration. Biochemistry. 1989;28(1):129-34.

124. Saeki D, Sugiura S, Baba T, Kanamori T, Sato S, Mukataka S, et al. Dynamic interaction between oppositely charged vesicles: aggregation, lipid mixing, and disaggregation. Journal of colloid and interface science. 2008;320(2):611-4.

125. Gonzalez-Rodriguez M, Rabasco A. Charged liposomes as carriers to enhance the permeation through the skin. Expert opinion on drug delivery. 2011;8(7):857-71.

126. Kim A, Lee EH, Choi S-H, Kim C-K. In vitro and in vivo transfection efficiency of a novel ultradeformable cationic liposome. Biomaterials. 2004;25(2):305-13.

127. Sapra P, Allen T. Ligand-targeted liposomal anticancer drugs. Progress in lipid research. 2003;42(5):439-62.

128. Grimaldi N, Andrade F, Segovia N, Ferrer-Tasies L, Sala S, Veciana J, et al. Lipid-based nanovesicles for nanomedicine. Chemical Society Reviews. 2016;45(23):6520-45.

129. Riaz MK, Riaz MA, Zhang X, Lin C, Wong KH, Chen X, et al. Surface functionalization and targeting strategies of liposomes in solid tumor therapy: A review. International journal of molecular sciences. 2018;19(1):195.

130. Zahednezhad F, Saadat M, Valizadeh H, Zakeri-Milani P, Baradaran B. Liposome and immune system interplay: Challenges and potentials. Journal of Controlled Release. 2019;305:194-209.

131. Olusanya TO, Haj Ahmad RR, Ibegbu DM, Smith JR, Elkordy AA. Liposomal drug delivery systems and anticancer drugs. Molecules. 2018;23(4):907.

132. Martin F, Boulikas T. The challenge of liposomes in gene therapy. Gene Ther Mol Biol. 1998;1:173-214.

133. Noble GT, Stefanick JF, Ashley JD, Kiziltepe T, Bilgicer B. Ligand-targeted liposome design: challenges and fundamental considerations. Trends in Biotechnology. 2014;32(1):32-45.

134. Tavano L, Muzzalupo R. Multi-functional vesicles for cancer therapy: the ultimate magic bullet. Colloids and Surfaces B: Biointerfaces. 2016;147:161-71.

135. Sawant RR, Torchilin VP. Challenges in development of targeted liposomal therapeutics. The AAPS journal. 2012;14(2):303-15.

136. Bunker A, Magarkar A, Viitala T. Rational design of liposomal drug delivery systems, a review: combined experimental and computational studies of lipid membranes, liposomes and their PEGylation. Biochimica et Biophysica Acta (BBA)-Biomembranes. 2016;1858(10):2334-52.

137. Knop K, Hoogenboom R, Fischer D, Schubert US. Poly(ethylene glycol) in drug delivery: pros and cons as well as potential alternatives. Angewandte Chemie. 2010;49(36):6288-308.

138. Clark AS, Vahdat LT. Chemotherapy-induced palmar-plantar erythrodysesthesia syndrome: etiology and emerging therapies. Supportive cancer therapy. 2004;1(4):213-8.

139. Garay RP, El-Gewely R, Armstrong JK, Garratty G, Richette P. Antibodies against polyethylene glycol in healthy subjects and in patients treated with PEG-conjugated agents. 2012.

140. Nichols JW, Sakurai Y, Harashima H, Bae YH. Nano-sized drug carriers: Extravasation, intratumoral distribution, and their modeling. Journal of Controlled Release. 2017;267:31-46.

141. Armstrong JK. The occurrence, induction, specificity and potential effect of antibodies against poly (ethylene glycol). Pegylated protein drugs: Basic science and clinical applications. 2009:147-68.

142. Rodriguez PL, Harada T, Christian DA, Pantano DA, Tsai RK, Discher DE. Minimal" self" peptides that inhibit phagocytic clearance and enhance delivery of nanoparticles. Science. 2013;339(6122):971-5.

143. Sugihara H, Yamamoto H, Kawashima Y, Takeuchi H. Effectiveness of submicronized chitosan-coated liposomes in oral absorption of indomethacin. Journal of liposome research. 2012;22(1):72-9.

144. Gottesmann M, Goycoolea FM, Steinbacher T, Menogni T, Hensel A. Smart drug delivery against Helicobacter pylori: pectin-coated, mucoadhesive liposomes with antiadhesive activity and antibiotic cargo. Applied Microbiology and Biotechnology. 2020;104:5943-57.

145. Hoang Thi TT, Pilkington EH, Nguyen DH, Lee JS, Park KD, Truong NP. The importance of poly (ethylene glycol) alternatives for overcoming PEG immunogenicity in drug delivery and bioconjugation. Polymers (Basel). 2020;12(2):298.

146. Kirpotin D, Park JW, Hong K, Zalipsky S, Li W-L, Carter P, et al. Sterically stabilized anti-HER2 immunoliposomes: design and targeting to human breast cancer cells in vitro. Biochemistry. 1997;36(1):66-75.

147. Nag OK, Yadav VR, Hedrick A, Awasthi V. Post-modification of preformed liposomes with novel non-phospholipid poly (ethylene glycol)-conjugated hexadecylcarbamoylmethyl hexadecanoic acid for enhanced circulation persistence in vivo. International journal of pharmaceutics. 2013;446(1-2):119-29.

148. Petros RA, DeSimone JM. Strategies in the design of nanoparticles for therapeutic applications. Nature reviews Drug discovery. 2010;9(8):615-27.

149. Matsumura Y, Maeda H. A new concept for macromolecular therapeutics in cancer chemotherapy: mechanism of tumoritropic accumulation of proteins and the antitumor agent smancs. Cancer research. 1986;46(12 Part 1):6387-92.

150. Nichols JW, Bae YH. EPR: evidence and fallacy. Journal of Controlled Release. 2014;190:451-64.

151. Adapted from 'Passive Targeting of Nanoparticles to Cancer Cells' by BioRender.com. (2022) Retrived from https://appbiorender.com/biorender-templates. 2022.

152. Pattni BS, Chupin VV, Torchilin VP. New developments in liposomal drug delivery. Chemical reviews. 2015;115(19):10938-66.

153. Cheng WW, Allen TM. Targeted delivery of anti-CD19 liposomal doxorubicin in B-cell lymphoma: a comparison of whole monoclonal antibody, Fab' fragments and single chain Fv. Journal of Controlled Release. 2008;126(1):50-8.

154. Miller K, Cortes J, Hurvitz SA, Krop IE, Tripathy D, Verma S, et al. HERMIONE: a randomized Phase 2 trial of MM-302 plus trastuzumab versus chemotherapy of physician's choice plus trastuzumab in patients with previously treated, anthracycline-naïve, HER2-positive, locally advanced/metastatic breast cancer. BMC cancer. 2016;16(1):1-11.

155. Cao Z, Tong R, Mishra A, Xu W, Wong GC, Cheng J, et al. Reversible cell-specific drug delivery with aptamer-functionalized liposomes. Angewandte Chemie International Edition. 2009;48(35):6494-8.

156. Li X, Ding L, Xu Y, Wang Y, Ping Q. Targeted delivery of doxorubicin using stealth liposomes modified with transferrin. International journal of pharmaceutics. 2009;373(1-2):116-23.

157. Song CK, Jung SH, Kim D-D, Jeong K-S, Shin BC, Seong H. Disaccharide-modified liposomes and their in vitro intracellular uptake. International Journal of Pharmaceutics. 2009;380(1-2):161-9.

158. Xie F, Yao N, Qin Y, Zhang Q, Chen H, Yuan M, et al. Investigation of glucose-modified liposomes using polyethylene glycols with different chain lengths as the linkers for brain targeting. International journal of nanomedicine. 2012:163-75.

159. Gao Y, Liu X, Chen N, Yang X, Tang F. Recent Advance of Liposome Nanoparticles for Nucleic Acid Therapy. Pharmaceutics. 2023;15(1):178.

160. Drummond DC, Hong K, Park JW, Benz CC, Kirpgtin DB. Liposome targeting to tumors using vitamin and growth factor receptors. 2000.

161. Gao J, Chen H, Yu Y, Song J, Song H, Su X, et al. Inhibition of hepatocellular carcinoma growth using immunoliposomes for co-delivery of adriamycin and ribonucleotide reductase M2 siRNA. Biomaterials. 2013;34(38):10084-98.

162. Carrasco-Triguero M, Yi J-H, Dere R, Qiu ZJ, Lei C, Li Y, et al. Immunogenicity assays for antibody–drug conjugates: case study with ado-trastuzumab emtansine. Bioanalysis. 2013;5(9):1007-23.

163. Almeida B, Nag OK, Rogers KE, Delehanty JB. Recent progress in bioconjugation strategies for liposome-mediated drug delivery. Molecules. 2020;25(23):5672.

164. Li L, Hou J, Liu X, Guo Y, Wu Y, Zhang L, et al. Nucleolin-targeting liposomes guided by aptamer AS1411 for the delivery of siRNA for the treatment of malignant melanomas. Biomaterials. 2014;35(12):3840-50.

165. Sonju JJ, Dahal A, Singh SS, Jois SD. Peptide-functionalized liposomes as therapeutic and diagnostic tools for cancer treatment. Journal of Controlled Release. 2021;329:624-44.

166. Song S, Liu D, Peng J, Deng H, Guo Y, Xu LX, et al. Novel peptide ligand directs liposomes toward EGF-R high-expressing cancer cells in vitro and in vivo. The FASEB Journal. 2009;23(5):1396-404.

167. Wang S, Chen Y, Guo J, Huang Q. Liposomes for Tumor Targeted Therapy: A Review. International Journal of Molecular Sciences. 2023;24(3):2643.

168. Gaspar M, Martins M, Corvo M, Cruz M. Design and characterization of enzymosomes with surface-exposed superoxide dismutase. Biochimica et biophysica acta (BBA)-biomembranes. 2003;1609(2):211-7.

169. Cruz MEM, Corvo ML, Martins MB, Simões S, Gaspar MM. Liposomes as tools to improve therapeutic enzyme performance. Pharmaceutics. 2022;14(3):531.

170. Zhang X, Qi J, Lu Y, He W, Li X, Wu W. Biotinylated liposomes as potential carriers for the oral delivery of insulin. Nanomedicine: nanotechnology, biology and medicine. 2014;10(1):167-76.

171. Raju A, Muthu MS, Feng S-S. Trastuzumab-conjugated vitamin E TPGS liposomes for sustained and targeted delivery of docetaxel. Expert opinion on drug delivery. 2013;10(6):747-60.

172. Abu-Dahab R, Schäfer UF, Lehr C-M. Lectin-functionalized liposomes for pulmonary drug delivery: effect of nebulization on stability and bioadhesion. European journal of pharmaceutical sciences. 2001;14(1):37-46.

173. Du J, Lu W-L, Ying X, Liu Y, Du P, Tian W, et al. Dual-targeting topotecan liposomes modified with tamoxifen and wheat germ agglutinin significantly improve drug transport across the blood− brain barrier and survival of brain tumor-bearing animals. Molecular pharmaceutics. 2009;6(3):905-17.

174. Eliasen R, Andresen TL, Larsen JB. PEG-lipid post insertion into drug delivery liposomes quantified at the single liposome level. Advanced Materials Interfaces. 2019;6(9):1801807.

175. Ringhieri P, Diaferia C, Galdiero S, Palumbo R, Morelli G, Accardo A. Liposomal doxorubicin doubly functionalized with CCK8 and R8 peptide sequences for selective intracellular drug delivery. Journal of Peptide Science. 2015;21(5):415-25.

176. Fathi S, Oyelere AK. Liposomal drug delivery systems for targeted cancer therapy: is active targeting the best choice? Future medicinal chemistry. 2016;8(17):2091-112.

177. Curcio M, Brindisi M, Cirillo G, Frattaruolo L, Leggio A, Rago V, et al. Smart lipid–polysaccharide nanoparticles for targeted delivery of doxorubicin to breast cancer cells. International Journal of Molecular Sciences. 2022;23(4):2386.

178. Tayo LL. Stimuli-responsive nanocarriers for intracellular delivery. Biophysical reviews. 2017;9(6):931-40.

179. Lou J, Best MD. A General Approach to Enzyme-Responsive Liposomes. Chemistry–A European Journal. 2020;26(39):8597-607.

180. Hu J, Wu D, Pan Q, Li H, Zhang J, Geng F. Recent Development of Photoresponsive Liposomes Based on Organic Photosensitizers, Au Nanoparticles, and Azobenzene Derivatives for Nanomedicine. ACS Applied Nano Materials. 2022;5(10):14171-90.

181. Paszko E, Ehrhardt C, Senge MO, Kelleher DP, Reynolds JV. Nanodrug applications in photodynamic therapy. Photodiagnosis and photodynamic therapy. 2011;8(1):14-29.

182. Krauss AC, Gao X, Li L, Manning ML, Patel P, Fu W, et al. FDA Approval Summary:(Daunorubicin and Cytarabine) Liposome for Injection for the Treatment of Adults with High-Risk Acute Myeloid LeukemiaFDA Approval:(Daunorubicin and Cytarabine). Clinical Cancer Research. 2019;25(9):2685-90.

183. Attia MF, Anton N, Wallyn J, Omran Z, Vandamme TF. An overview of active and passive targeting strategies to improve the nanocarriers efficiency to tumour sites. Journal of Pharmacy and Pharmacology. 2019;71(8):1185-98.

184. Kievit FM, Zhang M. Cancer nanotheranostics: improving imaging and therapy by targeted delivery across biological barriers. Advanced materials. 2011;23(36):H217-H47.

185. Sato YT, Umezaki K, Sawada S, Mukai S-a, Sasaki Y, Harada N, et al. Engineering hybrid exosomes by membrane fusion with liposomes. Scientific reports. 2016;6(1):21933.

186. Zhang W, Ngo L, Tsao SC-H, Liu D, Wang Y. Engineered Cancer-Derived Small Extracellular Vesicle-Liposome Hybrid Delivery System for Targeted Treatment of Breast Cancer. ACS Applied Materials & Interfaces. 2023.

187. Liu A, Yang G, Liu Y, Liu T. Research progress in membrane fusion-based hybrid exosomes for drug delivery systems. Frontiers in Bioengineering and Biotechnology. 2022;10.

188. Qiao L, Hu S, Huang K, Su T, Li Z, Vandergriff A, et al. Tumor cell-derived exosomes home to their cells of origin and can be used as Trojan horses to deliver cancer drugs. Theranostics. 2020;10(8):3474.

189. Li Y-J, Wu J-Y, Liu J, Xu W, Qiu X, Huang S, et al. Artificial exosomes for translational nanomedicine. Journal of nanobiotechnology. 2021;19:1-20.

190. Marqués-Gallego P, de Kroon AI. Ligation strategies for targeting liposomal nanocarriers. BioMed research international. 2014;2014.

191. de Lima PHC, Butera AP, Cabeça LF, Ribeiro-Viana RM. Liposome surface modification by phospholipid chemical reactions. Chemistry and Physics of Lipids. 2021;237:105084.

192. Liu Y, Cai Y, Liu W, Li X-H, Rhoades E, Yan EC. Triblock peptide–linker–lipid molecular design improves potency of peptide ligands targeting family BG protein-coupled receptors. Chemical Communications. 2015;51(28):6157-60.

193. Xia G, An Z, Wang Y, Zhao C, Li M, Li Z, et al. Synthesis of a novel polymeric material folate-poly (2-ethyl-2-oxazoline)-distearoyl phosphatidyl ethanolamine tri-block polymer for dual receptor and pH-sensitive targeting liposome. Chemical and Pharmaceutical Bulletin. 2013:c12-00951.

194. Gao H, Li M, Wu Y. Novel amphiphilic dextran copolymers nanoparticles for delivery of doxorubicin. Journal of applied polymer science. 2011;120(4):2448-58.

195. Yari H, Nkepang G, Awasthi V. Surface modification of liposomes by a lipopolymer targeting prostate specific membrane antigen for theranostic delivery in prostate cancer. Materials. 2019;12(5):756.

196. Mare R, Paolino D, Celia C, Molinaro R, Fresta M, Cosco D. Post-insertion parameters of PEG-derivatives in phosphocholine-liposomes. International journal of pharmaceutics. 2018;552(1-2):414-21.

197. Uster PS, Allen TM, Daniel BE, Mendez CJ, Newman MS, Zhu GZ. Insertion of poly (ethylene glycol) derivatized phospholipid into pre-formed liposomes results in prolonged in vivo circulation time. FEBS letters. 1996;386(2-3):243-6.

198. Sou K, Endo T, Takeoka S, Tsuchida E. Poly (ethylene glycol)-modification of the phospholipid vesicles by using the spontaneous incorporation of poly (ethylene glycol)-lipid into the vesicles. Bioconjugate chemistry. 2000;11(3):372-9.

199. Allen TM, Sapra P, Moase E. Use of the post-insertion method for the formation of ligand-coupled liposomes. Cellular and Molecular Biology Letters. 2002;7(2):217-9.

200. Liu Y, Zhao Z, Li M. Overcoming the cellular barriers and beyond: Recent progress on cell penetrating peptide modified nanomedicine in combating physiological and pathological barriers. Asian Journal of Pharmaceutical Sciences. 2022.

201. Kamps J, Scherphof G. Liposomes in biological systems. Liposomes, a Practical Approach. 2003:267-88.

202. Pagano RE, Weinstein JN. Interactions of liposomes with mammalian cells. Annual review of biophysics and bioengineering. 1978;7(1):435-68.

203. Pagano RE, Takeichi M. Adhesion of phospholipid vesicles to Chinese hamster fibroblasts: Role of cell surface proteins. The Journal of cell biology. 1977;74(2):531-46.

204. Adapted from 'Non-phagocytic nanopartilce internalisation pathways' by BioRender.com (2022). Retrieved from https://app.biorender.com/biorender-templates.

205. Zaabalawi A, Azzawi M. Chapter 6 - Cellular interactions of nanoparticles within the vasculature. In: Kesharwani P, Singh KK, editors. Nanoparticle Therapeutics: Academic Press; 2022. p. 247-63.

206. Dutta D, Pulsipher A, Luo W, Mak H, Yousaf MN. Engineering cell surfaces via liposome fusion. Bioconjugate Chemistry. 2011;22(12):2423-33.

207. Knoll G, Burger K, Bron R, van Meer G, Verkleij AJ. Fusion of liposomes with the plasma membrane of epithelial cells: Fate of incorporated lipids as followed by freeze fracture and autoradiography of plastic sections. The Journal of cell biology. 1988;107(6):2511-21.

208. Sandra A, Pagano R. Liposome-cell interactions. Studies of lipid transfer using isotopically asymmetric vesicles. Journal of Biological Chemistry. 1979;254(7):2244-9.

209. Kuypers F, Roelofsen B, Berendsen W, Op den Kamp J, Van Deenen L. Shape changes in human erythrocytes induced by replacement of the native phosphatidylcholine with species containing various fatty acids. The Journal of cell biology. 1984;99(6):2260-7.

210. Lev S. Non-vesicular lipid transport by lipid-transfer proteins and beyond. Nature reviews Molecular cell biology. 2010;11(10):739-50.

211. Ferrell Jr JE, Lee KJ, Huestis WH. Lipid transfer between phosphatidylcholine vesicles and human erythrocytes: exponential decrease in rate with increasing acyl chain length. Biochemistry. 1985;24(12):2857-64.

212. Martin FJ, MacDonald RC. Phospholipid exchange between bilayer membrane vesicles. Biochemistry. 1976;15(2):321-7.

213. Nichols JW, Pagano RE. Kinetics of soluble lipid monomer diffusion between vesicles. Biochemistry. 1981;20(10):2783-9.

214. De Cuyper M, Joniau M, Dangreau H. Intervesicular phospholipid transfer. A free-flow electrophoresis study. Biochemistry. 1983;22(2):415-20.

215. Phillips MC, Johnson WJ, Rothblat GH. Mechanisms and consequences of cellular cholesterol exchange and transfer. Biochimica et Biophysica Acta (BBA) - Reviews on Biomembranes. 1987;906(2):223-76.

216. Stoll C, Stadnick H, Kollas O, Holovati JL, Glasmacher B, Acker JP, et al. Liposomes alter thermal phase behavior and composition of red blood cell membranes. Biochimica et Biophysica Acta (BBA)-Biomembranes. 2011;1808(1):474-81.

217. Rahman Y, Cerny E, Patel K, Lau E, Wright B. Differential uptake of liposomes varying in size and lipid composition by parenchymal and Kupffer cells of mouse liver. Life sciences. 1982;31(19):2061-71.

218. Hsu M, Juliano R. Interactions of liposomes with the reticuloendothelial system: II. Nonspecific and receptor-mediated uptake of liposomes by mouse peritoneal macrophages. Biochimica et Biophysica Acta (BBA)-Molecular Cell Research. 1982;720(4):411-9.

219. Rejman J, Oberle V, Zuhorn IS, Hoekstra D. Size-dependent internalization of particles via the pathways of clathrin-and caveolae-mediated endocytosis. Biochemical journal. 2004;377(1):159-69.

220. Kang JH, Jang WY, Ko YT. The effect of surface charges on the cellular uptake of liposomes investigated by live cell imaging. Pharmaceutical research. 2017;34(4):704-17.

221. Düzgüneş N, Nir S. Mechanisms and kinetics of liposome–cell interactions. Advanced drug delivery reviews. 1999;40(1-2):3-18.

222. Düzgünes N, Wilschut J, Fraley R, Papahadjopoulos D. Studies on the mechanism of membrane fusion. Role of head-group composition in calcium-and magnesium-induced

fusion of mixed phospholipid vesicles. Biochimica et Biophysica Acta (BBA)-Biomembranes. 1981;642(1):182-95.

223. Papahadjopoulos D, Poste G, Schaeffer B. Fusion of mammalian cells by unilamellar lipid vesicles: influence of lipid surface charge, fluidity and cholesterol. Biochimica et Biophysica Acta (BBA)-Biomembranes. 1973;323(1):23-42.

224. Holovati JL, Gyongyossy-Issa MI, Acker JP. Effect of liposome charge and composition on the delivery of trehalose into red blood cells. Cell Preservation Technology. 2008;6(3):207-18.

225. Ahmad I, Allen TM. Antibody-mediated specific binding and cytotoxicity of liposome-entrapped doxorubicin to lung cancer cells in vitro. Cancer research. 1992;52(17):4817-20.

226. Goren D, Horowitz AT, Tzemach D, Tarshish M, Zalipsky S, Gabizon A. Nuclear delivery of doxorubicin via folate-targeted liposomes with bypass of multidrug-resistance efflux pump. Clinical Cancer Research. 2000;6(5):1949-57.

227. Gustafson HH, Holt-Casper D, Grainger DW, Ghandehari H. Nanoparticle uptake: The phagocyte problem. Nano Today. 2015;10(4):487-510.

228. Lee KD, Nir S, Papahadjopoulos D. Quantitative analysis of liposome-cell interactions in vitro: rate constants of binding and endocytosis with suspension and adherent J774 cells and human monocytes. Biochemistry. 1993;32(3):889-99.

229. Hoekstra D, Scherphof G. Effect of fetal calf serum and serum protein fractions on the uptake of liposomal phosphatidylcholine by rat hepatocytes in primary monolayer culture. Biochimica et Biophysica Acta (BBA)-Biomembranes. 1979;551(1):109-21.

230. Rapoport EM, Khasbiullina NR, Komarova VA, Ryzhov IM, Gorbatch MM, Tuzikov AB, et al. Localization of synthetic glycolipids in the cell and the dynamics of their insertion/loss. Biochimica et Biophysica Acta (BBA)-Biomembranes. 2021;1863(9):183645.

231. Gao X, Yue T, Tian F, Liu Z, Zhang X. Erythrocyte membrane skeleton inhibits nanoparticle endocytosis. AIP Advances. 2017;7(6):065303.

232. Thatte HS, Schrier SL. Comparison of transferrin receptor-mediated endocytosis and drug-induced endocytosis in human neonatal and adult RBCs. 1988.

233. Colin FC, Schrier SL. Spontaneous endocytosis in human neonatal and adult red blood cells: Comparison to drug-induced endocytosis and to receptor-mediated endocytosis. American journal of hematology. 1991;37(1):34-40.

234. Harisa GE-dI, Ibrahim MF, Alanazi FK. Characterization of human erythrocytes as potential carrier for pravastatin: an in vitro study. International Journal of Medical Sciences. 2011;8(3):222.

235. Chabanel A, Flamm M, Sung K, Lee M, Schachter D, Chien S. Influence of cholesterol content on red cell membrane viscoelasticity and fluidity. Biophysical journal. 1983;44(2):171-6.

236. Holovati JL, Acker JP. Emerging role for use of liposomes in the biopreservation of red blood cells. Transfusion Medicine and Hemotherapy. 2011;38(2):99-106.

237. Cyboran-Mikołajczyk S, Sareło P, Pasławski R, Pasławska U, Przybyło M, Nowak K, et al. Impact of Liposomal Drug Formulations on the RBCs Shape, Transmembrane Potential, and Mechanical Properties. International Journal of Molecular Sciences. 2021;22(4):1710.

238. Mourtas S, Michanetzis GP, Missirlis YF, Antimisiaris SG. Haemolytic activity of liposomes: effect of vesicle size, lipid concentration and polyethylene glycol-lipid or arsonolipid incorporation. Journal of biomedical nanotechnology. 2009;5(4):409-15.

239. Cooper R, Arner E, Wiley J, Shattil S. Modification of red cell membrane structure by cholesterol-rich lipid dispersions. A model for the primary spur cell defect. The Journal of clinical investigation. 1975;55(1):115-26.

240. Korchagina E, Henry S. Synthetic glycolipid-like constructs as tools for glycobiology research, diagnostics, and as potential therapeutics. Biochemistry (Moscow). 2015;80(7):857-71.

241. Henry S, Williams E, Barr K, Korchagina E, Tuzikov A, Ilyushina N, et al. Rapid one-step biotinylation of biological and non-biological surfaces. Scientific reports. 2018;8(1):1-6.

242. Henry SM, Bovin NV. Kode Technology–a universal cell surface glycan modification technology. Journal of the Royal Society of New Zealand. 2019;49(2):100-13.

243. Lan C-C, Blake D, Henry S, Love DR. Fluorescent function-spacer-lipid construct labelling allows for real-time in vivo imaging of cell migration and behaviour in zebrafish (Danio rerio). Journal of Fluorescence. 2012;22(4):1055-63.

244. Ilyushina NA, Chernyy ES, Korchagina EY, Gambaryan AS, Henry SM, Bovin NV. Labeling of influenza viruses with synthetic fluorescent and biotin-labeled lipids. Virologica Sinica. 2014;29(4):199-210.

245. Hadac EM, Federspiel MJ, Chernyy E, Tuzikov A, Korchagina E, Bovin NV, et al. Fluorescein and radiolabeled Function-Spacer-Lipid constructs allow for simple in vitro and in vivo bioimaging of enveloped virions. Journal of virological methods. 2011;176(1-2):78-84.

246. Barr K, Korchagina E, Ryzhov I, Bovin N, Henry S. Mapping the fine specificity of ABO monoclonal reagents with A and B type-specific function-spacer-lipid constructs in kodecytes and inkjet printed on paper. Transfusion. 2014;54(10):2477-84.

247. Barr K, Korchagina E, Popova I, Bovin N, Henry S. Monoclonal anti-A activity against the FORS1 (Forssman) antigen. Transfusion. 2015;55(1):129-36.

248. Chesla S, Henry S, Eatz R, Sinor L. Solid phase syphilis test utilizing KODE technology. Transfusion. 2010;50:196A-7A.

249. Georgakopoulos T, Komarraju S, Henry S, Bertolini J. An improved Fc function assay utilizing CMV antigen-coated red blood cells generated with synthetic function–spacer–lipid constructs. Vox sanguinis. 2012;102(1):72-8.

250. Oliver C, Blake D, Henry S. In vivo neutralization of anti-A and successful transfusion of A antigen–incompatible red blood cells in an animal model. Transfusion. 2011;51(12):2664-75.

251. Henry SM. Modification of red blood cells for laboratory quality control use. Current opinion in hematology. 2009;16(6):467-72.

252. Harrison AL, Olsson ML, Jones RB, Ramkumar S, Sakac D, Binnington B, et al. A synthetic globotriaosylceramide analogue inhibits HIV-1 infection in vitro by two mechanisms. Glycoconjugate journal. 2010;27(5):515-24.

253. Henry SM, Tuzikov AB, Bovin NV. Kode Technology Illustrated Technical Manual, First Edition: The University of Auckland Research Repository; 2023. Available from: https://researchspace.auckland.ac.nz/handle/2292/62953.

254. Frame T, Carroll T, Korchagina E, Bovin N, Henry S. Synthetic glycolipid modification of red blood cell membranes. Transfusion. 2007;47(5):876-82.

255. Heathcote D, Carroll T, Wang JJ, Flower R, Rodionov I, Tuzikov A, et al. IMMUNOHEMATOLOGY: Novel antibody screening cells, MUT+ Mur kodecytes, created by attaching peptides onto red blood cells. Transfusion. 2010;50(3):635-41.

256. Nagappan R, Flegel WA, Srivastava K, Williams EC, Ryzhov I, Tuzikov A, et al. COVID-19 antibody screening with SARS-CoV-2 red cell kodecytes using routine serologic diagnostic platforms. Transfusion. 2021;61(4):1171-80.

257. Tesfay MZ, Kirk AC, Hadac EM, Griesmann GE, Federspiel MJ, Barber GN, et al. PEGylation of vesicular stomatitis virus (VSV) extends virus persistence in blood circulation of passively immunized mice. Journal of virology. 2013:JVI. 02832-12.

258. Raghuraman P. Antibiofilm Function-Spacer-Lipid Coatings On Medical Surfaces: Auckland University of Technology; 2021.

259. Poudyal A. Kode Technology Modification of Nanofibres to Capture Particulates: Auckland University of Technology; 2020.

260. Zalygin A, Solovyeva D, Vaskan I, Henry S, Schaefer M, Volynsky P, et al. Structure of Supramers Formed by the Amphiphile Biotin-CMG-DOPE. ChemistryOpen. 2020;9(6):641.

261. Slivka E, Tuzikov A, Khaidukov S, Komarova V, Henry S, Bovin N, et al. Influence of the Lipid Moiety Structure on the Insertion/Release of Glycolipids in/from the Cell: A Study with Synthetic Analogs. Russian Journal of Bioorganic Chemistry. 2022;48(5):932-6.

262. Avanti Polar LIpids. DOPE [Available from: https://avantilipids.com/product/850725.

263. Hult AK, Frame T, Chesla S, Henry S, Olsson ML. Flow cytometry evaluation of red blood cells mimicking naturally occurring ABO subgroups after modification with variable amounts of function-spacer-lipid A and B constructs. Transfusion. 2012;52(2):247-51.

264. Sneath JS, Sneath P. Transformation of the Lewis groups of human red cells. Nature. 1955;176(4473):172-.

265. Marcus DM, Cass LE. Glycosphingolipids with Lewis blood group activity: uptake by human erythrocytes. Science. 1969;164(3879):553-5.

266. Oliver C, Blake D, Henry S. Modeling transfusion reactions and predicting in vivo cell survival with kodecytes. Transfusion. 2011;51(8):1723-30.

267. Has C, Sunthar P. A comprehensive review on recent preparation techniques of liposomes. Journal of liposome research. 2020;30(4):336-65.

268. Vemuri S, Rhodes C. Preparation and characterization fo liposomes as therapeutic delivery systems: a review. Pharmaceutica Acta Helvetiae. 1995;70:95-111.

269. Akbarzadeh A, Rezaei-Sadabady R, Davaran S, Joo SW, Zarghami N, Hanifehpour Y, et al. Liposome: classification, preparation, and applications. Nanoscale research letters. 2013;8(1):102.

270. Szoka F, Papahadjopoulos D. Procedure for preparation of liposomes with large internal aqueous space and high capture by reverse-phase evaporation. Proc Natl Acad Sci U S A. 1978;75(9):4194-8.

271. Batzri S, Korn ED. Single bilayer liposomes prepared without sonication. Biochimica et Biophysica Acta (BBA)-Biomembranes. 1973;298(4):1015-9.

272. Deamer D, Bangham A. Large volume liposomes by an ether vaporization method. Biochimica et Biophysica Acta (BBA)-Biomembranes. 1976;443(3):629-34.

273. Vemuri S, Rhodes C. Preparation and characterization of liposomes as therapeutic delivery systems: a review. Pharmaceutica Acta Helvetiae. 1995;70(2):95-111.

274. Meure LA, Foster NR, Dehghani F. Conventional and dense gas techniques for the production of liposomes: a review. Aaps Pharmscitech. 2008;9(3):798-809.

275. Li C, Deng Y. A novel method for the preparation of liposomes: freeze drying of monophase solutions. Journal of pharmaceutical sciences. 2004;93(6):1403-14.

276. Kikuchi H, Yamauchi H, Hirota S. A Spray-Drying Method for Mass Production of Liposomes. Chem Pharm Bull. 1991;39:1522.

277. Jahn A, Vreeland WN, Gaitan M, Locascio LE. Controlled vesicle self-assembly in microfluidic channels with hydrodynamic focusing. Journal of the American Chemical Society. 2004;126(9):2674-5.

278. Angelova MI, Dimitrov DS. Liposome electroformation. Faraday discussions of the Chemical Society. 1986;81:303-11.

279. Elizondo E, Moreno E, Cabrera I, Cordoba A, Sala S, Veciana J, et al. Liposomes and other vesicular systems: structural characteristics, methods of preparation, and use in nanomedicine. Progress in molecular biology and translational science. 2011;104:1-52.

280. Mendez R, Banerjee S. Sonication-based basic protocol for liposome synthesis. Lipidomics: Springer; 2017. p. 255-60.

281. Olson F, Hunt C, Szoka F, Vail W, Papahadjopoulos D. Preparation of liposomes of defined size distribution by extrusion through polycarbonate membranes. Biochimica et Biophysica Acta (BBA)-Biomembranes. 1979;557(1):9-23.

282. Ong SGM, Chitneni M, Lee KS, Ming LC, Yuen KH. Evaluation of extrusion technique for nanosizing liposomes. Pharmaceutics. 2016;8(4):36.

283. Hamilton Jr RL, Goerke J, Guo L, Williams MC, Havel RJ. Unilamellar liposomes made with the French pressure cell: a simple preparative and semiquantitative technique. Journal of lipid research. 1980;21(8):981-92.

284. Traïkia M, Warschawski DE, Recouvreur M, Cartaud J, Devaux PF. Formation of unilamellar vesicles by repetitive freeze-thaw cycles: characterization by electron microscopy and 31P-nuclear magnetic resonance. European Biophysics Journal. 2000;29(3):184-95.

285. Mayer L, Hope M, Cullis P. Vesicles of variable sizes produced by a rapid extrusion procedure. Biochimica et Biophysica Acta (BBA)-Biomembranes. 1986;858(1):161-8.

286. Bangham AD, Standish MM, Watkins JC. Diffusion of univalent ions across the lamellae of swollen phospholipids. Journal of Molecular Biology. 1965;13:238-52.

287. Zhang H. Thin-Film Hydration Followed by Extrusion Method for Liposome Preparation. Liposomes: Methods and Protocols. 2017;1522:17-22.

288. Adapted from 'Liposome preparation via thin film hydration' by BioRender.com(2021) Retrieved from https://app.biorender.com/biorender-templates.

289. rGuimarães D, Cavaco-Paulo A, Nogueira E. Design of liposomes as drug delivery system for therapeutic applications. International Journal of Pharmaceutics. 2021;601:120571.

290. Bhattacharjee S. DLS and zeta potential–what they are and what they are not? Journal of controlled release. 2016;235:337-51.

291. Malvern. Zetasizer nano user manul MAN0485 2013. Available from: https://www.chem.uci.edu/~dmitryf/manuals/Malvern%20Zetasizer%20ZS%20DLS%20user%20manual.pdf.

292. Stetefeld J, McKenna SA, Patel TR. Dynamic light scattering: a practical guide and applications in biomedical sciences. Biophysical reviews. 2016;8(4):409-27.

293. Malvern. Dynamic Light Scattering: An introduction in 30 Minutes [Technical Note]. 2010 [cited 2022 June 24]. Available from: https://www.malvernpanalytical.com/en/learn/knowledge-center/technical-notes/TN101104DynamicLightScatteringIntroduction.

294. Malvern. What does polydispersity mean? [Technical Note]. [cited 2023 10 May]. Available from: https://www.materials-talks.com/wp-content/uploads/2017/10/What-does-polydispersity-mean.pdf.

295. Chen C, Zhu S, Huang T, Wang S, Yan X. Analytical techniques for single-liposome characterization. Analytical Methods. 2013;5(9):2150-7.

296. Bibi S, Kaur R, Henriksen-Lacey M, McNeil SE, Wilkhu J, Lattmann E, et al. Microscopy imaging of liposomes: from coverslips to environmental SEM. Int J Pharm. 2011;417(1-2):138-50.

297. Baxa U. Imaging of liposomes by transmission electron microscopy. Characterization of Nanoparticles Intended for Drug Delivery: Springer; 2018. p. 73-88.

298. Weissenberger G, Henderikx RJ, Peters PJ. Understanding the invisible hands of sample preparation for cryo-EM. Nature methods. 2021;18(5):463-71.

299. Dubochet J, Chang J-J, Freeman R, Lepault J, McDowall A. Frozen aqueous suspensions. Ultramicroscopy. 1982;10(1-2):55-61.

300. Dubochet J, Adrian M, Lepault J, McDowall AW. Emerging techniques: Cryo-electron microscopy of vitrified biological specimens. Trends in Biochemical Sciences. 1985;10(4):143-6.

301. Almgren M, Edwards K, Karlsson G. Cryo transmission electron microscopy of liposomes and related structures. Colloids and Surfaces A: Physicochemical and Engineering Aspects. 2000;174(1):3-21.

302. Robson A-L, Dastoor PC, Flynn J, Palmer W, Martin A, Smith DW, et al. Advantages and Limitations of Current Imaging Techniques for Characterizing Liposome Morphology. Frontiers in Pharmacology. 2018;9(80).

303. Drulyte I, Johnson RM, Hesketh EL, Hurdiss DL, Scarff CA, Porav SA, et al. Approaches to altering particle distributions in cryo-electron microscopy sample preparation. Acta Crystallogr D Struct Biol. 2018;74(Pt 6):560-71.

304. Clogston JD, Patri AK. Zeta potential measurement. Characterization of nanoparticles intended for drug delivery: Springer; 2011. p. 63-70.

305. Domínguez A, Fernández A, González N, Iglesias E, Montenegro L. Determination of critical micelle concentration of some surfactants by three techniques. Journal of chemical education. 1997;74(10):1227.

306. Scholz N, Behnke T, Resch-Genger U. Determination of the critical micelle concentration of neutral and ionic surfactants with fluorometry, conductometry, and surface tension—a method comparison. Journal of fluorescence. 2018;28(1):465-76.

307. Shanks P, Franses E. Estimation of micellization parameters of aqueous sodium dodecyl sulfate from conductivity data. The Journal of Physical Chemistry. 1992;96(4):1794-805.

308. Lah J, Pohar C, Vesnaver G. Calorimetric study of the micellization of alkylpyridinium and alkyltrimethylammonium bromides in water. The Journal of Physical Chemistry B. 2000;104(11):2522-6.

309. Ghosh S, Krishnan A, Das PK, Ramakrishnan S. Determination of critical micelle concentration by hyper-Rayleigh scattering. Journal of the American Chemical Society. 2003;125(6):1602-6.

310. Surfactant micelle characterization using dynamic light scattering 2016 [Available from: https://www.malvernpanalytical.com/en/learn/knowledge-center/application-notes/AN101104SurfactantMicelleCharacterization.

311. Patist A, Bhagwat S, Penfield K, Aikens P, Shah D. On the measurement of critical micelle concentrations of pure and technical-grade nonionic surfactants. Journal of Surfactants and Detergents. 2000;3(1):53-8.

312. Cui X, Mao S, Liu M, Yuan H, Du Y. Mechanism of surfactant micelle formation. Langmuir. 2008;24(19):10771-5.

313. Critical micelle concentration (CMC) and surfactant concentration.: Kruss Scientific; [Available from: https://www.kruss-scientific.com/en/know-how/glossary/critical-micelle-concentration-cmc-and-surfactant-concentration.

314. Stauffer CE. The measurement of surface tension by the pendant drop technique. The journal of physical chemistry. 1965;69(6):1933-8.

315. Berry JD, Neeson MJ, Dagastine RR, Chan DY, Tabor RF. Measurement of surface and interfacial tension using pendant drop tensiometry. Journal of colloid and interface science. 2015;454:226-37.

316. Hansen F, Rødsrud G. Surface tension by pendant drop: I. A fast standard instrument using computer image analysis. Journal of colloid and interface science. 1991;141(1):1-9.

317. Kwok D, Vollhardt D, Miller R, Li D, Neumann A. Axisymmetric drop shape analysis as a film balance. Colloids and Surfaces A: Physicochemical and Engineering Aspects. 1994;88(1):51-8.

318. Saad SM, Policova Z, Neumann AW. Design and accuracy of pendant drop methods for surface tension measurement. Colloids and Surfaces A: Physicochemical and Engineering Aspects. 2011;384(1-3):442-52.

319. Alnoush W, Sayed A, Alyafei N. Optimization of contact angle and interfacial tension measurements for fluid/rock systems at ambient conditions. MethodsX. 2019;6:1706-15.

320. Kalyanasundaram K, Thomas J. Environmental effects on vibronic band intensities in pyrene monomer fluorescence and their application in studies of micellar systems. Journal of the American Chemical Society. 1977;99(7):2039-44.

321. Piñeiro L, Novo M, Al-Soufi W. Fluorescence emission of pyrene in surfactant solutions. Advances in colloid and interface science. 2015;215:1-12.

322. Zana R, Levy H, Kwetkat K. Mixed micellization of dimeric (Gemini) surfactants and conventional surfactants. I. Mixtures of an anionic dimeric surfactant and of the nonionic surfactants C12E5and C12E8. Journal of colloid and interface science. 1998;197(2):370-6.

323. Scholz N, Behnke T, Resch-Genger U. Determination of the critical micelle concentration of neutral and ionic surfactants with fluorometry, conductometry, and surface tension—a method comparison. Journal of fluorescence. 2018;28:465-76.

324. Lin M, Qi X-R. Purification method of drug-loaded liposome. Liposome-based drug delivery systems. 2021:111-21.

325. Dimov N, Kastner E, Hussain M, Perrie Y, Szita N. Formation and purification of tailored liposomes for drug delivery using a module-based micro continuous-flow system. Scientific reports. 2017;7(1):12045.

326. Alves NJ, Cusick W, Stefanick JF, Ashley JD, Handlogten MW, Bilgicer B. Functionalized liposome purification via liposome extruder purification (LEP). Analyst. 2013;138(17):4746-51.

327. Lin S-Y, Lin Y-Y, Chen E-M, Hsu C-T, Kwan C-C. A study of the equilibrium surface tension and the critical micelle concentration of mixed surfactant solutions. Langmuir. 1999;15(13):4370-6.

328. Eastoe J, Dalton J. Dynamic surface tension and adsorption mechanisms of surfactants at the air–water interface. Advances in colloid and interface science. 2000;85(2-3):103-44.

329. Cho D, Narsimhan G, Franses EI. Adsorption dynamics of native and pentylated bovine serum albumin at air–water interfaces: surface concentration/surface pressure measurements. Journal of colloid and interface science. 1997;191(2):312-25.

330. Simeonov A, Davis MI. Interference with fluorescence and absorbance. Assay Guidance Manual [Internet]. 2018.

331. Yu Q, England RM, Gunnarsson A, Luxenhofer R, Treacher K, Ashford MB. Designing Highly Stable Poly (sarcosine)-Based Telodendrimer Micelles with High Drug Content Exemplified with Fulvestrant. Macromolecules. 2022;55(2):401-12.

332. Bae W, Yoon T-Y, Jeong C. Direct evaluation of self-quenching behavior of fluorophores at high concentrations using an evanescent field. PloS one. 2021;16(2):e0247326.

333. Mukerjee P. The nature of the association equilibria and hydrophobic bonding in aqueous solutions of association colloids. Advances in Colloid and Interface Science. 1967;1(3):242-75.

334. Blandamer MJ, Cullis PM, Soldi LG, Engberts JBFN, Kacperska A, Van Os NM, et al. Thermodynamics of micellar systems: Comparison of mass action and phase equilibrium models for the calculation of standard Gibbs energies of micelle formation. Advances in Colloid and Interface Science. 1995;58(2):171-209.

335. Khan H, Seddon JM, Law RV, Brooks NJ, Robles E, Cabral JT, et al. Effect of glycerol with sodium chloride on the Krafft point of sodium dodecyl sulfate using surface tension. Journal of colloid and interface science. 2019;538:75-82.

336. Avanti Polar Lipids. Equipment (Avanti Mini Extruder) [Available from: https://avantilipids.com/divisions/equipment-products.

337. Mui B, Chow L, Hope MJ. Extrusion technique to generate liposomes of defined size. Methods in enzymology. 2003;367:3-14.

338. Mayer L, Hope M, Cullis P, Janoff A. Solute distributions and trapping efficiencies observed in freeze-thawed multilamellar vesicles. Biochimica et Biophysica Acta (BBA)-Biomembranes. 1985;817(1):193-6.

339. Costa AP, Xu X, Burgess DJ. Freeze-anneal-thaw cycling of unilamellar liposomes: effect on encapsulation efficiency. Pharmaceutical research. 2014;31(1):97-103.

340. Wnętrzak A, Łątka K, Dynarowicz-Łątka P. Interactions of alkylphosphocholines with model membranes—the Langmuir monolayer study. The Journal of Membrane Biology. 2013;246(6):453-66.

341. De Almeida RF, Fedorov A, Prieto M. Sphingomyelin/phosphatidylcholine/cholesterol phase diagram: boundaries and composition of lipid rafts. Biophysical journal. 2003;85(4):2406-16.

342. Kinnunen P, Alakoskela JM, Laggner P. Phase behavior of liposomes. Methods Enzymol. 2003;367:129-47.

343. Liposome: Encapsula's Scientific Blog. The number of lipid molecules per liposome. 2009 [Available from: http://www.liposomes.org/2009/01/number-of-lipid-molecules-per-liposome.html#:~:text=As%20an%20example%20the%20number,size%20liposome%20is%20about%2080047.

344. Karmakar S. Particle size distribution and zeta potential based on dynamic light scattering: techniques to characterise stability and surface distribution of charged colloids particle. Recent Trends Materials: Physics Chem. Recent Trends Mater Phys Chem. 2019:117-59.

345. Zidovska A, Ewert KK, Quispe J, Carragher B, Potter CS, Safinya CR. Block liposome and nanotube formation is a general phenomenon of two-component membranes containing multivalent lipids. Soft Matter. 2011;7(18):8363-9.

346. Zidovska A, Ewert KK, Quispe J, Carragher B, Potter CS, Safinya CR. The effect of salt and pH on block liposomes studied by cryogenic transmission electron microscopy. Biochimica et Biophysica Acta (BBA)-Biomembranes. 2009;1788(9):1869-76.

347. Greenall MJ, Gompper G. Bilayers connected by threadlike micelles in amphiphilic mixtures: a self-consistent field theory study. Langmuir. 2011;27(7):3416-23.

348. Bojarski C, Domsta J. Theory of the influence of concentration on the luminescence of solid solutions. Acta Physica Academiae Scientiarum Hungaricae. 1971;30(2):145-66.

349. Svensson L, Rydberg L, Hellberg Å, Gilliver L, Olsson M, Henry S. Novel glycolipid variations revealed by monoclonal antibody immunochemical analysis of weak ABO subgroups of A. Vox sanguinis. 2005;89(1):27-38.

350. Korchagina E, Tuzikov A, Formanovsky A, Popova I, Henry S, Bovin N. Toward creating cell membrane glyco-landscapes with glycan lipid constructs. Carbohydrate research. 2012;356:238-46.

351. Fung M, Grossman B, Hillyer C, Westhoff C. Technical manual 18th edition. AABB Bethesda Maryland USA. 2014.

352. Grilfols. Blood Grouping Reagent DG Gel 8 AB [package insert on the internet]. Diagnostic Grifols, SA. Spain2013; cited 2021.

353. Mosca M, Ceglie A, Ambrosone L. Effect of membrane composition on lipid oxidation in liposomes. Chemistry and Physics of Lipids. 2011;164(2):158-65.

354. Siukstaite L, Rosato F, Mitrovic A, Müller PF, Kraus K, Notova S, et al. The two sweet sides of Janus lectin drive crosslinking of liposomes to cancer cells and material uptake. Toxins. 2021;13(11):792.

355. Omidvar R, Ayala YA, Brandel A, Hasenclever L, Helmstädter M, Rohrbach A, et al. Quantification of nanoscale forces in lectin-mediated bacterial attachment and uptake into giant liposomes. Nanoscale. 2021;13(7):4016-28.

356. Ayala YA, Omidvar R, Römer W, Rohrbach A. Thermal fluctuations of the lipid membrane determine particle uptake into Giant Unilamellar Vesicles. Nature Communications. 2023;14(1):65.

357. Notova S, Bonnardel F, Rosato F, Siukstaite L, Schwaiger J, Lim JH, et al. The choanoflagellate pore-forming lectin SaroL-1 punches holes in cancer cells by targeting the tumor-related glycosphingolipid Gb3. Communications Biology. 2022;5(1):954.

358. Omidvar SR, Rohrbach A. Showcasing research from Professor Römer's laboratory, Signalling Research Centres BIOSS and CIBSS, Faculty of Biology, University of Freiburg, Germany. Quantification of nanoscale forces in lectin-mediated bacterial attachment and uptake into giant liposomes. Nanoscale. 2021;13:4016.

359. Ribeiro JP, Villringer S, Goyard D, Coche-Guerente L, Höferlin M, Renaudet O, et al. Tailor-made Janus lectin with dual avidity assembles glycoconjugate multilayers and crosslinks protocells. Chemical Science. 2018;9(39):7634-41.

360. Villringer S, Madl J, Sych T, Manner C, Imberty A, Römer W. Lectin-mediated protocell crosslinking to mimic cell-cell junctions and adhesion. Scientific reports. 2018;8(1):1-11.

361. Nakamura K, Yamashita K, Itoh Y, Yoshino K, Nozawa S, Kasukawa H. Comparative studies of polyethylene glycol-modified liposomes prepared using different PEG-modification methods. Biochimica et Biophysica Acta (BBA)-Biomembranes. 2012;1818(11):2801-7.

362. Cosco D, Tsapis N, Nascimento TL, Fresta M, Chapron D, Taverna M, et al. Polysaccharide-coated liposomes by post-insertion of a hyaluronan-lipid conjugate. Colloids and Surfaces B: Biointerfaces. 2017;158:119-26.

363. Szoka F, Jacobson K, Derzko Z, Papahadjopoulos D. Fluorescence studies on the mechanism of liposome-cell interactions in vitro. Biochimica et Biophysica Acta (BBA)-Biomembranes. 1980;600(1):1-18.

364. Henry S, Barr K, Oliver C. Modeling transfusion reactions with kodecytes and enabling ABO-incompatible transfusion with function-spacer-lipid constructs. ISBT Science Series. 2012;7(1):106-11.

365. Woodle MC. Surface-modified liposomes: assessment and characterization for increased stability and prolonged blood circulation. Chemistry and Physics of Lipids. 1993;64(1):249-62.